Aus dem Adolf-Butenandt-Institut der
Ludwig-Maximilians-Universität
München
Lehrstuhl: Molekularbiologie
Direktor: Prof. Dr. Peter B. Becker
Arbeitsgruppe: Prof. Dr. Gunnar Schotta

Deletion of Setdb1 in Sox17 lineage cells impairs early embryonic development in the mouse

Dissertation zum Erwerb des Doktorgrades der
Naturwissenschaften (Dr. rer. Nat.) an der Medizinischen Fakultät
Der Ludwig-Maximilians-Universität München

Vorgelegt von

Rui Fan

Aus
Shi Jia Zhuang, China

2015

Gedruckt mit Genehmigung der Medizinschen Fakultät der Ludwig Maximilians-Universität München

Betreuer: Prof. Dr. Gunnar Schotta

Zweitgutachter: Prof. Dr. Axel Imhof

Dekan: Prof. Dr. med. Dr. h. c. Maximilian Reiser, FACR, FRCR

Tag der mündlichen Prüfung: 24. 02. 2015

Eidesstattliche Versicherung

Ich erkläre hiermit an Eides statt,
dass ich die vorliegende Dissertation mit dem Thema

“Deletion of Setdb1 in Sox17 lineage cells impairs early embryonic development in the mouse”

selbständig verfasst, mich außer der angegebenen keiner weiteren Hilfsmittel bedient und alle Erkenntnisse, die aus dem Schrifttum ganz oder annähernd übernommen sind, als solche kenntlich gemacht und nach ihrer Herkunft unter Bezeichnung der Fundstelle einzeln nachgewiesen habe.

Ich erkläre des Weiteren, dass die hier vorgelegte Dissertation nicht in gleicher oder in ähnlicher Form bei einer anderen Stelle zur Erlangung eines akademischen Grades eingereicht wurde.

Ort, Datum

Unterschrift Rui Fan

ABSTRACT

Over the last decades, epigenetic mechanisms have been related to severe diseases (Dambacher et al. 2010) and developmental defects (Hahn et al. 2010). For my thesis, I mainly focused on the functional study of Setdb1, which is a histone methyltransferase that mediates H3K9 methylation, during endoderm development. Previous studies have already shown that Setdb1 could di- and tri-methylate H3K9 in euchromatin (Wang et al. 2003) and deletion of Setdb1 results in the lethality of embryos at a very early embryonic stage (Dodge et al. 2004). Additionally, Chip-Seq data showed that Setdb1 binds to pluripotency-associated genes and development regulators in ES cells (Bilodeau et al. 2009, Yuan et al. 2009). These results indicate the potential functions of Setdb1 in regulating mouse development.

During early embryonic development, three germ layers start to be formed at gastrulation stage (Takaoka et al. 2012). In order to study the spatial and temporal function of Setdb1 in endoderm development we specifically deleted Setdb1 in Sox17 lineage cells. In order to specifically test the function of Setdb1 in definitive endoderm, we additionally introduced a GFP-reporter gene. GFP is activated by the expression of Cre recombinase. Thus, we assume that GFP positive cells have also deleted Setdb1. By monitoring the Setdb1 deleted cells, we found that mutant embryos which showed a broad GFP signal even outside endoderm were severely developmentally retarded. In contrast, a specific GFP signal in the endoderm region correlated with milder endoderm-related defects. In the subsequent studies I focused on embryos with specific deletion of Setdb1 in the endoderm. In order to further characterize the phenotype we performed immunohistochemistry to check for structural changes. Setdb1 mutant embryos cannot complete axis rotation and show progressive deterioration of the hindgut region. In mutant embryos the hindgut diverticulum is formed but loses the contact with splanchnopleura. Moreover the size of the dorsal aorta is much bigger in mutant embryos. During development the diverticulum cannot further develop resulting in perturbed mesoderm development. Whole mount embryo immunostaining revealed an increase in apoptotic cells in the posterior part of mutant embryos and the reduced expression of endoderm genes in the primitive streak region. Interestingly we found that Setdb1 mutant cells display altered morphogenesis and cover part of the node region. We assume that impaired signal transmission through the cilia on the surface of the node contributes to the developmental defect of Setdb1 mutant embryos. To identify genes which are regulated by Setdb1, mutant and control embryos at E7.75 were collected for microarray analysis. Several genes belonging to different biological processes were found to be dysregulated. AFP, which is a visceral endoderm gene, is upregulated in Setdb1 mutant embryos. However, through the whole mount embryo immunostaining, AFP positive cells are mainly restricted to the extra-embryonic part indicating that the loss of Setdb1 in visceral endoderm does not affect the development of the embryonic part. We also generated Setdb1$^{flox/flox}$; Sox17-cre; GFP-reporter ES cells and induced differentiation of these cells into endoderm cells. RNA-seq analysis revealed that endoderm commitment genes are upregulated in the mutant cells. We therefore assume that Setdb1 balances the expression of the endoderm differentiation program.

ABSTRACT

Epigenetische Mechanismen haben eine grosse Bedeutung bei der Krankheitsentstehung und für die Embryonalentwicklung. In meiner Arbeit habe ich mich auf die Funktionen der Histon-Methyltransferase Setdb1 bei der Endodermentwicklung konzentriert. Voherige Studien konnten zeigen, dass Setdb1 essentiell für die Embryonalentwicklung ist und Histon H3 an Lysin 9 di- oder trimethylieren kann. Desweiteren bindet Setdb1 in Maus ES Zellen an Gene die mit Pluripotenz assoziiert sind. Diese Daten lassen eine mögliche Funktion von Setdb1 in der Regulation der Embryonalentwicklung vermuten.

Während der Embryonalentwicklung, bei der Gastrulation, formen sich drei Keimblätter: Ektoderm, Mesoderm und Endoderm. Um die Funktion von Setdb1 in der Endodermentwicklung zu studieren, schalteten wir Setdb1 in Endodermzellen aus, die das Markergen Sox17 exprimieren. Außerdem kreuzten wir ein Cre/GFP-Reportersystem in diese Mauslinie, um die Deletion von Setdb1 in Sox17 exprimierenden Zellen durch GFP-Expression erkennen zu können. Anhand der GFP Expression konnten wir feststellen, dass in unserem Mausmodell die Embryonen Setdb1 entweder global ausschalteten, oder Setdb1 spezifisch nur in Endoderm-Zellen verloren. Ich fokussierte mich in meiner Arbeit auf Mausembryonen mit spezifischer Depletion von Setdb1 in Endodermzellen. Embryonen in denen Setdb1 im Endoderm deletiert ist, führen keine embryonale Drehung durch und zeigen eine Schädigung der embryonalen Darmregion. Außerdem ist die dorsale Aorta erweitert und die Embryonen zeigen Defekte in der Mesodermentwicklung, welche wahrscheinlich von einer Fehlentwicklung des Diverticulums herrührt. Weiterhin konnten wir durch Immunfärbungen einen Anstieg der Apoptose im posterioren Bereich dieser Embryonen feststellen. Desweiteren konnten wir eine veränderte Morphogenese von Setdb1 depletierten Zellen detektieren und eine Veränderung des Embryonalknotens durch diese Zellen. Wir vermuten, dass eine veränderte Signaltransduktion an dieser wichtigen embryonalen Struktur für einen Teil des Phänotyps in unserem Mausmodell verantwortlich ist.

Um Gene zu identifizieren die durch Setdb1 reguliert werden, führten wir auch Microarray-Studien mit Embryonen vom Stadium E7.75 durch und konnten mehrere deregulierte Gene identifizieren. Von unserem Setdb1$^{flox/flox}$; Sox17-cre; GFP-Reporter Mausmodell stellten wir auch ES Zellen her. Durch induzierte Endodermentwicklung in Setdb1-depletierten Zellen konnten wir mittels RNA-Seq Analysen feststellen, dass Gene, die Endodermdifferenzierung vermitteln, hochreguliert waren in. Folglich, scheint Setdb1 die Expression des Endoderm Differenzierungssystems zu regulieren.

1. INTRODUCTION

1.1 Chromatin structure

The genetic information in cells is stored in the DNA sequence. Compaction of the DNA makes the long double stranded DNA fit into the nucleus and highly organized. DNA wraps around the histone octamer containing two molecules each of the four histones, H2A, H2B, H3, and H4 to form the nucleosome which is the fundamental repeating unit of chromatin. Furthermore, the crystal structure of the histone octamer is revealed in details at 2.8A resolution.

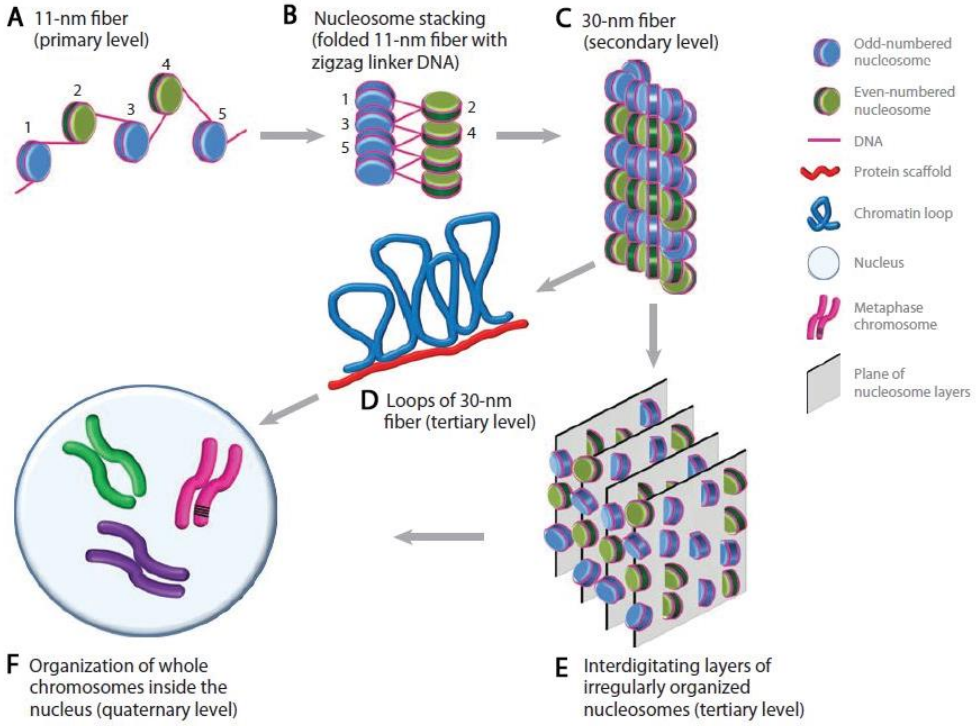

Figure 1.1 Different levels of chromatin compaction (Sajan et al. 2012). **A)** Multiple nucleosomes in a row form the 11-nm fiber as the primary level of chromatin compaction. **B)** The 11-nm fiber folds on itself to form two columns of nucleosomes. **C)** The folded 11-nm fiber forms the 30-nm chromatin fiber which is considered as the secondary level of compaction. **D)** The 30-nm fiber is twisted and forms a more compact fiber (blue) with some portions attached to a protein scaffold (red). **E)** The 30-nm fiber may also form the interdigitating layer which is another tertiary level of compaction. **F)** The three-dimensional organization of entire chromosomes considered as the quaternary level.

Ten years ago, it was found that H3 and H4 first form a tetramer which is comprised of two H3-H4 dimers through a strong 4-helix bundle (4-HB) between the two H3 molecules. H2A and H2B form the dimers first then interact with a H3 and H4 tetramer through a weak 4-helix bundle (4-HB) between H2B and H4 (Bönisch et al. 2012). Additionally, all of the nucleosomes contain one molecule of the linker protein H1 which binds at or near the nucleosome dyad axis and interacts with the linker

DNA. H1 could wrap another 20 base pairs of the octamer leading to 2 turns around it (Olins et al. 2003). A lot of non-histone proteins are also involved in the construction of chromatin which makes the structure of the chromatin more complicated. The strings of nucleosomes could be organized to the higher ordered 30 nm fibers which are considered as the secondary level of chromatin organization. Furthermore, the 30 nm fibers could be arranged in loops that constitute the tertiary structure of chromatin (Woodcock et al 2001). Recent research results identify there is another structure existence of interdigitating layers with irregularly organized nucleosomes in the metaphase chromosome are also considered as tertiary structure of chromatin. The loops of the 30 nm fibers and interdigitating layers of nucleosomes could be condensed and form the quaternary structure of chromatin in a complex context (Sajan et al. 2012).

1.2 Epigenetic mechanism regulates gene transcription

Chromatin is a rather complicated complex. More and more factors have been found involved in maintaining the stable structure of chromatin and contributing to gene regulation. The DNA sequence is not the only factor which could decide on gene regulation even though the DNA sequence is the direct template for the DNA transcription and RNA translation. The transcription mechanism on chromatinized DNA is nearly the same among different species. First, the activators could bind the core promoter region and then the adaptors such as SAGA and other mediators are recruited. These bound activators could in turn facilitate the binding of general transcriptional factors. Pol II sitting at the core promoter form the pre-initiation complex with TFIID, TFIIA, and TFIIB and so on (Green et al. 2005). Pol II could position at the single strand DNA which are cleaved by TFIIF and further recruit the elongation factors to perform the RNA synthesis.

1.2.1 Histone modification

Even though the gene expression directly connects to the DNA transcription and RNA translation, there are still several different factors playing important roles for gene expression regulation. Histone modifications as important components of the epigenetic regulation mechanisms also regulate the gene expression.

First, the Pol II binds to the promoter region of genes then recruits different factors to the core promoter to form the pre-initiation complex and initiate the transcription and elongation. However, the structure of the nucleosome is not static all the time. A lot of protein complexes could induce the change of the nucleosome structure and further alter the gene expression. One of the major classes of the chromatin regulators are histone modifications including methylation, acetylation, ubiquitiantion, ADP-ribosylation, sumolation and phosphorylation. These modifications could be divided into two different subgroups according to their functions. One subgroup is related to the gene repression, such as H3K9me, H4K20me and H3K27me. The other subgroup is associated with active transcription

including acetylation and methylation of H3K4 and H3K36. The precise mechanism of histone modification involved in the chromatin structure change remains to be unclear but some hypotheses have been gradually accepted. First, most of these modifications can change the charge of nucleosome which could alter the interaction between DNA and histones. For example, histone acetylation could neutralize the positive charge of specific lysine sites leading to an open chromatin architecture (Shahbazian et al. 2007). The other idea is that the different histone modifications could recruit different factors to specific loci of the chromatin which could alter the DNA transcription. One of the examples is that H3K9me could facilitate the binding of HP1 which further forms heterochromatin (Ayyanathan et al. 2003). These different effects could also happen on one modification. Additionally, in some cases different modifications could alter the modification state of each other. A well-characterized example is the H2BK123ub1 could promote H3K4me3 and H3K79me3 (Lee et al. 2010).

At the first beginning, histone modification was considered to be relative stable and to exist on the histone residues permanently. The only way to remove them is through exchange of the histone variants and dilution during DNA replication. But with the identification of enzymes which could remove these histone modifications, a different view was generated. Now histone modifications are considered to be rather dynamic (Kooistra et al. 2012). The balance between the addition and removal of histone modification is very important for the proper expression of specific genes. Several important questions regarding their molecular mechanism and biological roles remain unclear and more work needs to be done to further our understanding.

1.2.2 Chromatin remodelers

Another major epigenetic regulatory mechanism involved in gene transcription is chromatin remolding. Chromatin remodeling complexes could alter the contacts between chromatin and DNA through the power of ATP hydrolysis (Clapier et al. 2009). The structural change of chromatin caused by remodelers could control gene expression by regulating DNA accessibility.

How is this regulation achieved? Two different outcomes of the chromatin remodeling are generally accepted. The remodelers could alter the nucleosome packaging to expose the transcription start site by nucleosome sliding, or nucleosome eviction, or localized unwrapping. The other category could access the transcription factors into specific DNA sites through change of the composition of the nucleosome. So far, four different families of chromatin remodeling complexes have been identified (Flaus et al. 2006). These remodeler families are SWI/SNF family remodelers, ISWI family remodelers, CHD family remodelers and INO80 family remodelers. They all share one similar ATPase domain which is split into two parts by different insertions. Each family contains different domains in or adjacent to the ATPase domain performing different biological function. Also there are some pioneering studies to show the important role of remodelers for gene regulation during development (Clapier et al. 2009).

1.2.3 Histone variants

Histone octamers are wrapped around by DNA sequence to form the core nucleosome particles. During replication the nucleosomes are disassembled and the existing histones will be randomly distributed to the newly formed nucleosome and 50% histones are freshly synthesized.

Three of these four canonical histones, H2A H2B and H3, have been proved to have several histone variants. The differences between these canonical histones and variants range from nearly nothing to divergent differences (Kamakaka et al. 2005). The variants are mainly distinguished by incorporation of the chromatin in a DNA replication-independent manner (Skene et al. 2013). Recently, histone variants received more and more attention in gene regulation because of the change of the chromatin state due to the replacement of the canonical histones by these variants. Some of these variants exist globally in eukaryotic animals, for example CenH3, H3.3, H2A.Z and H2A.X. These variants are proven to be involved in the structure and stability of the nucleosome. The other variants do not exist globally like MacroH2As, H2A.Bbd and Rotifer H2As. They are expressed exclusively in specific species or cell lineages (Talbert et al. 2010). The difference between these canonical histones and variants could be found in just a few amino acids (H3.3) or in the histone tails (MacroH2A) or in the histone fold domains (H2ABbd) (Li et al. 2007). These histone variants are also involved in regulating transcriptional activity. One well-characterized variant is H2A.Z which prefers to sit at promoters. Upon transcription initiation, H2A.Z is evicted and the transcription could be activated (Zhang et al. 2005). In ES cells, loss of H2A.Z impedes the binding of Oct4 in the promoter regions of pluripotency genes which impairs the pluripotency of ES cells.

1.3 H3K9-specific methyltransferase

Epigenetic modifications are related to diverse biological processes. There are active and inactive epigenetic modifications which could regulate the binding of transcription factors to the naked DNA sequences resulting in the expression or the repression of specific genes. Cells with the expression of specific genes patterns could exhibit different functions. Inappropriate expression pattern in the cells leads to apoptosis and disease.

The DNA sequences wrapping around the histones to form nucleosomes. The nucleosomes could be further compacted to form chromatins. The tails of the highly organized chromatin could be modified by different histone post-translational modifications (PTMs) including phosphorylation, acetylation, ubiquitination, and methylation and so on (Figure1.2 A). These modifications can contribute to gene expression and cell fate decisions through the change of the chromatin structure or affect the interaction of protein complexes with the DNA sequence. Histone methylation has been reported on arginine, lysine and histidine (Greer et al. 2012). The methylation on lysine is more extensively studied and occurs as mono-, di-, or trimethylated form on H3K4, H3K9, H3K27, H3K36, H3K79, H4K20 and others (Figure1.2 B) (Zhang et al. 2001). Among them H3K4, H3K36 and H3K79 are

considered as the transcriptionally active markers and H3K9, H3K27 and H4K20 are related to transcriptional repression. H3K9 methylation is a significant repressive modification which is catalyzed by several different methyltransferases such as Suv39h1, Suv39h2, G9a, Glp1 and Setdb1. In mammals, these methyltransferases have a pivotal role in different biological processes and early embryonic development. Loss of these methyltransferases leads to the alteration of H3K9 methylation and severe growth defects.

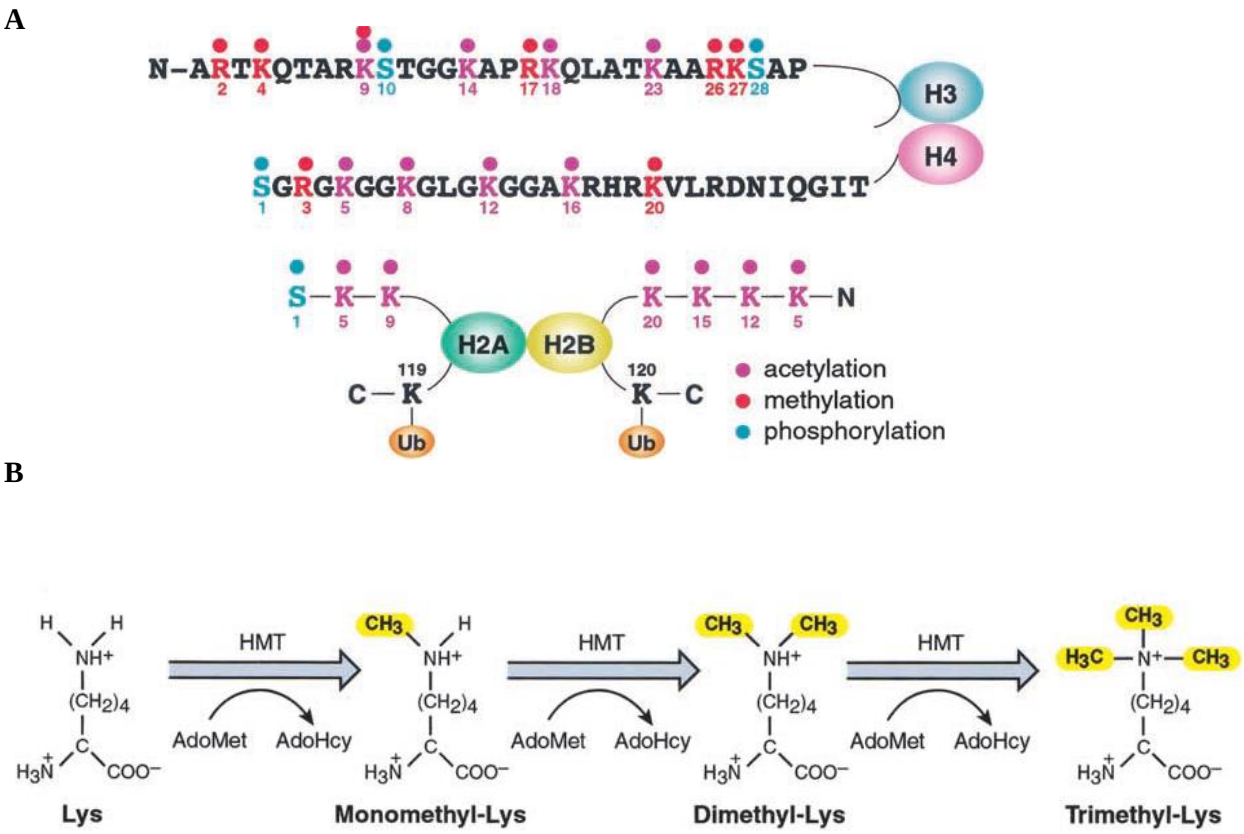

Figure 1.2 Sites of post-translational modifications on histone tails and the structure of lysine methylation (Zhang et al. 2001). A) The modifications shown include acetylation (purple), methylation (red), phosphorylation (green), and ubiquitination (orange) on the tails of H3, H4, H2A and H2B. **B)** Molecular structure of lysine and mono-, di-, and tri-methyl-lysine.

1.3.1 Suv39h1 and Suv39h2

Suv39 h1 and h2 were the first identified mammalian lysine-preferring histone methyltransferases and SET domain-containing proteins. The SET domain in Suv39h1 and h2 is found and conserved in several different proteins from different species. Most of these SET domain containing proteins are considered as chromatin modifiers (Jenuwein et al. 1998). The SET domain is also present in several different protein families, for example, polycomb and trithorax group (Pc-G and trx-G), acting as repressors and activators respectively. Among all of these SET domain-containing protein families, Suv39h family proteins also contain a chromo-domain (The Chromatin Organization Modifier), which is also conserved and characterized as a chromatin regulator motif. Homologues of Suv39h families

have been identified in different species, for example CLR4 in yeast (Allshire et al. 1995), Su(var)3–9 in drosophila (Sass et al.1998), Suv39h1 and h2 in mouse, and SUV39H1 in human (Rea et al. 2000). SUV39h1 and SUV39h2 are the most studied histone methyltransferases (HKMTs), which play very important role in pericentric heterochromatin establishment and gene repression (Peters et al. 2001). Heterochromatin protein 1 (HP1) could contribute to the heterochromatin formation and also mediate gene silencing. HP1 involves two important conserved chromo shadow domain and chromo domain and is able to localize at the methylated H3 peptide. In return, HP1 can recruit H3K9-specific methyltransferases and propagate the H3K9 methylation (Bannister et al. 2001).

In Drosophila, Position effect variegation (PEV) is an interesting way to study heterochromatin mediated gene silencing. A euchromatic gene will be silenced when it is placed in the neighborhood of heterochromatins. It has been proposed that HP1a and HP1b could be recruited via the SUV39h mediated H3K9me3 in pericentric heterochromatin and further interact with DNA methyltransferase 3b (Lehnertz et al. 2003). In Suv39h dn ES cells, H3-K9 trimethylation is drastically decreased in heterochromatin but the mono- and di-methylation in the euchromatin is not impaired. Suv39h1 and h2 double null mouse could be born but at only sub-Mendelian ratios and show a severe retardation phenotype. Loss of Suv39h1 and h2 severely affect the genetic stability through impairing the chromosome segregation during mitosis and meiosis (Peters et al. 2003).

1.3.2 G9a and Glp1

G9a and Glp1 are SET-domain-containing molecules which could mainly mono- and di-methylate H3K9. Recently, the function of G9a and Glp1 has been found to be involved in diverse biological processes therefore more and more interest has been raised on the study of these two methylases (Shinkai et al. 2011). G9a was the second reported HKMT. G9a deficient cells lacked nearly all the H3K9me2 and show a significant decrease in H3K9me1 which demonstrate that G9a is a major H3K9me1 and H3K9me2 HKMT mainly in euchromatin (Rice et al. 2003). Glp1 encode the G9a like protein and methylates the same substrate on histones as G9a. However G9a and Glp1 cannot compensate for the function of each other that means the levels of H3K9me1 and H3K9me2 are severely reduced upon the deletion of either G9a or Glp1 and double knockout of G9a and Glp1 could not further reduce the methylation level. G9a and Glp1 could perform the methylation function through the formation of homomeric and heteromeric complexes (Tachibana et al. 2005). Additionally, the G9a–Glp1 heterocomplex also need the binding of Wiz, a multi-zinc finger-containing molecule. The binding of wiz to the heterocomplex is more stable than the interaction with the homocomplex. Therefore it is speculated that the G9a–Glp1–Wiz complex exists as the dominant intracellular form (Ueda et al. 2006).

The relationship between H3K9 methylation and DNA methylation is very complicated. There is a paper showing that the G9a–Glp1 complex silences transcription through mediating not only H3K9

but also DNA methylation (Tachibana et al. 2008). DNMT1 can regulate the chromatin structure by loading of G9a and knockdown of DNMT1 reduces H3K9me2 levels in human cells (Estève et al. 2006). The function of G9a and Glp1 is also closely related to early mouse embryonic development. Loss of either G9a or Glp1 results in the lethality of the mouse embryos at around E9.5 and the development of the embryos is severely retarded (Tachibana et al. 2005). The epigenetic change through G9a also plays a very important role in repression of Oct4 during further development (Feldman et al. 2006). The mono- and di-methylation levels in H3K9 are drastically reduced and the location of HP1 is also dispersed in G9a or Glp1 mutant cell lines. G9a mediated methylation can induce heterochromatinization via the binding of HP1 in the promoter region of Oct4, subsequently Dnmt3a/3b which is recruited by HP1 cause the DNA methylation at Oct4 promoter.

1.3.3 Setdb1

Setdb1 was first identified in a human myelogenous leukemia cell line (Nomura et al. 1994). Setdb1, called Eset in mouse, was isolated from mouse hematopoietic cells through a yeast two-hybrid library of ERG and is 92% identical to human Setdb1 (Yang et al. 2002). Setdb1 consists of Tudor, MBD1 and SET domain. These domains have potential functions to mediate the interaction of proteins and regulated gene expression. Additionally, Setdb1 can form different complexes with different partners. These different complexes are involved in different biological processes.

Gel filtration experiments in HeLa cells showed that Setdb1 is co-eluted with a 200kD protein. Through Setdb1 immunoprecipitation and Mass spectrometric analysis this big protein was identified as mouse ATFa-associated Modulator (Atf7IP) (Wang et al.2003). Knock-down of Atf7ip cannot affect the expression level of Setdb1 but it results in a decrease of H3K9me3 and the increased level of H3K9me2 both in vitro and in vivo (Wang et al. 2003). In a reconstituted chromatin transcription system, Atf7ip improves the repression function of Setdb1 through the conversion of H3K9me2 to H3K9me3 in the promoter region of specific genes. In a yeast two-hybrid experiment using the PHD finger and bromodomain of Kap1 as bait, Schultz (Schultz et al. 2003) found that Kap1 was associated with Setdb1. The pull down experiment with flag-tagged Setdb1 also proved that Kap1 is an interactor of Setdb1 in HEK293 cells. In the KRAB–Kap1 repression system, Setdb1 could enhance the H3K9 methylation and the binding of HP1a on an endogenous promoter region. Based on their results they suggested that Kap1 acts as a molecular scaffold protein which could bind to specific promoter regions through the KRAB proteins and then recruits Setdb1 to establish the H3K9me3. Further H3K9me3 recruits HP1 to facilitate the nucleation of facultative heterochromatin and repress the gene expression (Schultz et al. 2003). However, H3K9me3 is not only used as a repressive marker in euchromatin. During the ES cell differentiation process, H3K9me3 which is assumed to be formed by Setdb1 in the upstream of mesendoderm genes can recruit the binding of Trim33 and displace HP1. Two nodal-induced Smad proteins cooperate to facilitate the activation of mesendoderm genes and initiate the mesendodermal cell commitment (Xi et al, 2011).

From in vivo and in vitro experiments, Sarraf showed that Mbd1 could bind Caf1 and Setdb1 with different domains, thus they suggested that these three proteins probably form a complex together (Sarraf et al. 2004). Co-IP experiments showed that Setdb1 and Mbd1 interacted with each other during all the cell cycle phases. Caf1 which functions in S phase could only be coimmunoprecipitated by the other two proteins at that time point. This experiment demonstrated that Caf-1/Mbd1/Setdb1 complex can only be formed during DNA replication and the H3K9me3 could be established by Setdb1 during the chromatin assembly before H3 and H4 dimers are loaded into DNA to form chromatin (Sarraf et al. 2004). Setdb1 is also involved in somatic cell reprogramming. Loss of Setdb1 affects the efficiency of reprogramming from somatic cells to iPS (Onder et al. 2012). Loss of Setdb1 also facilitates the reprogramming of the pre-iPSC which is an intermediated stage of iPSC into the iPSC through loss of H3K9me3 in the promoter regions of pluripotent factors (Chen et al. 2013).

1.4 Lineage decisions during early embryonic development

Differentiation and proliferation of the pluripotent cells during early embryonic development are extremely important for the normal growth of the animals. After fertilization, zygotes start to perform division and proliferation. Spatial and temporal regulation of specific gene expression and a diversity of signaling pathways are involved in these processes (Saiz et al. 2013). The first cell fate decision occurs in the morula stage and two different cell lineages, trophectoderm cell lineage and inner cell mass (ICM), are generated based on the distinct apical-basal polarity and transcription factor network (Takaoka et al. 2012). These two different cell types in the blastocyst show exclusive expression between the trophectodom cell lineage markers Cdx2 and the pluripotency-associated transcription factors Oct4 and Nanog. Before the cell fate decision occurred these markers are expressed randomly in the blastocyst, gradually the Cdx2 is restricted to the outside cells which becomes trophectoderm and Oct4 and Nanog are confined to the inner cell mass (Niwa et al. 2005).

The second wave of differentiation during early embryonic development happens in the ICM which can differentiate into epiblast and primitive endoderm, however the mechanism underlying this process is still elusive (Morris 2011; Yamanaka 2011). It coincides with a variety of cell behaviors and selective apoptosis (Plusa et al. 2008) and not only relies on the position of the cells (Chazaud et al. 2006). Considering the gene expression regulation related to this process, Gata6 and Nanog co-express in the ICM. During further development, Gata6 positive cells move out from ICM and are restricted to the primitive endoderm region. Nanog positive cells become mutual exclusive with Gata6 and only exist in the epiblast.

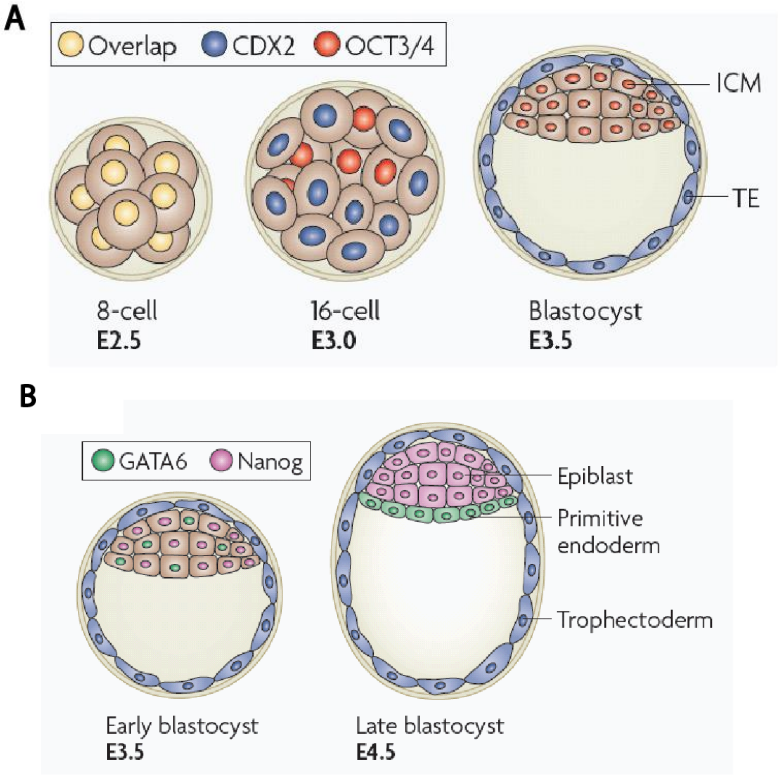

Figure 1.3 Lineage segregation in the blastocysts (Arnold et al. 2009). **A)** At E2.5, the overlapped expression of two transcription factors, Cdx2 and Oct4, in the blastomere. At E3.0, the expression of Cdx2 and Oct4 becomes exclusive. At blastocyst stage Oct4 positive cells localize in the inner cell mass and Cdx2 positive cells are restricted to the outside to form Trophectoderm. **B)** At early blastocyst stage, the transcription factors Nanog and Gata6 are randomly and exclusively expressed in the inner cell mass. At E4.5 the Gata6 positive cells move to the distal surface of the ICM to form primitive endoderm and Nanog positive cells give rise to the pluripotent epiblast.

The formation and correct placement of the primitive streak is an important step for the onset of gastrulation to form three different germ layers (Tam et al. 2007). The Nodal signaling pathway is important for the epiblast patterning and the correct placement of the primitive streak. Cer1 and Lefty1 which act as the antagonists of Nodal could regulate the activity of Nodal signaling and guarantee the correct movement of the primitive streak from the anterior to the posterior epiblast (Perea et al. 2002). Wnt3 signaling is also necessary for the primitive streak formation at the posterior epiblast and is considered to activate a feedback loop to maintain Nodal expression (Ben et al. 2006).These three germ layers, ectoderm, mesoderm and definitive endoderm, are formed from the epiblast through the primitive streak (Figure 1.4) (Sebastian et al. 2009). Mesoderm is formed by the ingression of the epiblast through the primitive streak to generate a new layer between epiblast and visceral endoderm. The endoderm germ layer is derived from the mesendoderm in the anterior primitive streak region. Mesendoderm can generate the precordial plate, the node, the notochord and the definitive endoderm (DE) cell lineages. The nascent DE cells move onto the outer surface of the embryo and disperse visceral endoderm cells. The formation of ectoderm does not need the migration of the epiblast though

the primitive streak. It is just derived from cells in the distal and anterior region of the epiblast and considered as the default state of epiblast differentiation (Camus et al. 2006). Mechanisms underlying these processes are rather complicated and genetic studies identified that several transcription factors cooperated with each other to pattern anterior-posterior polarity in the mouse embryo and orchestrate the three germ layers formation.

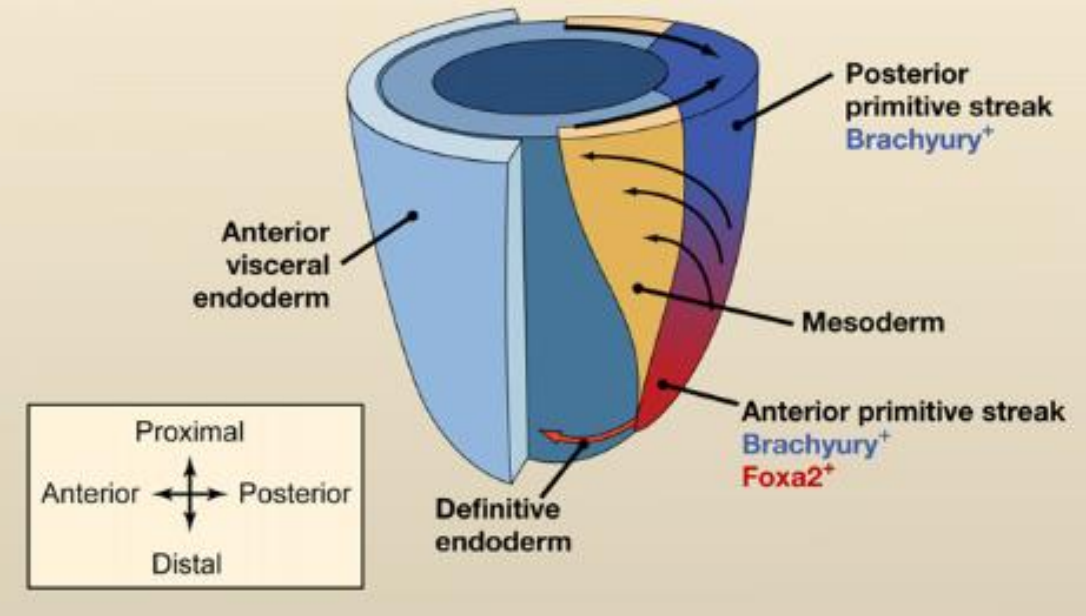

Figure 1.4 Mouse germ layer formation (Murry et al. 2008). Epiblast egresses from the primitive streak to form mesoderm and endoderm. Brachyury and Foxa2 are mesendoderm markers.

1.5 Wnt and Nodal signaling pathways regulate endoderm differentiation during early embryonic development

Cell fates could be specified through different signals during development. A number of signaling pathways, for example Wnt, TGF-beta, FGF and BMP4, have been identified. The interplay of several different signaling pathways could strictly regulate the development of tissue and organs.

During development, the Wnt signal plays very important roles for cell fate specification in proliferation, migration and cell death. So far at least three Wnt signaling pathways are identified containing the canonical Wnt/ beta-Catenin signaling pathway, the 'non-canonical' Wnt/Ca2+ pathway and the Wnt/PCP pathway (Cadigan et al. 2006). The canonical Wnt signaling pathway is well understood and is conserved in different species. In the absence of Wnt signal, Beta-catenin could interact with a destructive complex containing CK1Alpha (Casein Kinase-1-Alpha), GSK3Beta (Glycogen Synthase Kinase-3-Beta), AXIN (Axis Inhibitor) and the APC (Adenomatous Polyposis Coli) protein. This interaction will induce the phosphorylation of beta-Catenin and promote the interaction with beta-TRCP (Beta-Transducin Repeat-Containing Protein), a component of the E3 ubiquitin ligase complex, which results in the ubiquitination of beta-Catenin and degradation by the proteasome. In the presence of Wnt signaling, Frizzled which is the receptor of Wnt will activate the

Dishevelled protein which could enhance the phosphorylation of GSK3 Beta. The activation of Dishevelled protein could inhibit the ability of GSK3 Beta. Afterwards beta-Catenin will be set free from the Axin complex and accumulates in the cytoplasm in an unphosphorylated state. Due to the accumulation beta-Catenin is translocated into the nucleus. Without the induction of Wnt signaling, LEF (Lymphoid-Enhancing Factor) and TCF (T-Cell Factor) cooperate with Groucho and CTBP (COOH-terminal Binding Protein) to repress gene expression. In the presence of Wnt signaling binding of beta-Catenin to TCF/LEF converts the repressive activity of TCF/LEF into transcriptional activity which could activate the specific target genes. The regulatory mechanism is also related to structural changes in chromatin. It has been shown that the histone acetyltransferase CBP (CREB-Binding Protein) and the chromatin-remodeling complex SWI/SNF could interact with beta-Catenin to activate transcription (Klaus et al. 2008). The Wnt family consists of at least 16 members in the mouse which is secreted cysteine-rich glycoproteins. The Wnt signaling pathway is an essential molecular pathway for the differentiation of the primitive streak (Nakanishi et al. 2009). Deletion of Wnt3a impairs the development of the mesendoderm lineage and instead promotes neuralization (Yoshikawa et al. 1997). Ablation of beta-catenin in the definitive endoderm results in the lethality of early embryos and switches the cell fate from endoderm to precardiac mesoderm (Lickert et al. 2002).

The nodal signaling pathway is another important molecular pathway which is implicated in the specification of the primary body axis and the formation of mesoderm and endoderm (Whitman. 2001). Nodal pathway ligands belong to the transforming growth factor-beta (TGF-β) superfamily which could bind the type I and type II serine-threonine kinase receptors. The activation of the type I and type II serine-threonine kinase receptors phosphorylate Smad2 and/or Smad3 in the cytoplasm which then interact with Smad4 to form a complex which translocates into the nucleus. In the nucleus the formed complex could interact with co-activators and other transcription factors to regulate gene expression. Additionally, Lefty and Cer1 are considered as extracellular inhibitors of the nodal signaling pathway and impair the binding of nodal to the receptor. In the mouse, nodal is expressed in early embryogenesis before and during gastrulation. Nodal signaling is crucial for the early patterning. Before gastrulation nodal is expressed throughout the epiblast and is important for the formation of extraembryonic ectoderm and visceral endoderm. Later the expression of nodal is localized to the posterior part of the embryos and contributes to the formation of the primitive streak (Norris et al. 1999). Upon loss of nodal, the primitive streak cannot be formed and expression of mesendoderm genes is decreased. The migration of the extra-embryonic mesoderm from the posterior streak is dramatically reduced in nodal mutant embryos (Brennan et al. 2001).

During embryogenesis, the expression of the core pluripotency transcription factors will be shut down and the inner cell mass starts to differentiate into epiblast and visceral endoderm. They further form the outer and inner layers of the gastrula embryo. The trophectoderm gives rise to the extraembryonic part which generates supportive tissue for the future development of the embryo through providing

nutrients and oxygen. During development a subset of the epiblast ingresses into the primitive streak and generates mesendoderm which further differentiates into mesoderm and endoderm.

The manipulation of early embryos is relatively difficult as they are very small and it is difficult to get enough litters, especially it is hard to collect enough material to perform molecular analyses. The establishment of in vitro differentiation systems from stem cells towards multiple cell lineages allows studying the molecular mechanism regulating cell lineage induction and specification. In vitro differentiation of ES cells into different cell lineages provides a system to study the influence of different factors during early embryogenesis. There is a correspondence of the developmental pathway of the cells in vivo and in vitro. The factors which could influence the developmental processes between ES cells and embryos are also similar. Thus in vitro study for the molecular mechanism of the early embryonic development is an efficient replacement for the in vivo study. Importantly, in vitro differentiation can produce enough material to study molecular mechanisms. ES cells are pluripotent and possess the potential to differentiate into almost all cell lineages. Therefore a lot of work has been conducted to establish proper methods to induce the differentiation of pluripotent stem cells into specific cell lineages. The easiest and most common way to generate three germ layers in vitro is to use the embryo body formation which was established around 30 years ago (Doetschman et al. 2005). The EB could also form three different germ layers but the structure of the EB is far less organized than the actual embryos and it is still difficult to study single cell lineages. For better analysis of specific cell lineage differentiation, it is required to use a defined situation to obtain a high purity of cells. Even though a lot of effort has been made it is still difficult to generate all different cell types (Nishikawa et al. 2007). So far some defined culture conditions have been identified and to some extent the change of the transcription factors for the specific stages in vitro could reflect the in vivo situation. Culturing the ES cells in the conventional serum-free medium could produce neuroectodermal cells which express the specific neuroectodermal genes such as Sox1 (Ying et al. 2003). Treatment of the ES cells with the combination of activin A and retinoic acid lead to the differentiation of ES cells into the mesoderm cell lineage (Oeda et al. 2013). Definitive endoderm and visceral endoderm can be derived by the culture in serum free medium through the intermediate stage of mesendoderm with the induction of different concentrations of activin A (Yasunaga ei al. 2006) and Wnt3a (Nakanishi et al. 2009). With the deeper understanding of the embryonic development, more methods will be established for different cell lineages differentiation.

1.6 Epigenetic mechanism regulation is connected to ES cell pluripotency and cell lineage commitment

During development, gene expression patterns are strictly controlled. It is required that some critical genes are spatially and temporally expressed according to the defined conditions. Chromatin conformation is altered during the cell fate change from the pluripotent stem cell to specific cell lineages. In ES cells and inner cell mass, chromatin is largely open while during development the chromatin of differentiated cells becomes blocked and heterogeneous (Orkin et al. 2011). It is known

that the chromatin structure affects cell fate determination. A large number of chromatin modifiers are indicated to interact with pluripotency factors and developmental regulators. Loss of these genes leads to severe defects in ES cells pluripotency and cell lineage commitment.

The NuRD complex could interact with the core pluripotency transcription factors Oct4 and Nanog (Liang et al. 2008) and loss of MBD3 which is a component of NuRD impairs the pluripotent state of ES cells (Kaji et al.2006). This could be caused by the abnormal differentiation to the trophectoderm cell lineage (Zhu et al. 2009). Polycomb complexes gain a lot of attention for the involvement in diverse biological processes and PcG proteins are also related to ES cell differentiation. Deletion of PcG proteins leads to developmental defects and embryonic lethality in mice (Surface et al. 2010). PcG proteins bind to a large cohort of developmental regulators and repress the expression of these genes in ESCs (Boyer et al. 2006). It is also interesting how PcG-repressed cell-lineage genes maintain the potential for activation during development. These genes are in a bivalent configuration enriched with H3K27me3 and H3K4me3 and can easily switch on or off during differentiation. Moreover there is also evidence that PcG proteins could mediate Hox gene repression through changes in chromatin structure (Eskeland et al. 2010). Chromatin modifier, such as Swi/Snf complexes, can occupy core pluripotency factors and repress their expression through chromatin compaction (Schaniel et al. 2009). Oct4 directly regulates the expression of the epigenetic regulators Jmjd1a and Jmjd2c. Both of these genes regulate the expression of Tcl and Nanog, through the demethylation of H3K9me3 and H3K9me2 in the promoter region (Loh et al. 2007).

1.7 The Functions of Setdb1 during development

Setdb1 was shown to be important for early embryonic development as loss of Setdb1 in the mouse leads to lethality of the embryos in the peri-implantation stage and the Setdb1 deleted blastocyst cannot give rise to ES cells. Additionally, loss of Setdb1 cannot alter the global level of di and tri methylation of H3K9 rather than in specific loci (Dodge et al. 2004). There is a study showing that Setdb1 cooperates with Oct4 to confine the expression of Cdx2 to maintain the pluripotent state of embryonic stem cells (Yuan et al. 2009). From Chip-seq data we know that Oct4 is enriched in the gene body of trophectoderm specific cell lineage genes, such as Cdx2 and Tcfa2a. Through coIP experiments, Oct4 and Setdb1 were shown to bind to each other. Deletion of Oct4 leads to the reduced binding of Setdb1 to Cdx2 and Tcfa2a and the enrichment of H3K9me3 and H3K9me2 at these loci is reduced. The loss of Setdb1 also reduces the enrichment of H3K9me3 and H3K9me2 at Tcfa2a and Cdx2 loci however does not harm the binding the Oct4 to these loci. Taken together, these results show that Oct4 recruits Setdb1 to repress the expression of Tcfa2a and Cdx2 through H3K9me.

A RNAi screening assay also proved that the knock-down of the genes which are associated with H3K9 methylation, H3K27 methylation and acetylation can impair the pluripotency of the ES cells (Lohmann et al. 2010). Disruption of the expression of Setdb1 produces a similar effect as the loss of

Oct4 in influencing the ES cell state. Setdb1 Chip-seq analysis shows that Setdb1 occupies the core promoter regions of 2232 genes. Among them, 48% of these genes show active transcription and are also occupied by Pol II and active transcription markers. Only 52% of Setdb1 binding sites appear to be transcriptionally repressed. Interestingly most of the repressed genes are developmental genes. 38% of the repressed genes show co-localization of Setdb1 and PRC subunit Suz12 which is a repressive factor (Hansen et al. 2008). Setdb1 functions as a methyltransferase and is implicated in the repression through H3K9 methylation. H3K9me3 Chip-seq indicated that nearly all of the H3K9me3 occupied euchromatin genes are also co-localized by H3K4me. There are only 22% of the genes which are localized by H3K9me3 also bound by Setdb1. This could be caused by other methyltransferases and demethylation on some sites. Setdb1-bound genes which have the highest density of H3K9me3 are also co-occupied by H3K4me3 and H3K27me3. Loss of Setdb1 in ES cells results in the deregulation of some of these genes which are occupied by Setdb1 and enriched for H3K9me3, H3K27me3 and H3K4me3. Some of these derepressed genes are also overlapped with targets of polycomb repressed genes (Lohmann et al. 2010). From these results, we assume that Setdb1 is involved in the regulation of some developmental genes and probably cooperate with PcG proteins to regulate gene expression on specific genomic loci.

AIM OF THE THESIS

Epigenetics is connected with diverse biological processes. More and more researches show that epigenetic alterations results in severe diseases and developmental defects. The mechanisms underlying these processes remain unclear. During development, transcription programs which are mediated by different transcription factors are changing in order to generate different cell lineages. It is still elusive how these transcription factors target specific binding sites in the genome. Histone lysine methylation is a very important modification which could control gene expression (Kouzarides. 2007). Our lab is interested in mechanisms of transcriptional repression by the histone modifications H3K9me3 and H4K20me3. Thus it was very interesting for us to determine the functions of Setdb1, which is a pivotal methyltransferase for H3K9me3 in euchromatin, during development.

As loss of Setdb1 leads to early embryonic lethality at around E6.0, it is difficult to study the function of Setdb1 during development. So far there is little knowledge about the function of Setdb1 in different developmental processes. In order to study the spatial and temporal function of Setdb1, we used conditional Setdb1 knockout mice and induced the deletion of Setdb1 specifically in endoderm.

In this work I addressed the following questions:

What is the phenotype when Setdb1 is specifically deleted in the endoderm lineage?

Upon loss of Setdb1, embryos die at a very early embryonic stage and ES cells cannot maintain pluripotency, but we have no clue if Setdb1 is also involved in endoderm development and if the specific loss of Setdb1 in the endoderm cell lineage causes any developmental defects. First, we need to investigate the phenotype upon deletion of Setdb1 in the endoderm. Second, if the embryos show phenotypic defects, we will identify the exact structural changes of the mutant embryos during development.

The potential regulatory mechanism of Setdb1 for endoderm lineage commitment

We already know that Setdb1 could interact with a lot of regulatory factors and regulates gene expression in several different cell types and biological processes. But we do not know if Setdb1 interacts with specific factors to regulate gene expression during endoderm development. Detecting the interactors of Setdb1 in this spatial and temporal time point could better help us to figure out the function of Setdb1 during endoderm development. It is important to figure out the potential mechanism how Setdb1 regulates genes expression in endoderm and if Setdb1 target genes directly or indirectly influence embryonic development. It is also interesting to identify if Setdb1 is involved in specific signaling pathways which are important for endoderm development.

2. RESULTS

2.1 Establishment of Setdb1 conditional knockout mice

2.1.1 Genomic locus of Setdb1 and knockout strategy

Setdb1 has been proven as a H3K9 trimethylase and plays an essential role during mouse development. Deletion of Setdb1 results in the lethality of early embryos. In order to overcome this early lethality issue, we used Setdb1 conditional knockout mice which allowed us to study the function of Setdb1 in specific tissues and time points. The figure below (Figure 2.1 A) shows the schematic of the conditional Setdb1 knockout allele. Setdb1 exon 4 is flanked by loxP sites and could be cut off by the introduction of Cre recombinase. There is a beta-galactosidase (β-gal) insertion which is flanked by FRT sites before exon 4. β-gal could be removed by introduction of Flp recombinase. As β-gal is under the control of the endogenous promoter of Setdb1, the expression of β-gal reflects the endogenous expression of Setdb1. Removal of exon 4 from the Setdb1 flox allele leads to a frame shift mutation in Setdb1 and could only give rise to a severely truncated protein.

In order to obtain $Setdb1^{flox/flox}$ mice, we first crossed $Setdb1^{\beta\text{-}gal/+}$ mice with Flp mice which could generate a $Setdb1^{flox/+}$ mouse line by removing the β-gal insertion. Then, we intercrossed $Setdb1^{flox/+}$ mouse with $Setdb1^{flox/+}$ mouse to get $Setdb1^{flox/flox}$ homozygous mice. Using $Setdb1^{flox/flox}$ mice, we can excise exon 4 by introducing the Cre recombinase at different time points and in different organs.

A

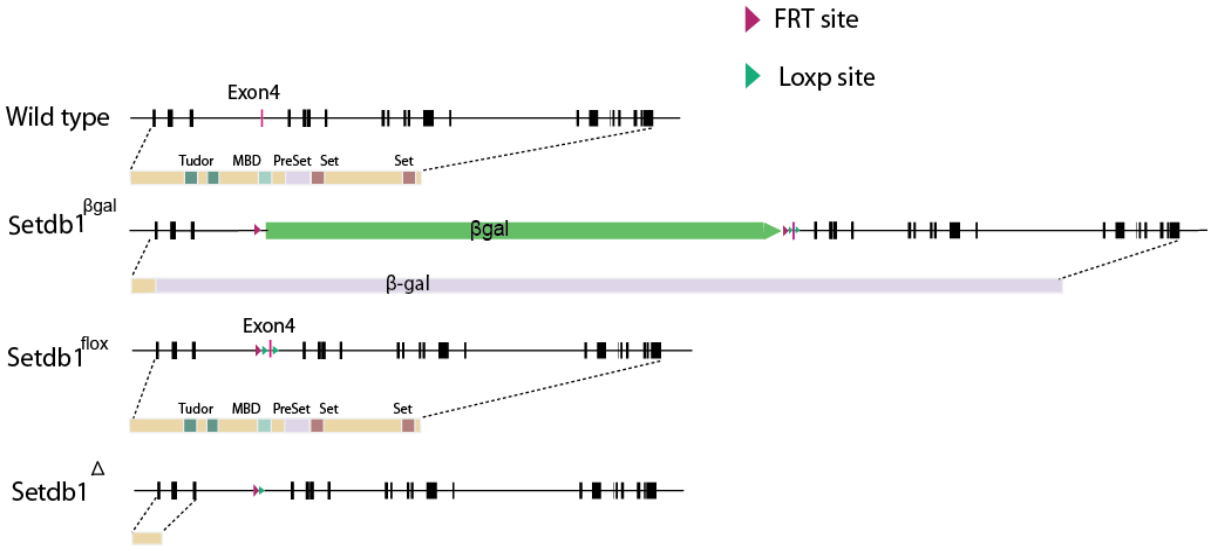

B

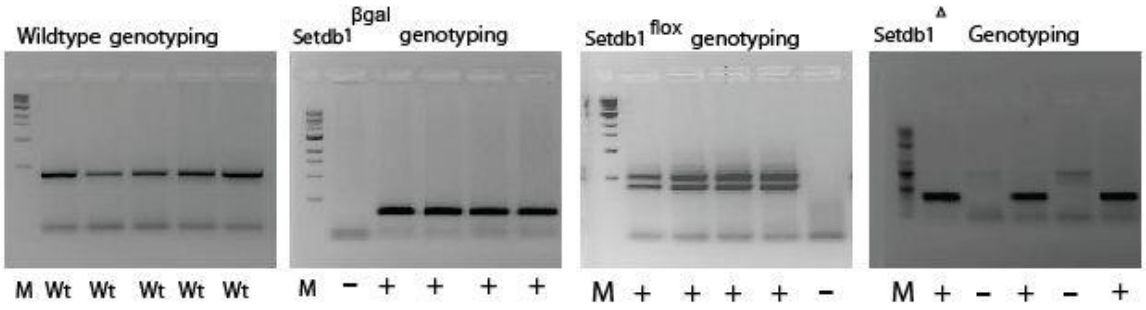

Figure 2.1 Schematic of Setdb1 knockout alleles and knockout strategy. A) Schematic of Setdb1 deletion strategy. The β-gal allele could be converted to a flox allele by introduction of Flp recombinase. Exon 4 could be excised by introduction of Cre recombinase. B) Gel pictures show genotyping results for individual Setdb1 alleles.

2.1.2 Generation of conditional Setdb1 knockout MEF and ES cell lines

Setdb1$^{flox/flox}$ MEFs and ES cells were obtained from Setdb1$^{flox/flox}$ mice. Exon 4 of Setdb1 can be deleted by the introduction of Cre recombinase. For the further analysis of the function of Setdb1, we deleted Setdb1 by infecting the Setdb1$^{flox/flox}$ MEFs with an adenovirus which expresses Cre-recombinase or control virus. Four days after infection, we tested the deletion rate of Setdb1 by PCR. A prominent PCR band detecting the deleted allele could be detected indicating efficient recombination of the loxP site (Figure 2.2).

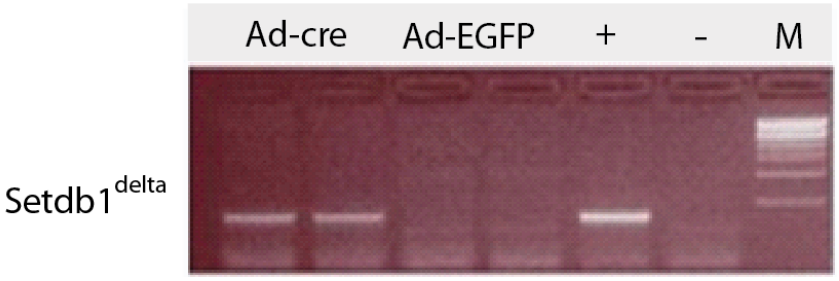

Figure 2.2 Deletion of Setdb1 with Cre-expressing adenovirus. Setdb1 delta band could be detected after the infection with adenovirus expressing Cre recombinase (Ad-Cre) but not with the control virus (Ad-GFP).

In order to get stable Setdb1 deficient cell lines, four days after virus infection single cells were selected. These cells were expanded and checked for deletion of Setdb1. The loss of Setdb1 was proven by PCR and western blot (Figure 2.3).

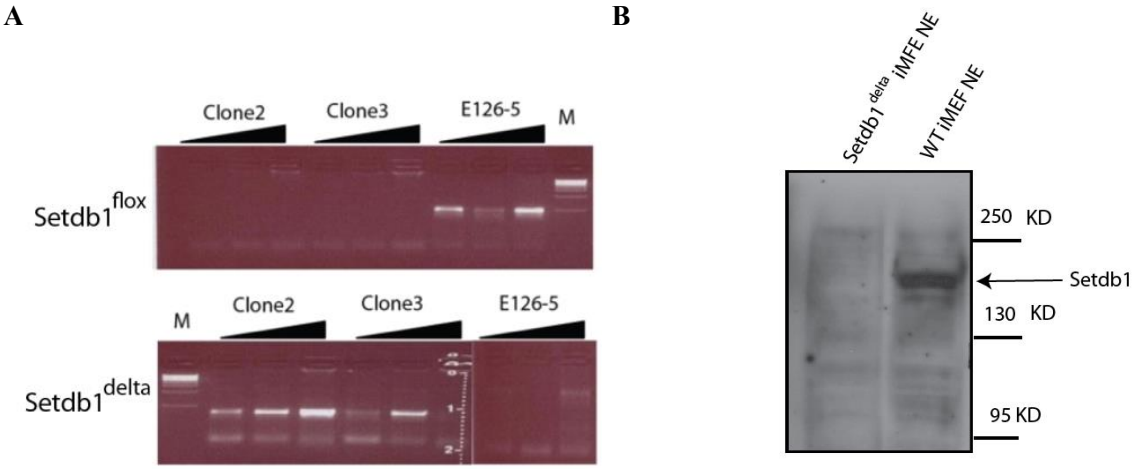

Figure 2.3 Setdb1 deletion in single cell clones. A) Loss of exon 4 of Setdb1 in independent knock-out clones. In the single cell clones, clone2 and clone3, no flox band could be detected but the flox band could be detected in the parental cell line (E126-5). The delta band is clearly detectable in the mutant clones but not in the parental cell line. **B)** Setdb1 protein is lost in Setdb1^{delta} iMEFs (clone2). Nuclear extract was isolated from mutant and wild type cell lines. As the commercial Setdb1 antibody is not promising for western blot (showing two bands), we used Setdb1 antibody which was generated by ourselves. The Setdb1 band is absent in the lane of Setdb1^{delta} iMEFs nuclear extract.

After generating Setdb1 deleted MEFs, we wanted to test if loss of Setdb1 leads to changes in the expression of genes which are controlled by this epigenetic regulatory mechanism. Imprinted genes are good candidates as it has been shown before that imprinting control region (ICR) present in the imprinted gene clusters are occupied by DNA methylation and H3K9me3. Changes in these modifications affect the expression of imprinted genes (Koerner et al. 2009). We checked two well-studied imprinted genes Igf2 and H19 in Setdb1 mutant MEFs. We found both of these genes are down-regulated (Figure 2.4).

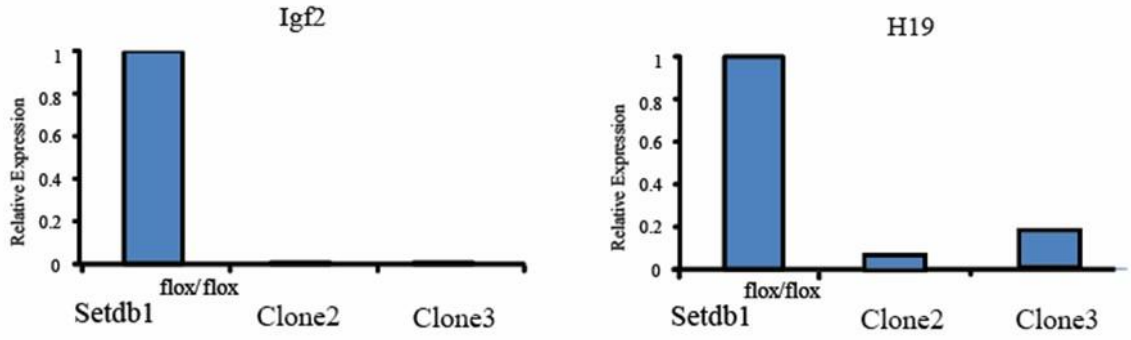

Figure 2.4 Loss of Setdb1 affects the expression of imprinted genes. Imprinted genes are tested in the parental cell line and two Setdb1 mutant cell clones (Clone2 and clone3). Igf2 and H19 are both down-regulated.

This result revealed that Setdb1 is important for the regulation of imprinted genes. In order to control the deletion of Setdb1 in cells more precisely, we infected Setdb1$^{flox/flox}$ pMEFs (E163-3) with inducible Cre recombinase virus. The stable transfected Cre recombinase is fused to a mutated

hormone binding domain of the estrogen receptor. Without stimulus of tamoxifen (4OHT), estrogen receptor fused to Cre recombinase is confined to the cytoplasm. However, addition of 4OHT will translocate Cre-ER recombinase into nuclei to excise loxP flanked target genes (Hirrlinger et al. 2009). The expression of imprinted genes was tested at day0 (without induction), day3, day5 and day7 after the induction of 4OHT in the Setdb1$^{flox/flox}$ pMEFs. At day3 after transfection, Setdb1 was lost and the expression of the imprinted genes Igf2 and H19 was reduced by half. These two genes were more strongly reduced at day5 and day7 after deletion of Setdb1 (Figure 2.5).

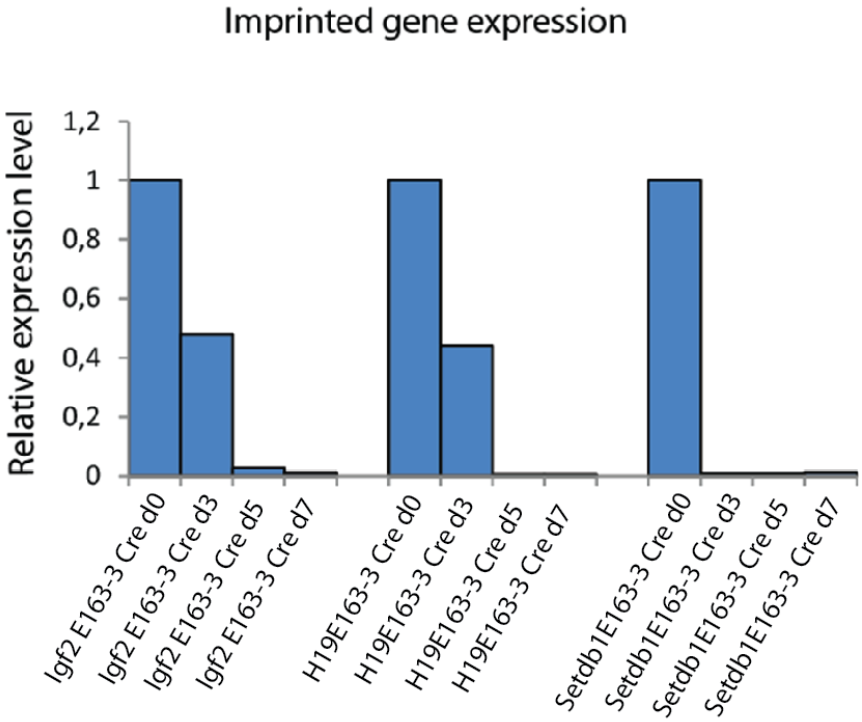

Figure 2.5 Imprinted genes Igf2 and H19 are reduced upon deletion of Setdb1 in the primary MEFs. The expression level of Igf2, H19 and Setdb1 in Cre transfected Setdb1$^{flox/flox}$ pMEFs (E163-3Cre) is tested upon deletion of Setdb1 at different days with 4OHT induction.

As was already shown, the deletion of Setdb1 in ES cells results in the differentiation of pluripotent ES cells into trophectoderm cell lineage (Yuan et al. 2009). In order to control the deletion of Setdb1 in ES cells, we infected Setdb1$^{flox/flox}$ ES cells (B32-3) with inducible Cre recombinase virus. The deletion rate of the inducible Cre in ES cells is efficient. We can see after 2 days induction with 4OHT, nearly 70% of Setdb1 is deleted in the genome and the RNA level is clearly reduced. At day 4 the deletion rate of Setdb1 reached 90% (Figure 2.6). According to this result, these inducible Cre construct transfected cells could be used to induce the deletion of Setdb1 in a simple way.

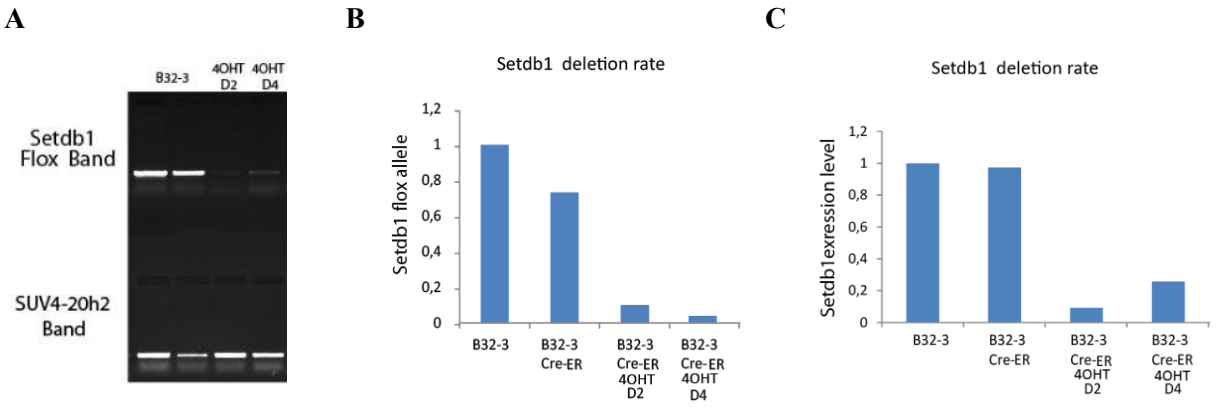

Figure 2.6 Deletion rate of Setdb1 in ES cells with inducible Cre. A) PCR for Setdb1 flox and delta allele. Strong band can be detected in Setdb1$^{flox/flox}$ ES cells (B32-3). Very weak Setdb1 flox band can be detected after day 2 and day 4 of 4 OHT induction. The Suv4-20h2 band acts as a control. **B)** qPCR analysis for the deletion of Setdb1 in the genomic level in Cre transfected Setdb1$^{flox/flox}$ ES cells (B32-3) after day 2 and day 4 with 4OHT induction. **C)** Quantification of Setdb1 transcripts in Cre transfected Setdb1$^{flox/flox}$ ES cells (B32-3) after day 2 and day 4 with 4OHT induction.

To check the spatial and temporal function of Setdb1 during mouse endoderm development, Setdb1 should be specifically deleted in endoderm lineage cells. We crossed Setdb1$^{flox/flox}$ mouse line with a Sox17-Cre mouse line. Sox17 is an endoderm lineage marker and is mainly activated in visceral and definitive endoderm (Kanai et al. 2002). Cre recombinase is under the control of the Sox17 promoter which means the Cre recombinase is only expressed in cells which initiate the expression of Sox17. When the Setdb1$^{flox/flox}$ mouse line is crossed with the Sox17-Cre mouse line, we get a Setdb1 mutant line with specific deletion in endoderm cells (Setdb1^{END}). In Setdb1^{END} mutant embryos, deletion of Setdb1 mainly happens in gastrulation stage corresponding to the expression of Sox17, thus we were able to obtain Setdb1^{END} ES cells.

Even though we got Setdb1$^{flox/flox}$; Sox17-cre mutant ES cells (Setdb1^{END}), it would be difficult to test the deletion rate of Setdb1 and differentiation efficiency cannot be guaranteed. Another drawback is that it would be difficult to get a pure endoderm cell population by in vitro differentiation as there is no proper endoderm surface marker for sorting. Thus we introduced the EGFP Cre-reporter which could be used for monitoring the differentiation and for sorting the differentiated cells for further analyses. The EGFP signal is activated by the Cre-mediated excision of a translation stop signal between CAG promoter and EGFP. Sorting for EGFP expression thus results in a pure endoderm cell population that has activated Sox17.

Our strategy was to cross Setdb1$^{flox/flox}$; Sox17-Cre mouse with the EGFP-reporter mouse line (Kawamoto et al. 2000). The following genotypes containing Setdb1$^{flox/flox}$, Sox17-Cre; EGFP-reporter as mutant mouse (Setdb1 EGFP mutant) and Setdb1$^{flox/+}$; Sox17-cre; GFP-reporter (Setdb1 EGFP control) as control mouse. We assume that deletion of exon 4 occurs in the same cells as activation of

the EGFP reporter (Figure 2.7). Using this system, we can thus perform in vitro and in vivo experiments to trace Setdb1 deleted cells and it is easy to sort differentiated cells for further analysis.

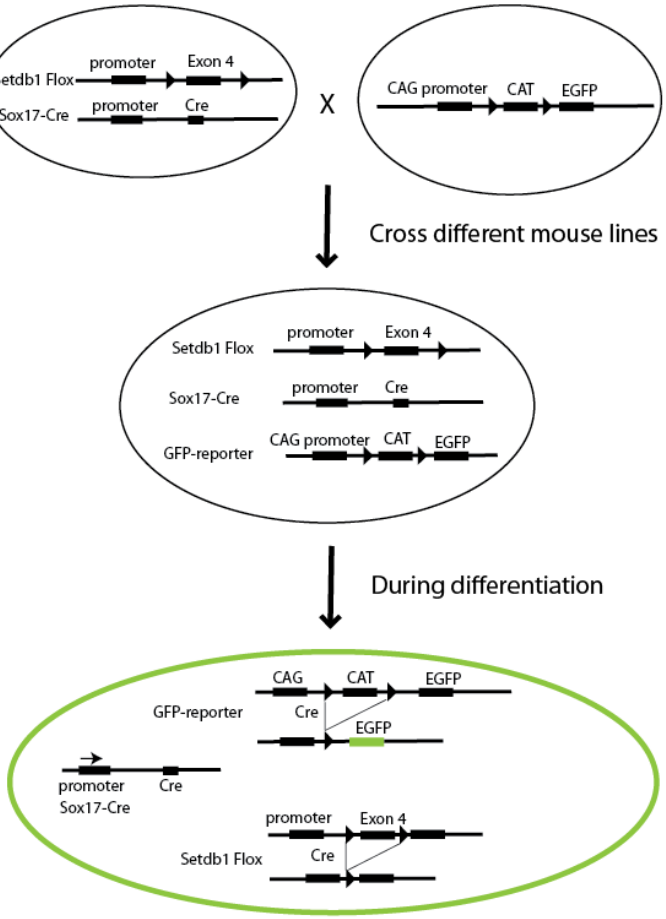

Figure 2.7 Schematic for obtaining the Setdb1 EGFP-reporter mouse line and Cre-mediated activation of EGFP during endoderm differentiation

In this strategy, we first needed to check if EGFP can be activated and if this activation is based on the expression of Sox17 in vivo. We performed a staining of Sox17 and EGFP in Setdb1 EGFP control embryos and embryos without Sox17-Cre (Figure 2.8). In the Sox17-Cre negative embryos, there is no EGFP staining meaning no EGFP leakiness happened in the embryos. For the embryos containing Sox17-Cre, we can see an overlap between Sox17 and EGFP staining. All of these EGFP positive cells are restricted to the endoderm region. The overlap of these two different staining indicates that the expression of EGFP is activated by the expression of Sox17.

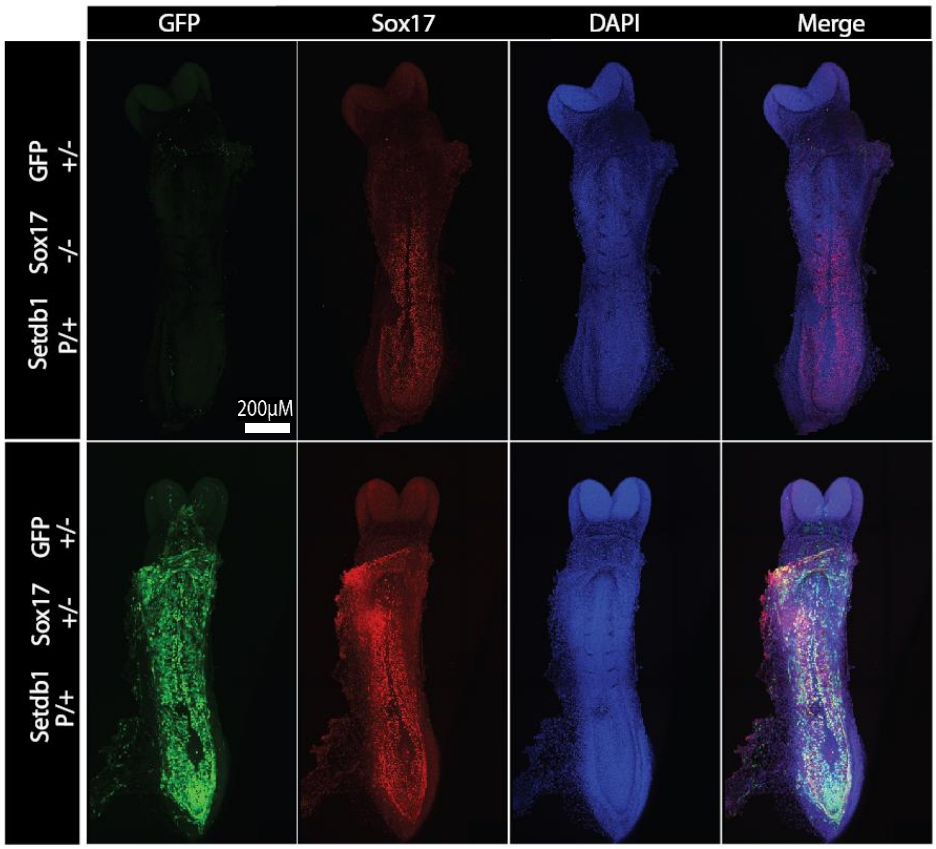

Figure 2.8 EGFP signal is activated by Sox17-Cre upon differentiation. In the Sox17-Cre negative embryos, there is no EGFP staining and Sox17 is restricted to the endoderm region. In the Sox17-Cre embryos (EGFP control embryos) Sox17 is expressed in the endoderm region and the EGFP staining is activated and overlapped with Sox17.

Based on the in vivo experiment, the EGFP reporter can be activated during development. We now used this system to derive Setdb1 EGFP control and mutant ES cells. Notably, our isolated Setdb1 EGFP ES cells cultured under standard ES cell conditions could show EGFP signals. This could be due to the transient expression of Sox17 in the blastocysts or spontaneous expression of Sox17 in ES cells which would lead to the permanent activation of EGFP reporter. Closer inspection revealed EGFP positive colonies during the first passages of the freshly isolated ES cells (Figure 2.9). That is probably due to the fact that in blastocyst stage embryos inner cell mass cells can randomly express Sox17 which is normally shut down during later development, however the EGFP reporter cannot be switched off even Sox17 expression ceases. In order to eliminate the EGFP positive ES cells we picked single colonies which were EGFP negative and expanded these colonies for further analyses. Upon in vitro endoderm differentiation, EGFP can only be activated in the Sox17 expressed endoderm cells.

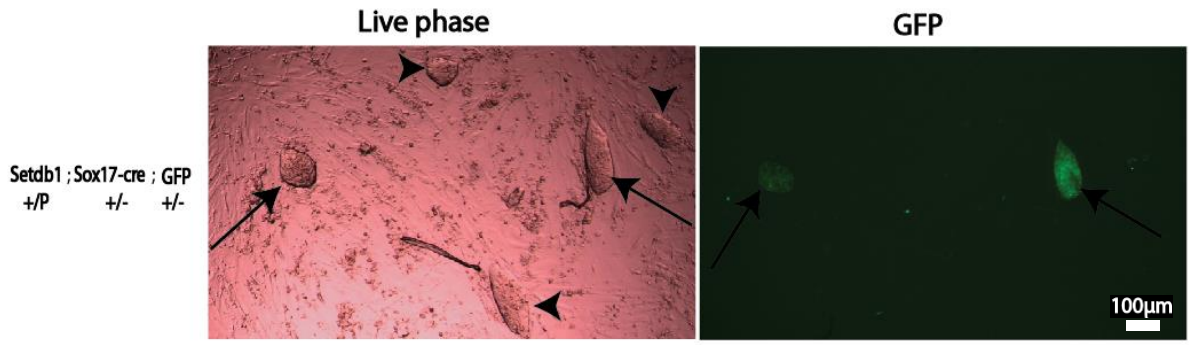

Figure 2.9 EGFP signal can be activated in the first passage of the isolated ES cells. We split the outgrowth of the inner cell mass from the blastocyst (EGFP control embryos) to get ES cell colonies. There are colonies showing EGFP signals. Arrows show the colonies with EGFP signal. Arrowheads point to the colonies without EGFP. We picked up and expanded the EGFP-negative cell colonies for further analyses.

2.1.3 Generation of Setdb1 knock-in cell lines

Setdb1 acts as a histone methyltransferase and does not contain a DNA binding domain. In order to understand targeting pathways, we wanted to screen for Setdb1 interaction partners. Some proteins were already identified to interact with Setdb1 in different cell types and biological processes (Fritsch et al. 2010; Wang et al, 2003). However, the interactors of Setdb1 in ES cells and endoderm cells are not clear. As the available Setdb1 antibodies in our hand were not applicable for IP experiments, in order to further figure out how Setdb1 performs its function in ES cells and during developmental processes we generated Setdb1 knock-in cell lines with a HA-3xFlag tag. The knock-in ES cell line was established by homologous recombination of HA-3xFlag tagged Setdb1 into the endogenous Setdb1 locus. This affinity-tag is fused to the C-terminus of Setdb1 and replaces the stop codon. There is a FRT-flanked neomycin cassette following the affinity-tag which could be used to carry out the neomycin selection (Figure 2.10 A). The insertion of the affinity tag was confirmed by PCR amplification in the knock-in specific regions and FLAG western blot (Figure 2.10 B). We could then use this Setdb1 knock-in cell line to perform pull down assays to identify interaction partners of Setdb1 at the endogenous expression level in ES cells and during differentiation.

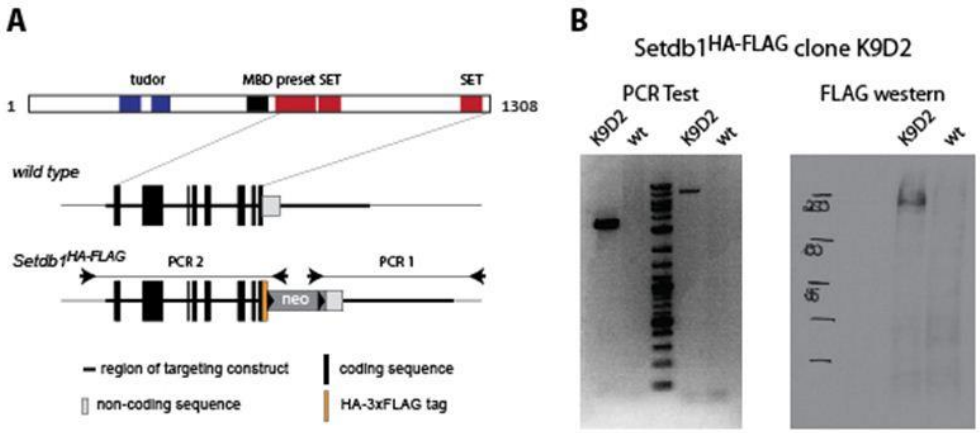

Figure 2.10 Generation of Setdb1 HA-3xFLAG knock-in ES cells. A) Targeting strategy for Setdb1 HA-3xFLAG ES cells. The HA-3xFLAG double tag replaces the STOP codon of Setdb1 and is followed by a FRT-flanked neomycin resistance gene which is used for positive selection. **B)** Successful homologous recombination in clone K9D2 was confirmed by PCR amplification of knock-in specific regions. Flag western blot of control vs. knock-in cells proofed expression of HA-3xFLAG-tagged Setdb1.

After the generation of the Setdb1 knock-in cell line, we performed pull-down experiments to identify the interaction partners of Setdb1 by using the 3xFLAG tag. First we optimized the condition for the Setdb1 pull down experiment. We tried to extract Setdb1 with different salt concentration. The biggest amount of soluble Setdb1 protein could be extracted with 300mM salt in comparison to the 150mM salt extraction with or without sonication (Figure 2.11A). Overnight incubation of the protein extract with the beads resulted in the binding of unspecific proteins. For example Kap1 can bind to the agarose beads in the wild type ES cell extract after overnight incubation but cannot bind to the beads after 2 hours of incubation (Figure2.11 B and C). In order to avoid the unspecific binding proteins, we decided to use mild binding conditions: 300mM salt extraction and 2 hour binding at 4 degree Celsius. Using this condition, Setdb1 can be highly enriched and only the strong interaction partners can bind to the beads (Figure 2.11 D and E). We eluted the binding proteins from beads and performed mass-spec analysis which could identify the strong and direct interactors of Setdb1.

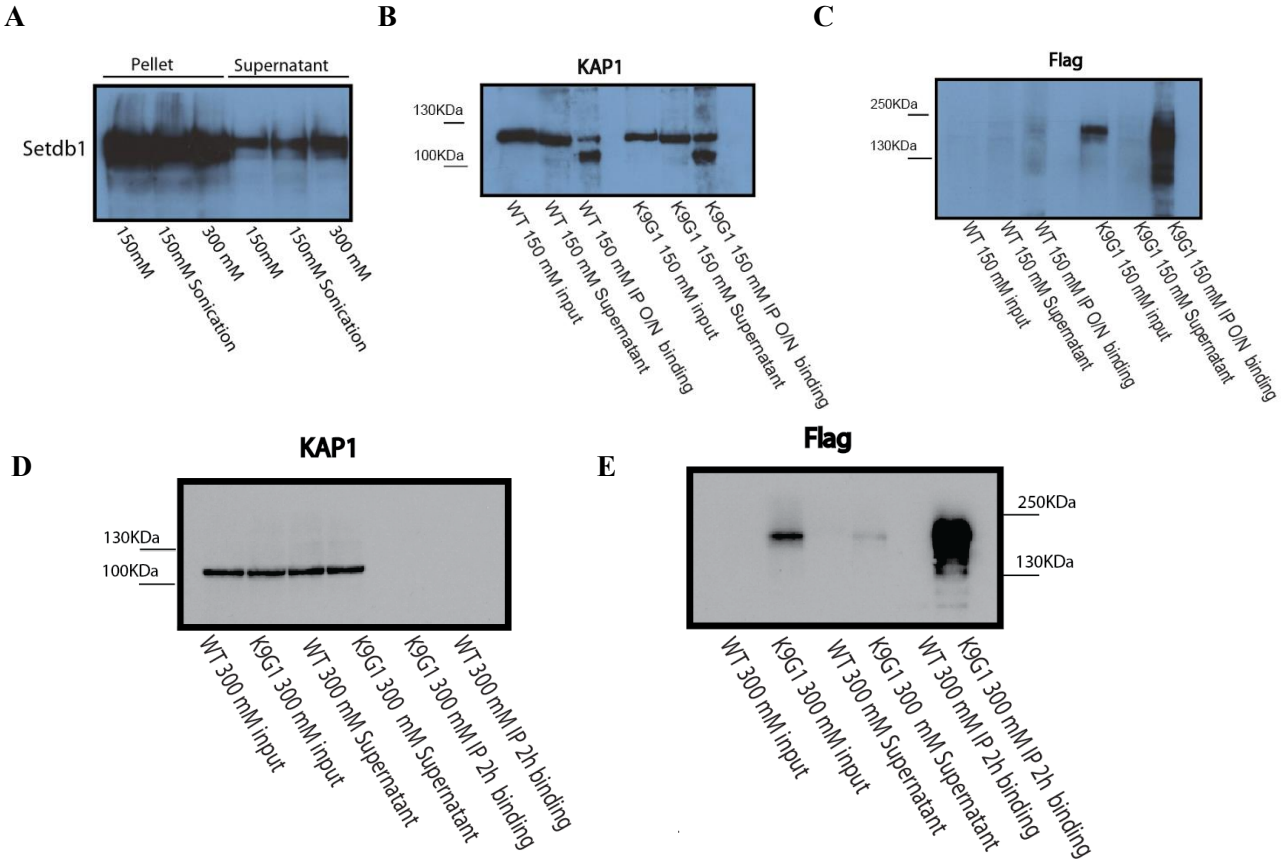

Figure 2.11 Optimization Setdb1 IP experiments. A) Extraction of Setdb1 from nuclei using different salt concentrations. 300mM salt without sonication could extract the highest amount of soluble Setdb1. **B)**

Unspecific binding of KAP1 to the FLAG beads. KAP1 could bind to the FLAG beads after o/n incubation with beads and nuclear extract of wild type ES cells. **C)** FLAG western blot proved the binding of Flag-tagged Setdb1 to the beads. **D)** No KAP1 binds to the beads and FLAG-tagged Setdb1 after 2 hours incubation. **E)** Setdb1 could be highly enriched with the beads after 2 hours incubation.

After the pull-down experiment, we run the eluted samples in an SDS-PAGE gel and cut each lane into 8 pieces. Through tryptic digestion, the proteins were cleaved into peptides and subjected to LC/MS/MS analysis. We performed two replicate experiments. In the first replicate, we could identify 147 proteins enriched by Setdb1. 191 proteins were identified as potential interactors of Setdb1 in the second replicate. When we compared the two datasets, we could find 110 proteins to overlap in the two replicates (Figure 2.12). By analyzing these data we found some binding proteins of Setdb1 in our list that had been previously reported to interact with Setdb1. For example, the interaction of Setdb1 and Atf7ip, Dnmt1, Glp1 and Trim28 has been found in different cells and biological processes (Fritsch et al. 2010). Atf7ip is the most enriched protein in our list. Atf7ip is a co-transcription factor which could interact with several different factors to regulate transcription and was found to form a complex with Setdb1 to facilitate the conversion of di-methylation to tri-methylation in HeLa cells. The pull down experiment proved the interaction of Setdb1 with Atf7ip in ES cells. Setdb1 plays an essential role for gene regulation in ES cells, however the mechanisms underlying its regulation are still elusive. Our finding that Atf7ip interacts with Setdb1 in ES cells suggests important function for Atf7ip in targeting Setdb1 to specific DNA regions or in regulating its activity.

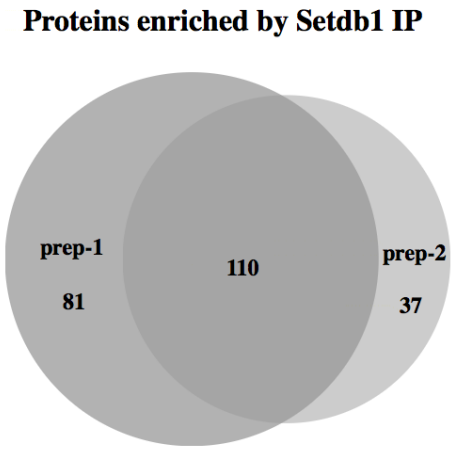

2.12 110 proteins were enriched with Setdb1 in 2 replicates of Setdb1-FLAG IP.

2.2 Phenotypic defects of mutant embryos upon deletion of Setdb1 in endoderm

2.2.1 Expression profile of Setdb1 during mouse development

In order to detect the expression of Setdb1 during early developmental stages of the embryos, we performed β-gal staining in Setdb1$^{\beta Gal}$ embryos and adult tissues. Because the β-gal gene is inserted before exon 4 and driven by the endogenous promoter of Setdb1, the expression of β-gal reflects the expression of Setdb1. First we isolated Setdb1$^{\beta gal}$ embryos at E7.5, E8.5 and E9.5. The β-gal staining was detected all over the embryos from E7.5 to E9.5 demonstrating that Setdb1 is expressed in the whole embryo during early embryonic development (Figure 2.13 A). We also performed cryostat sections to check the expression of Setdb1 in different adult organs. Brain and testis show the strongest expression of β-gal. Some of these organs are derived from the endoderm cell lineage, for example liver, spleen and pancreas (Figure 2.13 B). The expression of Setdb1 during different development stages suggests an important function of Setdb1 during early embryonic development and endoderm development in the later stages.

A

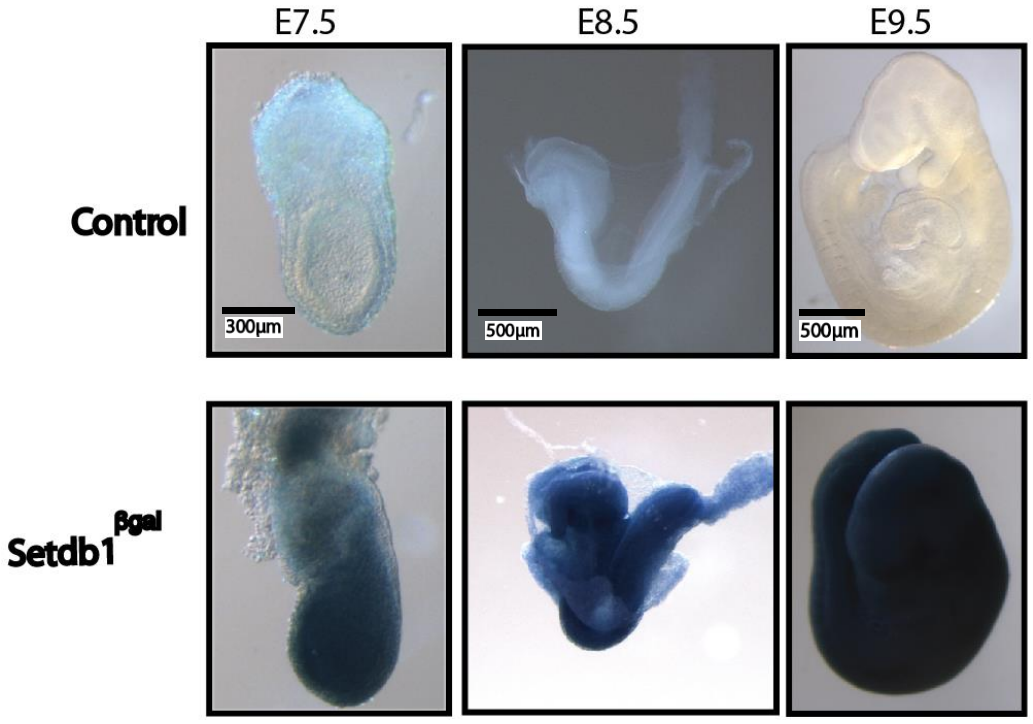

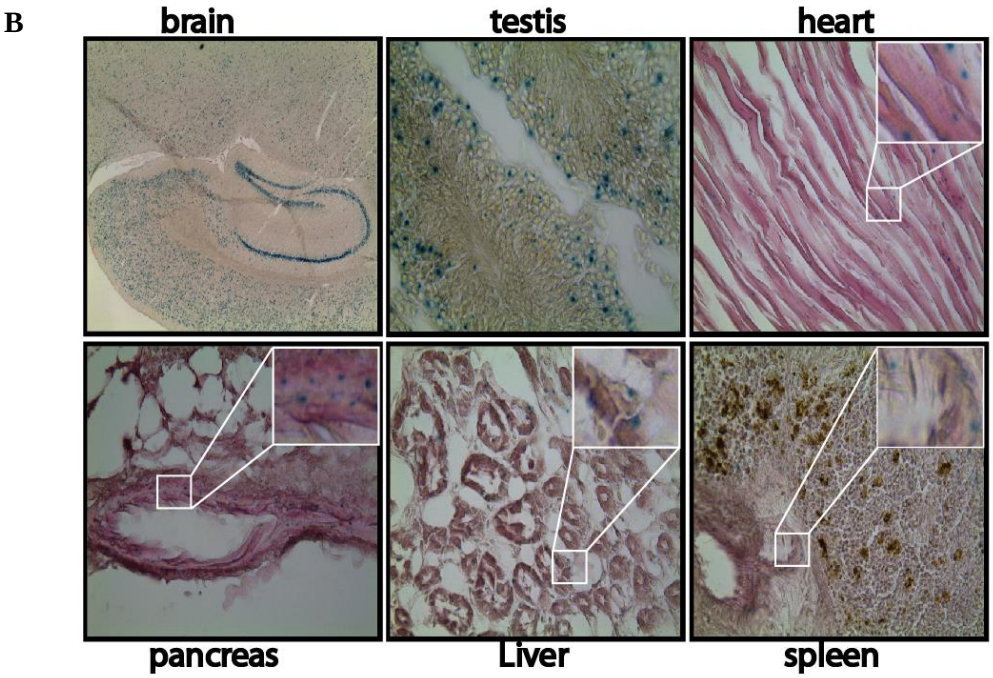

Figure 2.13 Setdb1 is expressed in early embryos and in different adult organs. A) From E7.5 to E9.5 the whole Setdb1$^{\beta\text{-gal}}$ embryos show the staining of β-gal. **B)** β-gal is expressed in different adult organs.

2.2.2 Early lethality of mouse embryos upon deletion of Setdb1 in endoderm

In order to investigate the functions of Setdb1 in the endoderm cell lineage, the Setdb1$^{flox/flox}$; Sox17-cre mutant mouse line (Setdb1^{END}) was generated. Early embryos at different stages from E7.5 to E9.5 were collected for phenotypic analysis. We found that the mutant embryos started to show a visible defect at E8.25. We could identify two different kinds of phenotypes (Figure 2.14). We call them type1 and type2 mutant phenotype. The type1 mutant embryos have nearly the same size as the WT embryos until E9.5. In general the embryos start to carry out the axis rotation at E8.5, but the type1 mutant embryos show a clear turning problem. At E9.5 the type1 mutant embryos cannot rotate and the posterior part of these embryos is strongly retarded. The other parts of the type1 mutant embryos are comparable to the control embryos. In comparison with type1 mutant embryos, type2 mutants show severe developmental defects. The type2 mutant embryos are smaller than the control embryos from E8.25 and also show the turning defect at E8.5. At E9.5, the type2 mutant embryos show severe growth retardation. Not only the posterior part but also the anterior part of the mutant embryos shows severe developmental defects.

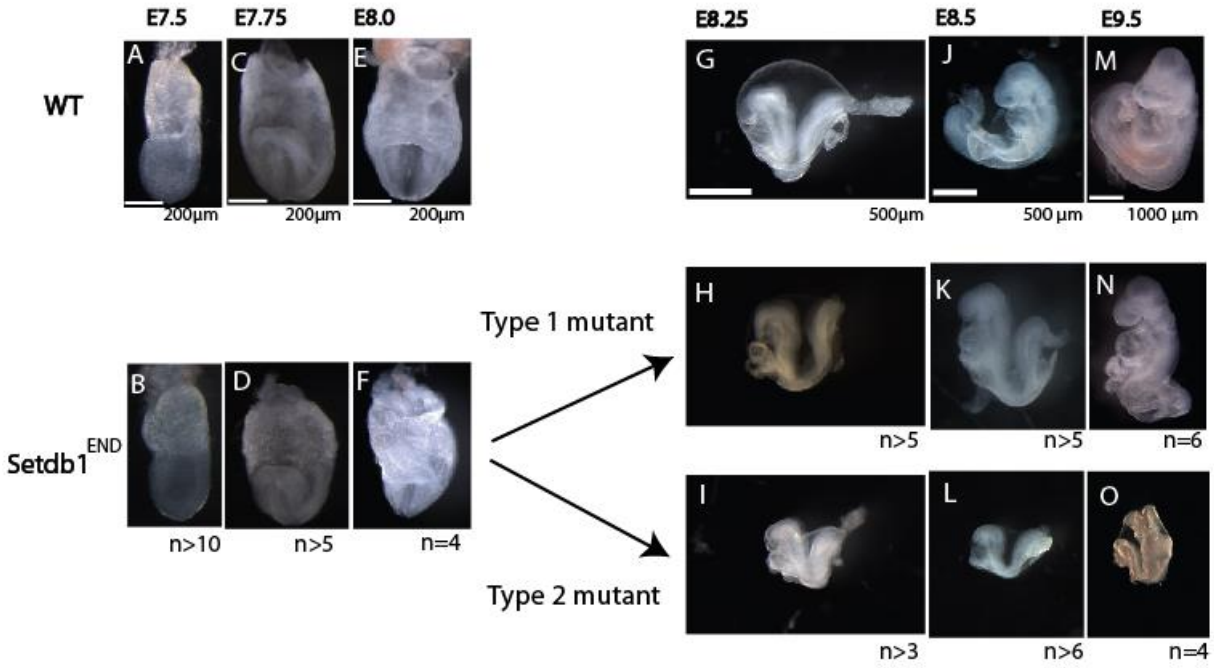

Figure 2.14 Development defects of the early embryos upon deletion of Setdb1 in the Sox17 lineage. From E7.5 to E8.0, the mutant embryos (Setdb1^{END}) are comparable to control embryos and did not show clear defects **(A, B, C, D, E and F).** At E8.25 mutant embryos start to show mild defects compared to control embryos **(G, H and I).** At E8.5 the control embryos perform axis rotation **(J)** but type1 mutant embryos **(K)** and type2 mutant embryos cannot rotate **(L)**. At E9.5 the type1 mutant embryos **(N)** have almost the same size as the control embryos **(M)** but the posterior part of the mutant embryos is smaller and cannot rotate. The type2 mutant embryos at E9.5 **(O)** show strong overall defects and a turning problem.

2.2.3 Sox17-mediated deletion of Setdb1 leads to two different phenotypes

As described before, we generated Setdb1 EGFP reporter mice and the EGFP reporter gene could help us to trace Sox17 lineage cells. By analyzing the expression of EGFP in the embryos, we found that not all of the EGFP staining was confined to the endoderm region and also a few embryos showed EGFP staining in other regions of the embryo. This EGFP expression pattern could be detected both in mutant and control embryos. Activation of EGFP reporter and deletion of Setdb1 is due to the expression of Sox17. So far, the fate of the Sox17 expressing cells in the morula is still elusive. Because in late stage blastocysts Sox17 is restricted to primitive endoderm, it is unclear that if these early Sox17 expressing cells in the morula are maintained in the blastocyst to contribute to the formation of other organs during development. Interestingly, the mutant embryos which show the overall EGFP staining in our experiment are severely retarded (Figure 2.15). This finding corresponded to our observation that there are two different kinds of phenotypic defects in Setdb1^{END} mutants (Figure 2.14). We assumed that the type1 mutant embryos are generated by the specific deletion of Setdb1 in the endoderm during development. In contrast, type2 mutant embryos are generated by an overall deletion of Setdb1.

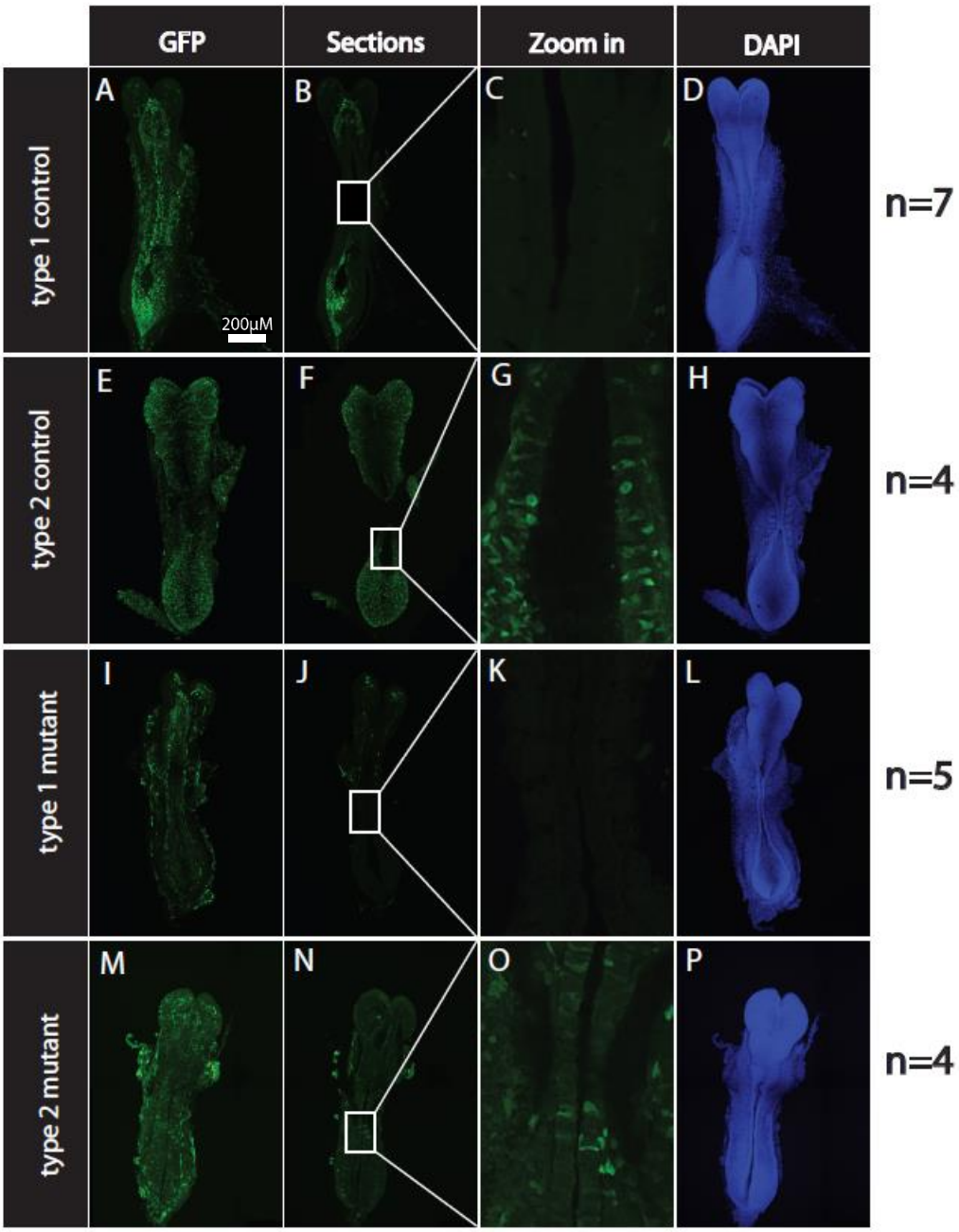

Figure 2.15 Two different EGFP expression patterns in control and mutant embryos. In type1 embryos the GFP signal is restricted to the endoderm region of the epiblast derivatives (**A, B, C** and **D** represent control embryos; **I, J, K** and **L** represent mutant embryos). There is no EGFP staining in the neural tube (**C** and **K**) in type1 embryos. The whole embryos show EGFP staining in type2 embryos (**E, F, G** and **H** represent control embryos; **M, N, O** and **P** represent mutant embryos). The EGFP signal can be detected in the neural tube of the type2 embryos (**G** and **O**).

2.2.4 Structural changes in the hindgut region in Setdb1^{END} mutant embryos

The Setdb1^{END} embryos show a clear developmental defect. Next, we wanted to specify marker changes by in situ experiments. In these experiments we focused on the function of Setdb1 in the definitive endoderm cells and only analyzed type1 mutant embryos which show the specific deletion

of Setdb1 in endoderm cells. We use different probes for Pyy, Trh, Nepn and Sox17 to detect these key markers of different embryonic regions. Pyy is a foregut region marker which is expressed in the foregut invagination. Trh is mainly expressed in neural tissues at roughly E9.0 (McKnight et al. 2007). Nepn is a midgut region marker and could only be recognized at the open region of the gut tube at the E8.5 embryos. Sox17 could be recognized in the hindgut region which is the closed region of the gut tub as well as in hemangioblasts and visceral endoderm (McKnight et al. 2010).

Comparing the Setdb1^{END} (mutant) and wild type embryos with these different probes (Figure 2.16), the expression of Pyy, Sox17, Trh does not show a clear difference between mutant and wild type embryos. As Sox17 is also expressed in the visceral endoderm, it is hard to judge the precise expression of Sox17 in definitive endoderm. According to Pyy, Trh and Nepn expression in the embryos we could judge that the development of the gut region and neural tube in the mutant embryos is not affected. The expression of these three markers is the same among mutant and control embryos. Thus deletion of Setdb1 in definitive endoderm does not affect the formation of the gut region.

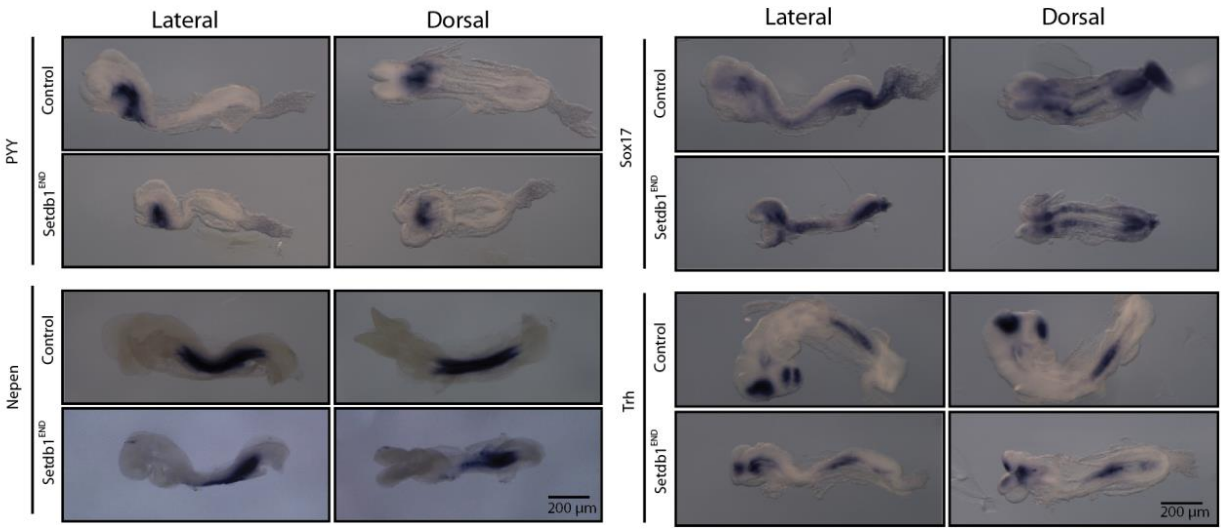

Figure 2.16 No difference in gut region and neural tissue marker expression between control and Setdb1^{END} (mutant) embryos at E8.5 by in situ hybridization. Pictures are taken from the lateral and dorsal side of the embryos. There is no difference that could be detected using these four different in situ markers.

Based on the expression of these markers, there is no difference in gut tube formation between control and mutant embryos. Further, we intended to identify any structural alterations of the gut region in mutant embryos. We collected mutant and control embryos from different developmental stages at E8.0, E8.5 and E9.5. These embryos were embedded in paraffin and used to generate sections of different layers of these embryos to identify structural changes. The structure of the mutant and control embryos at E8.0 is almost the same and the shape and the position of the endoderm cells is also very similar (Figure 2.17). These analyses revealed that endoderm could be properly formed in the mutant embryos at E8.0.

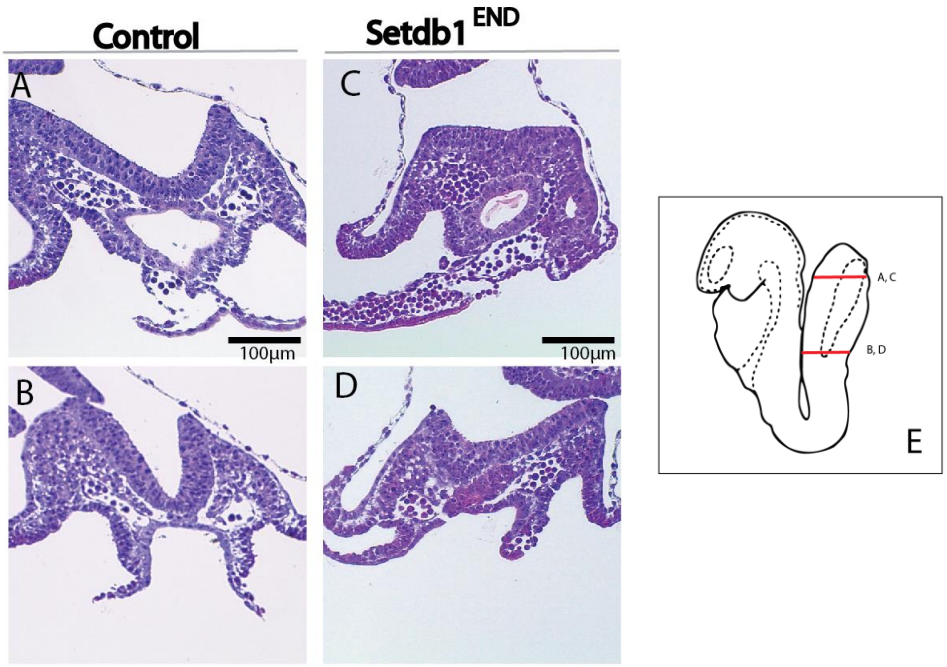

Figure 2.17 No structural change of the hindgut region upon deletion of Setdb1 at E8.0. A, B, C and D) H&E staining of paraffin sections of control and Setdb1^{END} (mutant) embryos at E8.0. E) The schematic of the position of the sections shown in A-D.

We chose another critical time point at which the mutant embryos show the axis turning problem at around E8.5. During mouse development, the hindgut diverticulum initiates to be closed from the hindgut region to the foregut region. We could see the hindgut diverticulum is already closed in both control and mutant embryos but the structure of that region is altered in the mutants. In control embryos the hindgut diverticulum is closed and in contact with the splanchnopleura (Figure 2.18 A, B, C and D). In mutant embryos the hindgut diverticulum could be formed but it is smaller and loses the contact with the splanchnopleura (Figure 2.18 E, F, G and H). Moreover the size of the dorsal aorta is much bigger in mutant embryos as compared to control embryos. Notably, the development of anterior parts of the mutant embryos such as neural tube and heart is normal.

As the splanchnopleura and is not derived from the endoderm lineage, we assumed the loss of the contact between diverticulum and splanchnopleura is caused by non-cell autonomous effects. This means lack of Setdb1 in endoderm cells does not only affect the development of the endoderm derived tissue but also the tissues close to endoderm.

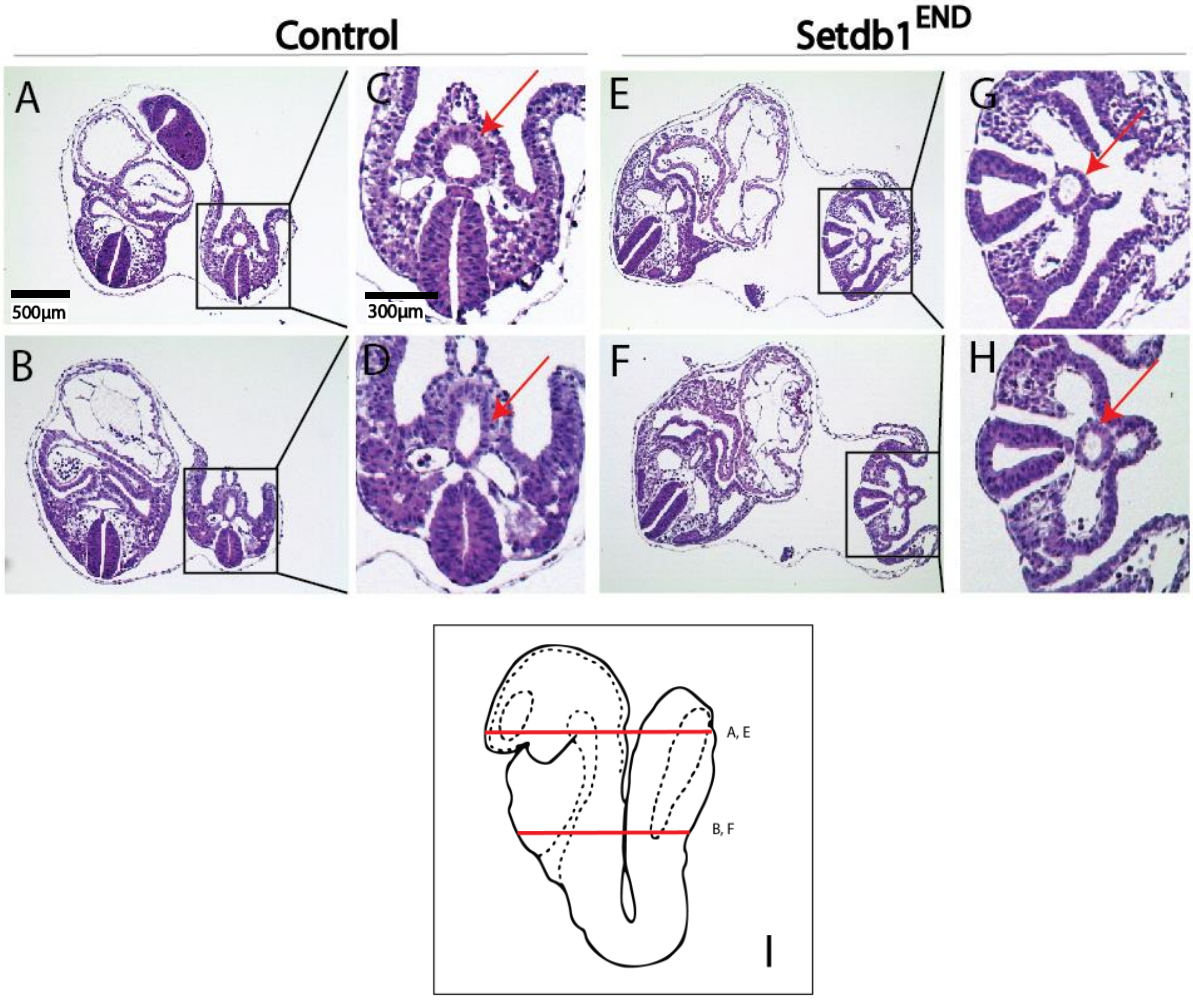

Figure 2.18 Defective gut development upon deletion of Setdb1 in the Setdb1^{END} (mutant) embryos at E8.5. A, B, E and F) H&E staining of paraffin sections at E8.0 from different layers. **C, D, G and H)** Enlarged picture from the square region. **I)** Schematic indicates the position of the different sections. Red arrows point to the defected region.

Immunohistochemistry was further conducted for later stages when the embryos already showed strong phenotypes at E9.5. We found that the anterior part of the mutant embryos showed a similar structure as the wild type embryos but the posterior gut region between mutant and control embryos was not comparable. At this developmental stage the mutant embryos already showed severe defects and the overall structure was severely affected. The hindgut diverticulum is surrounded by the splanchnopleura in control embryos but the hindgut diverticulum could not properly interact with other tissues and was stuck in the dorsal aorta in mutant embryos (Figure 2.19 arrow). This is consistent with our findings in E8.5 embryos. We thus conclude that deletion of Setdb1 in endoderm results in defective development of the posterior part of the mutant embryos.

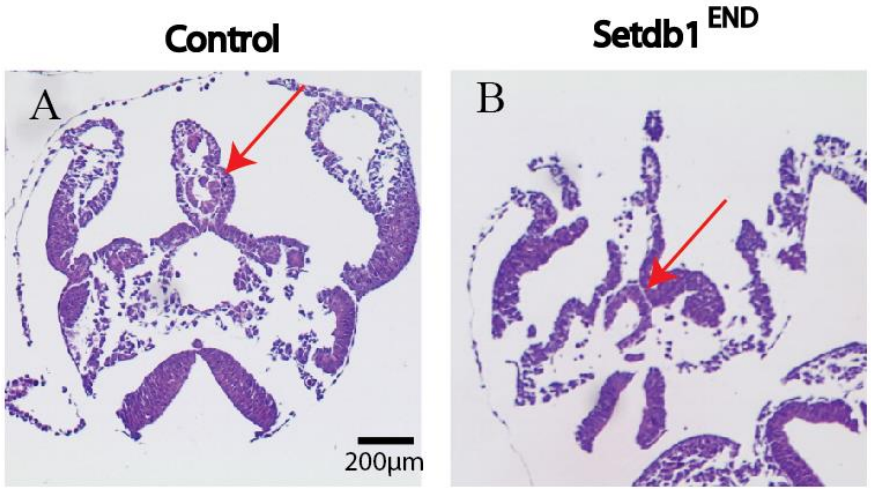

Figure 2.19 The posterior part of the Setdb1^{END} (mutant) embryos is strongly defective upon deletion of Setdb1 at E9.5. **A)** The gut region is surrounded by the splanchnopleura in the control embryo. **B)** The gut is stuck in the dorsal aorta in the mutant embryo and the posterior region is underdeveloped**.** Arrows show hindgut diverticulum.

The histological analysis at E8.5 revealed that the diverticulum in the mutant embryos cannot be well connected to the mesoderm derivatives. Furthermore the dorsal aortal is much bigger in the mutant embryos. As Sox17 lineage tracing experiments showed that Sox17 progenitor cells contribute to the formation of blood vessels we tested if the formation of the vasculature is affected upon deletion of Setdb1.

Platelet endothelial cell adhesion molecule (Pecam-1) is proved to be related to the formation of the vasculature and mediates cell-cell adhesion. Pecam1 is expressed in all endothelial cells and is first detected in the yolk sac and subsequently within the embryo itself (Baldwin et al. 1994). By staining of Pecam1 in the mutant embryos we found that the expression of pecam1 is not affected but the blood vessels are bigger in the mutant embryos in the comparison with the control embryos. This is consistent with our histological analysis. Based on this result we conclude that the formation of the vasculature is not generally affected by loss of Setdb1.

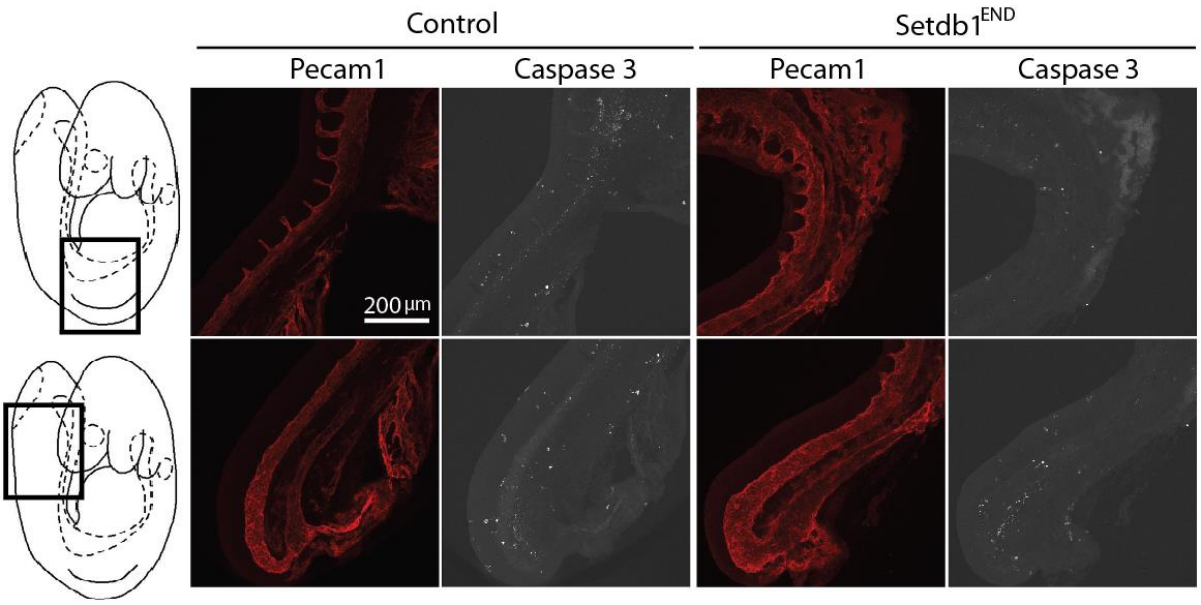

Figure 2.20 Whole mount immunostaining of control and Setdb1^{END} (mutant) embryos at E9.0 for Pecam1 and Caspase3. In mutant embryos, the blood vessels which are stained with Pecam1 (red) are wilder than in control embryos. The squares on the left side show the position of the images in the embryos.

2.3 Molecular changes during embryonic development upon deletion of Setdb1

2.3.1 Gene expression changes upon deletion of Setdb1 in endoderm at E7.75

From our previous analysis, we demonstrated a developmental defect by loss of Setdb1 in the endoderm region. In the next step, we tried to identify the molecular mechanism that are regulated by Setdb1 during endoderm development. One approach is to identify genes which are deregulated upon deletion of Setdb1 in endoderm then to test potential functions of these candidates. We collected 4 mutant embryos and 4 control embryos at E7.75 which were used for expression microarray analysis (Figure 2.21). As there is no obvious phenotypic defect at E7.5 and the axis turning problem take place at E8.5. Additionally, Sox17 in definitive endoderm is activated at around E6.5 thus the best time point to tell direct deregulated genes caused by deletion of Setdb1 is between E7.5 and E8.5. The visceral endoderm also shows the expression of Sox17 at roughly E4.5 and is partially replaced by definitive endoderm. The obvious developmental defect takes place at E8.5 in mutant embryos thus it is assumed the loss of Setdb1 in visceral endoderm does not affect the development of embryonic part. We decide to collect the embryos at E7.75 and try to identify the target genes of Setdb1 in the visceral and definitive endoderm. The mutant embryos at this stage do not show obvious phenotype (Figure 2.21).

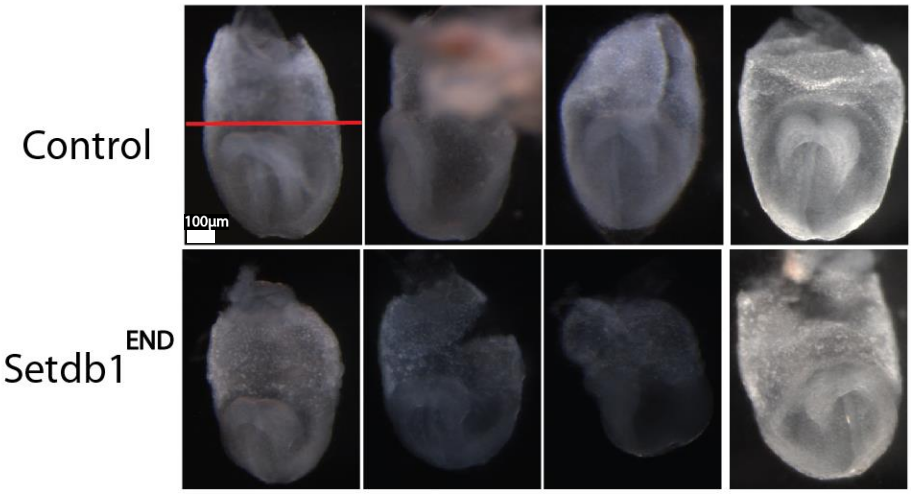

Figure 2.21 Embryos which are collected for microarray analysis at E7.75. No phenotypic difference between 4 control and 4 $Setdb1^{END}$ (mutant) embryos. The upper part of the visceral endoderm among control and mutant embryos was used for genotyping (shown by red line).

The microarray expression analysis revealed 936 genes to be significantly dysregulated in Setdb1 mutant embryos (FDR <10%) and most of these dysregulated genes are upregulated. This is consistent with the function of Setdb1 as a repressive histone methyltransferase (Figure 2.22 A). The expression level of Setdb1 is reduced by around 1/3 which is consistent with the specific deletion of Setdb1 in the endoderm lineage. From the list of dysregulated genes we found that a number of non-endoderm

lineage genes are derepressed. For example, Gabrr1 and Sycp3 which are related to neuronal development and meiosis are strongly increased in mutant embryos. Interestingly, we further detected upregulation of genes which are indicative of an undifferentiated or pluripotent state (e.g., Dppa2, Rex2). Several microRNAs were also found upregulated in Setdb1 mutant embryos. The mir302 cluster, for example, has been shown to maintain a pluripotent state (Anoky et al. 2011) (Figure 2.22 B). In contrast, endoderm lineage markers, for example Sox17 and Cer1, are repressed. These data suggest that loss of Setdb1 leads to the derepression of different cell lineage genes and perturbs the normal expression of endoderm genes.

A

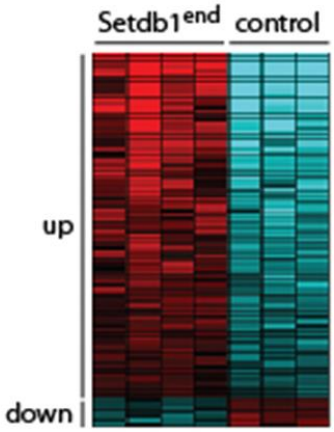

B

Gene	Description	fc	control	mutant
Gabrr1	GABA C receptor, subunit rho 1	10,24	125	1245
Mpv17l	Mpv17 transgene, kidney disease mutant-like	4,84	180	861
Sycp3	synaptonemal complex protein 3	4,78	49	227
Zfp558	zinc finger protein 558	3,59	76	267
Mael	maelstrom homolog	3,41	40	131
Zfp640	zinc finger protein 640	3,54	22	71
Dppa2	developmental pluripotency associated 2	2,75	128	350
Rex2	reduced expression 2	2,72	336	911
Mir302b	microRNA 302b	2,04	250	461
Mir302c	microRNA 302c	1,93	182	311
Mir302a	microRNA 302a	1,68	277	416
Mir302d	microRNA 302d	1,67	431	632

C

Gene	Description	fc	control	mutant
Slc2a2	solute carrier family 2 member 2	0,57	844	480
Setdb1	SET domain, bifurcated 1	0,62	868	541
Cer1	cerberus 1 homolog	0,65	1221	788
Sox17	SRY-box containing gene 17	0,74	504	374

Figure 2.22 Affymetrix expression analyses in E7.75 embryos. A) Heat map showing the top 100 dysregulated genes in 4 Setdb1^{END} (mutant) and 3 control embryos. **B)** List of top up-regulated genes. **C)** List of selected down-regulated genes. Fc = fold change; numbers in control and mutant column represent normalized intensity values of the selected probesets.

Through the microarray expression data, we identified some genes which are deregulated in mutant embryos at E7.75 (head fold stage). Next, we sought to validate these most dysregulated genes and check if these genes are also affected in E8.25 and E9.0 mutant embryos. We collected three mutant and three control embryos at E8.25 and one mutant and one control embryos at E9.0. We isolated RNA from these samples and carried out RT-qPCR analyses. We could detect that Gabrr1 and Mpv17l as the most upregulated genes in our microarray data show higher expression level in the mutant embryos in both E8.25 and E9.0 stages. Rex2 which contributes to the pluripotency of ES cells was also upregulated. Tbx4 showed no change. Cer1 which is an endoderm cell lineage gene is down-regulated in the mutant embryos (Figure 2.23). The expression level change of these genes at E8.25 and E9.0 between control and mutant embryos corresponds with the microarray expression data. The expression level of Setdb1 was reduced to 2/3 in the mutant embryos compared to control embryos. In summary, the RT-qPCR analysis revealed that dysregulated genes in E7.75 embryos are also dysregulated at later developmental stages in Setdb1^{END} embryos.

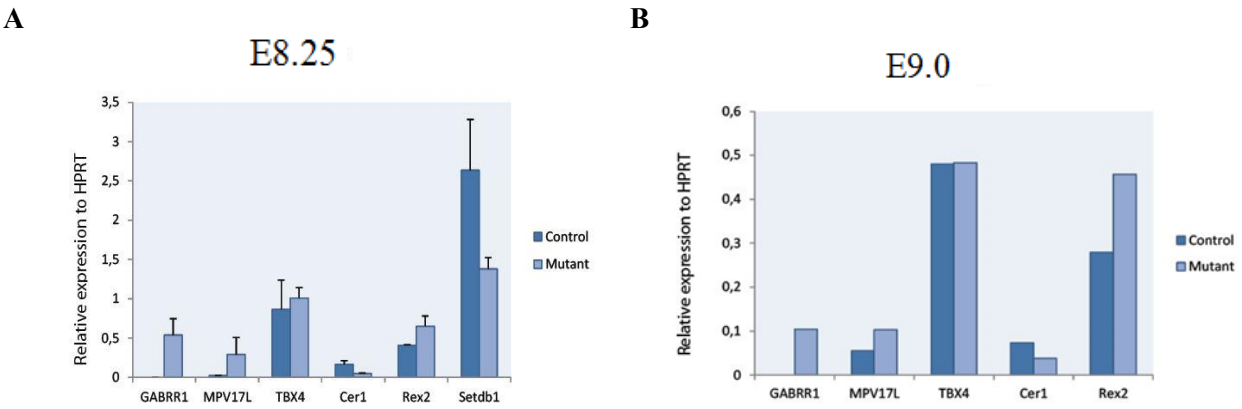

Figure 2.23 RT-qPCR analysis of dysegulated genes in E8.25 and E9.0 Control and Setdb1^{END} (mutant) embryos. A) RT-qPCR analysis of Setdb1 and candidate genes in E8.25 Control and Setdb1^{END} (mutant) embryos. Error bars represent ± standard error of the mean (SEM) of three biological replicates. **B)** RT-qPCR analysis of Setdb1 and candidate genes in E9.0 Control and Setdb1^{END} (mutant) embryos. The relative expression of these genes is normalized to HPRT.

Another up-regulated gene, AFP, is normally expressed in visceral endoderm in the primitive streak stage and covers the surface of embryos. During development the expression of AFP is gradually restricted to the extra visceral endoderm region until the early neural plate stage (Viotti et al. 2011). Interestingly, in Sox17 mutant embryos the expression of AFP cannot be restricted to the visceral endoderm at the neural plate stage and is also detectable in the posterior and lateral regions of the embryonic gut region, which demonstrates that the visceral endoderm cannot be properly replaced by definitive endoderm (Kanai et al. 2002). As the loss of Setdb1 in Sox17 positive cells causes a similar phenotype to Sox17 mutant embryos we decided to test if the replacement of the visceral endoderm by definitive endoderm is also deteriorated in Setdb1^{END} mutant embryos. We performed whole mount immunostaining and observed that AFP in mutant embryos is much stronger than in control embryos (Figure 2.24). When we closely analyzed the staining we found that the expression of AFP is mainly confined to the extra embryonic part but there are still some cells in the embryonic part showing slight expression of AFP. We assume that loss of Setdb1 leads to increased expression of AFP in visceral endoderm, which results in the difficulty or delay of the replacement of visceral endoderm cells by definitive endoderm cells.

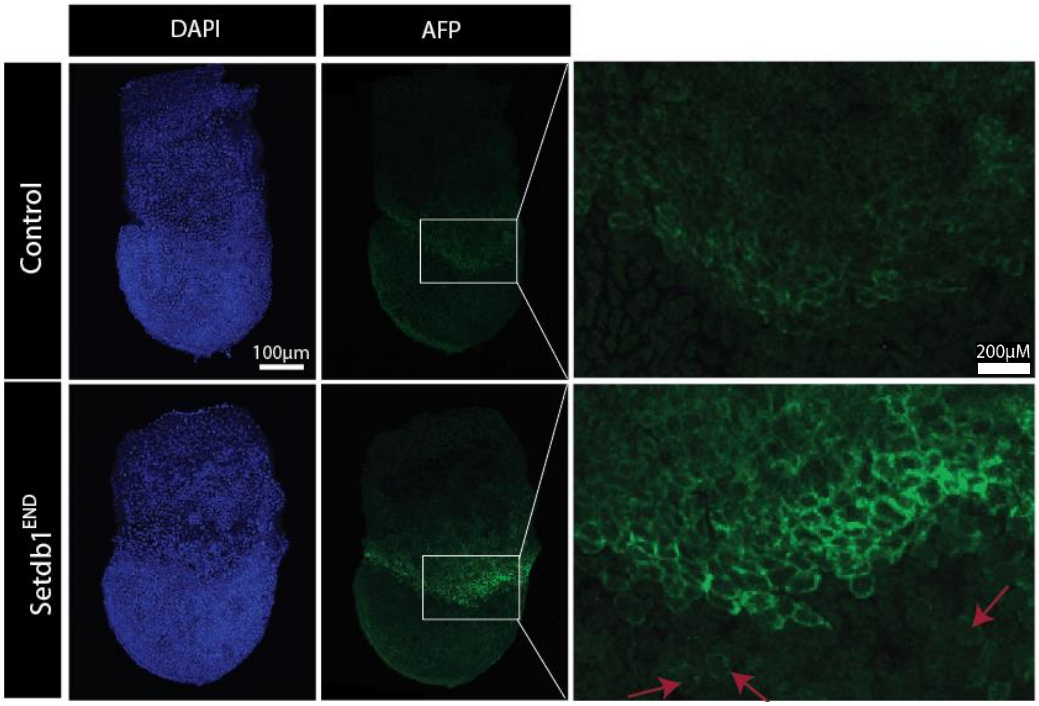

Figure 2.24 Overexpression of AFP upon deletion of Setdb1. The staining of AFP in Setdb1^{END} (mutant) embryos is much stronger than in control embryos. Red arrows show AFP positive cells in embryonic region in Setdb1^{END} mutant embryos

To test if deletion of Setdb1 in visceral endoderm would lead to defects in visceral endoderm development, we dissected embryos at around E8.5 and performed staining for AFP. We could identify upregulation of AFP in the yolk sac, which is derived from visceral endoderm, but there is no abnormal expression of AFP in other parts of the embryo (Figure 2.25). This suggests that deletion of Setdb1 in visceral endoderm due to expression of Sox17 does not influence the development of the embryonic part and the formation of yolk sac despite the upregulation of AFP as visceral endoderm gene. Thus the defect in development of the definitive endoderm is likely to be cell-intrinsic. However, we still need to test if other genes that could influence the function of the yolk sac are dysregulated at these later stages.

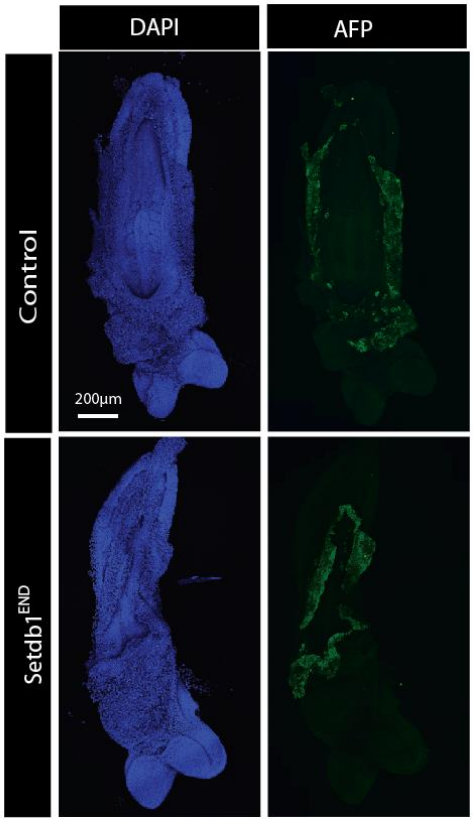

Figure 2.25 Upregulation of AFP upon deletion of Setdb1 in the Yolk sac at E8.5 Setdb1^{END} (mutant) embryos. The staining of AFP in mutant embryos is much stronger than control embryos. However AFP staining is restricted to the yolk sac and cannot be detected in other regions.

2.3.2 Endoderm specific transcription factors are reduced in the posterior region of the embryos

Setdb1 mutant embryos show the gut region defect and therefore set out to test if the major endoderm transcriptional factors are affected by deletion of Setdb1 in endoderm cells. We isolated E7.5 embryos and performed whole mount immunostaining for Foxa2 and Sox17. Both genes are expressed in the endoderm lineage and Foxa2 is additionally detected in the headfold region. At E7.5, the mutant embryos have no obvious phenotype, however the staining of the two markers is already reduced in the posterior part of the mutant embryos (Figure 2.26 A). The expression of Sox17 is also strongly reduced in the posterior region of the mutant embryos at E8.0 (Figure 2.26 B). Thus, it is possible that deletion of Setdb1 affects the expression of key endoderm transcription factors in specific regions of the embryo which could lead to the further impairment of development.

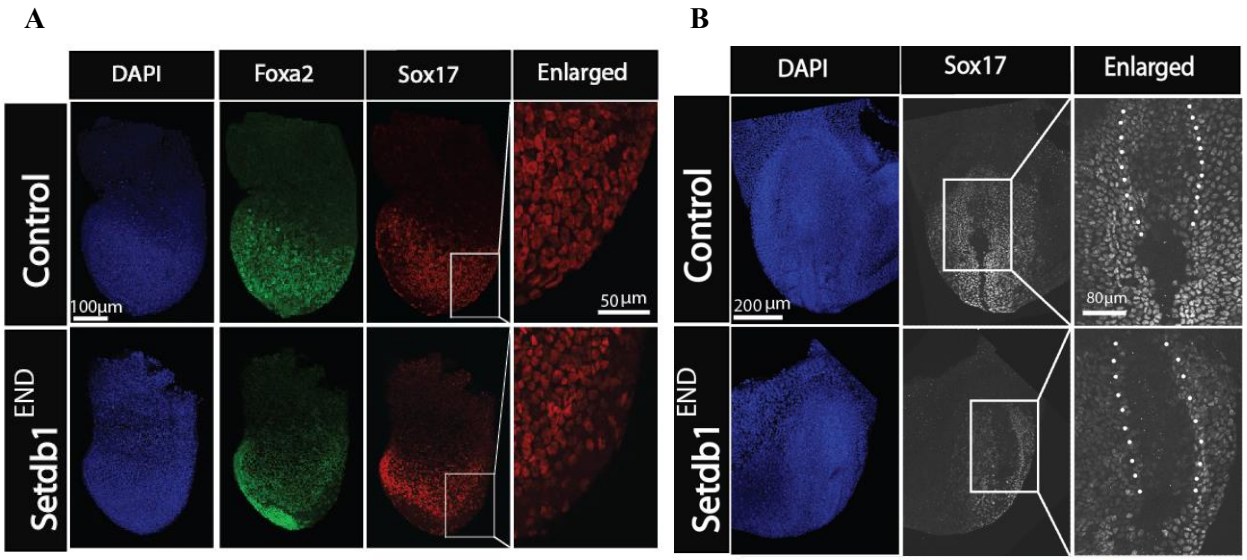

Figure 2.26 Reduction of endoderm markers in the posterior part of Setdb1^{END} (mutant) embryos. A) The staining of Sox17 (red) and Foxa2 (green) localize in the entire endoderm region of control and mutant embryos. There are less Sox17 expressing cells and weaker staining of Sox17 in the posterior region of mutant embryos**. B)** At head fold stage, the staining of Sox17 is reduced in primitive streak region of mutant embryos.

2.3.3 Increased apoptosis in the posterior part of the mutant embryos upon deletion of Setdb1

In order to figure out the possible molecular mechanism which causes the developmental defect in Setdb1^{END} mutant embryos, we first tested if the deletion of Setdb1 affects cell survival. As the defective phenotype becomes obvious at around E8.25 we stained the embryos at E8.25 with the apoptotic marker Caspase3. At E8.25, the mutant embryos showed reduced Sox17 staining around the node region and coincidently the apoptotic marker was increased (Figure 2.27 A). The frequency of apoptotic cells in the dorsal side of the mutant embryos was also increased (Figure 2.27 B). As there are no endoderm cells localized in that region the increased apoptosis in the dorsal side of the mutant embryos is probably caused by a secondary effect. In order to check apoptosis in more detail, we stained paraffin sections of control and mutant embryos at E8.5 with Caspase3 (Figure 2.28). More apoptotic cells were found in the mutant embryos and they were mainly restricted to the mesoderm.

These results suggest that loss of Setdb1 in endoderm cells leads to a slight increase in apoptosis. However the markedly increased apoptosis around endodermal cells implies that endoderm cells without Setdb1 may affect the normal development of adjacent cells.

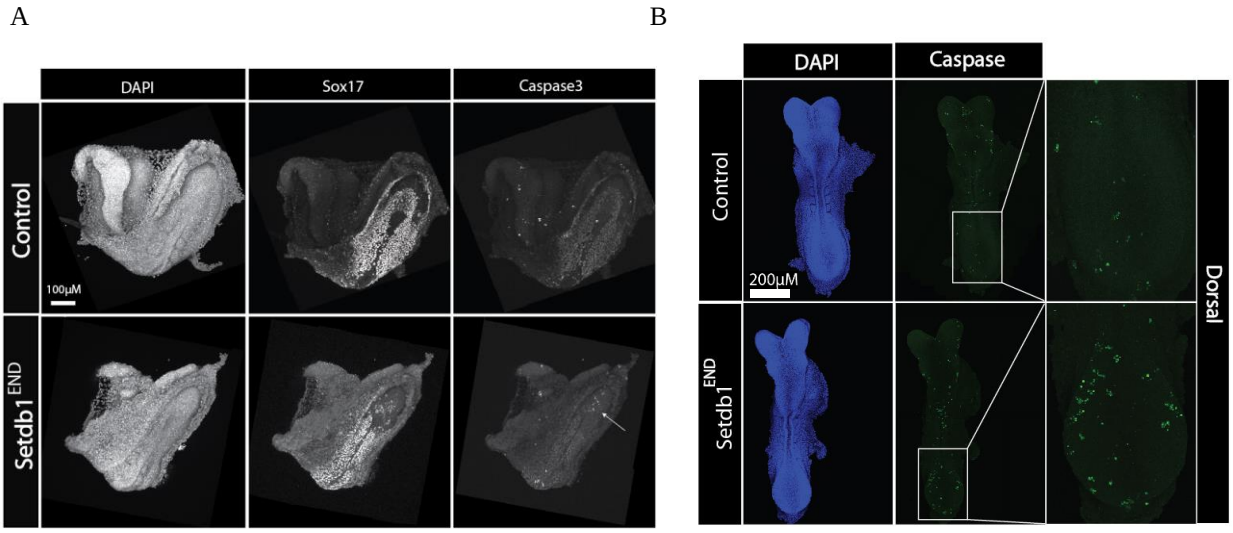

Figure 2.27 Increase of apoptotic marks in the posterior part of the Setdb1^{END} (mutant) embryos at E8.5. **A)** Embryos are stained with Sox17 (red) and Caspase3 (green). The staining of Sox17 is reduced around the node region and the Caspase3 staining is increased. **B)** Caspase3 staining in the dorsal side of the posterior part of the mutant embryos is increased.

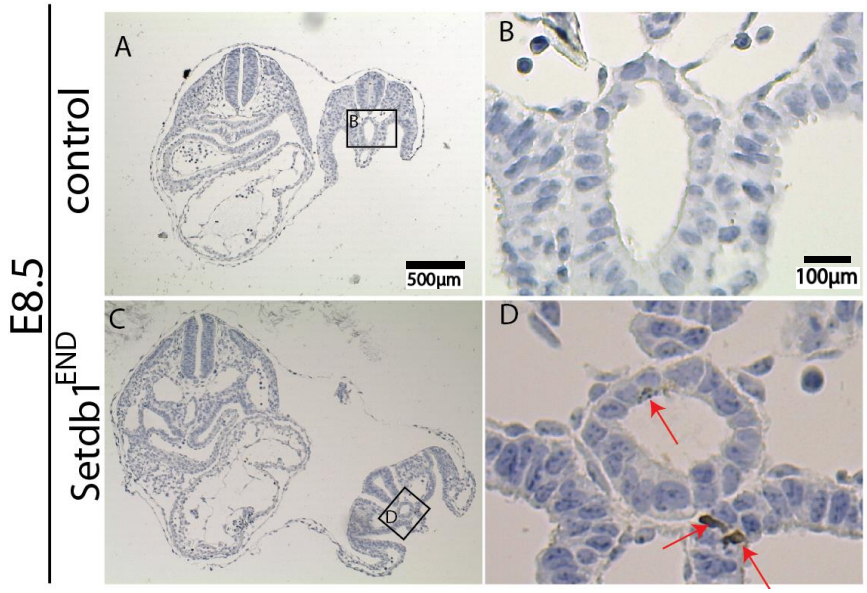

Figure 2.28 Transverse sections of the Setdb1^{END} (mutant) embryos show more apoptotic staining. Transverse sections of control and mutant embryos were stained with Caspase3 and Hematoxylin (**A** and **C**). **B** and **D** marked by the rectangle are shown in the magnified view. Increase of apoptotic marks in the posterior part of the mutant embryos. The apoptotic staining is pointed by the red arrow (**B** and **D**).

We then asked if proliferations of endoderm cells or cells adjacent to endoderm are affected upon deletion of Setdb1. H3S10 phosphorylation is a post transcriptional modification on histone H3 and plays an important role in mitosis. The emergence of H3S10 phosphorylation during prophase, prometaphase and metaphase inhibits the deposition of H3K9 methylation and HP1 in heterochromatin (Duan et al. 2008). With the staining of H3S10 phosphorylation proliferating cells can be identified.

We co-stained the embryos with Sox17 and H3S10ph. The Sox17 staining in the posterior part of the mutant embryos is reduced which is consistent with the staining before (Figure 2.29). There is no obvious difference in H3S10ph staining between control and mutant embryos. We further confirmed this result through staining with Ki67 which can be detected during all cell active phases (G1, S, G2 and mitosis) but is absent from non-proliferating cells (Scholzen et al. 2000). Transverse sections of E8.5 embryos were stained with Hematoxylin and Ki67. In comparison with control embryos, no marked difference could be detected in Setdb1^{END} mutants. The endoderm and non-endoderm derived organs show comparable proliferation between control and mutant embryos (Figure 2.30). Thus our results reveal that lack of Setdb1 in the endoderm region does not affect the proliferation of these cells.

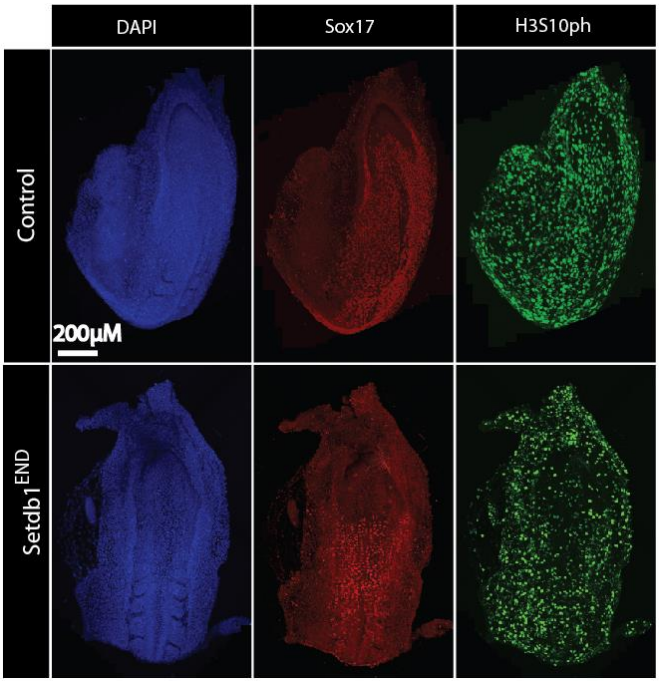

Figure 2.29 No obvious change of H3S10 phosphorylation staining in the posterior part of Setdb1^{END} (mutant) embryos in comparison with control embryos. Sox17 (red) and H3S10ph (Green) are stained in control and mutant embryos. The images are taken from the posterior side.

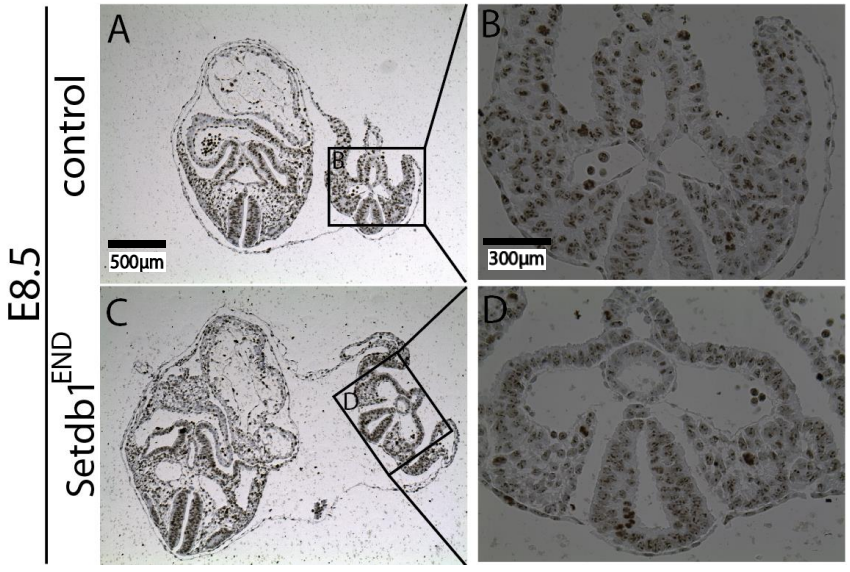

Figure 2.30 Transverse sections of embryos show comparable proliferation between control and Setdb1^{END} (mutants) embryos. Transverse sections of control and mutant embryos were stained with Ki67 (grey) and Hematoxylin (blue) (**A and C**). **B** and **D** marked by the rectangle are shown in the magnified view. No marked change in proliferation between control and mutant embryos could be detected.

2.3.4 Aberrant coverage of the node region in Setdb1^{END} embryos

In order to further dissect the endoderm defects in Setdb1^{END} mutant embryos we carefully analyzed Setdb1-deleted cells by tracing the EGFP Cre reporter. Based on this reporter we can recognize Setdb1 mutant cells and try to detect differences of Sox17 lineage cells with and without Setdb1. First, we collected E8.0 Setdb1 EGFP control and mutant embryos and performed Sox17 and EGFP staining. No obvious difference could be detected between control and mutant embryos. However, it appeared as if the node region and the midline were smaller and narrower in Setdb1^{END} embryos (Figure 2.31). Additionally, EGFP positive cells could be detected which lost expression of Sox17 in the primitive streak region. These data support our finding that loss of Setdb1 leads to an altered expression of important endoderm lineage markers.

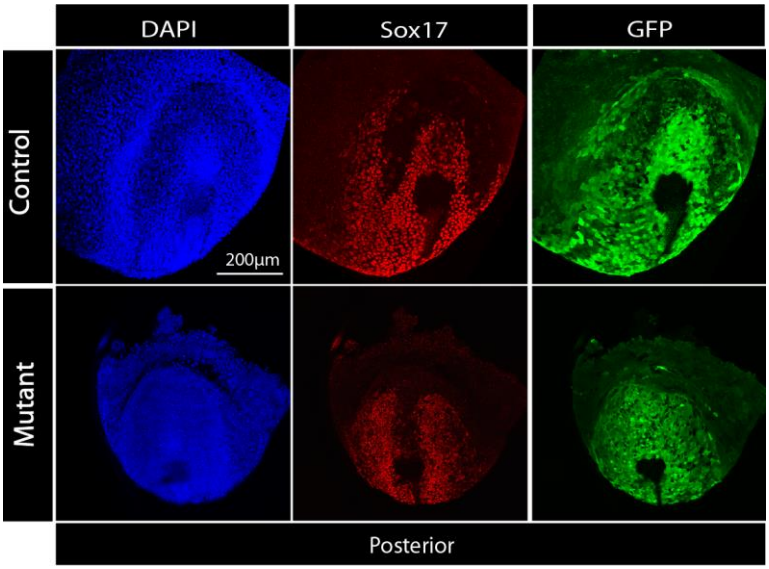

Figure 2.31 EGFP and Sox17 expression in Setdb1 EGFP control and mutant embryos at E8.0. Control and mutant embryos were stained for DNA (DAPI), Sox17 (red) and EGFP (Green).

Based on the increased apoptosis in the posterior part of the mutant embryos and the loss of endoderm marks in the primitive streak, we assumed that the node which is localized in this region may also be affected. The mouse embryo node region and axial midline arise from the anterior primitive streak and is an important organizer for left-right asymmetry and body axes formation (Kinder et al, 2011). The node produces the nodal flow to determine left-right asymmetry through the lateral plate mesoderm (LPM) (Saund et al. 2012). Recently, endoderm has also been related to the left-right asymmetry. It has been shown that mice lacking Sox17 show a defect in left-right asymmetry. The phenotype of Setdb1 mutant embryos looks similar to node deleted embryos (Yoshiba et al. 2012). Thus we wanted

to check if loss of Setdb1 in the endoderm lineage affects the normal development of the node. T is a major transcription factor whose expression is initiated in the primitive streak. It is required for normal development of mesoderm and for anterior-posterior axes formation. T is expressed in the node, notochord and tail bud at later development stages. Staining embryos with T would allow us to check if the node region is impaired by deletion of Setdb1 in endoderm. We isolated EGFP control and mutant embryos at roughly E8.5 and performed a staining for EGFP and T.

The comparison between control and mutant embryos showed us that T can be expressed in the mutant embryos and its staining is comparable to control embryos. However the GFP positive cells in the mutant embryos cannot be confined to the proper endoderm cell region and these cells converge into the center of the node region. Thus, the EGFP positive cells cover the T positive cells (Figure 2.32 L and P).

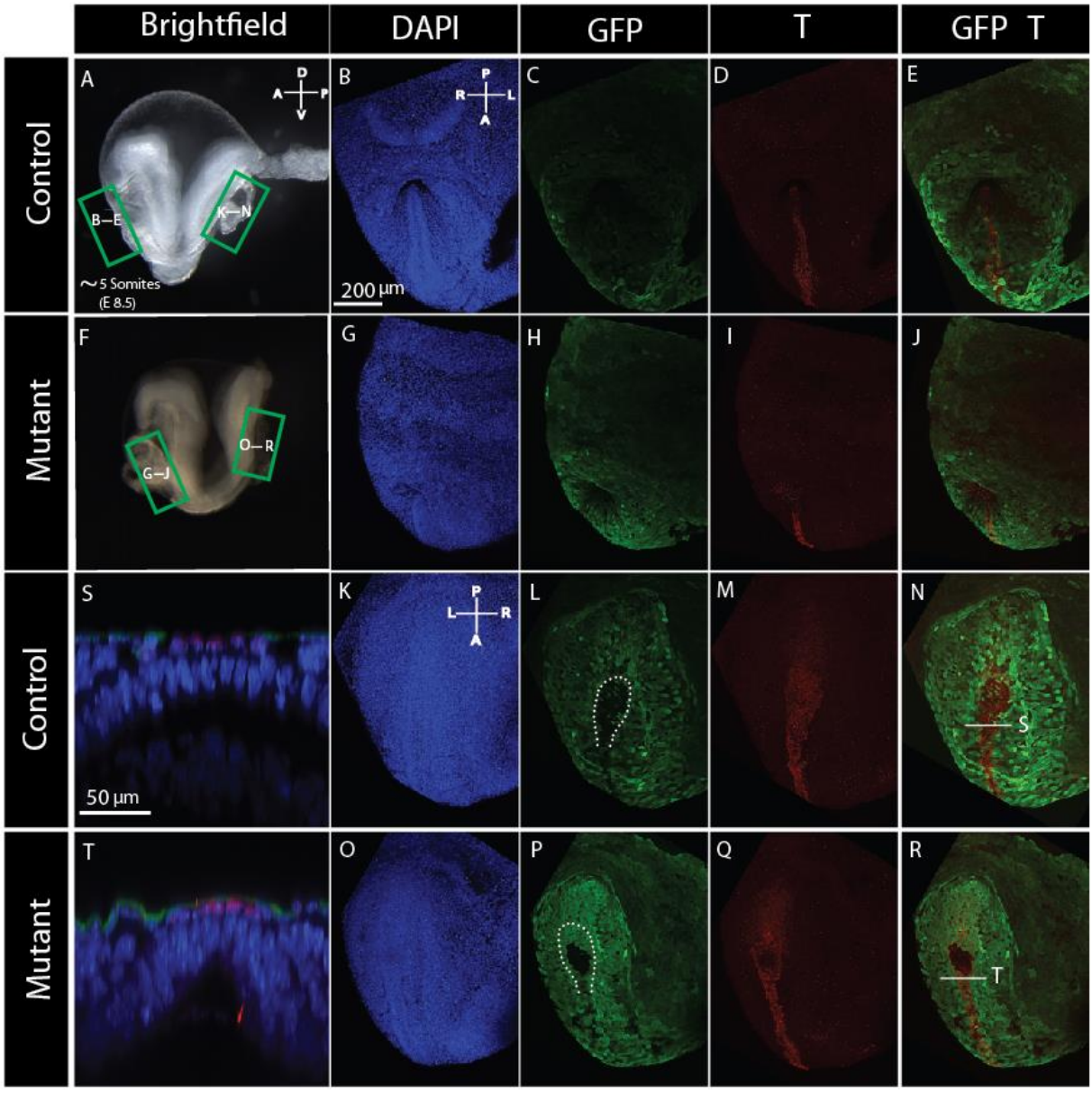

Figure 2.32 Co-staining of EGFP and T in Setdb1 EGFP control and mutant embryos at E8.5. **A and F)** Schematic of pictures taken in different regions of control and mutant embryos. The analyzed embryos have around 5 somites. **B and G)** DAPI staining in the embryonic anterior part. **C and H)** EGFP staining in the embryonic anterior part. **D and I)** T staining in the embryonic anterior part. **E and J)** Merge of EGFP and T in the embryonic anterior part. **K and O)** DAPI staining in the embryonic posterior part. **L and P)** EGFP staining in the embryonic posterior part. EGFP cells cover part of the node region. Dashed lines indicate the node region. **M and Q)** T staining in the embryonic posterior part. **N and R)** Merge of EGFP and T in the embryonic posterior part. Solid white line demarcates the transverse section through node region. **S)** EGFP positive cells stay adjacent to the T positive cells (red). **T)** EGFP positive cells cover the T positive cells.

The transverse sections also show the coverage of the GFP positive cells over the T positive cells in the node region of mutant embryos (Figure 2.32 S and T). As the node is an essential organizer for the embryonic development and the signals generated by the node are transmitted through the Cilia on its surface (Yoshiba et al. 2012), the coverage of the node region by different type of cells can impair the transition of the signals and affect the development of the embryos. This phenotype could be one of the reasons for impaired development of Setdb1^{END} embryos. However, further analyses are necessary to better specify the identity and molecular properties of the cells that cover the node region in Setdb1^{END} embryos.

2.4 Characterization of in vitro differentiated Setdb1 mutant endoderm cells

2.4.1 Establishment of an in vitro endoderm differentiation system

Loss of Setdb1 in endoderm cells leads to developmental defective embryos. To better characterize the molecular changes in mutant endoderm cells, we needed to obtain more and pure endoderm cells. Due to the complicated embryonic structure, it is difficult to get enough and pure Setdb1 mutant endoderm cells from these embryos. Thus we established an in vitro endoderm differentiation system in which we could differentiate ES cells specifically into endoderm cells.

By adding Wnt3a and Activin A into the culture medium, endoderm-specific transcription factors can be activated and ES cells initiate the differentiation into endoderm cells (Figure 2.33 A and B). Upon endoderm commitment pluripotency markers are shut down. Using this method, we could get more and purer endoderm cells for molecular studies.

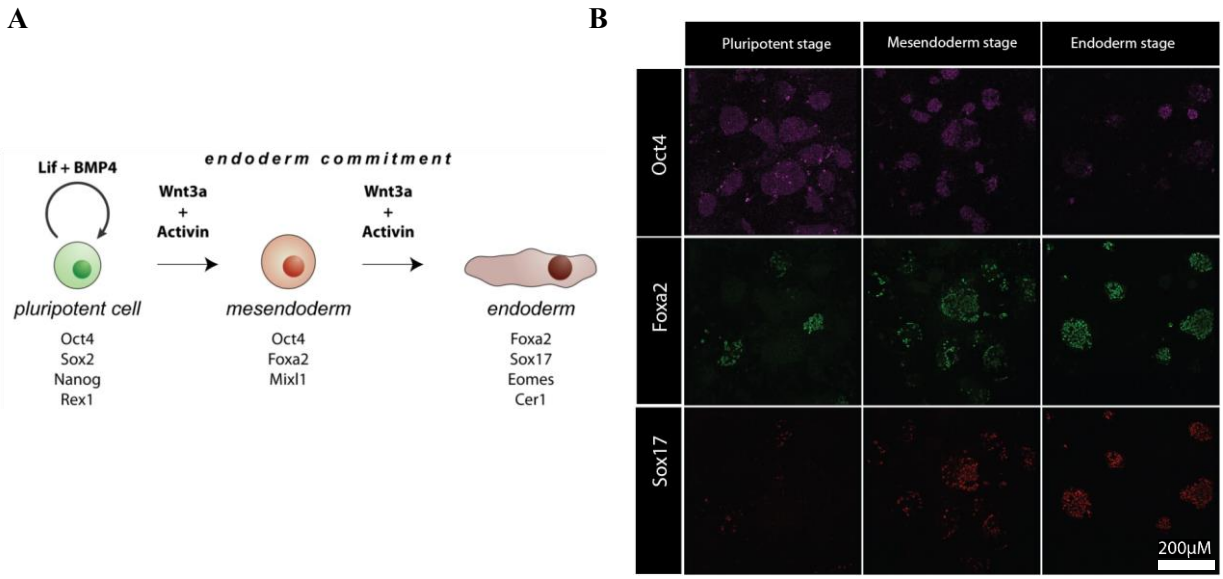

Figure 2.33 In vitro differentiation of pluripotent ES cells into endoderm cells. A) Schematics of ES cell differentiation into endoderm cells. In pluripotent cells, pluripotency markers can be identified. By adding Wnt3a and Activin A, pluripotent cells differentiate into mesendoderm cells and mesendoderm genes are activated. Mesendoderm cells can further differentiate into endoderm cells with the expression of endoderm specific markers. **B)** Immunofluorescence staining of different markers during differentiation. At the pluripotency stage most of the cells show Oct4 staining. At mesendoderm stage some colonies show endoderm transcriptional factor Sox17 and Foxa2 but most of the cells still show Oct4 staining. At endoderm stage the pluripotency marker Oct4 is shut down and the endoderm lineage markers Sox17 and Foxa2 are activated in most of the cells.

For the next experiments we used our ES cell line in which deletion of Setdb1 could be induced by addition of 4OHT. With this system we wanted to test if deletion of Setdb1 in ES cells impairs the differentiation of these ES cells into the endoderm lineage. We started the differentiation of the inducible ES cell lines with 4OHT or without 4OHT induction at day 0. The cells without the

treatment of 4OHT could differentiate efficiently and generated Foxa2 and Sox17 double positive cells. When Setdb1 was deleted at day 0, it was hard to find Foxa2 and Sox17 double positive cells after differentiation (Figure 2.34). Most of Setdb1 deleted cells cannot survive during the differentiation process. This result revealed that Setdb1 is important for the differentiation of pluripotent cells into endoderm cells.

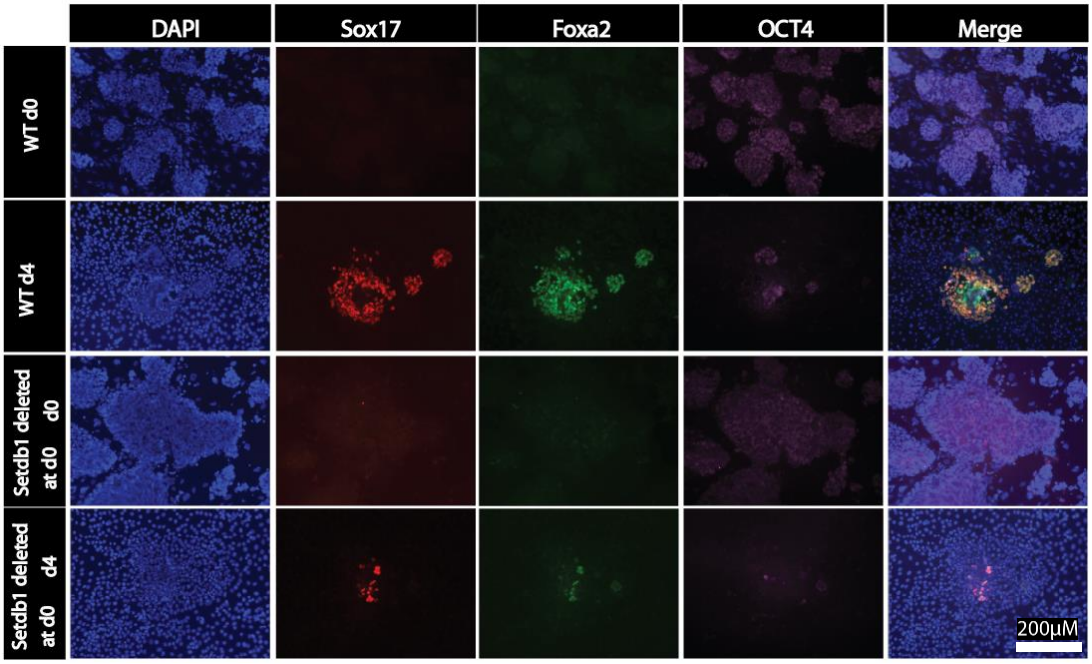

Figure 2.34 ES cell can hardly differentiate into endoderm cells upon deletion of Setdb1. In wildtype (WT) cells, the addition of 4OHT which is used to delete Setdb1 at d0 does not impair the differentiation of ES cells. But when Setdb1 is deleted in ES cell, most of these cells cannot survive until day4 of differentiation and only few Sox17 and Foxa2 double positive cells can be generated without Setdb1.

These data suggest an important function of Setdb1 for endoderm commitment. However this situation does not perfectly fit with the in vivo situation. It is difficult to control the time point of Setdb1 deletion in the inducible-Cre systerm. In order to better mimic the in vivo situation of Setdb1^{END} mutant embryos we decided to isolate Setdb1$^{flox/flox}$; Sox17-Cre mutant (Setdb1^{END}) ES cell lines. We crossed the Setdb1$^{flox/flox}$ with Sox17-Cre mice and isolated blastocysts to obtain Setdb1$^{flox/flox}$; Sox17-Cre ES cell lines. Then we performed differentiation experiments with these cell lines to test if these cells can differentiate or if they show phenotypic defects.

After 4 days of differentiation, we stained the cells with Foxa2 and Sox17. Both control and mutant cell lines can differentiate and show the Foxa2 and Sox17 staining (Figure 2.35). The differentiated mutant cells did not show obvious defects. This suggests that loss of Setdb1 in the endoderm cells does not affect the development of the cells. This situation is thus comparable to the in vivo situation. Even though the endoderm cells can be generated during differentiation, the molecular changes in the Setdb1 mutant endoderm cells need to be investigated

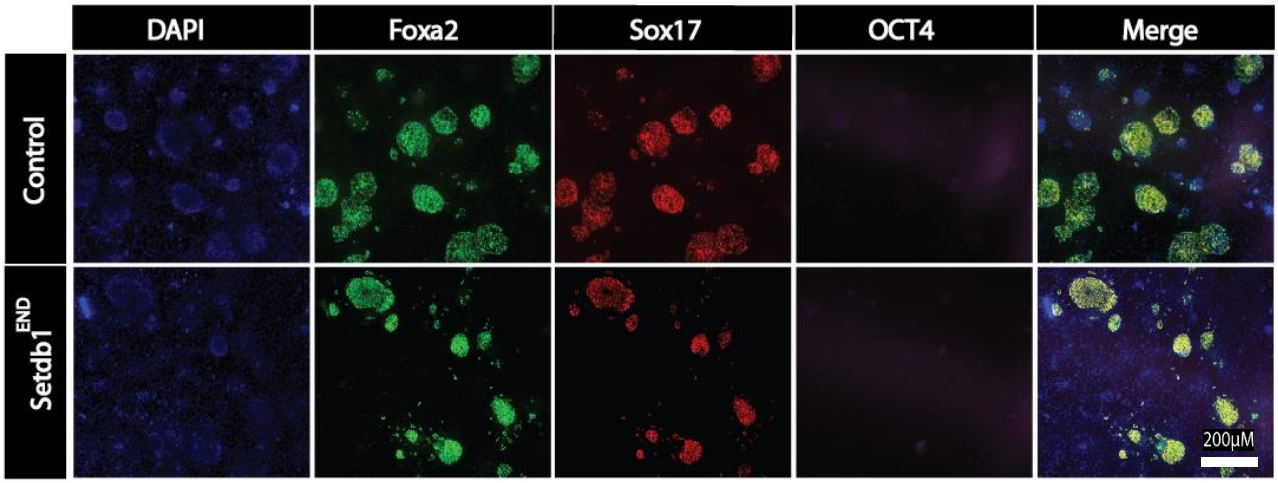

Figure 2.35 Setdb1$^{flox/flox}$; Sox17-Cre mutant ES cells (Setdb1^{END}) could differentiate into the endoderm lineage at day4 of differentiation. On day4 of differentiation both control and mutant cell lines showed a high differentiation efficiency. These cells were stained with Foxa2 (green) and Sox17 (red).

2.4.2 No alteration in histone modifications upon deletion of Setdb1 in endoderm cells

In order to trace the Setdb1 mutant endoderm cells we introduced the Cre based EGFP reporter gene into Setdb1$^{flox/flox}$; Sox17-cre mutant ES cells (Setdb1^{END}) (Figure 2.5). We then tested the Setdb1 EGFP reporter ES cells in the in vitro differentiation system. After four days of differentiation, Sox17 starts to be activated and EGFP could be detected in all Sox17 positive cells. On day 5 of differentiation, higher numbers of Sox17-expressing cells were detected and the EGFP signal completely overlapped with the Sox17 staining (Figure 2.36). This test confirmed the activity of the Sox17-driven Cre recombinase upon endoderm differentiation in vitro and demonstrates that the EGFP positive cells represent the Setdb1 mutant endoderm cells.

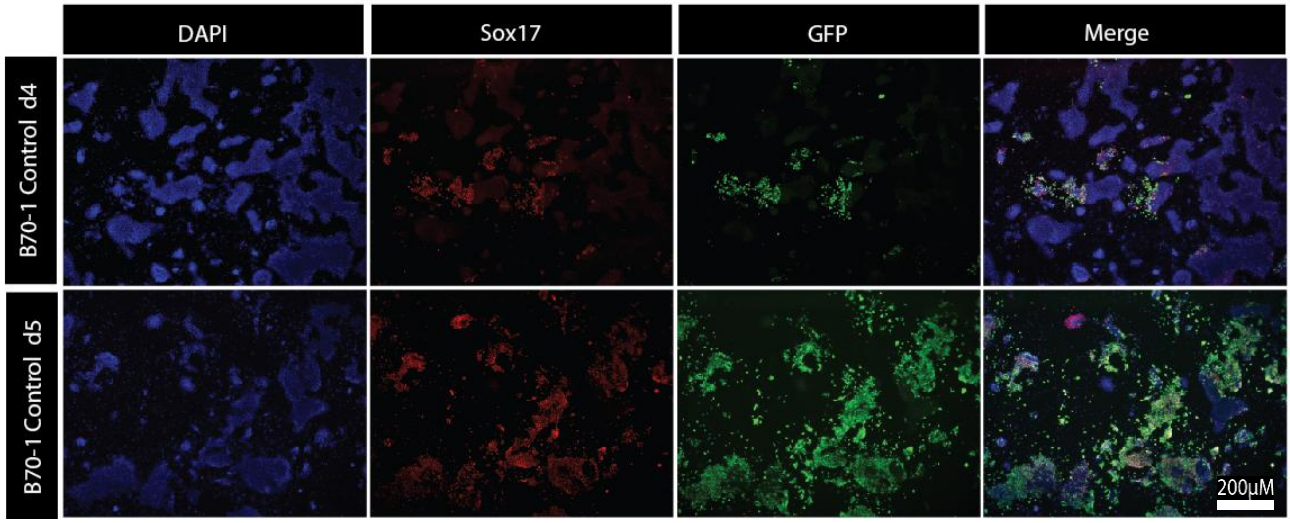

Figure 2.36 EGFP signal could be activated in Setdb1 EGFP control cell lines (B70-1) during endoderm differentiation. Day4 and day5 differentiated cells were stained with Sox17 (red) and GFP (Green). At day4,

Sox17 and EGFP start to be activated. At day5 the cells are highly differentiated. Both stainings almost overlapped.

Based on these experiments, we know that EGFP can be used as a reporter to for the deletion of Setdb1 during differentiation. Then we wanted to isolate pure Setdb1 mutant endoderm cells and check which genes are affected and if histone modifications are altered in these cells upon deletion of Setdb1. We differentiated control and mutant cells for 7 days and performed staining for Sox17 and EGFP. Both EGFP control (B70-1) and mutant (B63-4) ES cell lines can be differentiated well. In the EGFP positive cells, Sox17 exactly overlapped with EGFP (Figure 2.37 A). The loss of Setdb1 in endoderm cells did not obviously affect the normal development of these cells. In the undifferentiated situation very few cells were EGFP positive (Figure 2.37 B). These EGFP positive cells are probably generated due to the spontaneous expression of Sox17 in the ES colonies (Niakan et al. 2010). After day 7 of differentiation, large numbers of EGFP positive cells could be detected (Figure 2.37 B).

A

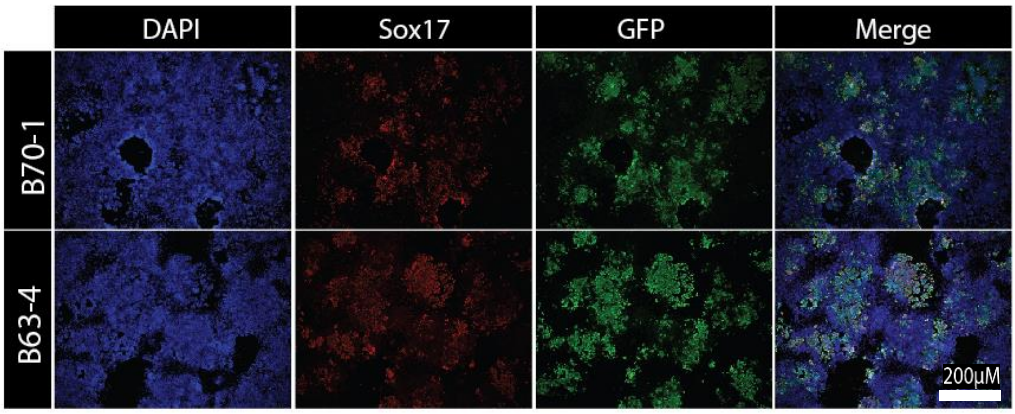

B

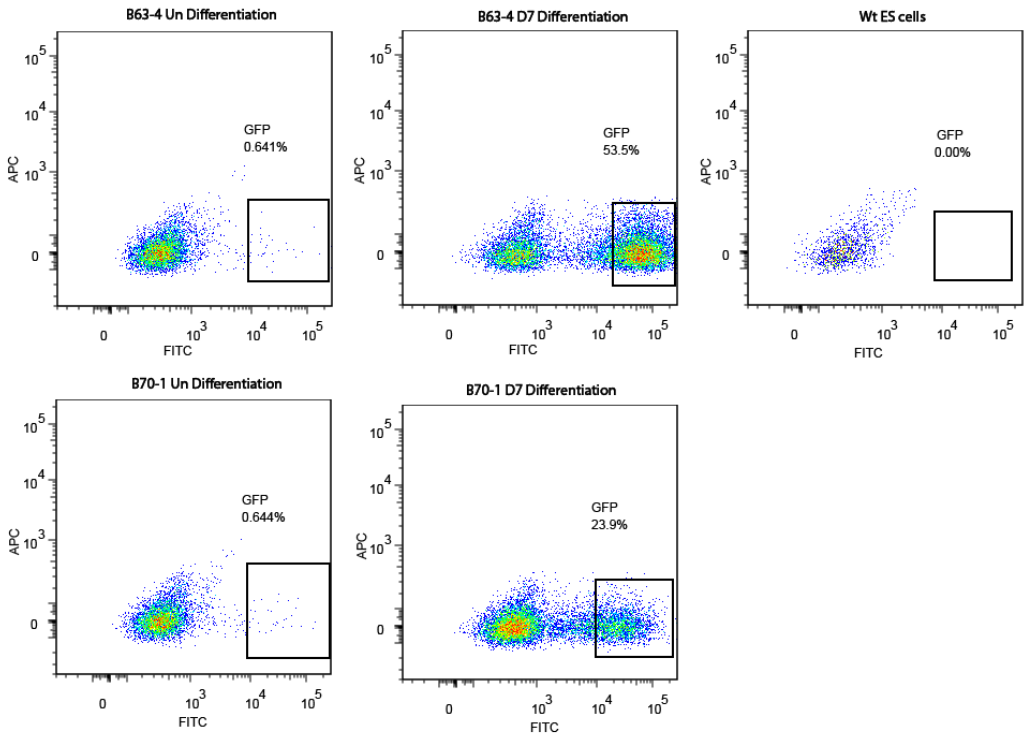

Figure 2.37 FACS analysis of Setdb1-deficient endoderm cells based on the EGFP Cre reporter. A) Overlap of Sox17 and EGFP signals in differentiated Setdb1 EGFP control (B70-1) and mutant (B63-4) cells. **B)** FACS analysis of EGFP positive cells. There is a very low percentage of EGFP positive cells in the undifferentiated EGFP reporter cell lines. The percentage of the EGFP positive cells markedly increased at day 7 of differentiation in both control (B70-1) and mutant (B63-4) cells. No GFP positive cells could be detected in the undifferentiated wild type ES cells.

We then FACS-sorted EGFP positive cells and isolated RNA to test expression levels of Setdb1 and selected candidate genes from the microarray expression analysis (Figure 2.38 A). Expression of Setdb1 could not be detected in the mutant EGFP cells demonstrating that Setdb1 was completely deleted during differentiation. We also tested the expression level of Gabrr1 and Cer1 which are the most up and down regulated genes in our microarray expression analysis in embryos. Gabrr1 was not activated in EGFP positive mutant cells. Cer1 which is an endoderm cell lineage gene is less expressed in differentiated Setdb1 mutant cells. We also performed western blot experiments to assess Setdb1 protein levels in the mutant cell lines during differentiation. Setdb1 was clearly reduced in the mutant cells (Figure 2.38 B). Thus, differentiated cells sorted by EGFP expression represent Setdb1 mutant endoderm cells and can be used for further molecular analyses.

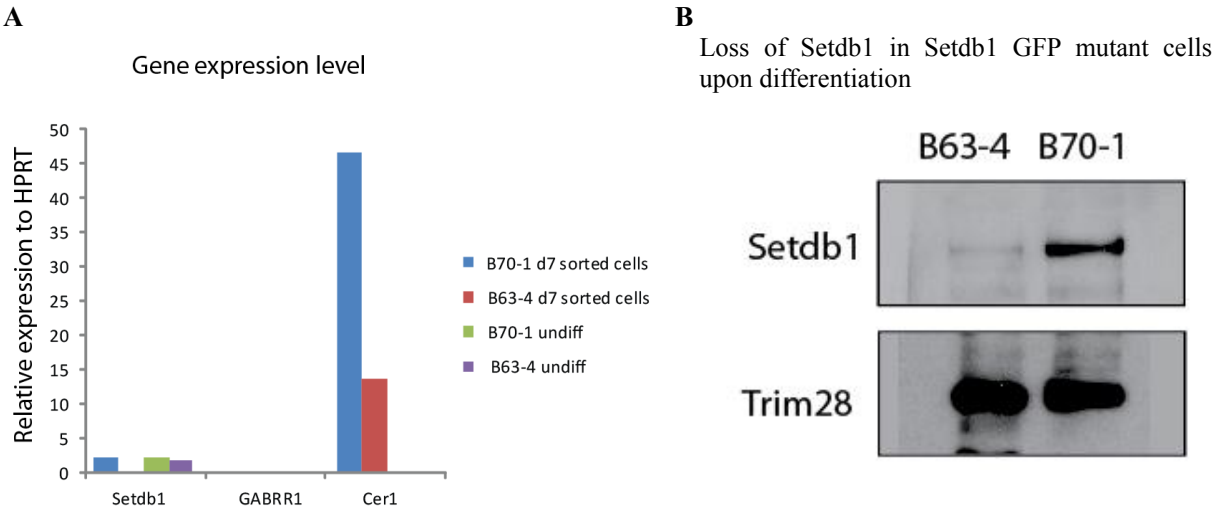

Figure 2.38 Changes in gene expression in Setdb1-deficient endoderm cells. A) Change in gene expression were tested by RT-qPCR. Setdb1 is hardly detectable in the differentiated Setdb1 EGFP mutant cells (B63-4). No expression of Gabrr1 was detected in both differentiated and undifferentiated cells. Cer1 is activated in Setdb1 EGFP mutant (B63-4) and control cells (B70-1). **B)** Western blot for Setdb1 and Trim28 (loading control). Setdb1 protein is strongly reduced in the differentiated Setdb1 EGFP mutant cells (B63-4).

Setdb1 was demonstrated as a histone methyltransferase which regulates different biological processes. Therefore we wanted to test if the loss of Setdb1 in endoderm cells affects overall histone modifications. H3K9ac, H3K9me2 and H3K9me3 were assessed in differentiated Setdb1 EGFP control and mutant cells. We extracted whole cell proteins and used Trim28 as loading control. We could not detect a significant change of the signals of H3K9ac, H3K9me2 or H3K9me3 between

control and mutant differentiated cells (Figure 2.39). These data demonstrate that the deletion of Setdb1 in endoderm cells does not result in global alternations of histone modifications but probably causes change on specific loci related to the spatial and temporal functions of Setdb1 as histone methyltransferase.

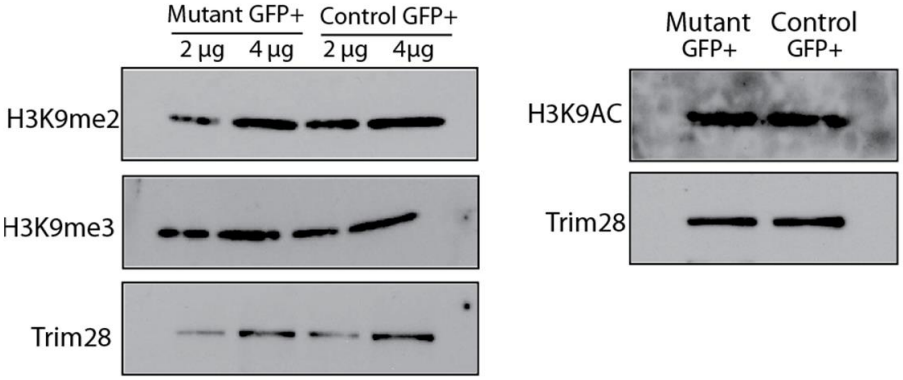

Figure 2.39 Analysis of histone modifications in endoderm differentiated cells. H3K9me2, H3K9me3 and H3K9ac were tested in whole cell extracts from differentiated control (B70-1) and mutant (B63-4) cells. No clear difference could be detected between control (B70-1) and mutant (B63-4) cells. Trim28 was used as loading control.

2.4.3 Molecular changes of the in vitro differentiated Setdb1 mutant cells

Although there were no global alterations in histone modifications in Setdb1 mutant endoderm cells we asked if gene expression is altered in mutant cells. Transcriptome analysis for sorted Setdb1 EGFP control and mutant cells was performed by RNA-seq analysis. Interestingly, we could find several genes which are related to endoderm development to be upregulated in mutant cells. For example, Mixl1 which is first expressed in the primitive streak of embryos and facilitates endoderm development is upregulated (Lim et al. 2009) (Figure 2.40 A). Eomes, Foxa1, Foxa3, Hnf1b and Cer1 as classical endoderm markers are also upregulated (Figure 2.40 B). Wnt3 and Nodal belonging to the Wnt and Tgf-β signaling pathway and involved in endoderm differentiation are also increased. Interestingly, Nanog and Sox2 considered as pluripotency-associated genes are up- and down-regulated separately in Setdb1 EGFP mutant endoderm cells. On the other hand, T (Izumi et al. 2007) and Tbx1 (Zhang et al. 2006) which are also important for the differentiation of mesendoderm are down-regulated. Even though these genes are expressed almost at the same time point and are important for the initiation of mesendoderm during in vitro and in vivo differentiation they have different roles for distinct cell lineage commitments (Izumi et al. 2007; Wang et al). The up-regulated genes (Mixl1, Nanog and so on) facilitate endoderm specification, however the down-regulated genes (T, Sox2 and so on) repressed endoderm commitment and induce the differentiation of the mesoderm and ectoderm lineages. These findings reveal that the genes which are related to endoderm differentiation are much easier to be activated in endoderm cells upon deletion of Setdb1.

A

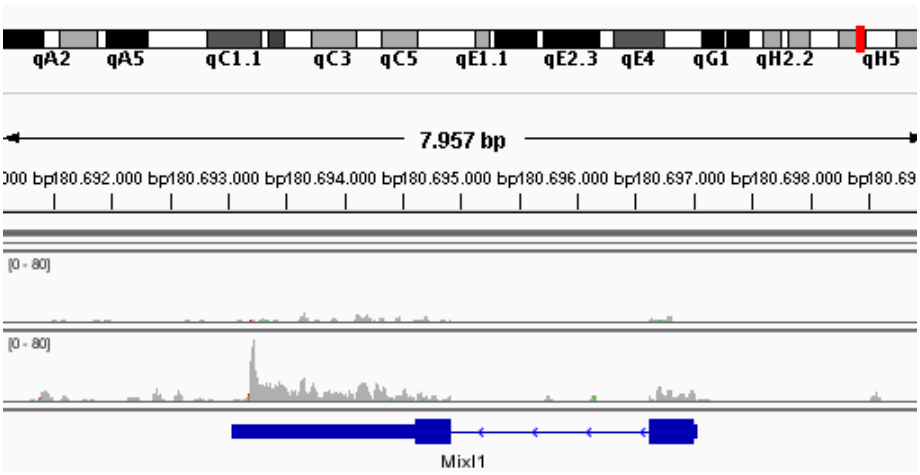

B

Genes	Description	FC
Nanog	Nanog homeobox	2.27
Wnt3	Wingless-related MMTV integration site 3	4.88
Nodal	Nodal	2.44
Mixl1	Mix1 homeobox-like 1	5.96
Eomes	Eomesodermin homolog	2.22
Foxa1	Forkhead box A1	3.01
Foxa3	Forkhead box A3	2.17
Cer1	Cerberus 1 homolog	2.33
Hnf1b	HNF1 Homeobox B	4.03
Foxj1	Forkhead box J1	2.12

C

Genes	Description	FC
Sox2	SRY -box 2	0.22
T	Brachyury	0.2
Tbx1	T-box 1	0.37

Figure 2.40 Dysregulated genes in differentiated Setdb1 EGFP mutant (B63-4) cells. A) RNA-seq analysis revealed increased transcription of Mixl1 in Setdb1 EGFP mutant endoderm cells. **B)** Genes related to endoderm lineage commitment are up-regulated in Setdb1 EGFP mutant endoderm cells. **C)** Genes related to mesoderm lineage commitment are down-regulated in Setdb1 EGFP mutant endoderm cells.

Next we wanted to test if the dysregulated genes in Setdb1 EGFP mutant cells are also dysregulated in Setdb1^{END} embryos. Mixl1 is a mesendoderm gene regulating the endoderm development and is speculated to be regulated by histone modifications induced by Setdb1 (Xi et al. 2011). We checked the expression level of Mixl1 in differentiated Setdb1 EGFP mutant cells by RT-qPCR. Mixl1 was indeed increased in the Setdb1 EGFP mutant endoderm cells in comparison to Setdb1 EGFP control cells (Figure 2.41 A). However, we did not identify an increase of Mixl1 in Setdb1^{END} mutant embryos at E8.0 and found only a slight increase of Mixl1 in E9.0 mutant embryos (Figure 2.41 B and C). We also confirmed the up-regulation of Nodal, Hnf1b and Foxa1 by RT-qPCR in mutant cells (Figure 2.41 B and C). However, these genes were not increased in Setdb1^{END} mutant embryos. There are two

possible reasons for this. One reason is that we differentiated ES cells until day7 and Sox17 starts to be activated at roughly day4. This means we analyze the cells 3 days after activation of Sox17. In embryos, Sox17 is activated at day 6.5. The time point of the differentiated endoderm cells used for RNA-seq would thus more correspond to E9.5 embryos. Unfortunately, E9.5 mutant embryos show severe defects and cannot be used for testing gene expression. The other possible reason for not finding consistent transcriptional changes between in vitro cells and embryos may be that the expression of these genes is not restricted to endoderm cells. A specific change in gene expression in endoderm is therefore hard to detectable.

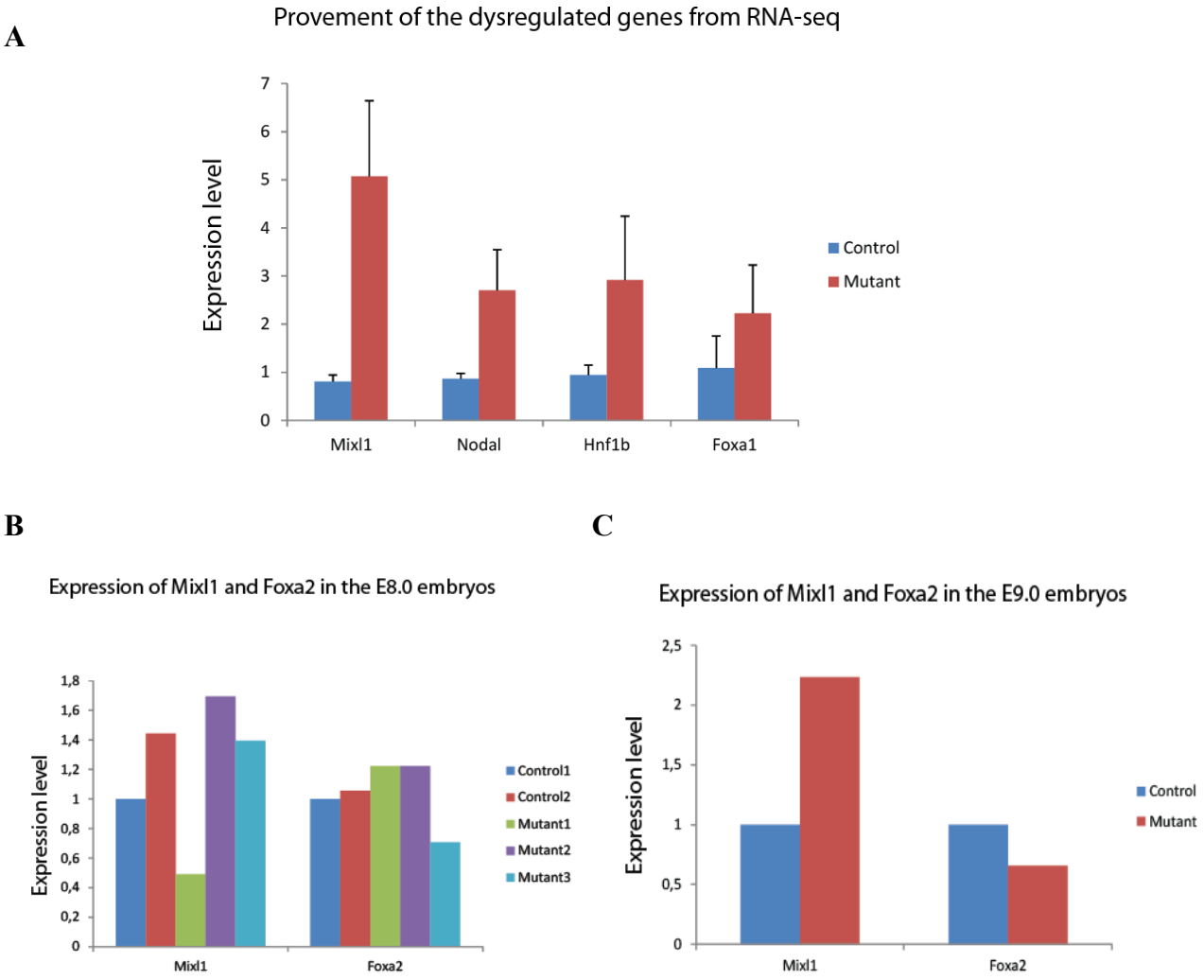

Figure 2.41 qRT-PCR analysis of selected dysregulated genes from RNA-seq analysis of differentiated cells. A) Confirmation of the up-regulated genes from the RNA-seq analysis in differentiated Setdb1 EGFP (mutant) cells. Error bars represent ± standard error of the mean (SEM) of three technical replicates. **B)** No expression change of Mixl1 in E8.0 Setdb1^{END} (mutant) embryos. **C)** Slight upregulation of Mixl1 in E9.0 Setdb1^{END} (mutant) embryo.

In ES cells, the histone modifications H3K9me3 and H4K20me3 occupy endogenous retroviruses (ERVs) according to genome wide analyses. Recent studies showed Setdb1 mediated H3K9me3 could

maintain silencing of these endogenous retroviruses (Rowe et al. 2010). Loss of Setdb1 in ES cell results in the decrease of H3K9me3 at ERV elements and de-repression of endogenous retroviruses (Rowe et al. 2010) (Matsui et al.2010). Therefore, we wanted to test if the loss of Setdb1 in endoderm progenitor cells also perturbs the silencing of ERV elements. We tested the expression of an abundant ERV subclass, IAP elements, in sorted Setdb1 EGFP mutant cells and Setdb1^{END} embryos (Figure 2.42). IAP elements are upregulated around 4 fold in the sorted cells and are upregulated around 7 fold in the E8.5 mutant embryos. This shows that during embryonic development Setdb1 functions in the repression of retrotransponsons. However, the level of up-regulation of IAPs is much lower than in Setdb1 mutant ES cells (Rowe et al. 2010).

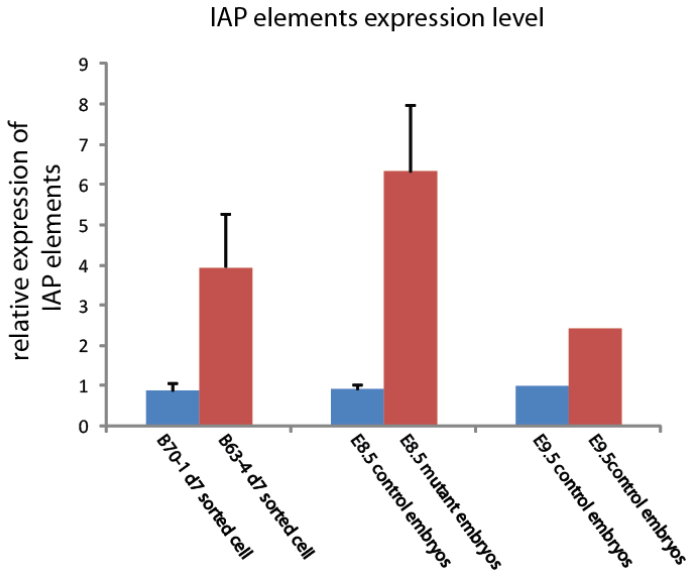

Figure 2.42 De-repression of IAP elements upon loss of Setdb1 in endoderm cells. The blue bars are the control cells and the red bars are the mutant cells. The IAP elements are de-repressed in the sorted Setdb1 EGFP mutant cells, E8.5 embryos and E9.5 embryos. Error bars in B70-1 and B63-4 d7 sorted cells represent ± standard error of the mean (SEM) of three technical replicates. Error bars in E8.5 control and mutant embryos represent ± standard error of the mean (SEM) of three technical replicates.

We observed a clear endoderm-related phenotype in Setdb1^{END} embryos, however, it is difficult to tell whether this defect is due to proliferation or apoptosis. We set out to test if apoptosis or proliferation is altered in our in vitro differentiation assay. We differentiated Setdb1 EGFP control and mutant cells into endoderm cells and then performed EGFP staining together with Ki67 or Caspase3. In both of control and mutant differentiated cells, high levels of both Ki67 and Caspase3 positive cells can be detected but due to the high numbers the staining is hard to be quantified (Figure 2.43).

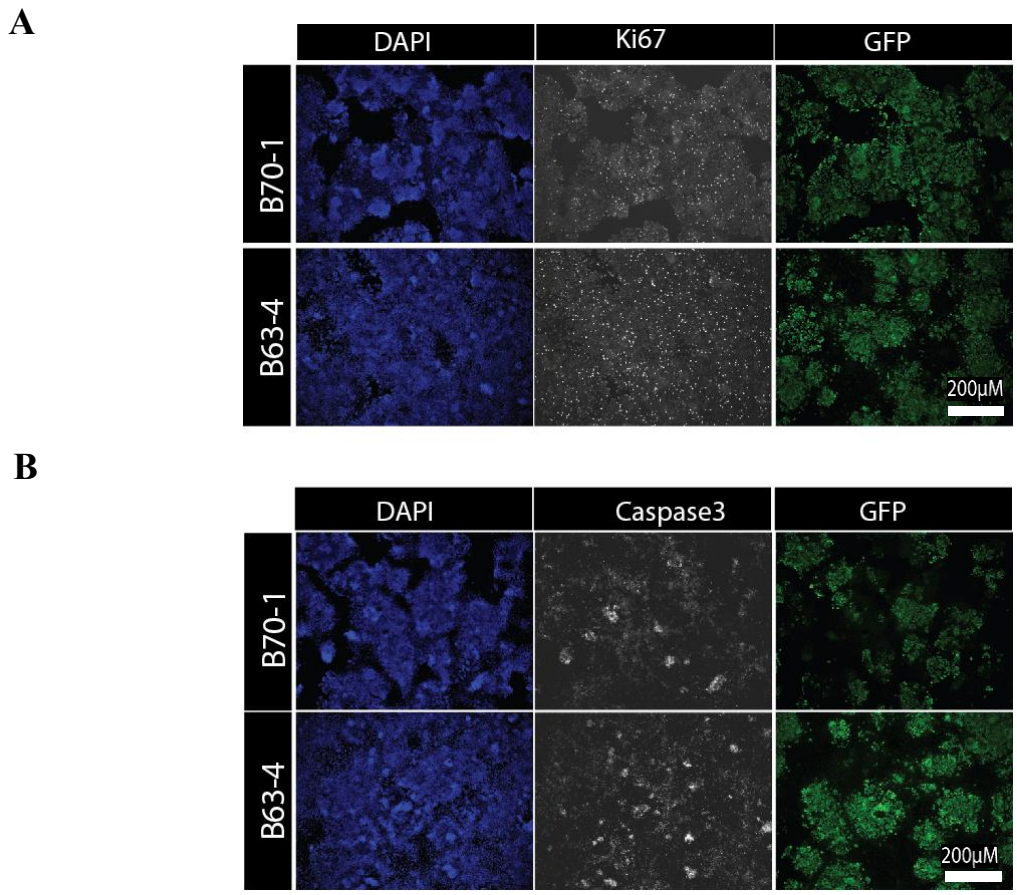

Figure 2.43 Immunofluorescence for Ki67 and Caspase3 in differentiated Setdb1 EGFP control (B70-1) and mutant (B63-4) cells. A) Co-staining of EGFP and Ki67 in differentiated Setdb1 EGFP control and mutant cells. **B)** Co-staining of EGFP and Caspase3 in differentiated Setdb1 EGFP control and mutant cells.

In order to better quantify apoptosis rate in Setdb1 EGFP control and mutant cells we performed FACS analyses (Figure 2.44). For the apoptosis analysis, we differentiated the Setdb1 EGFP control and mutant cells and then stained these cells with AnnexinV which is a specific PS (phosphatidylserine)-binding protein and can be used to detect apoptotic cells. In our FACS analysis, we could detect more apoptotic cells in the Setdb1 EGFP mutant cells. The increase in apoptosis in the mutant cells could be one of the reasons why loss of Setdb1 in the endoderm results in the developmental defect.

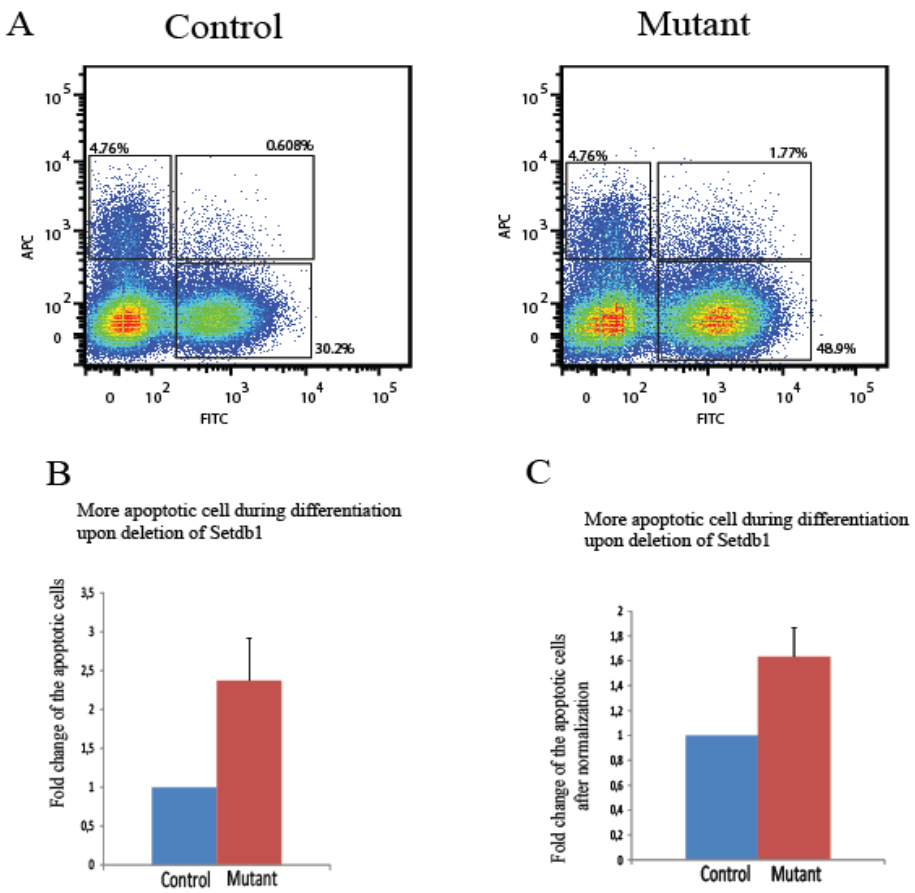

Figure 2.44 Loss of Setdb1 in endoderm cells causes more apoptosis. A) FACs analysis for AnnexinV (APC) and EGFP (FITC) in differentiated Setdb1 EGFP control (B70-1) and mutant (B63-4) cells. **B)** Quantification of the FACs analysis. Overall more apoptotic cells can be detected in differentiated Setdb1 EGFP mutant (B63-4) cells. Error bars represent ± standard error of the mean (SEM) of three technical replicates. **C)** Apoptotic is increased in differentiated Setdb1 EGFP mutant (B63-4) cells. Error bars represent ± standard error of the mean (SEM) of three technical replicates.

3 DISCUSSIONS

3.1 Setdb1 is implicated in the endoderm specification

Setdb1 is involved in several different biological processes. However, the specific function of Setdb1 during development remained largely uncharacterized because of the early lethality of the mutant embryos. According to the X-gal staining of Setdb1 β-gal embryos, we could demonstrate the expression of Setdb1 in whole embryos during gastrulation stage. Through X-gal staining of adult organs we also found expression of Setdb1 in several adult cell lineages. For example, there is a high expression level of Setdb1 in the brain and testis and intermediate expression level in the liver, pancreas and spleen, which are the endoderm derivatives (Figure 2.13 B). Thus we hypothesized that Setdb1 has a potential role in endoderm development. These endoderm derived organs are related to several severe diseases like, for example, type I diabetes caused by the destruction of pancreatic β-cells (Lee et al. 2011). In this work, I tried to figure out the spatial and temporal functions of Setdb1 in endoderm development and to understand the mechanism of endoderm development (Dodge et al. 2004). Because of the early lethality of Setdb1 mutant embryos at peri-implantation stage it was difficult to study the function of Setdb1 in the later development. Thus we used Setdb1 conditional knock-out mice. Setdb1 is deleted in Sox17 lineage cells with a Cre-recombinase under control of the Sox17 promoter. Setdb1^{END} mutant embryos show clear defect. Interestingly, two different kinds of defective phenotype could be identified (Figure 2.14). This is probably because of the different deletion ways of Setdb1 in the embryos due to distinct expression profiles of Sox17.

Sox17 was first identified in 1995 and belongs to Sox gene family due to a high level of amino-acid identity (Dunn et al. 1995). Members of the Sox gene families are related to cell type specification and tissue differentiation during development. Because of the general function of Sox genes during development, Sox17 was also considered to be implicated in mouse development (Kanai et al. 2002). Detailed functional analysis about Sox17 was conducted during the last years. Sox17 was first identified as a transcription factor for mouse spermatogenesis (Kanai et al. 1995) but is expressed at around post-implantation stage in the visceral and definitive endoderm. Deletion of Sox17 severely impairs axis rotation as well as mid- and hindgut formation (Kanai et al. 2002). Recently it was found that the expression of Sox17 can also be detected in the inner cell mass. At the 32 cell stage, the expression of Sox17 is first observed and with the expansion of the blastocyst the expression of Oct4 and Sox17 overlap in some cells. After the 128 cell stage Sox17 expression in the epiblast is shut down and restricted to the primitive endoderm region adjacent to the blastocoel cavity (Niakan et al. 2010). Further functional analysis demonstrated that deletion of Sox17 leads to a failure in the establishment of the left-right embryonic patterning (Viotti et al. 2012). Interestingly, another paper reported that the deletion of Sox17 could cause two different phenotypes. One phenotype shows strong defects where the whole bodies of the embryos are retarded. The other phenotype shows a mild defect

with rotation problem and retarded posterior part (Kim et al. 2007). However the reasons for these two different phenotypes are unclear.

Embryos with deletion of Setdb1 in the Sox17 lineage (Setdb1^{END}) show similar phenotypes as the Sox17 mutant embryos (Kim et al. 2007). In order to trace the fate of the Setdb1 deleted cells an EGFP-based Cre reporter was used to monitor the deletion of Setdb1 in individual cells. The EGFP reporter features a stop codon flanked by LoxP sites upstream of an EGFP transgene. Expression of Cre results in a removal of the stop codon through the recombination and activation of EGFP. First when we checked the control embryos for EGFP expression, a very interesting phenomenon was identified. In some embryos the EGFP staining could only be detected in the endoderm region and blood vessels which are considered to be derived from Sox17 progenitor cells (Engert et al. 2009). However in other embryos the EGFP cells were localized everywhere throughout the mutant embryo (Figure 2.15). We further analyzed the mutant embryos with the Sox17-Cre, EGFP-reporter system. Consistently, some mutant embryos only showed the EGFP signal in the definitive endoderm and vessels at E8.5 but others showed the overall staining in the embryos. Interestingly, mutant embryos which showed the EGFP staining in the whole embryos were strongly retarded and we call it type 2 mutant phenotype. However, the embryos with confined EGFP staining in the endoderm region and blood vessels showed a milder phenotype which we considered as type 1 mutant phenotype (Figure 2.14 and 2.15). Based on this observation, the generation of these two different phenotypes from mutant embryos could be explained by different expression patterns of Sox17. In the morula, Sox17 is expressed in some cells and then shut down in the blastocyst. Activation of Sox17 in the epiblast starts in the definitive endoderm at around E6.0 (Kanai et al. 2002). However, the fate of the Sox17 expressing cells in the morula is still unclear. Our results suggest that type 1 mutant embryos start to lose Setdb1 mainly at the primitive streak stage and thus mutant embryos show endoderm-specific defects. In type 2 mutant embryos, Sox17 is likely activated at an earlier stage in the blastocysts resulting in the loss of Setdb1 even outside endoderm. According to the two different phenotypes caused by the different expression patterns of Sox17, we hypothesize that the cells expressing Sox17 in blastocyst also contribute to the later development of the embryos; however, specific loss of Setdb1 in the later Sox17 lineage affects endoderm development.

In my work, I mainly focused on the functions of Setdb1 in definitive endoderm by studying the type 1 mutant embryos. Three different germ layers emerge at around E6.5 and ingress from the primitive streak. In type 1 mutant embryos, Setdb1 start to be deleted in the definitive endoderm at this time point. From E6.5 to E8.0, no obvious phenotype can be detected in the mutant embryos. However upon E8.5, which is the time point of the embryo axis rotation, mutant embryos show a turning defect and retardation of the posterior part (Figure 2.14). Importantly, the head and the heart could be formed properly. In order to figure out the exact structural changes of the embryos upon deletion of Setdb1 at this stage, we performed immunohistochemistry staining from E8.0 to E9.5. At E8.0, the paraffin sections did not show differences in the gut region between control and mutant embryos. We could

identify that endoderm and mesoderm are in contact with each other in both control and mutant embryos. However when we checked the embryos at E8.5 which already showed the turning defect we found a big difference in the hindgut region between control and mutant embryos. In control embryos, the hindgut diverticulum keeps contact with the mesoderm and gradually moves forward with the surrounding of the mesoderm. But in E8.5 mutant embryos we found the mesoderm derived splanchnopleura detached from the endoderm (Figure 2.18). In addition, the dorsal aortal in mutant embryos is much bigger than in control embryos. During development, the hindgut diverticulum of the mutant embryos cannot move forward with the surrounding of the mesoderm; instead is arrests in the dorsal aorta resulting in perturbed mesoderm development. Thus loss of Setdb1 in the definitive endoderm affects the further development of the gut region. However, the anterior part of the mutant embryo is not affected suggesting this defect to be mainly caused by the abnormal development of the definitive endoderm.

In the next steps we investigated possible reasons for the endoderm phenotype. First we investigated the expression of major endoderm genes in Setdb1 mutant embryos. The whole mount immunostaining revealed a reduced expression of Foxa2 and Sox17 in the primitive streak of mutant embryos (Figure 2.26). Next, we checked if deletion of Setdb1 in endoderm cells affects apoptosis and proliferation of these cells. The whole mount embryo staining was performed with Caspase3 which is an apoptotic marker and H3S10ph which is proliferation marker (Figure 2.27 and Figure 2.29). We detected an increase in apoptotic cells in the posterior part of the mutant embryos. However, most of the Caspase3 staining was localized in the dorsal side of the mutant embryos (Figure 2.27 and Figure 2.28). Through H3S10ph staining in the whole embryos and immunohistochemistry staining by Ki67 as a proliferation marker, we could not detect a difference between control and mutant embryos (Figure 2.29 and Figure 2.30). This indicates that deletion of Setdb1 does not strongly affect the normal development of the endoderm cells and rather induced defects in neighboring cells. The node is localized in the posterior part of the embryos and performs important organizer roles for embryos development. Destruction of the node will severely affect the embryonic development. Therefore we checked if the node region is affected upon the deletion of Setdb1 in endoderm. Notably, endoderm lies adjacent to the node and the loss of Sox17 in the definitive endoderm impairs the establishment of left-right asymmetry through the lack of Connexin45 in the endoderm cells which has been implicated to the signal relay (Giepmans. 2004). In order to check the formation of the node, we stained the embryos with T. T is a mesendoderm transcription factor and serves as a marker which is first activated in the primitive streak and is then expressed in the node, notochord and tail bud. T plays essential role for embryonic development. Lack of T results in the disruption of the node and impairs the extension of the notochord precursors. When we conducted T staining in the embryos there was no change of T in the node region.

In order to check the cell fate of the mutant cells we crossed Setdb1$^{flox/flox}$; Sox17-Cre mice with an EGFP Cre-reporter mouse. The expression of EGFP through Cre mediated recombination is irreversibly activated, thus we can trace the mutant endoderm cells. In Setdb1 EGFP control embryos at E8.5, the EGFP positive cells surround the node region, and there is clear boundary between the endoderm region and the node region. However, in E8.5 Setdb1 EGFP mutant embryos, the EGFP positive cells are not well organized. The EGFP positive cells converge into the node region. There is no clear boundary between the endoderm region and the node region and the surface of the node region is partially covered by EGFP positive cells (Figure 2.32). Presumably the deletion of Setdb1 in the endoderm cells changed the property of these cells in a way that they cannot be maintained in the proper endoderm position. There is a recent study (Yoshiba et al. 2012) revealing that the node region consists of two different cell types: perinodal crown cells sitting on the edge of the node region and pit cells located in the central region of the node. It is suggested that the nodal flow is sensed dependent on Pdk2 located on the surface of the cilia of the crown cells. In Setdb1 mutant embryos, the EGFP positive cells cover part of the surface of the node region where the crown cells reside. Based on this observation, we assumed that coverage by the EGFP cells impairs the signal transmission through the cilia of the crown cells. Thus the node cannot function well as an organizer for normal development of the mutant embryos. This could be one of the possibilities which cause the endoderm phenotype. But some questions remain unanswered. It is unclear why the Setdb1 mutant cells cannot be confined to the endoderm region and if the mutant cells really affect the function of the node as a developmental organizer.

Overall, our findings reveal that the deletion of Setdb1 in endoderm cells impairs the normal development of the embryos. We found not only the Setdb1 deleted endoderm cells to be defective but also the tissue close to endoderm is affected. We assume that loss of Setdb1 in endoderm cell impairs the development of the embryos through both cell-autonomous and non-cell autonomous effects.

3.2 Setdb1 regulates gene expression in different biological processes

3.2.1 Setdb1 regulates gene expression during early embryonic development

Setdb1 control and mutant embryos were collected at E7.75 (head fold stage) and subjected to microarray expression analysis. The defect of the mutant embryos was not obvious at E7.75, however, dysregulated genes might be direct target genes of Setdb1 in definitive endoderm or visceral endoderm. Totally, we found 936 genes were significantly dysregulated in the mutant embryos (FDR <10%). Consistent with the function of Setdb1 as a repressive histone methyltransferase, among the top100 dysregulated genes, there are more up-regulated genes than down-regulated genes. Interestingly, most of the up-regulated genes in mutant embryos are normally not expressed or just kept at a very low level in early embryonic development. These genes are closely connected to different specific cell lineages and conduct functions in different adult organs.

Synaptonemal complex protein (Sycp3) is first expressed in leptotene spermatocytes and shut down in late meiotic cells (Lammers et al. 1994). There is a study showing that Sycp3 plays an essential role in testicular development and fertility in the male mouse (Yuan et al. 2000). Loss of Sycp3 in female mice causes defective meiotic chromosome segregation and early embryonic lethality (Yuan et al. 2002). Gabrr1 is the most up-regulated gene in Setdb1^{END} embryos and belongs to the GABA receptor rho subunit family which is mainly expressed in the brain (García et al. 2011). GABA is the major inhibitory neurotransmitter in the brain which could activate subclasses of GABA receptors rho1, rho2 and rho3 subunits (Alakuijala et al. 2005). We also detect up-regulation of Dppa2 which is associated with undifferentiated or pluripotent ES cells (Watabe et al. 2012). Several microRNAs were found up-regulated and could potentially result in the defect in Setdb1 mutant embryos. The mir302 cluster has been shown to be activated in the ES cells by Sox2 and Oct4 (Card et al. 2008) and contributes to the maintenance of the pluripotent state (Anokye et al. 2011). Some genes which are related to endoderm development are down-regulated upon deletion of Setdb1. The expression of Cer1 starts from E5.5 in the lateral region (Torres et al. 2007) and then continues in definitive endoderm from E7.5. During later development, Cer1 could be detected in the foregut endoderm and the mesoderm (Iwashita et al. 2013). Sox17 is considered as a transcription factor mediating endoderm differentiation and is specifically expressed in the definitive endoderm region at E8.5. The expression of these two important endoderm genes was reduced according to the expression analysis and the reduction of Sox17 was proven by whole mount immunostaining (Figure 2.26). These results indicate that Setdb1 could restrict the expression of genes which contribute to different development processes and ensures endoderm lineage differentiation.

Sox17 is activated in the primitive endoderm which further develops into visceral endoderm. This expression profile of Sox17 results in the deletion of Setdb1 in visceral endoderm. Visceral endoderm is important for the morphogenesis and patterning of the epiblast and is involved in the nutrient uptake and transport (Srinivas. 2006). From our data we could identify the up-regulation of AFP which is secreted in the visceral endoderm during the fetal life (Kwon et al. 2006). Because visceral endoderm is replaced by definitive endoderm during development (Kwon et al.2008), we wanted to investigate if the up-regulation of this visceral endoderm marker would be indicative of defective morphogenesis od definitive endoderm. Embryos were stained with AFP antibody and the up-regulation of AFP was confirmed at E7.5 in the mutant embryos but the staining was confined to the extraembryonic part (Figure 2.24). At E8.5, we could identify an increase in AFP staining in the yolk sac (Figure 2.25). According to this result, we speculate that even though visceral endoderm genes are up-regulated in mutant embryos this does not interfere with the normal function of endoderm cells to replace visceral endoderm. Therefore we speculate that the defective phenotype of the mutant embryos is mainly caused by definitive endoderm defects at a later stage. But the visceral endoderm will form the yolk sac in the later development stages which uptake and breakdown the macronutrient from mother. We

cannot exclude that changes in gene expression in the extra embryonic part could also impair the development of embryo (Follit et al. 2014).

We further tested if the expression level of dysregulated genes in E7.75 embryos is altered in later developmental stages. We checked the genes which are most dysregulated in mutant embryos at E8.5 and E9.0. Consistent to the analysis at E7.75, at later developmental stages Gabrr1 and Mpv17l which are the most up-regulated genes show marked increase and Cer1 which is the most down-regulated gene is markedly reduced. Thus we could validate the microarray date and found the same dysregulated genes in the mutant embryos at later stages. Due to the complexity of early embryonic development and the expression profile of Sox17 in the early embryos, it is difficult to distinguish if these dysregulated genes are from visceral endoderm or definitive endoderm lineage cells. Additionally how these dysregulated genes affect the normal development of the embryos still needs to be investigated.

3.2.2 Setdb1 regulates the expression of imprinted genes

In mammalian genomes, there is a group of genes which is imprinted. These imprinted genes inherit the epigenetic markers from their parental origin which will affect their expression. These genes are expressed from one parental allele but are repressed from the other parental allele (Ideraabdullah et al. 2008). So far around 100 genes have been identified as imprinted genes, most of the clusters contain genes for noncoding RNAs which has been shown to repress the proximal protein-coding genes (Rougeulle et al. 2002). These imprinted genes could be either maternally or paternally expressed through the regulation of the corresponding imprinting control region (ICR). These ICRs are modified by either DNA methylation or histone modifications.

The question is to understand how the methylated ICR could affect the activity of the nearby genes? Interestingly, methylation markers are deposited in the paternal germ line in intergenic regions leading to the heritable repression from the paternally inherited chromosome. In contrast, methylation markers in the female germline are not placed in intergenic regions but are rather located on the promoters of imprinted genes (Bartolomei et al. 2011). So far, the best studied example of the repression of paternally methylated ICRs locating to an intergenic region is Igf2 and H19 (Hark et al. 2000). The enhancer region for both of the genes is located downstream of H19. The ICR placed upstream of the transcriptional start site of H19 containing a binding site for CTCF. This insulator protein can bind to the unmethylated maternal ICR and blocks the interaction with the enhancer of Igf2 rendering the inactivation of Igf2. However H19 could be activated by the interaction of the enhancer with the H19 promoter. In the paternal chromosome as CTCF could not bind to the methylated ICR the expression of Igf2 will be activated by the interaction between the enhancer and promoter. In contrast to paternally methylated ICRs, a maternally methylated ICR regulates the promoters of the imprinted genes for Igf2r and Airn (Sleutels et al. 2002). The ICR region located in the CpG-Island could act as promoter of Airn. In the paternally derived chromosome the CpG-island in the intron is unmethylated,

therefore the expression of Airn as a noncoding RNA could restrict the expression of Igf2r. In the maternally inherited chromosome the ICR is methylated, thus the Airn will be repressed and Igf2r is activated. There is evidence showing that the Airn ncRNA could recruit repressive histone modifications to inactivate the gene expression on the paternal chromosome (Nagano et al. 2008). Another interesting finding connects H3K9me3 to the regulation of H19 and Igf2 loci (Monnier et al. 2013). Transcribed H19 ncRNA cooperates with Mbd1 to repress the expression of Igf2. Loss of H19 results in the reduction of H3K9me3 in the DMR region (differentially methylated region is also called imprinting control region). As it is already known Mbd1 could form a complex with Setdb1 to repress gene expression and to maintain the H3K9me3 methylation during the replication. We assume that Setdb1 is also involved in the regulation of imprinted genes. We tested the expression level of these imprinted genes in Setdb1 mutant immortalized MEFs and primary MEFs. In both different cell types we could find the alteration of gene expression (Figure 2.4 and 2.5). Interestingly and surprisingly, both of the Igf2 and H19 genes are markedly reduced upon deletion of Setdb1. As chromatin long distance interaction is a major regulatory mechanism for Igf2 and H19, and enhancers of both genes are located downstream of these genes, we assume that Setdb1 is involved to regulating the chromatin structure of this locus. Loss of Setdb1 interferes with the interaction of enhancer with promoter of both genes. Thus, both genes cannot be activated upon deletion of Setdb1.

3.2.3 IAP elements are derepressed upon deletion of Setdb1 during early embryonic development

In mammals, more than 10% of the genome is derived from endogenous retrovirus (ERV) sequences which can be divided into three classes (Initial sequencing and comparative analysis of the mouse genome). In the normal situation, ERVs are transcriptionally silent in the host genome. But these parasitic sequence elements could also be reactivated and cause dysregulation of nearby cellular genes and also induces new mutations via replicative transposition (Walsh et al.1998). The intracisternal A type particle (IAP) retrovirus is one of the most aggressive parasitic sequence in the mouse genome.

Kap-1 which is a corepressor for the DNA sequence-specific KRAB-ZFP has been identified to be involved in the repression of endogenous retroviruses (ERVs) during early embryogenesis (Rowe et al. 2010; Wolf et al. 2007). Upon loss of KAP1 in ES cells, a range of ERVs, for example murine leukemia virus and IAP elements will be de-repressed. Also in early embryonic development IAP elements are reactivated upon deletion of Kap1. It has been further demonstrated that Kap1 deletion leads to the changes in DNA methylation and H3K9me3 on IAP elements. Kap1 mediated silencing is mediated by recruiting the histone methyltransferase Setdb1, heterochromatin protein 1 (HP1) and the NuRD histone deacetylase complex (Sripathy et al. 2006). Matsui showed that loss of Setdb1 in ES cells results in the reactivation of IAP elements and loss of H3K9me3 from these elements (Matsui et al. 2010). As Setdb1 plays a major role for the repression of ERV in ES cells and neural progenitor cells (Tan et al. 2012) it was interesting to identify if Setdb1 has a role for IAP silencing in endoderm

cells. First, we isolated mutant embryos at E8.5 and E9.5 and checked the expression of IAP elements. Interestingly, we found that IAP elements are also de-repressed in the mutant E8.5 and E9.5 embryos. Also in the sorted Setdb1 EGFP mutant endoderm cells reactivation of IAP elements was identified (Figure 2.42). But the up-regulation of these IAP elements in endoderm cells was much lower than in ES cells. These results illustrate that Setdb1 contribute to the silencing of endogenous retroviruses during endoderm development but a regulatory mechanism which is likely comparable to ES cells. However, if the depression of IAP elements influences expression of other genes and could impair development of the embryos needs to be clarified.

3.3 Loss of Setdb1 affects the properties of endoderm cells during in vitro

In vitro differentiation of ES cells become a very powerful method to study the molecular mechanism underlying specific cell lineage commitments. In our experiments the ES cells were differentiated into endoderm lineage cells by adding Activin A and Wnt3a (Yang et al. 2014). Upon differentiation, at day 2-3 the ES cells reach the mesendoderm stage and Foxa2 is activated. Sox17 will be activated at around day 4. As we are using EGFP reporter cells, the green signal start to be activated at day 4. For RNA-seq analysis, EGFP positive cells were sorted at day seven when the Setdb1 has been removed (proved by western and RT-PCR) (Figure 2.38). From the RNA-seq analysis, we could found that genes which facilitate endoderm development were up-regulated and the genes which repress the endoderm commitment were down-regulated (Figure 2.39).

Nanog and Sox2 are both highly expressed in stem cells and are involved in ES cell pluripotency and self-renewal. These genes have different potential for further cell lineage commitment (Wang et al. 2012). Nanog represses embryonic ectoderm differentiation and overexpression of Nanog facilitates endoderm lineage specification. In contrast to Nanog, Sox2 increases the differentiation to ectoderm but represses the commitment to the endoderm cell lineage (Thomson et al. 2011). Very interestingly from our RNA-Seq results we could see the up-regulation of Nanog but decreased expression of Sox2 in Setdb1 EGFP mutant cells. This means the cells are in a state more like endoderm cells. Mixl1 which is a mesendoderm gene is around 6 fold up-regulated in the differentiated Setdb1 mutant cells. This gene was shown to be related to endoderm development (Hart et al. 2002). Loss of Mixl1 in the embryos at E7.0 leads to a thickened primitive streak which lacks a morphologically recognizable node. At E8.5 the anterior-posterior axis of the mutant embryos is much shorter and the midline structure is strongly retarded. Mixl1 as a mesendoderm gene and plays an important role for the normal development of mesoderm and endoderm. However, overexpression of Mixl1 in the ventral marginal zone of Xenopus embryos leads to the repression of dorsal and ventral mesoderm differentiation and promoted the expansion of endoderm (Lemaire et al. 1998). The enforced expression of Mixl1 in mesodermal and endodermal precursors during mouse ES cell differentiation will cause different effects (Lim et al. 2009). By constitutive expression of Mixl1 during the mesoderm differentiation it is difficult to generate hematopoietic cells. Enforced overexpression of

Mixl1 during the endoderm differentiation from ES cells will increase the expression of definitive endoderm genes and promote the formation of endoderm cells. During differentiation, Activin A could induce the expression of Mixl1. There are H3K9me3 and H4K16ac deposited in the promoter region of Mixl1. Under the induction of Nodal TGF-β signals, Smad4-Smad2/3 and Trim33-Smad2/3 complexes will be formed and bind to H3K9me3 in promoter region of Mixl1 (Xi et al. 2011). The binding of this complex will displace HP1 and initiate the transcription through the recruitment of Pol II. From this experiment we know the poised H3K9me3 in the promoter region of Mixl1 works as bait which could induce the binding of the activating complex. Setdb1 which acts as a histone methyltransferase could stimulate the histone modification in the promoter region of this main regulator. We assume that the deposit of H3K9me3 is formed through the interaction of Setdb1 with the core pluripotency transcription factors. Thus we postulate that the lack of Setdb1 in endoderm cells will reduce the H3K9me3 in the promoter region of Mixl1 which will lead to the removal of HP1 in this region. The expression of Mixl1 will be activated. Eomes is considered to be upstream of Mixl1 and is also upregulated in the Setdb1 mutant differentiated cells. During embryonic development, Mixl1 expression in the primitive streak was lost in Eomes knock-out mice. There are papers showing that Eomes plays a pivotal role in mesendoderm differentiation and Mixl1 could facilities the differentiation of definitive endoderm. Both genes will repress the expression of T during differentiation. T which is down-regulated in Setdb1 EGFP mutant cells is necessary for the development of the mesoderm (Wilson et al. 1995). This means both Mixl1 and Eomes have the opposite role to T. This is also consistent with our result of upregulation of Eomes and Mixl1 but the down regulation of T in the differentiated cells upon deletion of Setdb1. It means that the differentiated mutant cells are prone to stay in the endoderm state. Foxa1, Foxa2 and Foxa3 are a family of transcription factors which are responsible for hepatocyte differentiation (Monaghan et al. 1993). All of these three genes start to be expressed in the endoderm region at around E6.5 to E8.0 and have been involved in gut development (Hiemisch et al.1997). Hnf1b is required for the organogenesis of the liver, the kidney and the pancreas and keeps expression for a long time. It is first detected in the visceral endoderm and activated in the definitive endoderm at around E8.0 (Coffinier et al. 1999). Our RNA-seq result indicates an increase of Foxa1, Foxa3 and Hnf1b. Interestingly Nodal and Wnt are also up-regulated in the differentiated mutant cells. Loss of Nodal will lead to the missing of the primitive streak and the Nodal signaling pathway is important for the formation of the endoderm. In the gastrulation stage, Wnt3 is expressed in the posterior epiblast and the primitive streak. The expression level of Wnt3 is a good biomarker for the potential of definitive endoderm development. ES cells are much easier to differentiate to endoderm cells with the higher level of Wnt3 (Jiang et al. 2013).

In summary, we could find most of the up-regulated genes (Mixl1, Eomes, Wnt3 and so on) are related to endoderm differentiation or initiation of endoderm commitment. But the down-regulated genes are more related to different cell lineages (Sox2 and T). Therefore, we think that cells without Setdb1 are

more responsive to external signals. With the external endoderm stimulus, the Setdb1 mutant endoderm lineage cells possess more endoderm properties.

However how does Setdb1 regulate the expression of these genes? As Setdb1 does not contain a DNA binding domain, there should be interaction partners of Setdb1 involved in its recruitment. In order to identify such interaction partners we performed Setdb1 pull down assays followed by mass-spectrometry identification.

Setdb1 was shown to be related to ES cell pluripotency by interacting with transcription factors. Loss of Setdb1 leads to the de-repression of the trophectoderm lineage gene Cdx2 in ES cells. The occupancy of Setdb1 in the promoter region of Cdx2 depends on the presence of Oct4. Setdb1 may form different complexes in different cell types. Additionally, Setdb1 was suggested to be involved in the establishment and maintenance of the H3K9me3 (Sarraf et al. 2004) and the extension of heterochromatin (Ichimura et al. 2005). Even though Setdb1 comprise an MBD-like domain, critical amino acid residues for binding methylated DNA are mutated. It is thus unlikely that Setdb1 could bind directly to target genes and thus there must be other interaction partners cooperating with Setdb1. Several different Setdb1 complexes have been identified from different cell types and stages, but proteins that would interact with Setdb1 in ES cells and endoderm cells are still not known (Schultz et al. 2003; Sarraf et al. 2004; Fritsch et al. 2010). In order to perform a detailed molecular analysis of Setdb1 in ES cells, we generated Setdb1 knock-in ES cells with an affinity-tag fused to the C-terminus of Setdb1. With this tool, we could identify interaction partners of endogenously expressed Setdb1. We carried out FLAG IP experiments and identified the Setdb1 interaction partners through mass-spec analysis. Interestingly, Atf7ip which has been identified as a factor interacting with Setdb1 in HeLa cells was also highly enriched in our IP experiments (Wang et al. 2003). This means that Setdb1 has the same regulatory mechanism in different cell types. DNA methylation has been known to be involved in gene repression. The function of DNA methylation is conducted by the binding of methyl-CpG binding domain proteins. Atf7ip is a very important factor which could facilitate gene repression through the binding to the transcriptional repression domain of Mbd1, one of at least five mammalian MBD proteins (Fujita et al. 2003). Setdb1 was also reported to be recruited to DNA methylated regions through Atf7ip to repress gene expression synergistically (Minkovsky et al. 2014). Because Atf7ip could facilitate the conversion of di-methylation to tri-methylation by Setdb1 and MBD1 can mediate the formation of heterochromatin (Uchimura et al. 2006), Setdb1 is possibly involved in Mbd1-dependent transcriptional repression through heterochromatin assembly.

From our list, we could also find Glp1, Dnmt1 and Kap1 binding to Setdb1. These interactors of Setdb1 have also been identified earlier (Fritsch et al. 2010). However, how Setdb1 is involved in different biological processes with these interactors and if the interaction is direct or indirect remain uncharacterized. Furthermore it needs to be clarified if the interaction partners that we found in ES cells also function in the context of endoderm differentiation.

4. MATERIAL AND METHOD

4.1 Cell biology methods

Cultivation of mammalian cells

MEF and ES cells are cultivated in High Glucose DMEM with L-Glutamine complemented with sodium pyruvate, fetal calf serum (Sigma), beta-mercaptoethanol, non-essential amino acids (PAA) and penicillin/streptomycin (PAA) in a 37°C incubator at 5% CO2. For ES cell culture medium is supplemented with leukemia inhibitory factor (LIF) and gelatinized tissue culture dishes or feeders covered dishes were used.

Immunofluorescence and microscopy

A Leica TCS SP5 confocal laser scanning microscope and a Zeiss LSM510 microscope were used to obtain the images. Sequential excitation at 405nm, 488 nm, 543 nm and 633nm are provided by diode, argon and helium-neon gas lasers, respectively. Emission detection ranges of the PMTs were adjusted to minimize crosstalk between the channels. Images were further analyzed using FiJi software.

Establishment of ES and MEFs cell lines

Blastocysts are isolated at 3.5 dpc with mouth pipette. Culture the blastocysts on the feeder coated 48 well plate with ES cell medium containing MEK-1 inhibitor. Until 5 to 7 days, the inner cell mass outgrow to form big colony then the colony can be trypsinized and transformed to bigger plate with feeders. The medium should be changed every day. At the first passages the cells could only be split when the colonies are formed as the new generated ES cells cannot grow very well at the first days. Embryos are isolated at E13.5. Removing head and livers from the embryos then chop these embryos into very small pieces with razor. Trypsinize the cell to single cells and then culture and expand the cells.

Endoderm differentiation experiment

Coat the plate with gelatin for half an hour later and then seed the Wnt3a feeders 3 hours before starting differentiation with 5-6x10^4 cells per 24 well. Trypsinize ES cells and pre-plate the ES cells two times to remove all the feeders. Seed 2-3x10^5 ES cells onto feeder (Wnt3a feeders) coated plate in 1 ml differentiation medium (Yang et al.2014) and change medium every day. For the feeder free endoderm differentiation experiment, skip the step of preparing the Wnt3a feeders instead add of Wnt3a into the differentiation medium. The culture plates need to be coated with gelatin half an hour

before the seeding. These cells need to be cultured for 6-7 days in the differentiation medium until they reach high differentiation efficiency.

FACS analysis the differentiated cells and FACS sorting

FACS Canto Flow Cytometer (BD Bioscience) was used to analyze the apoptosis of the differentiated control and mutant cells. After 7 days of differentiation Setdb1 EGFP reporter cells were stained with AnnexinV which is an apoptotic marker and were analyzed with the FACS machine to calculate the proportion of the apoptotic cells in the differentiated GFP positive cells. The cells used for the RNA-seq were sorted directly after day 7 of differentiation.

4.2 Molecular biology methods

Cloning of candidate proteins

CDNAs were reverse-transcribed from the RNA template purified from either mouse fibroblasts or embryonic stem cells. Primers were designed with gateway att-side overhangs. Cloning was performed using gateway cloning system (Invitrogen) following the manufacturer's instructions. Primers used for cloning are listed in Table 4.3.

RT-qPCR for monitoring different gene expression level

RNA of cells was harvested by using RNEasy (Qiagen). 100ng~1.25µg RNA was used for cDNA synthesis using Superscript III Kit (Invitrogen) and random hexameric primers (NEB). qPCR reactions were carried out in technical triplicates using a Roche Light Cycler 480 with FAST SYBR® Master Mix (Applied Biosystems), and gene-specific primers. Ct-values were normalized to the geometric mean of Actin or HPRT for each individual cDNA and fold changes where calculated by the 2-DDCt-method (Vandesompele et al. 2002). qPCR primers are listed in Table 4.4.

4.3 Biochemical Methods

Determination of protein concentration

The concentration of proteins was determined by Bradford assay (Bradford.1979) (Compton et al.1985).

SDS page gel

Separation of proteins by SDS-PAGE was performed in the Perfect Blue Dual gel Twin system (Peqlab) using precast gel cassettes (Invitrogen). Resolving and stacking gels were prepared according to the manufacturer's instructions using 30% (v/v) polyacrylamide solution (Rotiphorese, 37.5:1

acrylamide/bisacrylamide) and resolving gel buffer (375mM Tris/HCl pH 8.8) or stacking gel buffer (125mM Tris/HCl pH 6.8) respectively. Prior to loading samples were mixed with Roti Load (Roth) and heat-denatured for 7 min at 95°C. Various molecular weight protein standards were used from Bio-Rad/Peqlab. Electrophoresis was performed at 40 - 80 mA at RT for varying time. SDS gels were either used for Coomassie staining, silver staining or western blotting.

Coomassie staining of protein gels

Proteins were visualized in SDS page by incubating in staining solution [0.1% Coomassie R250, 10% acetic acid, 25% methanol] for 15 min at room temperature. Destain solution [8% acidic acid, 25% methanol in water] was used to remove excessive staining solution.

Silver staining of protein gels

SDS page was fixed in fixation solution [10% acetic acid, 30% isopropanol] for at least 2 h or overnight at room temperature. The gel was washed 3x 20 min in 30% ethanol followed by sensitizing using 0.01% $Na_2S_2O_3$ for 1 min at room temperature and washed 3x 30 sec with water. Staining solution [0.1% $AgNO_3$ in H_2O] was applied for 1 h at room temperature while shaking. The gel was again washed 3x 30 sec with water and incubated with the developer solution [3% Na_2CO_3, 0.05% formaldehyde, 0.02% $Na_2S_2O_3$ in H_2O] until the bands were clear. Reaction was stopped by adding 5% glycine solution. The gel was rinsed in water and stored in water at 4°C until analysis.

Western blot

Proteins separated by SDS-PAGE were transferred to a PVDF membrane (Roth). Transfer was achieved with a wet blot system (Criterion Blotter, Bio-Rad). Before the transfer, the polyacrylamide gel and the PVDF membrane were activated in MeOH and rinsed in blotting buffer [25mM Tris, 192 mM glycine, 10% methanol]. The transfer was performed at 400 mA for 1 h at 4°C. The membranes are incubated in Blocking Buffer [1 x PBS, 2.5% BSA and 2.5% milk] for 1 h at RT in order to saturate free binding sites on the membrane and hence minimize the non-specific background. After blocking the membranes were incubated either for 2.5 h at RT or o/n at 4°C with an appropriate dilution of the primary antibody. The membranes were extensively washed for 3 x 20 min in PBST Buffer [1 x PBS, 0.1% (v/v Tween 20)]. The HRP-coupled secondary antibody was incubated for 1-1.5 h at room temperature in the appropriate dilution in blocking buffer. The membranes were again washed 3x 20 min in PBST and exposed to X ray films using ECL developer solution mix (Amersham biosciences).

Generation of Setdb1 antibodies

Setdb1 antibody was raised in mouse immunized with peptide derived from the mouse protein. Antibody serum was tested on extracts from mouse embryonic stem cells and Setdb1 deleted MEFs.

Figure 4.1 Peptides used for antibody generation

Expression and purification of GST tagged proteins from E. coli

GST fusion proteins were expressed from pGEX6P1 vector in E. coli Bl21 (Stratagene). Bacteria were induced at OD=0.6 by adding 1 mM IPTG at 37°C for 3 h or overnight at 25°C. Harvested cells were resuspended in Lysis buffer [20 mM Tris pH 7.5, 150 mM NaCl, 2 mM EDTA, 1mM DTT, complete (Roche)] and disrupted using a Branson sonicator. Suspension was adjusted to 1% Triton and incubated for 30 min at 4°C. Cell debris was removed by centrifugation 60 min 12000 rpm 4°C. GST tagged proteins were bound to Glutathione-S-Sepharose beads (Amersham Biosciences) for 1 h 4°C rotating. After washing with 10x volume of wash buffer I [20mM Tris pH 7.5, 500 mM NaCl, 2 mM EDTA, 1% Triton-X-100 and 1mM DTT], wash buffer II [20 mM Tris pH 7.5, 150 mM NaCl, 2 mM EDTA, 0.1% TritonX-100 und 1mM DTT] and wash buffer III [20 mM Tris pH 7.5, 150 mM NaCl, 2 mM EDTA und 1mM DTT] bound proteins were eluted with elution buffer [10mM Tris (pH 8.0) and 10 mM Glutathion], dialyzed against 1xPBS, 20% glycerol then snap frozen and stored at -80°C.

Co-immunoprecipitation

Nuclei from wild type and Setdb1 HA-FLAG ES cells were isolated by spinning through a Ficoll gradient. The nuclear pellet was resuspended in low salt IP Buffer [50mM Tris pH 7.5, 150mM NaCl, 1mM EDTA, 20% glycerol, 0.1% NP40, proteinase inhibitor cocktail (Roche)] followed by addition of benzonase and incubation for 15 min at 37°C. Adjust salt concentration to 300mM and incubate for 30 mins on ice followed by mild sonication 2x 10 sec at amplitude 10 in a Branson sonifier. Insoluble proteins were separated by spinning for 30 min at 13000 rpm at 4°C and repeated once. The extract was incubated with anti-flag M2 agarose beads for 2 hours at 4°C on a rotating wheel. The beads were washed in IP buffer containing 300 mM NaCl for five times and eluted with SDS sample buffer. Proteins were separated on SDS-polyacrylamidgels and analyzed by western blotting using antibodies for different purposes.

4.4 Embryology methods

Whole mount embryo X-gal staining

Embryos were dissected carefully then fix embryos with 4% paraformaldehyde/PBS at 4°C [E7.5/5min;E8.5/10min]. After washing with LacZ rinse solution [2mM MgCl2; 0.02% NP-40; 0.01% sodium deoxycholate in PBS] the embryos were stained with X-gal staining solution [1mg/ml dimethylformamide; 5mM potassium ferricyanide; 5mM potassium ferrocyanide in LacZ rinse solution] O/N at 37°C.

In situ hybridization

Dissect embryos in autoclaved PBS and fix in 4% paraformaldehyde (PFA) in PBS at 4°C overnight. Add 1 ml prehybridization buffer [50% Formamide, 5xSSC pH5.4, 1%SDS, 50µg/ml yeast tRNA, 50 µg/ml Heparin] to the embryos and swirl for 5 min then replace with 2 ml fresh prehybridization buffer and incubate at 70°C for at least 2 hours. Replace the prehybridization buffer with hybridisation mix including 500ng to 1.0 µg/mL DIG. Labeled RNA probe which has been denatured at 80°C for 5 min was incubated with embryos overnight at 70°C. The next day, quick wash with 1 ml of hybridization buffer at 70°C and 3x30 min wash with prewarmed solution I [50% formamide, 5X SSC, pH 4.5, 1% SDS] at 70°C. Afterwards wash 3 times with TNT [10 mM Tris-HCl, pH 7.5, 0.5 M NaCl , 0.1% Tween-20] at RT for 5 min followed by treatment with 100µg/ml RNase A for 60 min in TNT at 37 °C. Then the embryos were washed with TNT: Solution II [50% formamide, 2X SSC, pH 4.5, 0.2% SDS in regular MilliQ H_2O] (1:1) for 5 min at RT then washed 3x30 min with solution II at 65 °C followed by 3 x wash for 5 min each in MAB [100mM Maleic acid, 150 mM NaCl, 2mM Levamisole, 0.1% Tween-20.] at RT. Add 1-2 ml of antibody solution and rock gently at 4°C overnight after the Preblock embryos in 10% lamb serum in MAB/2% blocking reagent for 2-3 hours at RT. In the third day carry out the whole day wash with MAB. Until the fourth day wash the embryos 3 x with NTMT [100 mM NaCl , 100 mM Tris-HCl, pH 9.5, 50 mM MgCl2 0.1Tween-20, 2 mM Levamisole] for 10 min at RT followed by the incubation of the embryos in 1-2 ml BM purple with levamisole at RT to develop colors. Stop the chromogenic reaction by washing 3 times in PBST with PH at 4.5.

The embryos could also be dehydrated by 25% MeOH/PBST, 50% MeOH/PBST, 75% MeOH/PBST and 100% MeOH for 10 min each and kept for a year at -20°C. Then the embryos could be redehydrated by MeOH/PBST (75%MeOH -> 50% MeOH -> 25% MeOH -> PBST) series in reverse for 5 min each.

Whole mount embryo immunostaining

Embryos were isolated in the dissection medium (PBS+) [PBS containing Mg_2+ ad Ca_2+]. Then these embryos were fixed for 20 min at RT in 2% PFA in PBS+ followed by permeabilizing for 10 to 15 min in the permeabilization solution [0.1 M Glycin/0.1% TritonX-100]. Transfer these embryos into

blocking solution [0.1% Tween-20; 10% FCS; 0.1% BSA; 3% Rabbit, Goat or Donkey serum]. 2-3 hours later the primary antibodies were added into blocking solution and incubated O/N at 4°C.The next day leave these embryos for another 2 hours at RT. After 3 times wash with PBST, these embryos were incubated with secondary antibody for minimum 3 hours at RT then wash with PBST for 3 times. Afterwards these embryos were dehydrated with a series of 30%, 60% and 80% Glycerol in PBST+ for 5 min each. Then embed the embryos in the embedding medium for the microscopy analysis.

Embryo preparation for paraffin section and Hematoxylin and Eosin (H&E) Staining

Embryos were fixed in 4% PFA at 4°C O/N and wash quickly with PBS. Different concentration of Ethanol was used to dehydrate the embryos (25%, 50%, 75%, 96% and 100% ethanol). Then Xylol was used to dehydrate the embryos followed by incubation in paraffin at 65°C O/N. Next day, the embryos could be embedded and oriented in the right direction.
The embedded embryos were sectioned from different layers by microtome. Fist these slide were deparaffinized in Xylene and then rehydrated by 100%, 96%, 75% and 50% ethanol. Afterwards these slides were stained with Hematoxylin and then counterstained with Eosin. After staining the slides were dehydrated and mounted with cytoseal.

4.5 Mouse methods

Generation of conditional mouse knock-out stains

Heterozygous mice with successful germ line transmission of the targeted allele were generated through the EUCOMM project. Setdb1 beta-gal mouse was introduced Flp recombinase to remove the beta-gal gene cassette resulting in “flox” alleles. To disrupt Setdb1 protein, homozygous Setdb1$^{flox/flox}$ mice were crossed with different Cre lines. To monitor the Setdb1 deleted cells Setdb1$^{flox/flox}$ mice were crossed with CAG-CAT-EGFP reporter mice (Nakamura et al. 2006).

Genotyping

Genomic DNA was isolated from tail biopsies. Proteinase K (Invitrogen) in tail buffer (50 TRIS pH 7.4, 100mM EDTA, 100mM NaCl, 1% SDS) at 55°C overnight was used to remove proteins. DNA was precipitated by high salt and isopropanol and resuspend in 1xTE buffer. Genotyping was performed as standard endpoint PCR reaction in 25µl volume.
For very less cell numbers of early embryos (earlier than E8.5), cells were lysed with Lysis buffer (50mM KCl, 10mM Tris HCl PH8.0, 2mM $MgCl_2$, 0.45% NP-40, 0.45% Tween20) and protein was degraded with Proteinase K at 55°C for at least 3 hours. Then inactivate proteinase K by heating at 95 °C for 10~20 Min.

Table 4.1 Cloning vectors

vector	company	description
pDonor Zeo	Invitrogen	Bacterial expression vector, containing att sides for gateway cloning
pEGFP N1	Invitrogen	Mammalian expression vector, C-terminal EGFP tag, CMV promoter, polyadenylation signal from SV40
pCMV myc	Invitrogen	Mammalian expression vector, N-terminal c-myc, HA tag, CMV promoter, polyadenylation signal from SV40
pGex6P1	Invitrogen	Bacterial expression vector, N-terminal GST tag, tac promoter, PreScission cleavage site
pET21	Novagen	Bacterial expression vector

Table 4.2 Bacteria strains

Strain	company	genotype
Bl21 (DE3)	NEB	F– ompT gal dcm lon hsdSB(rB- mB-) λ(DE3 [lacI lacUV5-T7 gene 1 ind1 sam7 nin5])
DH5 alpha	Promega	F- endA1 glnV44 thi-1 recA1 relA1 gyrA96 deoR nupG Φ80dlacZΔM15 Δ(lacZYA-argF)U169, hsdR17(rK- mK+), λ–
Stellar	clontech	F–, ara,Δ(lac-proAB) [Φ80d lacZΔM15], rpsL(str), thi, Δ(mrr-hsdRMS-mcrBC), ΔmcrA, dam, dcm

Table 4.3 Primer sequence

Genotyping primer For Setdb1 mouse		
Setdb1 flox	F	TCTTTGAGCCAGAGCAAGCAGG
Setdb1 flox	R	TGGCAGCTCACAAGCACATTCA
setdb1 beta-gal	F	AGTAAATCTTTGAGCCAGAGCAAGC
setdb1 beta-gal	R	TTCTTCTGTTAGTCCCAACCCCTT
Setdb1 flp	F	GTGGATCGATCCTACCCCTTGCG
Setdb1 flp	R	GTCCAACTGCAGCCCAAGCTTCC
Setdb1 delta	F	AGTAAATCTTTGAGCCAGAGCAAGC
Setdb1 delta	R	TCACAGAGATCCACCTGCCTTTCCT
Setdb1 Sox17-cre	F	GTGTATAAGCCCGAGATGG
Setdb1 Sox17-cre	M	CTCAACTGTTCAAGTGGCAG
Setdb1 Sox17-cre	R	GATCTATGGTGCCAAGGATGAC
Cloning primer		
Setdb1 698f		GGGGACAAGTTTGTACAAAAAAGCAGGCTACACC ATGTTGGACATCACCTATG
Setdb1 1308f		GGGGACCACTTTGTACAAGAAAGCTGGGTCAAGA AGTCTCCCTCTGCATT
Mutagenesis primer		
Setdb1 H1241L f		CCGCTACCTCAATCTGAGTTGCAGCCCCAAC
Setdb1 H1241L r		GTTGGGGCTGCAACTCAGATTGAGGTAGCGG
Setdb1 H1241R f		GCCGCTACCTCAATAGGAGTTGCAGCCCCAAC
Setdb1 H1241R r		GTTGGGGCTGCAACTCCTATTGAGGTAGCGGC
Setdb1 C1243A f		CTACCTCAATCACAGTGCCAGCCCCAACCTGTTTG
Setdb1 C1243A r		CAAACAGGTTGGGGCTGGCACTGTGATTGAGGTAG

Table 4.4 Primers used for quantitative PCR

Gene		Sequence
HPRT	F	ATGAGCGCAAGTTGAATCTG
HPRT	R	CAGATGGCCACAGGACTAGA
GAPDH	F	TCAAGAAGGTGGTGAAGCAG
GAPDH	R	GTTGAAGTCGCAGGAGACAA
Oct4	F	AGACCATGTTTCTGAAGTGCCCG
Oct4	R	CGCCGGTTACAGAACCATACTCG
IAP U3	F	CGA GGG TGG TTC TCT ACT CCA T
IAP U3	R	GAC GTG TCA CTC CCT GAT TGG
IAP pol	F	CTT GCC CTT AAA GGT CTA AAA GCA
IAP pol	R	GCG GTA TAA GGT ACA ATT AAA AGA TAT GG
IAP global	F	CGGGTCGCGGTAATAAAGGT
IAP global	R	ACTCTCGTTCCCCAGCTGAA
Igf2r	F	GCTGCCAGCCTTCAGATTCACA
Igf2r	R	TTCTTGCAGGCTGCAGTAGTCCTC
Airn	F	AGCCCTTCCTTTCTTGTTTCCTTG
Airn	R	AAATCTCACTATTCCCGCTCCCTG
Igf2	F	GGGAGCTTGTTGACACGCTTCA
Igf2	R	AAGTACGGCCTGAGAGGTAGACACG
H19	F	CATGTCTGGGCCTTTGAA
H19	R	TTGGCTCCAGGATGATGT
Setdb1 Exon4	F	AGCAGAACTCCAAAAGACCAGAAGC
Setdb1 Exon4	R	TCTTGCCCAGAATCCGCATG
Gabrr1	F	CACACCACCACAAAACTAGCC
Gabrr1	R	TGGCAGGAAAGTAGGTTTGG
Mpv17L	F	TCATGTACTGGCCCTTTGTG
Mpv17L	R	TATGGACTGCAGTGTACCATCG
Rex2	F	TGTTTGCTCCTCACCAAGAA
Rex2	R	CCTCCGATGAGAAGTCCAAA
Cer1	F	ACTGTGCCCTTCAACCAGAC
Cer1	R	CATTTGCCAAAGCAAAGGTT
Tbox4	F	GAGGATGTTCCCCAGCTACA

Tbox4	R	ATCCGGGTGCACATAAAGTC
Foxa1	F	CCTCCGATGAGAAGTCCAAA
Foxa1	R	TGTTAGGGACTGTGAAGATG
Nodal	F	TTCAAGCCTGTTGGGCTCTAC
Nodal	R	TCCGGTCACGTCCACATCTT
Hnf1b	F	AGGGAGGTGGTCGATGTCA
Hnf1b	R	TCTGGACTGTCTGGTTGAACT
Wnt3	F	GGAGCGACAGTCAGATCTCC
Wnt3	R	AGAAGAGACCTGCCTCCACA

Table 4.5 Antibodies used for immunofluorescence and western blot

Antibody	**company**
Setdb1	Santa Cruz
Flag	Sigma
Sox17	Acris/Novus
Foxa2	Abcam
Brachyury	Santa Cruz
Pecam1	BD science
H3K9me1	IMP
H3K9me2	IMP
H3K9me3	IMP
H4K20me3	IMP
H3K9AC	Abcam
GFP	Aves
Ki67	Zytomed
Caspase3	Zytomed
H3S10ph	Abcam

ABBREVIATIONS

ADP: adenosine diphosphate

ATP: adenosine triphosphate

BSA: bovine serum albumin

cDNA: complementary DNA

CKO: conditional knock-out

DAPI: 4,6-Diamino-2-phenylindol

DNA: deoxyribonucleic acid

ESCs: embryonic stem cells

GFP: Green Fluorescent Protein

GST: Glutathion-S-Transferase

H3K9me3: trimethylation of histone H3 at lysine 9

H4K20me3: trimethylation of histone H4 at lysine 20

HMTase: histone lysine methyaltransferase

HP1: heterochromatin protein 1

kb: Kilobases

kDa: Kilodalton

KO: knockout

miRNA: microRNA

mRNA: messenger RNA

ncRNA: non coding RNA

PCR: polzmerase chain reaction

qRT-PCR: quantitative Real-time polymerase chain reaction

RNA: Ribonucleic acid

SET: suppressor of variegation, enhancer of zeste and trithorax

Setdb1: SET domain, bifurcated 1

Suv39h1: suppressor of variegation 3-9 homolog 1

Suv39h2: suppressor of variegation 3-9 homolog 2

Suv4-20h1: suppressor of variegation 4-20 homolog 1

Suv4-20h2: suppressor of variegation 4-20 homolog 2

XEN: extraemryonic endoderm

ACKNOWLEDGEMENTS

First I would like to thank my supervisor Gunnar Schotta who provides me the position and interesting project. During my PHD period he taught me not only the knowledge of my project but also the rigorous scientific attitude to my work.

I thank my colleagues Alexander Nuber, Alessandra Pasquarella, Dennis Sadic who start with me together in the lab and provide a lot of technic support in my whole PHD life. Filippo Cernilogar for the help of Chip experiment. It is also a nice working atmosphere with Sahra Pilz, Gustavo Pereira de Almeida and Maryam Kazerani in the lab.

I am really thankful to my former colleagues Silvia Dambacher, Matthias Hahn, Maike Schulte and Stanimir Dulev for the help in my experiment and interesting discussion about my project.

I thank my collaborators Silvia Engert, Stefan Hasenöder and Dapeng Yang from Lickert lab teaching me the technics about mouse development. Irmler Martin for the microarrary analysis.

I am really lucky to work in the stimulating environment of the Becker department.

Finally, I express great gratitude towards my wife Jianhua Li to be always standing by my side to support me.

CURRICULUM VITAE

Personal information

Name	Rui Fan
Date of birth	1983.06.13
Place of birth	Shi Jia Zhuang. He Bei province. China
Nationality	Chinese

Education background

09, 2003 - 07, 2006 Bachelor degree in Animal science

Northwest A&F University (NWSUAF).

Graduation thesis: The analysis of the content of the fatty acids in different lactation periods of Xinong saanen dairy goats

Professor Dr. Jun Luo

09, 2006 – 08, 2009 Master degree in Animal genetics

Graduation thesis： Diversity and Population Structure in Nine Chinese Indigenous Goat Breeds

Professor Dr. Jun Luo

09, 2009– ongoing PHD in Dr. rer. Nat

Adolf Butenandt Institute, Ludwig-Maximilian University Munich

Professor Dr. Gunnar Schotta

Table 1. Affymetrix array data list of Setdb1^{END} embryos. These genes which are more than 1.2 fold change are listed.

Gene symbol or ID	Ratio Mut/Ctrl	rawp
Slc13a4	0,48	3,22E-03
Reep6	0,60	1,63E-02
Klb	0,57	2,58E-03
Slc2a2	0,57	2,34E-03
Xlr5c	0,59	6,95E-04
Chd7	0,82	2,11E-01
Gar1	0,69	1,23E-02
Capn2	0,71	2,21E-02
Chd7	0,85	2,82E-01
Setdb1	0,62	7,17E-05
Nolc1	0,75	6,53E-02
Xlr5c	0,64	1,84E-03
Rnf213	0,81	2,07E-01
Epb4.1l3	0,79	1,58E-01
Rbm25	0,77	1,11E-01
Rbm25	0,77	1,16E-01
Supt16h	0,80	1,50E-01
Slc7a7	0,61	3,10E-04
Slc20a1	0,68	2,22E-03
Sgk1	0,62	7,99E-04
Ddx21	0,76	6,06E-02
Pbrm1	0,82	1,98E-01
Slc16a6	0,66	1,83E-03
Naa15	0,80	1,30E-01
Rad54l2	0,80	1,43E-01
Trim44	0,82	1,76E-01
Cer1	0,65	1,33E-04
Chd7	0,90	4,09E-01
Cldn2	0,69	4,39E-03
C330019G07Rik	0,89	3,52E-01
GENSCAN00000007344	0,82	1,63E-01
Marcksl1	0,74	4,63E-02
Rbm47	0,69	7,62E-03
Chd7	0,89	3,46E-01
Dnajc13	0,78	7,94E-02
2210011C24Rik	0,64	9,62E-04
Ckap2l	0,77	4,10E-02
Purb	0,85	2,59E-01
Chd7	0,93	4,83E-01
Chd7	0,91	3,97E-01
Thoc4	0,73	3,44E-03
Foxc2	0,77	7,37E-02
Stox2	1,04	6,85E-01
Eif3b	0,80	8,51E-02
Kif5b	0,88	3,11E-01
Ncl	0,83	1,76E-01
Kdr	0,74	1,68E-02
Pbrm1	0,83	2,16E-01
Myo9a	0,87	2,85E-01
Hnrnpu	0,84	2,16E-01
Igf2bp1	0,89	3,59E-01
Opa3	0,77	3,83E-02
Tcf15	0,70	1,36E-04
Rrp1b	0,81	1,31E-01
Zfp259	0,74	5,96E-03
Srsf2ip	0,88	3,01E-01
Elovl6	0,82	1,35E-01
Ppp1r7	0,82	1,38E-01
Odc1	0,70	1,92E-03
Srp72	0,83	1,49E-01
Srrm2	0,83	1,84E-01
Yars	0,79	6,97E-02
Stxbp4	0,93	4,62E-01
Zbed3	0,79	4,70E-02
A530032D15Rik	0,80	7,75E-02
4932438A13Rik	0,90	3,81E-01
Ltn1	0,78	4,92E-02
Smc3	0,88	3,34E-01

Igfbp5	0,77	3,05E-02
Ftsj3	0,80	6,12E-02
Ckap5	0,84	1,84E-01
Cdk12	0,89	3,46E-01
Xlr3c	0,73	1,21E-03
Zc3h4	0,82	1,27E-01
Usp8	0,83	1,35E-01
Rbms1	0,82	9,42E-02
Podxl	0,84	1,69E-01
Prpf40a	0,83	1,34E-01
Pabpc4	0,79	3,83E-02
Ltbr	0,71	3,56E-05
Sfrp1	0,88	3,04E-01
Ltn1	0,81	7,39E-02
Aff4	0,92	4,39E-01
Trip12	0,86	2,26E-01
Sel1l3	0,71	5,19E-04
Eif3a	0,81	7,88E-02
GENSCAN00000029169	0,74	1,94E-03
Mtap4	0,85	2,14E-01
Hspa4	0,83	1,11E-01
Scpep1	0,74	4,52E-03
Arid3c	0,69	1,08E-04
C230081A13Rik	0,94	4,83E-01
Srrm1	0,85	2,06E-01
Xlr3a	0,74	1,74E-03
Luzp1	0,86	2,65E-01
Pabpc4	0,80	4,38E-02
Rnasen	0,91	3,91E-01
Eif3j	0,80	5,39E-02
Pabpc4	0,80	4,83E-02
Hnrnpa3	0,87	2,63E-01
Hnrnpa3	0,87	2,63E-01
Wnk3-ps	0,83	1,17E-01
Dhx8	0,82	7,86E-02
Brwd3	0,83	1,53E-01
Pabpc1	0,85	1,90E-01
Gnl3l	0,81	6,94E-02
4932438A13Rik	0,96	5,81E-01
Eif3j	0,79	3,67E-02
Lyar	0,83	1,23E-01
ENSMUST00000150411	0,77	6,81E-03
Hnrnpa3	0,86	2,52E-01
Adamts9	0,83	1,32E-01
Arhgap11a	0,82	1,16E-01
Tet1	0,93	4,86E-01
Srgap1	0,82	9,42E-02
Dhx29	0,81	5,40E-02
Pabpc4	0,80	5,81E-02
Actn4	0,86	2,58E-01
Nf2	0,85	1,90E-01
Myo9a	0,91	4,24E-01
Tgs1	0,84	1,37E-01
4932438A13Rik	0,92	4,53E-01
Tet3	0,85	1,97E-01
Pvr	0,74	1,45E-03
Ddx24	0,81	4,19E-02
Psmc2	0,77	3,03E-03
Nfe2l2	0,79	2,42E-02
Hnrnpa3	0,87	2,53E-01
Odc1	0,74	2,04E-03
GENSCAN00000041795	0,80	3,76E-02
Ywhab	0,84	1,33E-01
Igf2bp1	0,84	1,32E-01
Bms1	0,83	1,14E-01
Sox17	0,74	8,67E-04
Hnrnpd	0,85	1,73E-01
Mns1	0,84	1,51E-01
Hnrnpa3	0,87	2,83E-01
Fus	0,86	1,83E-01
Crebbp	0,92	4,53E-01
Ddx46	0,92	4,33E-01
Hnrnpa3	0,88	2,90E-01

Ltn1	0,82	8,01E-02
Ogfr	0,81	4,42E-02
Gemin5	0,81	7,37E-02
Eif3c	0,87	2,48E-01
Smarca4	0,90	3,67E-01
Hnrnpul2	0,87	2,63E-01
Slc16a1	0,75	3,07E-03
Ubqln2	0,86	2,30E-01
Mprip	0,94	5,27E-01
Csda	0,85	1,48E-01
Zdbf2	0,83	9,37E-02
Bmpr2	0,87	2,67E-01
Mettl1	0,75	4,65E-03
Chd8	0,85	1,69E-01
Dkc1	0,86	1,79E-01
Hnrnpa3	0,87	2,53E-01
Sart1	0,91	3,72E-01
1200009O22Rik	0,76	1,18E-03
Hnrnpa0	0,82	5,25E-02
Actn1	0,87	2,42E-01
Slco3a1	0,80	1,81E-02
Chd7	0,96	5,70E-01
Aak1	0,85	1,76E-01
Ddc	0,79	1,56E-02
Fscn1	0,88	2,60E-01
Kpnb1	0,84	1,07E-01
Ddx23	0,83	9,66E-02
Ccdc86	0,82	8,39E-02
Usp7	0,88	2,65E-01
Nudt11	0,75	1,76E-03
Trps1	0,90	3,41E-01
Zfp398	0,79	1,70E-02
Ralbp1	0,87	2,02E-01
Clint1	0,83	6,70E-02
Cltc	0,83	8,65E-02
Arhgap1	0,84	9,65E-02
Bat2l2	0,92	4,76E-01
Setx	0,87	2,36E-01
Chd7	0,88	2,51E-01
Zc3h18	0,84	1,09E-01
Sall4	0,85	1,46E-01
Srp68	0,86	1,75E-01
Ltn1	0,82	6,32E-02
GENSCAN00000006406	0,81	2,58E-02
Lpgat1	0,78	4,03E-03
Frmd4a	0,87	2,24E-01
Igf2bp3	0,86	1,65E-01
Pbrm1	0,87	1,98E-01
Pde3a	0,78	8,20E-03
Hectd1	0,87	2,17E-01
Nhs	0,81	2,79E-02
Psmd1	0,85	1,21E-01
Chd7	0,89	3,24E-01
Caprin1	0,84	8,50E-02
Hsp90b1	0,86	1,53E-01
Dhcr24	0,83	5,09E-02
Ankrd17	0,92	4,29E-01
Fam98a	0,78	2,57E-03
Whsc1	0,90	3,60E-01
Nono	0,87	2,12E-01
Setd5	0,92	4,30E-01
Vim	0,85	1,59E-01
Tnks	0,90	3,22E-01
Gm340	0,91	4,11E-01
Xpnpep1	0,83	6,49E-02
Mdn1	0,83	7,38E-02
Zmiz1	0,96	5,96E-01
Gprc5c	0,84	8,28E-02
Wbp11	0,86	1,87E-01
Dnmt1	0,87	2,18E-01
Ddx18	0,81	1,57E-02
Pitpna	0,80	1,52E-02
Zeb2	0,96	5,82E-01
E430025E21Rik	0,86	1,64E-01

Tcf25	0,84	8,48E-02
Hcfc1	0,88	2,40E-01
Nfyc	0,79	2,81E-03
GENSCAN00000005602	0,81	2,64E-02
4732471D19Rik	0,91	3,95E-01
Trip4	0,81	2,47E-02
Stip1	0,83	6,43E-02
Ssrp1	0,82	4,55E-02
Vcp	0,85	9,44E-02
Pa2g4	0,81	1,57E-02
Sec63	0,88	2,75E-01
Hs6st2	0,83	4,53E-02
Mcm6	0,85	1,04E-01
Bbx	0,87	1,96E-01
Rest	0,88	2,47E-01
Chd7	0,97	6,32E-01
Hdgf	0,87	1,84E-01
GENSCAN00000044609	0,83	5,42E-02
5730590G19Rik	0,94	5,27E-01
4933411K20Rik	0,83	5,33E-02
Zmym4	0,88	2,35E-01
Usp42	0,86	1,33E-01
2010305A19Rik	0,76	4,86E-04
Chd7	0,87	2,23E-01
Spna2	0,89	2,88E-01
Nmt2	0,83	4,46E-02
2610507B11Rik	0,88	2,55E-01
Gna11	0,80	6,43E-03
Rangap1	0,82	4,32E-02
Mis12	0,79	3,72E-03
C79407	0,89	2,71E-01
Hadha	0,85	9,96E-02
Nudc	0,84	6,66E-02
D8Ertd82e	0,86	1,61E-01
Prc1	0,81	1,82E-02
Zfp568	0,83	5,07E-02
Gtf2i	0,89	2,51E-01
Mia3	0,90	3,35E-01
Lars	0,85	9,53E-02
Polr3c	0,84	6,61E-02
Hnrnpab	0,83	3,03E-02
4932438A13Rik	0,95	5,37E-01
Fam98b	0,87	1,89E-01
4931431F19Rik	0,81	1,06E-02
Igf2bp2	0,88	2,41E-01
Cdr2	0,78	2,12E-03
Ppfibp1	0,83	4,65E-02
Zscan4-ps2	0,84	7,44E-02
Zfp710	0,84	7,42E-02
Npc1	0,83	4,75E-02
Abcf1	0,88	2,12E-01
Lrpap1	0,82	2,79E-02
Hsp90aa1	0,84	5,87E-02
Supt5h	0,88	2,14E-01
Dnajc13	0,87	2,05E-01
Tpm3	0,84	5,50E-02
Slc39a7	0,83	3,92E-02
Myo1b	0,85	1,08E-01
Smchd1	0,87	1,71E-01
Birc6	0,88	2,54E-01
Arhgef5	0,85	9,25E-02
Ebf1	0,85	1,04E-01
Ankrd13a	0,85	1,01E-01
Nup214	0,88	2,55E-01
GENSCAN00000033295	0,83	3,34E-02
Anks4b	0,78	9,28E-04
Smarca5	0,90	3,18E-01
Heatr1	0,83	3,22E-02
2900092E17Rik	0,79	3,80E-03
Sh3kbp1	0,93	4,40E-01
Prss12	0,76	1,31E-03
Dhx38	0,89	2,77E-01
Ube4b	0,93	4,47E-01

Rprd2	0,89	2,98E-01
Inpp5a	0,81	8,63E-03
Fam83b	0,80	7,06E-03
Arl2bp	0,82	1,75E-02
Hsp90aa1	0,86	1,16E-01
Gm5471	0,81	8,55E-03
Ppm1g	0,82	1,50E-02
Hyou1	0,87	1,73E-01
Ezr	0,85	1,00E-01
Ncapd2	0,89	2,68E-01
Rapgef2	0,93	4,42E-01
Zfp57	0,83	3,13E-02
GENSCAN00000044605	0,85	7,20E-02
Gnl2	0,86	1,15E-01
Synj2	0,80	6,37E-03
Sec16b	0,81	9,99E-03
Dnajc11	0,85	6,76E-02
Zeb1	0,88	2,21E-01
Pdxdc1	0,85	7,97E-02
Nrp2	0,90	2,80E-01
Smarcd1	0,86	1,05E-01
Nudt10	0,75	2,19E-03
Elac2	0,84	2,75E-02
ENSMUST00000120104	0,82	2,35E-02
Fat3	0,92	4,26E-01
Taf3	0,90	3,17E-01
Nudc	0,88	1,94E-01
Dennd5b	0,88	1,72E-01
Lad1	0,84	5,01E-02
Grinl1a	0,86	8,78E-02
Polr1a	0,86	1,27E-01
Ltn1	0,86	1,04E-01
Hdlbp	0,93	4,67E-01
GENSCAN00000048589	0,87	1,25E-01
Ildr1	0,78	1,56E-03
Zfp106	0,97	6,50E-01
Rcor1	0,86	8,67E-02
Ppp3ca	0,91	3,31E-01
Pla2g6	0,85	6,80E-02
Rapgef1	0,93	4,36E-01
Coq5	0,84	4,18E-02
Smurf1	0,86	8,21E-02
Fam3c	0,82	8,34E-03
Psmc1	0,80	2,75E-03
Nasp	0,89	2,29E-01
ENSMUST00000120860	0,81	7,89E-03
Sae1	0,85	5,49E-02
Zfp281	0,88	1,94E-01
Smarca5	0,91	3,42E-01
Qrich1	0,88	1,93E-01
Anp32b	0,86	9,07E-02
GENSCAN00000031128	0,81	2,88E-03
Hsp90aa1	0,86	1,04E-01
Eme1	0,83	1,24E-02
Golm1	0,94	4,89E-01
Tbl1x	0,90	3,18E-01
Smyd5	0,84	4,49E-02
GENSCAN00000016966	0,86	9,09E-02
Ddx18	0,82	7,19E-03
Ctnnd1	0,89	2,52E-01
Tex2	0,82	1,14E-02
Samhd1	0,88	1,63E-01
Myh10	0,90	3,02E-01
Sdha	0,86	7,01E-02
Ddx6	0,88	1,50E-01
Tsr1	0,83	1,78E-02
Mapk14	0,82	1,15E-02
Mtap	0,83	7,42E-03
Cdca2	0,84	2,99E-02
Tmx2	0,76	2,06E-03
D10Wsu52e	0,84	1,97E-02
Ide	0,84	2,50E-02
Myst2	0,85	4,34E-02
Ltn1	0,87	1,31E-01

Map3k1	0,90	3,07E-01
Tpm3	0,88	1,71E-01
Huwe1	0,95	5,44E-01
Mybl2	0,90	2,96E-01
Ly75	0,87	1,25E-01
Neo1	0,91	3,25E-01
X02935	0,83	1,20E-02
Sept9	0,93	4,44E-01
Nacc1	0,89	1,89E-01
Thoc5	0,90	2,51E-01
Dnajb11	0,81	1,98E-03
Acsl1	0,85	4,48E-02
Acaca	0,89	2,10E-01
Ptpdc1	0,83	6,90E-03
Fam180a	0,82	2,36E-03
Zfp300	0,80	7,33E-04
Epb4.1	0,99	7,27E-01
Epb4.1l2	0,91	3,51E-01
Colec12	0,96	5,78E-01
Rrp1	0,91	2,95E-01
Gpd2	0,87	1,10E-01
Ube2r2	0,91	3,17E-01
Ppp2r5d	0,91	2,94E-01
ENSMUST00000119244	0,85	4,01E-02
Brpf1	0,89	2,09E-01
2610002D18Rik	0,81	1,27E-03
Fbxo11	0,92	3,58E-01
Etf1	0,84	1,02E-02
4932438A13Rik	0,96	5,71E-01
1810055G02Rik	0,86	4,89E-02
Ddx19a	0,84	1,11E-02
Lias	0,81	1,45E-03
Snx19	0,87	7,69E-02
Stau1	0,91	2,91E-01
Cttn	0,90	2,45E-01
Wwp1	0,87	5,86E-02
Kcna1	0,86	3,33E-02
Carm1	0,92	3,41E-01
Cdkl3	0,85	2,06E-02
Txnrd1	0,88	7,87E-02
Ahsa1	0,83	2,31E-03
Ddx42	0,89	1,37E-01
Rsl1d1	0,87	6,95E-02
Cdv3	0,87	4,60E-02
Cops8	0,86	2,63E-02
Sec62	0,88	6,84E-02
Eif4g2	0,88	7,46E-02
1300018J18Rik	1,14	1,18E-01
4930432O21Rik	1,11	3,68E-01
Cnot6l	1,16	3,60E-02
Ormdl2	1,12	2,69E-01
Prdx5	1,14	1,52E-01
Paqr3	1,15	7,75E-02
Ndufs4	1,16	8,22E-02
Fhit	1,20	5,33E-03
Olfr920	1,16	8,11E-02
Crot	1,18	2,07E-02
Dnase1l3	1,19	1,27E-02
Edil3	1,28	2,23E-03
Fut10	1,17	5,06E-02
Apoa1bp	1,14	1,90E-01
Ppie	1,17	7,78E-02
E2f1	1,18	3,78E-02
Lsm10	1,11	4,95E-01
Esco2	1,20	9,14E-03
Lamp2	1,21	7,44E-03
Degs2	1,20	1,22E-02
ENSMUST00000058162	1,21	4,67E-03
Pex7	1,13	3,44E-01
Tm2d3	1,13	3,92E-01
Cyp17a1	1,28	1,65E-03
1700080G18Rik	1,16	1,69E-01
Wnt5b	1,20	2,31E-02

Srsf7	1,17	1,29E-01
Paip2	1,17	8,54E-02
Zfp747	1,19	5,72E-02
GENSCAN00000036079	1,15	2,24E-01
Krtcap3	1,19	3,93E-02
Cblc	1,26	1,18E-03
Cdc7	1,17	1,46E-01
Fancf	1,18	9,79E-02
Atg4c	1,15	2,46E-01
Sec61g	1,19	6,49E-02
Ms4a10	1,25	9,26E-04
A930001N09Rik	1,21	1,34E-02
Gabre	1,20	4,13E-02
Acpp	1,23	7,08E-03
Golga7	1,24	2,46E-03
Taf1d	1,18	1,11E-01
Sdhc	1,20	3,23E-02
Il15	1,23	5,41E-03
Cox7b	1,20	4,97E-02
Hist1h1d	1,21	2,32E-02
Efcab2	1,16	2,53E-01
Prrg1	1,21	2,32E-02
Tmem208	1,23	6,93E-03
Gm5465	1,20	3,34E-02
GENSCAN00000019883	1,22	1,10E-02
Zc4h2	1,18	1,20E-01
Fbxo8	1,19	8,59E-02
Mov10l1	1,32	1,82E-03
Cox6c	1,23	6,48E-03
Dpm3	1,18	1,38E-01
Pebp1	1,23	8,11E-03
ENSMUST00000082933	1,17	1,73E-01
Trappc2	1,20	4,98E-02
Hexb	1,20	4,98E-02
Ube2b	1,17	1,74E-01
Tmem82	1,26	2,13E-03
Amn1	1,21	5,31E-02
Rln3	1,24	5,70E-03
E330020D12Rik	1,23	9,79E-03
2410076I21Rik	1,24	9,23E-03
Cldn10	1,18	1,62E-01
Dbi	1,25	4,68E-03
Hace1	1,21	4,84E-02
Ppox	1,24	6,54E-03
Mlxipl	1,22	2,52E-02
ENSMUST00000083299	1,18	1,56E-01
Dkk1	1,22	2,72E-02
Dppa4	1,26	3,38E-03
Ssbp2	1,24	1,06E-02
Ndufb11	1,23	1,22E-02
2410089E03Rik	1,41	3,59E-03
Rnf5	1,20	7,71E-02
Rps27a	1,19	1,41E-01
Cmpk1	1,21	4,56E-02
Romo1	1,21	5,39E-02
Trappc2	1,21	3,79E-02
Gabarapl2	1,20	8,50E-02
2310004I24Rik	1,21	7,50E-02
Dexi	1,22	2,03E-02
Zfp560	1,19	1,32E-01
Wdr86	1,23	1,54E-02
AK132964	1,22	2,78E-02
Mthfd2l	1,26	4,69E-03
AI597479	1,18	2,22E-01
2410004B18Rik	1,18	2,51E-01
Rpl12	1,18	2,03E-01
Dcaf6	1,24	1,44E-02
Cryl1	1,20	1,01E-01
Ccng2	1,22	3,68E-02
Klhl13	1,24	1,86E-02
Dnahc6	1,20	8,80E-02
1700034H14Rik	1,18	2,63E-01
ENSMUST00000101869	1,20	1,06E-01
Cda	1,24	1,38E-02

1700094D03Rik	1,18	3,01E-01
Ndufa13	1,23	2,77E-02
Gm13290	1,32	8,39E-04
Tasp1	1,25	1,42E-02
Lmbr1l	1,24	1,60E-02
Cox6c	1,25	5,94E-03
Atp5j2	1,22	5,86E-02
1700012B15Rik	1,28	1,60E-03
0610010O12Rik	1,24	1,72E-02
ENSMUST00000082581	1,18	2,62E-01
Fbxl5	1,23	2,39E-02
H2afv	1,27	2,04E-03
Pebp1	1,26	6,47E-03
Tmem128	1,20	1,29E-01
Rbm44	1,47	5,67E-03
Pramel3	1,22	6,80E-02
Mrpl32	1,19	2,19E-01
Hsbp1	1,25	9,95E-03
ENSMUST00000102009	1,18	3,02E-01
ENSMUST00000102009	1,18	3,02E-01
ENSMUST00000102009	1,18	3,02E-01
ENSMUST00000102009	1,18	3,02E-01
ENSMUST00000102009	1,18	3,02E-01
ENSMUST00000102009	1,18	3,02E-01
EU599041	1,41	2,35E-03
Pole2	1,23	5,27E-02
Mir15b	1,36	7,32E-04
Stard3	1,21	1,02E-01
Cenpq	1,24	3,78E-02
Tssc4	1,21	1,24E-01
Shcbp1	1,27	4,92E-03
Arsk	1,25	1,68E-02
ENSMUST00000083703	1,20	1,70E-01
Slc10a4	1,27	5,96E-03
Ccdc58	1,21	1,36E-01
4930579G24Rik	1,20	1,96E-01
Tmem163	1,27	9,81E-03
NR_002841.1	1,25	1,91E-02
Pramel3	1,23	7,25E-02
AA474408	1,25	3,22E-02
Lipo1	1,23	8,83E-02
Akap7	1,26	8,94E-03
Tbcel	1,24	3,54E-02
C330021F23Rik	1,26	1,14E-02
Gtf2b	1,21	1,56E-01
Tomm7	1,25	2,80E-02
Pcmtd2	1,24	3,76E-02
Gstm1	1,46	3,75E-03
9430023L20Rik	1,23	1,00E-01
Apoc3	1,27	1,33E-02
Atf7ip	1,36	8,06E-04
Zfand2b	1,23	8,99E-02
Rad1	1,21	1,43E-01
Romo1	1,25	4,03E-02
NM_025969.1	1,20	2,60E-01
Snora3	1,24	6,07E-02
Rab39b	1,25	3,59E-02
Gm13152	1,33	2,75E-04
Elmod2	1,21	2,05E-01
ENSMUST00000099185	1,31	2,69E-03
Cercam	1,26	2,68E-02
Selk	1,24	4,99E-02
Bcl10	1,22	1,03E-01
Gm16386	1,29	4,71E-03
Rxrg	1,34	1,59E-03
Gm13152	1,30	1,51E-03
Ppil5	1,23	1,05E-01
1700029I01Rik	1,38	8,46E-04
Scai	1,24	6,44E-02
Snora3	1,24	6,77E-02
Lsm5	1,22	1,36E-01
Efna3	1,26	3,18E-02
Gstp1	1,32	1,31E-03

Klk1b27	1,27	1,29E-02
Rnf13	1,23	9,51E-02
Cenpw	1,25	4,03E-02
Tmsb4x	1,29	7,28E-03
Ndufc1	1,25	3,34E-02
Sgpp1	1,23	1,21E-01
Rps14	1,23	1,54E-01
Cpt1c	1,29	1,00E-02
Serf1	1,28	8,60E-03
Aplp1	1,41	1,61E-03
Lrrc3b	1,36	6,34E-04
AK010586	1,38	8,26E-04
Zfp595	1,24	1,08E-01
Pdcd10	1,21	2,11E-01
Mterfd1	1,24	8,46E-02
Gpr85	1,28	7,52E-03
Fdxacb1	1,25	6,30E-02
Gulp1	1,25	7,65E-02
Mboat1	1,35	1,78E-03
Pde6d	1,24	8,05E-02
Nudt14	1,23	1,52E-01
Lsm5	1,23	1,53E-01
H2-Ke6	1,29	7,88E-03
Tcn2	1,34	9,83E-04
BC088983	1,23	1,32E-01
ENSMUST00000083907	1,25	7,40E-02
Fgg	1,37	1,54E-03
GENSCAN00000042973	1,29	1,43E-02
Med21	1,22	2,04E-01
Ndufb11	1,28	1,58E-02
Cpne3	1,32	8,45E-04
Ndufb2	1,24	1,48E-01
Rxrb	1,25	9,76E-02
Tmem54	1,31	9,80E-03
Cox6b1	1,30	1,15E-02
Pramel3	1,28	2,66E-02
GENSCAN00000037690	1,31	5,35E-03
1110003E01Rik	1,28	1,36E-02
Myl6	1,31	6,69E-03
Ccbl2	1,34	1,70E-03
EU599041	1,48	1,19E-03
Pafah1b3	1,27	4,79E-02
Lgals1	1,31	4,85E-03
ENSMUST00000093641	1,27	3,82E-02
Mterf	1,24	1,52E-01
Sh3gl2	1,31	5,24E-03
Hist1h4i	1,32	3,45E-03
Aldh6a1	1,33	5,61E-03
Qtrt1	1,28	3,25E-02
Myl6	1,30	1,59E-02
Trpc6	1,30	1,58E-02
Vamp7	1,27	6,74E-02
Snora73a	1,22	2,70E-01
Fzd8	1,27	6,28E-02
0610009B22Rik	1,24	1,58E-01
Gstm2	1,30	1,68E-02
Snora70	1,26	1,01E-01
ENSMUST00000093713	1,27	5,90E-02
Anxa2	1,29	2,84E-02
Rpl22l1	1,26	9,65E-02
Snord104	1,31	1,19E-02
Myl6	1,31	1,19E-02
Klhl32	1,29	1,61E-02
Il10rb	1,30	1,76E-02
Ndufc1	1,29	2,31E-02
Hrsp12	1,26	1,14E-01
ENSMUST00000082561	1,28	4,63E-02
Myl6	1,31	1,32E-02
Myl6	1,31	8,81E-03
Vnn1	1,34	9,51E-04
Ndufa3	1,32	9,84E-03
Gm10374	1,34	4,26E-03
Wdr90	1,32	1,27E-02
Myl6	1,31	1,09E-02

Rpl22l1	1,27	7,43E-02
Vamp4	1,30	2,33E-02
Rdm1	1,34	2,75E-03
Snord35a	1,28	8,21E-02
Snora61	1,24	2,83E-01
Snora7a	1,28	7,41E-02
Mtch1	1,37	6,91E-04
Brp44l	1,22	3,79E-01
Tmem159	1,31	1,89E-02
Gstm6	1,28	9,45E-02
Gm13139	1,41	8,04E-04
Aim2	1,36	5,28E-03
Rpl13	1,28	1,08E-01
Tmco6	1,27	1,11E-01
Snord33	1,25	2,55E-01
Mif4gd	1,28	8,56E-02
Npnt	1,41	1,68E-03
Mterf	1,29	3,76E-02
Snhg1	1,25	2,37E-01
ENSMUST00000091320	1,31	1,83E-02
Lsm7	1,28	8,64E-02
NM_028615	1,39	1,78E-03
Hormad1	1,44	5,81E-04
NM_001082620.1	1,51	1,66E-03
Slc25a14	1,32	2,67E-02
Fcgr3	1,37	4,23E-03
Btg2	1,33	6,31E-03
2610524H06Rik	1,35	3,94E-03
Stra13	1,33	1,98E-02
Krcc1	1,31	3,19E-02
Dnajb9	1,27	1,54E-01
E130120F12Rik	1,32	2,96E-02
B230315N10Rik	1,31	4,92E-02
Fabp7	1,31	4,09E-02
Ldoc1	1,50	9,06E-04
Cetn2	1,33	1,48E-02
Klhl24	1,42	3,14E-05
Ly96	1,30	9,78E-02
1700030C10Rik	1,39	1,46E-03
Trpc1	1,36	1,22E-02
Lekr1	1,31	4,17E-02
Tmem38b	1,29	1,51E-01
Smpdl3a	1,30	8,84E-02
Atp5l	1,30	8,98E-02
Dppa5a	1,36	6,27E-03
ENSMUST00000049869	1,33	3,74E-02
Hspb1	1,41	3,78E-04
ENSMUST00000083266	1,26	2,76E-01
Lsm7	1,30	9,59E-02
ENSMUST00000137320	1,30	9,89E-02
Tmed6	1,38	1,02E-03
Spopl	1,33	3,09E-02
Lcmt2	1,39	2,22E-03
Pdp1	1,37	4,76E-03
Hspb1	1,41	3,48E-04
Meig1	1,25	4,34E-01
Lgals9	1,40	3,43E-03
Nckap1l	1,43	5,52E-04
NM_001081226.1	1,35	2,05E-02
Pnliprp2	1,48	6,67E-05
Gls	1,32	6,46E-02
Zfp640	1,45	1,56E-04
Rac3	1,31	1,01E-01
AK044970	1,40	3,12E-03
AK044970	1,40	3,12E-03
AK044970	1,40	3,12E-03
ENSMUST00000082919	1,32	7,84E-02
Atp5l	1,31	1,33E-01
Cml3	1,44	2,44E-03
Ankrd10	1,32	1,04E-01
Nxt2	1,37	8,55E-03
AU022751	1,41	1,46E-03
Ugt2b38	1,33	6,92E-02

NC_005089	1,34	5,15E-02
Spry3	1,40	4,43E-03
Gnpda2	1,35	2,64E-02
Tktl2	1,51	6,38E-04
Atp5l	1,33	1,06E-01
Hist1h2bc	1,43	2,54E-04
Npbwr1	1,44	1,41E-04
Mir20a	1,47	2,22E-03
Acat1	1,38	1,53E-02
Bves	1,42	2,50E-03
Spp2	1,42	8,42E-04
ENSMUST00000093682	1,36	4,42E-02
1700029I01Rik	1,51	1,04E-04
Atp5l	1,33	1,44E-01
Stag3	1,41	4,72E-03
Crip1	1,35	5,67E-02
Atp5l	1,34	1,07E-01
Atp5l	1,34	1,16E-01
Sec61b	1,38	2,87E-02
1810037I17Rik	1,33	1,51E-01
Ndufb8	1,36	8,98E-02
Ms4a4d	1,44	1,89E-03
ENSMUST00000142348	1,38	2,70E-02
3110007F17Rik	1,44	1,85E-03
Slc7a13	1,39	2,34E-02
ENSMUST00000082651	1,36	6,86E-02
Ccl27a	1,40	1,98E-02
Ccl27a	1,40	1,98E-02
Btla	1,45	7,44E-03
Hsd3b4	1,44	2,33E-03
Hsd3b4	1,44	2,33E-03
S100a1	1,40	2,66E-02
Dhrs7	1,44	3,86E-03
ENSMUST00000067345	1,46	4,14E-03
Sec61b	1,39	6,53E-02
Clec2j	1,58	7,17E-05
Sec61b	1,40	3,80E-02
Akr1c12	1,45	2,63E-03
Scarna13	1,40	2,98E-02
Ugt2b34	1,47	4,65E-04
3110057O12Rik	1,40	4,90E-02
Ccl27a	1,41	3,33E-02
Ndufb7	1,42	2,07E-02
Gm10752	1,37	1,11E-01
3110007F17Rik	1,48	1,55E-03
Cd28	1,56	1,14E-04
Klk1b24	1,62	2,91E-05
Grcc10	1,41	3,34E-02
3110007F17Rik	1,49	1,58E-03
Enpp3	1,61	1,05E-03
D6Mm5e	1,54	5,00E-04
Fthl17	1,43	2,25E-02
ENSMUST00000083155	1,44	1,73E-02
Fkbp6	1,55	5,03E-05
Gstp2	1,55	2,56E-05
Cyp4a12a	1,54	7,98E-04
Fxyd5	1,60	4,59E-04
Snora73b	1,39	1,07E-01
Plac8	1,44	4,02E-02
Hist1h1c	1,52	6,12E-04
Mir7-1	1,41	7,38E-02
Rpl13a	1,42	6,75E-02
Trim13	1,47	4,62E-03
Fut9	1,50	4,56E-03
Gstp2	1,58	3,25E-05
Rnf17	1,56	1,55E-04
Apoa2	1,50	2,35E-03
Gm13235	1,67	4,88E-05
ENSMUST00000082475	1,52	4,65E-04
Actr6	1,43	6,29E-02
Fthl17	1,48	1,10E-02
Trp53inp1	1,48	5,03E-03
Sepw1	1,51	3,42E-03
Hist1h2ae	1,51	3,67E-03

4833442J19Rik	1,52	1,22E-03
Gm13051	1,67	5,64E-05
Rex2	1,68	3,81E-05
ENSMUST00000088218	2,29	8,84E-03
Fsd1l	1,55	2,12E-03
Emcn	1,58	1,55E-03
ENSMUST00000101881	1,45	6,55E-02
A830018L16Rik	1,55	2,45E-03
Tex12	1,60	6,10E-04
Uqcr11	1,47	3,68E-02
Mirlet7f-1	1,68	1,24E-03
Tspo	1,47	5,11E-02
Snora28	1,47	5,04E-02
Mir302d	1,47	6,60E-02
ENSMUST00000083025	1,52	1,20E-02
Tc2n	1,53	7,08E-03
Uqcr11	1,49	4,02E-02
Gm13154	1,70	3,10E-05
Mir302a	1,50	4,42E-02
Tdgf1	1,64	1,56E-04
Bst1	1,56	7,02E-03
Mir301b	1,68	5,25E-05
Rnu3b4	1,55	1,16E-02
Rnu3b4	1,55	1,16E-02
Rnu3b4	1,55	1,16E-02
Rnu3b4	1,55	1,16E-02
Gm15107	1,59	7,19E-03
1110001J03Rik	1,50	6,70E-02
ENSMUST00000082466	1,55	1,51E-02
BC035947	1,75	1,56E-04
NC_005089	1,58	1,30E-02
Dppa2	1,70	1,07E-05
ENSMUST00000157774	1,61	9,76E-03
Serpina1a	1,73	4,39E-05
Apoc2	1,77	5,89E-05
Rps12	1,56	2,74E-02
Tuba3a	1,70	2,69E-03
Mir19b-1	2,00	9,96E-04
ENSMUST00000099683	1,64	2,34E-03
ENSMUST00000083959	1,53	1,44E-01
Gpx3	1,90	4,73E-04
ENSMUST00000099046	1,64	5,70E-03
Myl4	1,81	1,34E-03
Afp	1,82	1,06E-04
Gm15107	1,67	6,68E-03
Gm15107	1,67	5,70E-03
Gm15107	1,69	4,69E-03
Gm15107	1,69	4,69E-03
Nat8	1,76	7,49E-05
Gm11275	1,74	8,76E-04
Gm15107	1,70	4,48E-03
Zfp600	1,82	9,33E-05
Gm5226	1,87	2,52E-05
Gm15107	1,72	1,24E-02
Gm773	1,77	2,37E-03
Serpinf2	1,81	9,30E-04
S100a11	2,02	8,81E-05
C330022B21Rik	1,80	1,98E-04
Mir302c	1,71	1,87E-02
Mir18	2,06	7,99E-06
Snora44	1,59	2,83E-01
ENSMUST00000083947	1,79	1,47E-03
1700110I01Rik	1,93	4,71E-05
Serpina1e	1,91	2,35E-05
S100a11	2,06	4,36E-05
Plbd1	2,11	7,39E-06
AI481877	2,03	1,99E-07
Serpina1a	1,82	2,66E-03
Zfp640	1,91	3,34E-04
Cyp2d26	1,79	8,46E-03
ENSMUST00000083028	1,82	2,42E-03
Akr1c19	1,84	3,39E-03
LOC280487	2,11	4,31E-04

Mir19b-2	1,85	2,27E-03
Gm15107	1,83	1,01E-02
Rnu1b1	1,91	2,38E-03
Mir302b	1,84	7,53E-03
Rnu1b1	1,91	2,74E-03
Rnu1b1	1,91	2,74E-03
Rnu1b1	1,91	2,74E-03
Dusp1	1,93	2,91E-05
Cyp4a12b	2,20	1,03E-03
Alb	1,82	1,76E-02
Hist1h2aa	1,86	6,42E-03
Spp1	1,85	2,24E-02
ENSMUST00000054349	2,15	1,46E-04
Gm15107	1,90	7,82E-03
Vmn2r-ps104	2,01	8,73E-05
Mir19a	2,12	1,55E-06
Rnu1b1	2,00	1,93E-03
Hist2h3c2-ps	2,09	1,49E-05
ENSMUST00000099056	1,97	2,00E-03
ENSMUST00000147569	1,96	3,66E-03
Rny1	1,88	8,99E-02
Hist1h2bg	2,14	8,58E-04
Rnu3a	1,98	2,25E-02
Akr1c13	2,16	4,25E-05
Lgals2	2,19	6,62E-05
Gm7120	2,25	1,23E-04
Mup1	2,09	1,02E-02
Ddx4	2,43	5,42E-04
ENSMUST00000099414	2,21	3,47E-04
2610305D13Rik	2,38	1,68E-04
S100g	2,26	3,04E-05
Khdc1a	2,24	7,53E-05
1700110I01Rik	2,36	2,80E-05
ENSMUST00000099042	2,16	4,20E-03
Ugt3a2	2,08	4,76E-02
Khdc1c	2,38	4,62E-05
Defb1	2,12	4,87E-02
3830403N18Rik	2,33	5,04E-04
Zfp640	2,34	8,79E-06
Slc25a31	2,46	1,83E-07
Gm13235	2,59	4,22E-05
Gm13235	2,59	4,22E-05
Xlr	2,37	6,90E-06
NC_005089	2,28	1,20E-02
Ccnb1ip1	2,36	1,09E-03
Mup7	2,32	1,11E-02
Mup1	2,33	1,36E-02
Mup3	2,35	5,97E-03
Rex2	2,72	3,02E-07
Dppa2	2,72	9,27E-05
Klk1b5	2,31	3,86E-02
Taf7l	2,71	1,11E-06
Ugt3a2	2,33	2,91E-02
ENSMUST00000099042	2,46	8,40E-04
Mup7	2,43	7,84E-03
Ube2l6	2,86	1,36E-06
Zfp640	2,62	1,05E-03
Mup1	2,52	1,18E-02
Keg1	2,43	6,44E-02
ENSMUST00000099046	2,53	5,55E-03
Sult1d1	2,59	5,41E-02
Mup7	2,69	8,95E-03
Zfp640	2,96	4,09E-04
Mup7	2,87	8,82E-03
Mael	3,27	1,54E-06
Akr1c21	2,95	1,88E-02
Zfp640	3,22	9,47E-05
Zfp558	3,50	2,72E-06
1700110I01Rik	3,34	2,08E-05
ENSMUST00000112652	3,44	1,17E-07
NM_001081285.1	3,27	5,96E-05
Hba-a1	3,69	6,53E-05
Hba-a1	3,72	6,89E-05
Kap	3,28	1,24E-02

Gm13242	4,56	1,13E-06
Hbb-b2	4,32	4,90E-05
Gm10324	4,37	3,72E-08
Hbb-b1	4,34	5,27E-05
Sycp3	4,67	5,07E-07
Rpl39l	4,47	4,26E-07
Mpv17l	4,79	3,33E-09
Tmem27	3,98	1,43E-02
Gabrr1	9,97	1,18E-08

Table 2. Mass spec list of Setdb1 Flag IPs from two repeats (MaxQuant analysis). K9G1 represents Setdb1-Flag knock in cell line.

Protein ID	Gene Names	Prep-1 K9G1/Con1	Prep-2 K9G1/Con2
IPI00844695	Setdb1	15234000	7011400
IPI00380770	Atf7ip	3513800	1940600
IPI00222310	2700007P21Rik	2912700	580930
IPI00121788	Msp23	754400	0,679023205
IPI00119581	Fbl	451090	3,455792835
IPI00108271	Elavl1	378180	1,255619364
IPI00620256	Lmn1	349470	161620
IPI00453821	Nup155	291910	2,046352418
IPI00752086	OTTMUSG00000015149	229650	1,57211372
IPI00132443	Hnrnpm	229440	209250
IPI00134994	Fam111a	103750	110430
IPI00849275	Kifc1	96576	51967
IPI00134621	Ran	92534	150800
IPI00122011	Kiaa0017	85799	207900
IPI00129535	Gtl1-13	57720	43447
IPI00556768	Thrap3	57506	55008
IPI00123181	Myh9	52693	52732
IPI00830976	mCG_19661	43921	60337
IPI00649060	Akap2	39776	29480
IPI00661618		24,77432583	1835400
IPI00831490	Igk-V33	20,75728639	0,169387879
IPI00828741	C130057N11Rik	17,4325835	0,430948802
IPI00230394	Lmnb1	10,40208692	1153300
IPI00458765	Khdrbs1	8,609508579	2,351754786
IPI00755318		8,059711822	1,650844173
IPI00229845	Jbp1	6,329589271	7,524176191
IPI00169625		5,790864814	0,065892418
IPI00312128	Krip1	4,591901973	2,007217343
IPI00831140	Vk	4,285798971	2,374933142
IPI00762625	Gm1499	4,060199094	1,465321458
IPI00944078	Camsap3	3,525870997	3,701954977
IPI00421108	Als4	3,033000163	181280
IPI00761741	CP1-10VL	2,714674601	0,908797109
IPI00230035	D1Pas1-rs2	2,682454644	2,447077182
IPI00323357	Hsc70	2,665181064	4,028557782
IPI00127653	Gpx5	2,625657009	1,415055445
IPI00115588	Nxf1	2,529104353	7,984461146
IPI00228617	Gnai2	2,164330055	33289
IPI00111265	Cappa2	2,149244783	193120
IPI00128441	Hnrnpr	1,932537974	163840
IPI00755119	Morc3	1,755902182	2,026194482
IPI00556799		1,704088946	0,737615459
IPI00816945	Nrsf	1,566101933	4,324622402
IPI00396739	Smarca5	1,564443215	1,185532792
IPI00475246	Igh	1,533822143	0,024505694
IPI00555042	Ehmt1	1,466704779	69395
IPI00131674	2210010C04Rik	1,465431677	0,445046698
IPI00420329	Ascc3l1	1,419159456	2,231763417
IPI00378855		1,351833195	0,758565921
IPI00785509	ENSMUSG00000076577	1,276045002	1,253294892
IPI00119478	Tmod3	1,251496105	4,178305667
IPI00395100	EG386551	1,236693376	5,992525861
IPI00653307	Ddx17	1,232398507	10,20751578
IPI00605227	mKIAA0138	1,220859388	41934
IPI00346834	Krt76	1,175764925	0,508735493
IPI00929832	Nup205	1,136992493	86036
IPI00405665	Kif20b	1,121632329	2,513671272
IPI00469323	Dnmt1	1,094593527	127350
IPI00808254		1,057979198	0,202269389
IPI00265358	Dhx38	1,046474445	108100
IPI00121596	Prp8	0,969196975	1,619869431
IPI00464383	Igk	0,939145426	1,014018907
IPI00263048	Numa1	0,892721572	1,169221316
IPI00123172	anti-MOG kappa	0,89022635	0,550355484
IPI00403589	Erh	0,87768683	0,266770466
IPI00421014		0,87522576	0,088366024

IPI00831162	G8(anti-MRBC) V-2/ J-L	0,871932005	0,690615938
IPI00720058	mKIAA0035	0,83663764	4,667275404
IPI00420481	Tpx2	0,836241519	0,911940406
IPI00115660	Tcof1	0,804229231	1,368369984
IPI00318048	Nol5a	0,774251694	290230
IPI00678584	Igl-V2	0,748202958	1,808299312
IPI00230044	Tpm3	0,747153942	84958
IPI00309398	Cdc46	0,722074481	2,274972444
IPI00226073	Hnrnpf	0,711749885	0,695848999
IPI00553499	IgG1 TS1 VL	0,707814758	1,080514227
IPI00460668	Baf190a	0,70499131	46086
IPI00623570	cbp37	0,652124721	3,624524953
IPI00462809		0,62956751	2,278531283
IPI00130343	Hnrnpc	0,614102277	3,078151528
IPI00458190	Pde4d	0,596916981	1,174069511
IPI00138207	ENSMUSG00000056850	0,588912051	0,073267885
IPI00663560		0,536877127	1,084742233
IPI00921658	Flna	0,521325752	0,832055571
IPI00127415	Npm1	0,517208629	0,544864637
IPI00319830	Elf	0,482388879	1,608726454
IPI00929786	Kiaa0731	0,426001085	68670
IPI00757312	Myh10	0,397899846	151880
IPI00124573	BC018507	0,397651913	1,138087227
IPI00850020	Igk-C	0,39557459	0,244950175
IPI00817029	Glyr1	0,358545395	0,148482186
IPI00224127	D2Wsu81e	0,337817702	0,466979773
IPI00269662	Hnrnpa3	0,332080059	1,088514764
IPI00653841	Capza1	0,330813955	184280
IPI00331424	Prp31	0,324340172	0,103910273
IPI00453826	Matr3	0,322711062	0,216374032
IPI00330000	Hist2h2aa1	0,311446268	3,589436313
IPI00623776	H4-12	0,287392197	3,871513356
IPI00331461	Rpl11	0,241641686	0,771918427
IPI00221581	Eif4b	0,241258916	3,099947114
IPI00221694	Bola2	0,229085772	1,276419748
IPI00323819	Rps20	0,226625867	8,368138483
IPI00129468	Cbx3	0,203910076	2,84096133
IPI00762198	Hbb-b1	0,186718863	38586
IPI00348270	Hist2h2bb	0,184701805	9,157242981
IPI00153400	H2afj	0,156490718	131640
IPI00282848	H3.3a	0,129058767	4,098003489
IPI00670422	Nhp2l1	0,043285703	4,863509116
IPI00108338	Mcm3	0,042250576	0,622419002
IPI00119667	Eef1a2	0,03560898	0,373263944

Table 3. List of dysregulated genes from Setdb1 mutant endoderm cells

Downregulated genes		Upregulated genes	
Gene names	log2 FoldChange	Gene names	log2 FoldChange
Eif2s3y	-7,97	4933413G19Rik	6,49
Uty	-7,78	Gm13394	5,91
Ddx3y	-6,42	4931409K22Rik	5,73
0610038L08Rik	-6,04	4930556G01Rik	5,69
Hist1h4m	-5,99	Gm12296	5,51
Klk13	-5,95	Gm26839	5,35
Kcns1	-5,68	Cd22	5,29
Unc45b	-5,34	Ppp1r1c	5,21
Cryab	-5,06	Gm26691	5,21
Dmrt3	-5,02	Cd79b	5,16
Nupr1	-4,98	Gm10304	5,16
2900055J20Rik	-4,83	Slc9a2	5,11
Chac1	-4,77	Lrrc24	5,06
Ankrd1	-4,72	Gm10434	5,03
Fstl3	-4,70	Ninj2	5,00
Ern2	-4,56	Gm13230	5,00
Ntf3	-4,56	Slc17a8	4,79
Gm20448	-4,56	Dpys	4,76
Smpdl3a	-4,45	Aldob	4,76
Hus1b	-4,40	Ddx43	4,76
Gm17203	-4,34	Ramp1	4,73
A230028O05Rik	-4,34	Gm26627	4,69
G0s2	-4,28	Sgcz	4,62
Dpcr1	-4,28	Gm11961	4,62
Gm24198	-4,28	Gm10248	4,62
Mfsd2a	-4,22	9330162012Rik	4,62
Kdm5d	-4,18	Lrrc26	4,55
Mir3060	-4,16	Cyp4a31	4,55
BC025920	-4,12	Fzd9	4,55
Gm22345	-4,09	Dcc	4,55
Gm25827	-4,09	mt-Te	4,55
uc_338	-4,09	Gm25683	4,55
Gm26559	-4,06	Gm16838	4,55
Astn1	-4,02	Vmn2r-ps20	4,55
Gm11821	-4,02	Rab19	4,47
Gm15580	-4,02	Tgm5	4,47
Gm15518	-4,02	Gm23297	4,47
Gm17219	-4,02	Gm17252	4,47
Nmrk1	-3,95	Slc17a1	4,39
C730034F03Rik	-3,95	1700093J21Rik	4,39
Gm12356	-3,95	Agbl1	4,39
Gm12264	-3,95	Dnaaf1	4,39
Gm5558	-3,95	Gm12596	4,39
Gm13814	-3,91	Aoah	4,30
Zfp641	-3,87	Ankrd22	4,30
Lox	-3,87	Them5	4,30
Neurl2	-3,87	Slfn8	4,30
E130304I02Rik	-3,87	Nlrp9b	4,30
Fam221a	-3,87	Krt77	4,30
Rxfp4	-3,87	Gm16129	4,30
Trank1	-3,87	Drr1	4,30
Gm13145	-3,87	Gm6058	4,30
2410004I01Rik	-3,87	Gm16190	4,23
Gm15735	-3,87	9530003J23Rik	4,21
Gm13657	-3,87	Lrat	4,21
Gm23468	-3,87	Stap1	4,21
Gm23115	-3,87	Gbx2	4,21
Gnb3	-3,83	Lbx2	4,21
Them6	-3,83	Olfr1258	4,21
Cryba1	-3,79	Slc14a1	4,21
Tex26	-3,79	Cacng3	4,21
1700023L04Rik	-3,79	Gm13385	4,21
Sh2d6	-3,79	Gm16124	4,21
Gpr20	-3,74	Gm12908	4,21
Gm20498	-3,70	Gm26189	4,21
Vstm2l	-3,70	4933416M07Rik	4,21
Tmem72	-3,70	4930467K11Rik	4,21
Gja5	-3,70	4930578M01Rik	4,21
Hist1h2aj	-3,70	Akr1c21	4,11

Gm13133	-3,70	Fam154a	4,11
Gm12117	-3,70	Gm498	4,11
AC144797.1	-3,70	Tlr13	4,11
Klk10	-3,67	Wnt8b	4,11
Lrrc18	-3,67	Gpr149	4,11
Gm3468	-3,65	Cyp2f2	4,11
RP23-296I6.9	-3,65	Ces1c	4,11
Jph2	-3,64	Gm5591	4,11
Oas1c	-3,60	Slco1a5	4,11
Lmx1a	-3,60	Gm9047	4,11
Treml4	-3,60	Gm17173	4,11
Fam71d	-3,60	Gm26706	4,11
5430421N21Rik	-3,60	Eif3j2	4,08
Gm12303	-3,60	Abca8b	4,00
Gm13069	-3,60	4921501E09Rik	4,00
Gm25284	-3,60	Ctla4	4,00
Gm26590	-3,60	Ifi44	4,00
Tmie	-3,58	Actl6b	4,00
Pnck	-3,57	Arhgap30	4,00
Gdnf	-3,56	Gm24611	4,00
Ptk6	-3,56	Nr2f1	4,00
Foxd4	-3,55	Sp110	4,00
Prr5l	-3,55	A530040E14Rik	4,00
Pparg	-3,51	Gm14139	4,00
Spata3	-3,51	Gm12760	4,00
Klk6	-3,51	Gm15347	4,00
Gpr17	-3,51	Gm7873	4,00
Gm10134	-3,51	Myrip	3,97
Foxe1	-3,51	Fa2h	3,95
Gm25612	-3,51	Btn1a1	3,89
Gm15458	-3,51	Fgf22	3,89
Gm24722	-3,51	Wdr64	3,89
4930532G15Rik	-3,51	Il2	3,89
Gm26578	-3,51	Hpca	3,89
Ccser1	-3,47	Adam5	3,89
Adora3	-3,40	Triml1	3,89
Scin	-3,40	Gm9936	3,89
Lipf	-3,40	BC094916	3,89
Ccdc135	-3,40	Gm14085	3,89
Plekhs1	-3,40	4932414N04Rik	3,89
Dbil5	-3,40	Gm5077	3,89
Ttll6	-3,40	Gm15651	3,89
Npas4	-3,40	Gm16111	3,89
Qrfpr	-3,40	Gm26783	3,89
Bhmt	-3,40	4833422M21Rik	3,89
Gm11620	-3,40	4930444E06Rik	3,87
4930512H18Rik	-3,40	Gpr68	3,86
Gm20678	-3,40	Pnpla1	3,85
Gm26568	-3,40	Tex19.1	3,83
Gm9949	-3,34	Fbxl8	3,83
1700039E22Rik	-3,34	Gm22450	3,83
Gm8177	-3,34	Gm7658	3,79
Six3	-3,32	4732419C18Rik	3,79
Ppp1r3c	-3,30	Gm24917	3,78
Nxnl2	-3,28	Nqo1	3,76
Ccdc151	-3,28	Apol7a	3,76
Gm12703	-3,28	Rhag	3,76
Gadl1	-3,28	Htr7	3,76
Casp16	-3,28	Zap70	3,76
Selenbp1	-3,28	Cdh15	3,76
Rps24-ps2	-3,28	S100b	3,76
Gm5535	-3,28	2810032G03Rik	3,76
Gm11451	-3,28	5330416C01Rik	3,76
Gm12607	-3,28	Cxcl11	3,76
4932702P03Rik	-3,28	Gm5580	3,76
Gm2301	-3,28	Gm10499	3,76
4930458D05Rik	-3,28	Gm15284	3,76
Myh15	-3,28	Sel1l2	3,76
Gm26787	-3,28	Gm10916	3,76
1700006J14Rik	-3,23	Fam155a	3,76
Tmem213	-3,22	Gm13532	3,76
Gm6478	-3,22	Gm12038	3,76
Gm12856	-3,22	Gm15367	3,76

Gm25445	-3,22	Gm12984	3,76
A930038B10Rik	-3,22	Gm14344	3,76
Gm7805	-3,20	Gm15510	3,76
Gm15869	-3,20	2900079G21Rik	3,76
Mgat3	-3,20	Gm1992	3,76
Slc13a2	-3,16	Gm17212	3,76
Trp53tg5	-3,16	Gm17168	3,76
4632428N05Rik	-3,16	Gm5784	3,76
Veph1	-3,16	Npm2	3,72
Tdrd12	-3,16	1700120E14Rik	3,72
Pet2	-3,16	Slc13a3	3,69
Ptger2	-3,16	Morn3	3,69
Slc25a34	-3,16	Gm8894	3,69
Ramp3	-3,16	Aox2	3,69
Lgr6	-3,16	Gm14150	3,69
Fhl4	-3,16	Pou1f1	3,62
Krt9	-3,16	Rnase6	3,62
4931415C17Rik	-3,16	Trim52	3,62
Egr4	-3,16	Fetub	3,62
Gm24608	-3,16	Cxcr2	3,62
Gm15836	-3,16	Itgax	3,62
Gm6322	-3,16	Palmd	3,62
Gm15785	-3,16	Slc39a12	3,62
Gm11199	-3,16	Trim58	3,62
4930457A20Rik	-3,16	Gm5867	3,62
Gm13861	-3,16	Krt14	3,62
Gm13609	-3,16	Gm9812	3,62
Gm15295	-3,16	Sprr1a	3,62
Gm13977	-3,16	Krt78	3,62
Mir1927	-3,16	A730017C20Rik	3,62
Gm20456	-3,16	Ces5a	3,62
Vmn2r-ps119	-3,16	Zfp804a	3,62
AC132867.1	-3,16	Gm6116	3,62
SNORA43	-3,16	Gm1070	3,62
Gm9918	-3,13	BC030870	3,62
Gm16326	-3,12	Olfr1006	3,62
Mdga1	-3,11	Scgb1b30	3,62
Gm16041	-3,11	Gm17396	3,62
Vcp-rs	-3,10	Gm7638	3,62
Dmrt1	-3,09	Gm12196	3,62
Hs3st3a1	-3,09	Gm13121	3,62
Mmp12	-3,09	1700123O12Rik	3,62
Selenbp2	-3,09	A530076I17Rik	3,62
Smpd5	-3,09	Gm14157	3,62
A730090N16Rik	-3,09	5133400J02Rik	3,62
Oxld1	-3,08	Gm14225	3,62
Ifit2	-3,08	Gm23094	3,62
Vps37d	-3,07	Serpina4-ps1	3,62
Nap1l2	-3,07	Gm20470	3,62
Gm3896	-3,07	n-R5s211	3,62
Grin2c	-3,07	Triml2	3,59
Podxl2	-3,06	Emx2	3,58
Lrguk	-3,05	Skiv2l-ps1	3,58
Tph2	-3,02	4930590J08Rik	3,55
Tacr2	-3,02	Rsph6a	3,55
Hcls1	-3,02	Tex33	3,55
Klra5	-3,02	Gm5177	3,55
Krt17	-3,02	Scnn1g	3,47
P2ry13	-3,02	Clvs2	3,47
Hspb2	-3,02	Gria1	3,47
Ttc39d	-3,02	Cpne6	3,47
Skint7	-3,02	Hgd	3,47
Gm5087	-3,02	Prss30	3,47
Vmn1r222	-3,02	Daf2	3,47
Gm24150	-3,02	Lrrn2	3,47
Mir34a	-3,02	Adcy10	3,47
Mir181b-2	-3,02	Hdc	3,47
Vmn1r4	-3,02	Slc2a2	3,47
Ccdc105	-3,02	Car5b	3,47
Olfr1397-ps1	-3,02	1700016D06Rik	3,47
Gm15791	-3,02	Hp	3,47
Gm12848	-3,02	Muc16	3,47
Gm15234	-3,02	Sdr42e1	3,47
Gm11523	-3,02	Sgcg	3,47

Gm16062	-3,02	Sec1	3,47
B230398E01Rik	-3,02	1700113H08Rik	3,47
Gm3164	-3,02	Odf3b	3,47
Hspe1-ps3	-3,02	Ces2a	3,47
Vmn1r39	-3,02	Tcl1b2	3,47
Palm2	-3,00	Gm25578	3,47
Rgs9	-2,97	Pabpn1l	3,47
1700084C01Rik	-2,97	Itgad	3,47
Gm9311	-2,97	Klf14	3,47
Dscam	-2,95	Nlrp4g	3,47
Gm24867	-2,95	Gm12838	3,47
Gm15549	-2,95	Gm13142	3,47
Gm11511	-2,95	Gm12327	3,47
Gm12972	-2,95	Gm15172	3,47
A830052D11Rik	-2,95	Gm13886	3,47
Epdr1	-2,92	Gm12798	3,47
Cr2	-2,92	Gm13807	3,47
Tfap2c	-2,92	Gm25925	3,47
Shh	-2,88	Gm25265	3,47
Asic5	-2,87	4930556I23Rik	3,47
Cd1d1	-2,87	Gm15689	3,47
Csf3r	-2,87	Cyp2c69	3,47
Nat8	-2,87	Gm6489	3,47
Vsig1	-2,87	Gm6625	3,47
Otud7a	-2,87	Olfr888	3,47
Cd200r3	-2,87	Gm16701	3,47
Kcnj9	-2,87	A930006I01Rik	3,42
BC028528	-2,87	RP24-312B12.1	3,42
Gpr37	-2,87	Agt	3,40
S1pr1	-2,87	Phactr3	3,39
D930020B18Rik	-2,87	1700022I11Rik	3,39
Gm9970	-2,87	Pde6b	3,39
Gm13242	-2,87	Tpte	3,39
Gm5581	-2,87	Aldh8a1	3,39
Gm8062	-2,87	Ccdc144b	3,39
Mroh5	-2,87	Cited4	3,39
Gm10369	-2,87	9030624G23Rik	3,39
Rpl10-ps2	-2,87	Gm22728	3,39
Lrrc55	-2,87	Gm25464	3,39
Gm23608	-2,87	Foxl2os	3,39
Ankrd65	-2,87	C3ar1	3,37
Gm13117	-2,87	Nlrp4e	3,36
Gm16181	-2,87	Gm26501	3,36
Gm12181	-2,87	Scn1a	3,34
Gm13418	-2,87	Pou2f2	3,30
Gm12928	-2,87	Fcrls	3,30
Rpl7a-ps12	-2,87	Gabrg2	3,30
Gm13466	-2,87	Krt24	3,30
Gm12337	-2,87	Gm16437	3,30
1700013G23Rik	-2,87	Ccdc172	3,30
Gm11934	-2,87	Mettl7b	3,30
Gm14547	-2,87	Serpinb11	3,30
Gm16563	-2,87	Il2ra	3,30
Gm15954	-2,87	Prkcq	3,30
Gm20686	-2,87	Procr	3,30
Raxos1	-2,87	Cacna1f	3,30
mmu-mir-7237	-2,87	Tbx22	3,30
Ppp1r1a	-2,86	Bean1	3,30
Klk12	-2,85	Cebpa	3,30
Bmp4	-2,85	Slc17a2	3,30
Tctex1d2	-2,83	Spata16	3,30
Zfp773	-2,83	Mpped1	3,30
Gm3636	-2,83	Ttc34	3,30
Frs3	-2,82	Cdcp2	3,30
Adamts20	-2,81	Pla2g4e	3,30
Gm12213	-2,81	Gm609	3,30
Gm26869	-2,81	Gm9901	3,30
Nfkbie	-2,80	Oscar	3,30
Ube2t	-2,79	1700019A02Rik	3,30
Hspa1l	-2,79	Syt10	3,30
Mlkl	-2,79	Gm22502	3,30
Ptchd2	-2,79	Gm23723	3,30
Klk9	-2,79	Gm22682	3,30

Olfr1372-ps1	-2,79	9230020A06Rik	3,30
Gm26770	-2,77	Gm5532	3,30
Drc1	-2,76	Olfr1247	3,30
Gm26925	-2,75	n-R5s158	3,30
2810029C07Rik	-2,74	Gm24671	3,30
Nod2	-2,73	Gm14425	3,30
Mab21l3	-2,73	Gm14006	3,30
Ccdc173	-2,71	Gm8805	3,30
Nphs1	-2,70	Gm12892	3,30
1700093K21Rik	-2,70	Gm14829	3,30
Slc10a2	-2,70	Hmgb1-ps4	3,30
2610034M16Rik	-2,70	Gm13165	3,30
Hao2	-2,70	C330018A13Rik	3,30
1700061I17Rik	-2,70	Gm13748	3,30
Cxcl1	-2,70	Gm13889	3,30
Kel	-2,70	BC052486	3,30
Zfp300	-2,70	Gm23751	3,30
Neurod1	-2,70	Gm6133	3,30
Fmo1	-2,70	Gm17660	3,30
Insm2	-2,70	Mir3090	3,30
Slitrk6	-2,70	Gm5435	3,30
Pcdhb13	-2,70	Gm19791	3,30
C130026I21Rik	-2,70	Gm26797	3,30
Try4	-2,70	mt-Tv	3,27
Gm9958	-2,70	Mgat4c	3,24
Kbtbd13	-2,70	Asic2	3,24
4931429L15Rik	-2,70	Ppara	3,24
Myl4	-2,70	Myot	3,24
n-R5s88	-2,70	Kcnj16	3,24
Foxr2	-2,70	Gm16222	3,24
Gm10575	-2,70	Gm25252	3,24
Gm10647	-2,70	Prkcg	3,22
Gm9143	-2,70	Hoxb6	3,21
Eif3s6-ps1	-2,70	Lin7b	3,21
Gm11605	-2,70	Hk3	3,21
Mdk-ps1	-2,70	Defb36	3,21
Gm16090	-2,70	Lgals7	3,21
Gm15984	-2,70	Gm12500	3,21
Gm15987	-2,70	Gm12098	3,21
Gm13448	-2,70	Gm11476	3,21
Gm15972	-2,70	4933424L21Rik	3,21
Gm15998	-2,70	4930570N19Rik	3,21
Gm12915	-2,70	Gm24018	3,21
Gm23663	-2,70	Lrtm2	3,20
Gm16538	-2,70	BC051019	3,18
Gm16199	-2,70	Gm24629	3,18
Nhlrc4	-2,70	Wnt2	3,16
Gm17149	-2,70	Atp2b2	3,16
Vmn2r115	-2,70	Cacna2d4	3,16
Vmn2r82	-2,70	Gm1123	3,16
Gm5117	-2,70	Tcstv3	3,15
Vmn2r-ps18	-2,70	S100a4	3,11
Vmn2r66	-2,70	Mpo	3,11
Gm25709	-2,70	Lect2	3,11
Gm26589	-2,70	Adam7	3,11
Gm26599	-2,70	Gpr115	3,11
2010300F17Rik	-2,70	Nppc	3,11
Gm26682	-2,70	Fcna	3,11
Ms4a4d	-2,68	Afm	3,11
Aipl1	-2,67	Clec4a2	3,11
Gm14091	-2,67	Klrb1c	3,11
Cckbr	-2,66	Sbk2	3,11
Myh7	-2,65	Apba2	3,11
Gm7173	-2,65	Acan	3,11
Mir302a	-2,65	Strc	3,11
Klk7	-2,64	Tspan8	3,11
Gm14252	-2,64	Tmprss11bnl	3,11
Erdr1	-2,64	Lgi4	3,11
B230314M03Rik	-2,63	Hoxa11	3,11
Gm14122	-2,62	Foxf2	3,11
Six3os1	-2,61	Clvs1	3,11
Alx1	-2,61	1700069L16Rik	3,11
Pde7b	-2,60	9930038B18Rik	3,11
Cxcl14	-2,60	Henmt1	3,11

Cd28	-2,60	0610008F07Rik	3,11
Bpifb2	-2,60	Olfr1388	3,11
Rho	-2,60	Tecrl	3,11
4930556J24Rik	-2,60	Lrrc15	3,11
Gm25188	-2,60	1700016K19Rik	3,11
Mir302b	-2,60	5830411N06Rik	3,11
AW011738	-2,60	Gsta2	3,11
Gm16057	-2,60	Gm23095	3,11
Gm26280	-2,60	Gm25681	3,11
1110019D14Rik	-2,60	Speer3	3,11
Akap5	-2,60	Gm8587	3,11
Chst1	-2,59	Ang6	3,11
Kctd1	-2,58	Dcdc5	3,11
Pgbd1	-2,57	Gm25538	3,11
Gm13033	-2,57	Skint5	3,11
DLEU2_1	-2,57	Gm7609	3,11
Tmem54	-2,56	Olfr1069-ps1	3,11
Phox2a	-2,56	Gm12985	3,11
Tmem59l	-2,56	Gm4852	3,11
Rcsd1	-2,56	Gm12785	3,11
9230105E05Rik	-2,56	Gm8624	3,11
Ier3	-2,55	Gm11734	3,11
Car3	-2,55	Gm12018	3,11
Gm6415	-2,55	Gm15485	3,11
Hey2	-2,53	Gm13536	3,11
Tagln	-2,53	BC039966	3,11
Plekhg6	-2,53	4930551O13Rik	3,11
Pitpnm3	-2,53	Gm15911	3,11
Rapsn	-2,51	4933406J10Rik	3,11
1700001P01Rik	-2,51	Gm13781	3,11
Rtn1	-2,51	A230004M16Rik	3,11
Enox1	-2,51	Gm15457	3,11
Cd163l1	-2,51	1500017E21Rik	3,11
6820408C15Rik	-2,51	Gm25460	3,11
Wnt6	-2,51	Gm24996	3,11
Zswim2	-2,51	Gm15825	3,11
Tnfsf9	-2,51	Ugt1a5	3,11
Npy6r	-2,51	Gm3371	3,11
Ccdc67	-2,51	4930433I11Rik	3,11
Abcg5	-2,51	Gm8878	3,11
Gm9294	-2,51	Gm10417	3,11
Cnrip1	-2,51	Gm17365	3,11
Gm6430	-2,51	Gm23019	3,11
Fam26f	-2,51	Gm25211	3,11
Foxc2	-2,51	Gm26822	3,11
Ofcc1	-2,51	Gm26877	3,11
Kcna3	-2,51	4930593A02Rik	3,11
Muc15	-2,51	C530050E15Rik	3,11
Fam181b	-2,51	Gm2445	3,11
Olfr352	-2,51	CT030684.1	3,11
A430110L20Rik	-2,51	RP23-302F9.2	3,11
Actg2	-2,51	Gpr152	3,07
Gm7099	-2,51	Anks4b	3,06
C230062I16Rik	-2,51	Guca1b	3,06
4930417O22Rik	-2,51	Gpr50	3,06
1700022K14Rik	-2,51	Tac1	3,06
Gm17374	-2,51	4932416K20Rik	3,06
Gm17382	-2,51	Guca2a	3,04
Gm11033	-2,51	Hmcn2	3,04
Gm11052	-2,51	Gm6471	3,04
Gm8152	-2,51	Gm12735	3,03
Gm13454	-2,51	Gm22044	3,02
Gm12899	-2,51	Gm5493	3,02
Gm12479	-2,51	Kcnma1	3,02
Gm8344	-2,51	Gm25618	3,01
Gm12168	-2,51	Ly9	3,00
Gm11805	-2,51	Nt5c1b	3,00
4930595D18Rik	-2,51	Lect1	3,00
Gm12001	-2,51	Spag6	3,00
Gm12104	-2,51	Spata18	3,00
Gm13524	-2,51	Arhgap25	3,00
4930423M02Rik	-2,51	Acsm5	3,00
Kis2	-2,51	Adam39	3,00

Gm15850	-2,51	Ms4a4b	3,00
Gm26215	-2,51	Rit2	3,00
Srpx	-2,51	Mro	3,00
Gm16549	-2,51	Psg16	3,00
Gm17528	-2,51	Gm12020	3,00
Gm20515	-2,51	Gm15808	3,00
Gm4705	-2,51	Gm13134	3,00
Vmn1r50	-2,51	Gm16070	3,00
Gm23092	-2,51	4930566F21Rik	3,00
Gm24243	-2,51	Gm26872	3,00
Gm26820	-2,51	A930011O12Rik	3,00
Gm26566	-2,51	5830416P10Rik	3,00
Gm10814	-2,51	Fcgr3	3,00
4930500F10Rik	-2,51	Srgn	2,98
Gm26856	-2,51	Cutal	2,97
Gm26962	-2,51	Sds	2,97
Zfp759	-2,49	Ano4	2,97
Scx	-2,46	3110043A19Rik	2,97
Ldoc1l	-2,46	Myt1l	2,97
Zc2hc1c	-2,46	Gm26519	2,96
Bdh2	-2,45	Gm25973	2,95
Map6	-2,45	Cabp1	2,92
Slc6a15	-2,44	Gm23445	2,92
Gpr87	-2,43	Cd5	2,90
Fam105a	-2,43	6330409D20Rik	2,89
Gm14269	-2,43	Pnpla5	2,89
C920009B18Rik	-2,43	Itk	2,89
Gm23971	-2,42	Adap2	2,89
Pnma2	-2,41	P2rx1	2,89
Tmsb4x	-2,41	Acot12	2,89
Pon1	-2,40	Tmco5	2,89
Oas1b	-2,40	Oca2	2,89
Barx2	-2,40	Siglecg	2,89
Ankar	-2,40	Adam18	2,89
Cd14	-2,40	Stac	2,89
Gm26132	-2,40	Nlrp4d	2,89
4930589L23Rik	-2,40	Cdhr3	2,89
Gm10305	-2,40	Banf2	2,89
Gm12568	-2,40	Pyhin1	2,89
Emx2os	-2,40	D630023F18Rik	2,89
Mpc1-ps	-2,40	Frrs1l	2,89
MIMT1_1	-2,40	Fam19a4	2,89
Enpp3	-2,40	Chst9	2,89
Tcerg1l	-2,39	Serpinb13	2,89
Gm10406	-2,38	Gm5540	2,89
Tspan2	-2,38	Txndc2	2,89
A330094K24Rik	-2,37	Creg2	2,89
Scrn2	-2,37	Vtcn1	2,89
Enpp2	-2,36	Pcdhb2	2,89
Zfyve28	-2,36	Abcd2	2,89
Nlrp6	-2,36	Gm5468	2,89
Actr3b	-2,36	Gpr97	2,89
Gm23037	-2,36	Olfr530	2,89
A130006I12Rik	-2,36	Olfr508	2,89
Rps13-ps4	-2,36	Gm10157	2,89
Npm3-ps1	-2,36	Foxd3	2,89
Gm11739	-2,36	A230006K03Rik	2,89
Gm15884	-2,36	Rpl32-ps	2,89
Mir1957	-2,36	Gm4950	2,89
Gm3200	-2,36	Gm10343	2,89
Cap2	-2,35	Gm1966	2,89
Slc26a4	-2,34	Amy1	2,89
Gm4799	-2,34	Olfr1272	2,89
Col8a2	-2,34	Gm23131	2,89
3930402G23Rik	-2,34	Gm22231	2,89
Pabpc4l	-2,33	Gm6565	2,89
Zfp90	-2,33	Gm15820	2,89
Mir200b	-2,33	Gm18859	2,89
E130309D14Rik	-2,33	Gm6325	2,89
Acta1	-2,33	Gm14985	2,89
Susd4	-2,32	Gm11407	2,89
Gcnt2	-2,31	Gm9378	2,89
Tmem181b-ps	-2,31	Gm11540	2,89
Zmat4	-2,30	Gm14620	2,89

Srd5a2	-2,30	Gm11284	2,89
Loxl1	-2,29	Gm14524	2,89
Il12rb1	-2,28	Gm1848	2,89
Adam21	-2,28	Gm12194	2,89
Glra2	-2,28	1810059H22Rik	2,89
Slc25a35	-2,28	5830418P13Rik	2,89
Crisp4	-2,28	Gm16170	2,89
Iqca	-2,28	Gm12122	2,89
Oxt	-2,28	Gm11192	2,89
1810062G17Rik	-2,28	Gm13116	2,89
Rhd	-2,28	Gm13523	2,89
Sirt4	-2,28	Gm16291	2,89
Pgpep1l	-2,28	Gm23757	2,89
Cyp2r1	-2,28	Gm24554	2,89
Nox1	-2,28	C030048H21Rik	2,89
Ces2g	-2,28	BC027582	2,89
Akap14	-2,28	1700099I09Rik	2,89
Tnfsf10	-2,28	Rnasek	2,89
Gm14117	-2,28	C330013E15Rik	2,89
Eif5al3-ps	-2,28	Gm6846	2,89
2900005J15Rik	-2,28	4930471D02Rik	2,89
Ncmap	-2,28	SMAD5-AS1_3	2,89
Gm6816	-2,28	AC091763.1	2,89
Fam211b	-2,28	Rbp3	2,86
Lmod1	-2,28	Rdh1	2,83
Gpr81	-2,28	4930511M11Rik	2,83
5330417H12Rik	-2,28	Hormad2	2,83
Fgf4	-2,28	Capn11	2,83
Ifi205	-2,28	Mir23a	2,83
Ifng	-2,28	A930033H14Rik	2,83
Olfr166	-2,28	5031415H12Rik	2,83
Gm10015	-2,28	Ccdc83	2,80
Gjc3	-2,28	Bai1	2,80
Ccdc176	-2,28	Htr2c	2,80
Fam57b	-2,28	Gm14412	2,80
Cfd	-2,28	Gm13141	2,80
Gm25813	-2,28	Gm11789	2,80
Gm22354	-2,28	Gm16572	2,80
Serpina3b	-2,28	Gm17146	2,80
Gm6969	-2,28	Mc1r	2,79
Klk11	-2,28	Msx1	2,78
Lilra5	-2,28	Gm17190	2,77
Lsmem1	-2,28	Tssk3	2,76
BC061237	-2,28	Spata20	2,76
Fnd3c2	-2,28	CK137956	2,76
Gm8098	-2,28	Nnmt	2,76
Btnl5-ps	-2,28	Neu4	2,76
Trbv5	-2,28	Vav1	2,76
Gm26014	-2,28	Colec11	2,76
Mir294	-2,28	Slc22a2	2,76
Gm11645	-2,28	Tssk2	2,76
Gm13552	-2,28	Pip5kl1	2,76
Gm15544	-2,28	E330013P04Rik	2,76
Gm14200	-2,28	Gm11353	2,76
Gm15885	-2,28	Mroh9	2,76
Gm11972	-2,28	Mageb3	2,76
Gm24592	-2,28	Mir1195	2,76
Gm23184	-2,28	Gm12230	2,76
n-R5s21	-2,28	Gm8569	2,76
Gm15567	-2,28	B230206L02Rik	2,76
A530072M11Rik	-2,28	Gm3470	2,76
Gm11659	-2,28	Gm20430	2,76
6330418K02Rik	-2,28	A330032B11Rik	2,76
Gm15598	-2,28	Cd6	2,75
2900053O20Rik	-2,28	Cd59b	2,74
Gm12002	-2,28	Gm27031	2,74
Gm15681	-2,28	Myh3	2,73
BC064078	-2,28	Evx2	2,72
AV039307	-2,28	Fer1l4	2,72
Gm25282	-2,28	Lrmp	2,72
Mir1969	-2,28	Lyl1	2,72
3632454L22Rik	-2,28	Tbc1d10c	2,72
Tmsb15b1	-2,28	Rims1	2,72

Gm16239	-2,28	Bcl11b	2,72
Gm16043	-2,28	Nrgn	2,72
Gm14027	-2,28	Sytl5	2,72
Gm17324	-2,28	Gm9989	2,72
Gm8237	-2,28	n-R5s56	2,72
Gm9027	-2,28	Mir345	2,72
Mir3092	-2,28	Gm13881	2,72
Mir3080	-2,28	Cfb	2,72
Gm5070	-2,28	9330185C12Rik	2,72
Gm23523	-2,28	Slc38a8	2,70
Gm6919	-2,28	Edn3	2,69
Gm26834	-2,28	Adamts2	2,69
Gm26667	-2,28	Hic1	2,69
Gm17634	-2,28	D630039A03Rik	2,69
3110045C21Rik	-2,28	Trim40	2,69
C130060C02Rik	-2,28	Gm6044	2,69
Gm26812	-2,28	Gm23140	2,69
Gm11214	-2,28	Ifi27l2b	2,68
Gcnt4	-2,26	Akr1c12	2,68
Txnip	-2,25	Gm16012	2,68
Zfp185	-2,25	Gm10544	2,68
Gm15777	-2,25	Gm26984	2,68
Mppe1	-2,24	Mixl1	2,67
Arrdc3	-2,24	Cd38	2,66
Mir378b	-2,23	Ptprb	2,65
Akap2	-2,23	Ptafr	2,65
AU040972	-2,23	Col23a1	2,64
Mrps36-ps1	-2,22	Tat	2,62
Slc45a3	-2,22	Mmp8	2,62
Ccdc109b	-2,22	Aldh1a3	2,62
Gm6781	-2,22	Gnrh1	2,62
Gm6382	-2,22	Abi3	2,62
Gm22615	-2,22	Hbq1a	2,62
Snx32	-2,22	Ccdc175	2,62
Gjb3	-2,21	Opn4	2,62
Stard8	-2,20	Adam2	2,62
Lamp3	-2,20	Iqcf3	2,62
Wdr96	-2,20	Nptx1	2,62
Sox2	-2,20	Tmeff2	2,62
Gm24582	-2,20	Spp2	2,62
Rpl30-ps3	-2,20	F13b	2,62
Gm6305	-2,20	Ccdc3	2,62
1700042O10Rik	-2,20	2310002L09Rik	2,62
Gm26102	-2,20	C8b	2,62
E030044B06Rik	-2,20	Slco1b2	2,62
Cyp2j9	-2,20	Adm	2,62
Gm5113	-2,19	Aqp9	2,62
Gm4737	-2,19	Mgll	2,62
Klk14	-2,19	Meox2	2,62
Mapk11	-2,19	Islr	2,62
Postn	-2,19	Bank1	2,62
Gm11457	-2,19	Esm1	2,62
Pyy	-2,19	5031434C07Rik	2,62
Ccdc103	-2,18	Fam179a	2,62
Ttll13	-2,18	Gm7729	2,62
Gm11400	-2,18	Pla2g4f	2,62
Gm1818	-2,18	BC053393	2,62
Tmem95	-2,18	Vstm2a	2,62
Igfbp5	-2,18	Clec4a1	2,62
Asah2	-2,18	4921517D22Rik	2,62
Tmem181b-ps	-2,18	C230029F24Rik	2,62
Rbbp8nl	-2,17	Gm9889	2,62
Phldb3	-2,17	Ppfia2	2,62
1500009L16Rik	-2,17	Gm9951	2,62
Pik3cd	-2,17	Rab39	2,62
Socs2	-2,17	Actbl2	2,62
Acta2	-2,16	Myh1	2,62
Efcab10	-2,16	Cts8	2,62
Chst10	-2,16	Gm15698	2,62
Phxr4	-2,16	Cfi	2,62
Bmp5	-2,16	Gm5670	2,62
Dhrs7c	-2,16	Rpl10l	2,62
Atg9b	-2,16	Fmr1nb	2,62
Tmem145	-2,16	Fbxw24	2,62

Ccr10	-2,16	Vmn1r51	2,62
Krt84	-2,16	Ifna13	2,62
Gm9888	-2,16	Mir186	2,62
Mir1188	-2,16	n-R5s7	2,62
Gm15750	-2,16	Cyp2c66	2,62
Gm12974	-2,16	A430093F15Rik	2,62
Gm15867	-2,16	Dsg1a	2,62
Gm26608	-2,16	Fam196b	2,62
Tal2	-2,16	Gm10287	2,62
Trim29	-2,14	Rbm44	2,62
Zfp658	-2,14	Actl7a	2,62
Dtwd1	-2,14	9230009I02Rik	2,62
Galnt18	-2,14	5730507C01Rik	2,62
Tmod4	-2,13	B430319F04Rik	2,62
Kcnq4	-2,13	Gm10634	2,62
Nrg1	-2,13	Defb28	2,62
AI987944	-2,13	Gm10766	2,62
Irf2	-2,13	Gm23940	2,62
Gm8113	-2,13	Gm26339	2,62
Thap3	-2,13	Ighg2b	2,62
Sebox	-2,11	Gm10941	2,62
Aanat	-2,11	Gm14401	2,62
Cnih3	-2,11	Gm5930	2,62
4930548H24Rik	-2,11	Gm2974	2,62
Gpm6a	-2,11	Gm6161	2,62
Upb1	-2,11	Gm11893	2,62
Bai3	-2,11	Gm13670	2,62
C130071C03Rik	-2,11	Gm13326	2,62
1700055D18Rik	-2,11	Gm13687	2,62
Gm6316	-2,11	Gm14127	2,62
5330430P22Rik	-2,11	Gm5386	2,62
Gm16305	-2,11	Gm13437	2,62
4930405P13Rik	-2,11	Gm12469	2,62
Gm6467	-2,11	Gm13148	2,62
Gm27028	-2,11	Gm11930	2,62
Trim54	-2,10	Gm14802	2,62
Camkmt	-2,10	Gm14097	2,62
Slc26a1	-2,09	Gm12958	2,62
2310002F09Rik	-2,09	Gm5860	2,62
Masp1	-2,09	Gm15412	2,62
Ins2	-2,09	Gm14204	2,62
Pim1	-2,09	Gm8093	2,62
3830408C21Rik	-2,09	Gm7613	2,62
Macc1	-2,09	Gm16174	2,62
Tnnc1	-2,08	Gm14703	2,62
Prss16	-2,08	Gm23957	2,62
Ccdc19	-2,08	Gm22762	2,62
P2ry14	-2,08	Mir1934	2,62
Tnfrsf18	-2,07	Gm24391	2,62
2810433D01Rik	-2,07	Gm25435	2,62
Gm16236	-2,07	Gm15796	2,62
Zfp239	-2,06	Gm16006	2,62
Gm8731	-2,06	Rpl29-ps1	2,62
Spock1	-2,05	Gm15717	2,62
Wdfy1	-2,05	Gm10612	2,62
Panx2	-2,04	Sox2ot	2,62
Vash2	-2,04	A530084C06Rik	2,62
Rnf144a	-2,04	Gm19840	2,62
Harbi1	-2,04	Gm16432	2,62
Slc6a4	-2,04	Hspa1a	2,62
Slc4a5	-2,04	Gm23153	2,62
Gm561	-2,03	Vmn2r-ps9	2,62
Zik1	-2,03	Igkv1-110	2,62
B3gnt5	-2,02	Igkv10-96	2,62
Nalcn	-2,02	Gm22287	2,62
Slc47a1	-2,02	Ighv5-6	2,62
Scarf2	-2,02	Topaz1	2,62
Slc41a1	-2,02	Gm24968	2,62
Edn1	-2,02	Gm4461	2,62
Cpb2	-2,02	2610316D01Rik	2,62
Rgn	-2,02	4833428L15Rik	2,62
Selp	-2,02	Rpl31-ps15	2,62
Car9	-2,02	Rmst	2,62

Rasl11a	-2,02	Gm26875	2,62
Lmod2	-2,02	Gm17619	2,62
Slc7a10	-2,02	1700101I11Rik	2,62
Dcx	-2,02	B230377A18Rik	2,62
Thy1	-2,02	Gm26849	2,62
Bcl2l10	-2,02	9630001P10Rik	2,62
Itgbl1	-2,02	mmu-mir-6975	2,62
Larp6	-2,02	Rgs8	2,61
Sapcd1	-2,02	1700019B03Rik	2,59
BC061194	-2,02	Tmem25	2,59
Rlbp1	-2,02	Pmel	2,58
Saa4	-2,02	Gm22170	2,58
Pfpl	-2,02	Slc44a5	2,58
Btbd16	-2,02	Peg10	2,58
Dao	-2,02	Olfr1513	2,58
Gm16516	-2,02	Gm10655	2,57
Rhbdl2	-2,02	Cldn24	2,57
4930412D23Rik	-2,02	Gm5878	2,57
Pnoc	-2,02	Gm26104	2,57
Vat1l	-2,02	Prox2	2,55
Irs3	-2,02	Nefh	2,55
Nr1h4	-2,02	4933431K23Rik	2,55
Gemin4	-2,02	Gm16049	2,55
Ppp1r3d	-2,02	Ak9	2,55
Ppp1r3g	-2,02	A730085K08Rik	2,55
Slc6a7	-2,02	Gm25327	2,55
Sox14	-2,02	Gm21814	2,55
Kdm4d	-2,02	A430057M04Rik	2,54
Pnma1	-2,02	F7	2,52
Usp17la	-2,02	Myct1	2,52
C1ra	-2,02	Prss27	2,52
Skint4	-2,02	Irgc1	2,52
Olfr1350	-2,02	Gm25008	2,52
Ces1d	-2,02	Cntnap5a	2,52
Scimp	-2,02	Klhl41	2,52
0610039K10Rik	-2,02	Gm15327	2,52
Ifitm6	-2,02	Gm24136	2,52
Amd-ps3	-2,02	Ifi27l2a	2,52
Gm10125	-2,02	Aass	2,52
Olfr926	-2,02	Scarna8	2,52
Rnu73b	-2,02	Slc9a9	2,50
Gm25357	-2,02	Nov	2,50
Gm25137	-2,02	Gm24406	2,50
Gm26065	-2,02	Gm15461	2,50
Gm24260	-2,02	Gm23287	2,50
Gm5908	-2,02	Foxf1	2,49
Rpl7a-ps3	-2,02	Ccdc154	2,47
Gm10244	-2,02	Slc28a3	2,47
Gm7457	-2,02	Il1r2	2,47
Rpl21-ps4	-2,02	Slc12a1	2,47
H2-Bl	-2,02	Calb1	2,47
Gm20775	-2,02	Trim63	2,47
Gm22657	-2,02	Hyal4	2,47
Gm831	-2,02	Tnfsf13b	2,47
Gm17546	-2,02	B3gnt3	2,47
Xirp1	-2,02	Glis1	2,47
Gm15366	-2,02	Brinp3	2,47
Gm15745	-2,02	Gp1bb	2,47
Gm9009	-2,02	Pkdrej	2,47
Gm9157	-2,02	Pla2g4a	2,47
Gm13328	-2,02	Krt6a	2,47
Gm12599	-2,02	Gm22304	2,47
Gm15197	-2,02	Olfr1331	2,47
Gm11628	-2,02	BC028471	2,47
Gm15207	-2,02	Gm22824	2,47
Gm15897	-2,02	Ces1b	2,47
Gm13525	-2,02	Ms4a6c	2,47
Naip3	-2,02	Gm13416	2,47
Gm14470	-2,02	Gm25654	2,47
Gm15452	-2,02	Gm17428	2,47
Gm15915	-2,02	Apol11b	2,47
Gm14009	-2,02	Gm20702	2,47
Gm2788	-2,02	Gm23144	2,47
Gm16084	-2,02	Gm22633	2,47

Gm11832	-2,02	Gm22618	2,47
2700069I18Rik	-2,02	Gm26580	2,47
Gm11269	-2,02	Mfsd2b	2,46
Has2os	-2,02	Samd5	2,46
Hnrnpa1l2-ps	-2,02	Tsga8	2,46
B230206H07Rik	-2,02	Gm16503	2,46
Cbfa2t2-ps1	-2,02	Rnf39	2,44
Gm15910	-2,02	Cntnap3	2,44
Gm13855	-2,02	Gm10113	2,44
Gm13031	-2,02	Gm26129	2,44
Gm22322	-2,02	C7	2,44
Gm8429	-2,02	Gm27026	2,44
Gm17112	-2,02	Apol8	2,43
Gm6659	-2,02	Pdxk-ps	2,42
Gm23162	-2,02	Tmem45a	2,42
Gm22933	-2,02	Maats1	2,42
Kcnj11	-2,02	Grik1	2,42
Igkv4-55	-2,02	Syt4	2,42
4930528D03Rik	-2,02	Rhoh	2,42
4921504A21Rik	-2,02	Piwil4	2,42
RP24-570C10.7	-2,02	Bcl2l15	2,42
RP24-194K24.6	-2,02	Ifltd1	2,42
mmu-mir-6353	-2,02	Gm22061	2,42
Foxc1	-2,02	Gm22353	2,42
Uprt	-2,00	Gm8618	2,42
Matn1	-2,00	Gm14088	2,42
Gm15774	-2,00	Gm5721	2,42
Pax9	-1,99	Gm15918	2,42
Zc3h8	-1,99	Gm16055	2,42
Myl7	-1,98	D430041D05Rik	2,41
Aug 00	-1,98	P2rx7	2,41
Myl9	-1,98	Wdr17	2,41
Eva1a	-1,98	Fau-ps2	2,40
Zkscan7	-1,98	Mgst2	2,40
Gm16102	-1,98	C3	2,40
Wdr54	-1,97	Pcp4l1	2,39
Galnt16	-1,97	Rrh	2,39
Zdhhc14	-1,97	Klra2	2,39
Kcnip1	-1,97	Mgp	2,39
4921518J05Rik	-1,97	4921513D11Rik	2,39
Gm9083	-1,97	Gm20760	2,39
Itprip	-1,97	Casc1	2,38
Antxr2	-1,96	Nr5a1	2,37
Rpl10-ps6	-1,96	Lrg1	2,37
Gm16246	-1,96	Gm11755	2,37
Gm19357	-1,96	Gm23137	2,37
PYURF	-1,96	Zfp422-rs1	2,37
B4galnt4	-1,96	Gfi1	2,37
Wdr86	-1,96	Pdf	2,36
Ikzf4	-1,95	Gm20681	2,36
Zkscan14	-1,95	Six2	2,35
Sult5a1	-1,95	Slc28a1	2,35
Zfp354b	-1,95	Gm15541	2,35
Amer2	-1,95	Gm16540	2,35
Zfp455	-1,95	Tmem178b	2,35
Gm7665	-1,95	Barhl2	2,34
Ahnak2	-1,95	AA414768	2,34
4632411P08Rik	-1,95	Akr1c13	2,34
Fam111a	-1,94	Gm13391	2,33
Pik3c2b	-1,94	Pgbd5	2,32
Scn2a1	-1,93	Gabra2	2,30
Tnfsf12	-1,93	Abhd3	2,30
Zfp462	-1,92	Crhr2	2,30
Psg17	-1,92	Gabra1	2,30
Tyrp1	-1,92	Hnf4g	2,30
Gip	-1,92	Alox12e	2,30
Gdap1	-1,92	Iyd	2,30
Gria4	-1,92	Tbata	2,30
Dnaic2	-1,92	Gas2l2	2,30
Bpifc	-1,92	Nell2	2,30
Rps27a-ps2	-1,92	Ly6h	2,30
n-R5s151	-1,92	Tff3	2,30
9130019P16Rik	-1,92	Mtl5	2,30

Gm14387	-1,92	Ankrd2	2,30
Gm13868	-1,92	Rp1	2,30
Gm8606	-1,92	Slc9a4	2,30
Gm11636	-1,92	Snph	2,30
1810012K08Rik	-1,92	Stmn3	2,30
Dlx6os1	-1,92	Cckar	2,30
Gm19898	-1,92	Pdcl2	2,30
E030018B13Rik	-1,92	Prok2	2,30
Gm10825	-1,92	Klrg1	2,30
Eid2b	-1,92	Lrrc23	2,30
Csf1	-1,91	2900092C05Rik	2,30
Utf1	-1,91	Dio1	2,30
Zbtb32	-1,91	Ccl7	2,30
Smyd1	-1,91	Fbxl21	2,30
Mmp19	-1,90	Darc	2,30
Treh	-1,90	4921524L21Rik	2,30
Gm11761	-1,90	Frmpd3	2,30
Zcchc24	-1,90	Hoxa6	2,30
Hmgn3	-1,89	Elfn2	2,30
A230107N01Rik	-1,89	Olfr1018	2,30
2700046G09Rik	-1,89	9530080O11Rik	2,30
Gadd45b	-1,89	Olfr1010	2,30
Zfp72	-1,89	B530045E10Rik	2,30
Paqr6	-1,88	Rps11-ps4	2,30
Gprc5a	-1,87	Nxph3	2,30
Cldn10	-1,87	Nxpe5	2,30
Slc22a6	-1,87	Ddi1	2,30
Pcsk2	-1,87	Olfr1366	2,30
1700023E05Rik	-1,87	Frmd3	2,30
Lyve1	-1,87	Tifab	2,30
Ptprm	-1,87	Olfr165	2,30
Rgl3	-1,87	Il31ra	2,30
Aicda	-1,87	Kcnb1	2,30
Olig1	-1,87	Hist1h2ba	2,30
Gm9806	-1,87	Gucy2g	2,30
1700084J12Rik	-1,87	Gm5447	2,30
Trim5	-1,87	5730596B20Rik	2,30
H2-Q7	-1,87	1700022P22Rik	2,30
Gm4945	-1,87	Olfr1501	2,30
Cys1	-1,87	BC021614	2,30
Vmn2r10	-1,87	Fcgr4	2,30
Tmem88b	-1,87	Orm2	2,30
E530001K10Rik	-1,87	9430002A10Rik	2,30
Gm13653	-1,87	Gm25793	2,30
A930003A15Rik	-1,87	Gm26062	2,30
Hoxb2	-1,87	Gm24412	2,30
1700028N14Rik	-1,87	Serpina3f	2,30
Nlrp12	-1,87	Gpr113	2,30
9230113P08Rik	-1,87	Xkr9	2,30
Gm5622	-1,87	Mrgprb5	2,30
Gm12488	-1,87	Rps8-ps1	2,30
Gm16758	-1,87	Eddm3b	2,30
Gm11465	-1,87	Gm5460	2,30
Gm25116	-1,87	Gm5830	2,30
Mir1950	-1,87	4930567H17Rik	2,30
Gm25348	-1,87	AU016765	2,30
mmu-mir-6363	-1,87	Gm12526	2,30
Fut1	-1,86	Olfr713	2,30
Fabp3	-1,86	Gm10638	2,30
Zcchc18	-1,85	Gm10654	2,30
Adamts19	-1,85	Rad21l	2,30
1500002C15Rik	-1,85	Gm21994	2,30
Ift57	-1,85	4833423E24Rik	2,30
Egf	-1,84	9430097D07Rik	2,30
Lphn2	-1,84	Igkv15-103	2,30
Exoc3l2	-1,84	Igkv12-46	2,30
Cyb5r2	-1,84	Gm26012	2,30
Mir302d	-1,84	Gm25803	2,30
Gm14410	-1,84	Gm4877	2,30
Rps15a-ps4	-1,84	Rnf148	2,30
Snord88a	-1,84	Gm13152	2,30
Uggt2	-1,83	Dear1	2,30
Rorc	-1,83	C030005K15Rik	2,30
Ppm1j	-1,83	Mir466i	2,30

Gm20939	-1,83	Gm15823	2,30
Gm9797	-1,83	Gm12933	2,30
Moxd1	-1,82	Gm14550	2,30
Pif1	-1,82	Gm12717	2,30
Bok	-1,82	Gm11488	2,30
Tm4sf5	-1,81	Gm13915	2,30
Irak3	-1,81	Gm7091	2,30
Slc30a10	-1,81	Gm11450	2,30
Hmgcs2	-1,81	Gm11380	2,30
Cd27	-1,81	Gpr144-ps	2,30
Hddc3	-1,81	Gm12969	2,30
Fez1	-1,81	Gm14827	2,30
Rhov	-1,81	Gm12233	2,30
BC106179	-1,81	Gm16010	2,30
Gm23054	-1,81	Gm12066	2,30
Lrch1	-1,81	1700061F12Rik	2,30
Gm10615	-1,81	4930550G17Rik	2,30
H2-T10	-1,81	Gm12764	2,30
Gm15799	-1,81	Gm16266	2,30
Mroh3	-1,81	Gm14873	2,30
4930480K23Rik	-1,81	Fam150a	2,30
Zfp69	-1,81	2310065F04Rik	2,30
Tfap4	-1,81	Gm11998	2,30
Capn6	-1,81	1700003G18Rik	2,30
Cntfr	-1,80	Gm22849	2,30
Pde1b	-1,80	Gm25558	2,30
Tmod2	-1,80	Gm25864	2,30
Zim1	-1,80	Gm22948	2,30
Nr0b1	-1,80	Gm23341	2,30
Rsad1	-1,80	Gm15810	2,30
Map9	-1,80	1110002E22Rik	2,30
Rnd3	-1,80	1700071M16Rik	2,30
Gm4924	-1,79	Vmn2r117	2,30
Slc26a11	-1,79	Gm9268	2,30
Gm9900	-1,79	Gm17191	2,30
Calr3	-1,79	Vmn2r80	2,30
Ccr1	-1,79	Nlrp1c-ps	2,30
Prtn3	-1,79	Mir3099	2,30
Myh13	-1,79	Gm20611	2,30
Gm5643	-1,79	Gm20618	2,30
Gm13196	-1,79	Gm25457	2,30
Gm15552	-1,79	Olfr893	2,30
Bbs10	-1,79	Gm379	2,30
Adarb2	-1,79	Gm23002	2,30
Clip3	-1,78	Gm22911	2,30
Serpine1	-1,78	Gm23151	2,30
Unc80	-1,78	Gm26285	2,30
Myl3	-1,78	Gm10243	2,30
Pxdc1	-1,77	Gm25313	2,30
Rasl11b	-1,77	Gm24517	2,30
Spata24	-1,77	Gm22756	2,30
Mettl7a1	-1,77	Gm26573	2,30
Actc1	-1,77	2310069G16Rik	2,30
Grk1	-1,77	5730422E09Rik	2,30
Best1	-1,77	4933408J17Rik	2,30
Ttc24	-1,77	4930461G14Rik	2,30
Lrrc37a	-1,77	1700015O11Rik	2,30
Gm13392	-1,77	Gm5523	2,30
Fam220a	-1,76	Gm26756	2,30
Gm5611	-1,76	Gm8824	2,30
Gucy2e	-1,76	Gm6283	2,30
Gprc5b	-1,76	Gm4804	2,30
Cyp26c1	-1,76	RP23-59B16.8	2,30
5430403G16Rik	-1,76	mmu-mir-6391	2,30
A530017D24Rik	-1,76	Nod1	2,29
2010001M06Rik	-1,75	A330008L17Rik	2,28
T	-1,75	Trhr2	2,28
Pkd1l1	-1,75	Gm22748	2,27
Hist2h3c2	-1,75	Adra2a	2,27
Pvt1	-1,75	Tmem40	2,27
Gck	-1,74	Spef1	2,26
Ddx58	-1,74	Styk1	2,26
Rpl15-ps2	-1,74	Tmed6	2,26

Sema3d	-1,73	Bglap3	2,26
Gpx8	-1,73	Ephx3	2,25
Zfp128	-1,73	Amica1	2,25
Agbl2	-1,73	Ablim2	2,24
Gm11282	-1,73	Klhl31	2,24
Slc6a20b	-1,72	Akr1c20	2,24
Trim34a	-1,72	Dach2	2,23
Zfp677	-1,72	Lct	2,23
Rbm24	-1,71	Col20a1	2,23
Unc93b1	-1,71	Ldhc	2,23
1700028K03Rik	-1,71	Pygo1	2,23
Tlx1	-1,71	Gm13535	2,23
Nudt22	-1,71	Fzd10	2,21
Xkr8	-1,71	Grin1	2,21
Csdc2	-1,71	Vipr2	2,21
Oprk1	-1,71	Rhbdl3	2,21
Zfp248	-1,70	Lrrc2	2,21
Meox1	-1,70	5031414D18Rik	2,21
Nkx2-1	-1,70	Hepacam2	2,21
Hlf	-1,70	1600029I14Rik	2,21
4930550C14Rik	-1,70	Grem2	2,21
G6pc2	-1,70	Lman1l	2,21
Apoa2	-1,70	Dsg3	2,21
1700008O03Rik	-1,70	Gm16135	2,21
Tnfaip8l2	-1,70	9430029A11Rik	2,21
Cd34	-1,70	Gm9719	2,21
Adora2b	-1,70	Gm20434	2,21
Spata9	-1,70	9330175E14Rik	2,21
Chat	-1,70	Trap1a	2,20
Cpn2	-1,70	Hsh2d	2,20
Clps	-1,70	Gm26326	2,20
Kcnk7	-1,70	Gm11869	2,20
Tectb	-1,70	Gpr3	2,19
Hspa12a	-1,70	Hist1h2ao	2,19
Adam23	-1,70	Ncan	2,18
Chit1	-1,70	Fgf9	2,18
Hc	-1,70	Slc5a11	2,18
Prom2	-1,70	Mcf2	2,18
Cort	-1,70	Zcwpw2	2,18
Nos3	-1,70	Scn10a	2,18
4930522N08Rik	-1,70	Ushbp1	2,18
Lmo3	-1,70	Gm9725	2,18
Fam24a	-1,70	2210406O10Rik	2,18
Bco2	-1,70	Elmod1	2,18
Trim42	-1,70	Gm8566	2,18
Trf	-1,70	Gm25801	2,18
Rnf43	-1,70	Gm10466	2,18
Sncb	-1,70	Slco1a6	2,18
Gm7008	-1,70	Spcs2-ps	2,18
Il5	-1,70	Gm25544	2,18
C1qc	-1,70	Gm12299	2,18
Il22ra1	-1,70	4930481A15Rik	2,18
Adh4	-1,70	Gm24400	2,18
Uts2r	-1,70	Gm17688	2,18
Il17f	-1,70	4930444M15Rik	2,18
Ctf1	-1,70	Gm26768	2,18
Gimap5	-1,70	RP23-386K20.2	2,18
4932442L08Rik	-1,70	2810455O05Rik	2,16
Zfp879	-1,70	Fam210b	2,15
4731417B20Rik	-1,70	Il16	2,15
Fcrl5	-1,70	Ambp	2,15
Neto1	-1,70	Gcnt3	2,15
Olfr1395	-1,70	Nek10	2,15
Otop1	-1,70	Fam221b	2,15
Gm9988	-1,70	Lax1	2,15
Kcnj15	-1,70	Gm9869	2,15
Gm25899	-1,70	Mtnr1a	2,15
2510046G10Rik	-1,70	Gm25698	2,15
Klk1b21	-1,70	Mir695	2,15
Olfr203	-1,70	Gm27042	2,15
Gm4841	-1,70	mmu-mir-8091	2,15
Mir496	-1,70	Elavl3	2,15
Mrgprb1	-1,70	Fgf17	2,14
Abcb5	-1,70	Pof1b	2,14

Gm16401	-1,70	Pear1	2,14
Gm14636	-1,70	Tbxa2r	2,14
Lst1	-1,70	Rbm42	2,14
Gm16589	-1,70	Gabbr2	2,14
4833422C13Rik	-1,70	Ak7	2,14
Defb30	-1,70	mt-Tq	2,14
Gm24430	-1,70	Nkx6-1	2,13
Gm11034	-1,70	Il1rl1	2,13
Gbp6	-1,70	Hkdc1	2,13
Gm11951	-1,70	Dnhd1	2,13
Gm22952	-1,70	4930518C09Rik	2,13
Gm8250	-1,70	Pde8a	2,13
Gm14513	-1,70	Gm22740	2,13
Gm11336	-1,70	Zfp703	2,11
Gm11446	-1,70	Aqp1	2,11
Gm14130	-1,70	1700006E09Rik	2,11
Gm12090	-1,70	Kcnq2	2,11
Gm15636	-1,70	Prl3c1	2,11
Gm6238	-1,70	Tekt1	2,11
Gm15840	-1,70	Snai2	2,11
Gm14044	-1,70	Pde6g	2,11
Gm14038	-1,70	4930426L09Rik	2,11
Gm6977	-1,70	Il1f5	2,11
Gm25780	-1,70	Pla2g2f	2,11
Gm25321	-1,70	Yipf7	2,11
C630028M04Rik	-1,70	Scnn1b	2,11
Gm15952	-1,70	Ooep	2,11
Gm13548	-1,70	Rag2	2,11
Gm12951	-1,70	Lum	2,11
Gm15328	-1,70	Cldn22	2,11
Gm14123	-1,70	Trim72	2,11
0610009E02Rik	-1,70	Olfr266	2,11
Gm15334	-1,70	P2ry4	2,11
Skint6	-1,70	Cnpy1	2,11
Gm13209	-1,70	Vwc2l	2,11
Gm15860	-1,70	Hsf3	2,11
Gm12680	-1,70	Gm9801	2,11
Gm13856	-1,70	Sdpr	2,11
Gm12100	-1,70	Frmpd4	2,11
4933406I18Rik	-1,70	Gm9867	2,11
Gm14343	-1,70	Spdya	2,11
Gm12290	-1,70	Tarm1	2,11
Gm24644	-1,70	Gsdmc2	2,11
Gm22516	-1,70	Gm10083	2,11
Gm25713	-1,70	Olfr1204	2,11
Gm26361	-1,70	Gm23510	2,11
Gm15978	-1,70	n-R5s197	2,11
Gm16137	-1,70	Olfr169	2,11
BC035044	-1,70	Trim10	2,11
Gm17226	-1,70	Anapc15-ps	2,11
Gm4462	-1,70	Olfr1242	2,11
Gm4613	-1,70	Gm23692	2,11
Gm17233	-1,70	Ighg1	2,11
D6Ertd527e	-1,70	Gm25756	2,11
Gm17175	-1,70	Gm25563	2,11
Gm8425	-1,70	Reg3a	2,11
Vmn2r18	-1,70	Gm14087	2,11
Gm17039	-1,70	Gm13297	2,11
Gm20512	-1,70	Gm15379	2,11
Gm20531	-1,70	Gm12803	2,11
Gm20405	-1,70	Gm9003	2,11
Vmn2r-ps114	-1,70	Gm13784	2,11
Gm10045	-1,70	Gm12436	2,11
Igkv5-43	-1,70	Gm23172	2,11
Gm23617	-1,70	Gm25271	2,11
Gm8212	-1,70	Gm23830	2,11
Gm21846	-1,70	Gm15562	2,11
Wdr49	-1,70	Gm24655	2,11
Gm21893	-1,70	Gm16712	2,11
Gm21984	-1,70	Gm26654	2,11
Gm8298	-1,70	Gm26871	2,11
Sox1	-1,70	A330033J07Rik	2,11
Gm26878	-1,70	5430400D12Rik	2,11

Gm26513	-1,70	Gm26911	2,11
1700112J16Rik	-1,70	Gm26980	2,11
4833407H14Rik	-1,70	Rassf10	2,11
4631405K08Rik	-1,70	RP24-86O15.2	2,11
Gm3809	-1,70	MEG3_1	2,11
Gm8957	-1,70	mmu-mir-6398	2,11
Gm8927	-1,70	RP24-300P2.1	2,11
RP23-304I16.1	-1,70	Mtmr10	2,11
RP23-477C13.2	-1,70	Mir5136	2,10
GNAS-AS1_1	-1,70	Nudt12	2,10
Atp6v0e2	-1,69	mt-Tf	2,10
Cep55	-1,68	Pcnxl2	2,09
Fam46b	-1,68	Crispld1	2,09
Wnt5a	-1,67	Prlr	2,09
Cacna1g	-1,67	1700064H15Rik	2,09
Zfp493	-1,67	Nmi	2,08
Mir143hg	-1,66	Edil3	2,08
Gm15453	-1,66	Slc25a21	2,08
Nkx2-5	-1,66	Rpl21-ps3	2,08
Pex11a	-1,66	Gm13062	2,08
Gpr44	-1,66	2810459M11Rik	2,07
Gm17231	-1,66	Aox4	2,07
Vwa2	-1,66	Proz	2,07
Prps2	-1,65	Gm22739	2,07
Traf5	-1,65	Mir342	2,07
A2m	-1,65	Gm13063	2,07
Mrgpre	-1,65	Gm24130	2,07
E130102H24Rik	-1,65	Gm25193	2,07
1700084E18Rik	-1,65	Gm24497	2,07
Gm17218	-1,65	Gm26522	2,07
Gm2885	-1,65	Gm27012	2,07
Gm26826	-1,65	Tbx2	2,07
AC124326.1	-1,65	Xirp2	2,06
Cuedc1	-1,64	Tecta	2,06
Bzrap1	-1,64	Gm13247	2,06
Gm26792	-1,64	mt-Atp8	2,06
Neurl1b	-1,64	Gm20712	2,05
Smim3	-1,64	Chsy3	2,05
Msh4	-1,64	D130043K22Rik	2,04
B3galt1	-1,64	Tnfrsf13b	2,04
Rnf182	-1,64	Slc10a4	2,04
Gm11025	-1,64	Gm9758	2,04
Gm25965	-1,64	Ugt2a3	2,04
0610040B10Rik	-1,64	Card11	2,04
Slc35e4	-1,63	9130409I23Rik	2,04
Syde1	-1,63	Foxn4	2,04
Gm15965	-1,63	Proser2	2,04
Tmem38b	-1,63	Olfr1102	2,04
A130014A01Rik	-1,63	Gm13015	2,04
H2-M3	-1,62	Gm216	2,04
1600016N20Rik	-1,62	Gm2178	2,04
Pcdhb17	-1,62	Gm11790	2,04
Fam78a	-1,62	Gm22204	2,04
Gm6612	-1,62	Gm4750	2,04
Gm3848	-1,62	Gm16378	2,04
Gm16214	-1,62	B230110C06Rik	2,04
Asic1	-1,62	Gm27002	2,04
Prph	-1,62	Mroh6	2,04
Rilpl1	-1,62	Wnt3	2,03
Axl	-1,62	Sgce	2,03
Chac2	-1,62	Akr1c19	2,03
A830018L16Rik	-1,62	Hapln4	2,02
Gm16233	-1,62	Mkx	2,02
Gm16136	-1,62	Etos1	2,02
Slc37a1	-1,62	AF366264	2,02
4930581F22Rik	-1,61	Fxyd4	2,01
Tuft1	-1,61	Tspan32	2,00
Popdc2	-1,60	Pcp2	2,00
1700003M02Rik	-1,60	Ttll8	2,00
N28178	-1,60	Slc5a9	2,00
Hhat	-1,60	Lhx5	2,00
Fam228b	-1,60	C1qb	2,00
Gm10069	-1,60	Sstr3	2,00
2500004C02Rik	-1,60	Gpr158	2,00

Anp32b-ps1	-1,60	Usp17ld	2,00
Gm12034	-1,60	Nlrp1b	2,00
n-R5s201	-1,60	Vmn1r58	2,00
4930448K12Rik	-1,60	1700062I23Rik	2,00
Gm15545	-1,60	Gm14022	2,00
Gm22942	-1,60	Abhd12b	2,00
Fbxo24	-1,60	1700025N21Rik	2,00
Gm16244	-1,60	Cd300lf	1,99
Gm23713	-1,60	Gm8251	1,99
Gm26680	-1,60	Dsg4	1,98
Gm26679	-1,60	Lcp2	1,98
Angel1	-1,60	Fgf7	1,98
Heg1	-1,60	Gm25039	1,98
Gal3st3	-1,60	C86695	1,98
Alcam	-1,60	4930556N08Rik	1,98
Igdcc3	-1,60	Gm11948	1,98
Gm20705	-1,60	1110002J07Rik	1,98
Plcd3	-1,59	Gm20033	1,98
Msl3l2	-1,59	1700092M07Rik	1,97
Cacng6	-1,59	Sost	1,97
1110046J04Rik	-1,59	Myt1	1,97
Trim43a	-1,59	Il1r1	1,97
St8sia4	-1,59	Pdzd9	1,97
Ribc1	-1,59	Vipr1	1,97
Hdac9	-1,59	Ptprh	1,97
AF529169	-1,59	Gm13420	1,97
Gm1826	-1,59	Gm25776	1,97
Timm10b	-1,59	Papln	1,95
Ldb3	-1,58	Cd72	1,95
Spata25	-1,57	Cntn1	1,95
2610015P09Rik	-1,57	Acat3	1,95
Akr1cl	-1,57	Ccdc146	1,95
Ugt8a	-1,57	mt-Tl1	1,95
Zfp3	-1,57	Gm572	1,95
Gm7327	-1,57	A830036E02Rik	1,95
6430503K07Rik	-1,57	Gm16154	1,95
A130066N16Rik	-1,57	Snord66	1,95
A930013B10Rik	-1,57	Kmo	1,95
Dytn	-1,57	2310026L22Rik	1,95
Ttpa	-1,57	Gm13986	1,95
Gm15198	-1,57	Gm25431	1,95
Gm15794	-1,57	Ctsc	1,95
Gm8216	-1,57	Rbpsuh-rs3	1,94
Gm7707	-1,57	Alpl	1,94
Gm20540	-1,57	Sv2c	1,94
Gm26693	-1,57	Depdc7	1,94
Gm26874	-1,57	Klf2	1,94
Ypel4	-1,57	Slc5a5	1,94
Adrb3	-1,57	Foxq1	1,94
Adm2	-1,57	Tnfaip2	1,93
Amigo2	-1,57	Gpr128	1,93
Arhgef39	-1,56	C1qtnf9	1,93
Sema3c	-1,56	Pnlip	1,92
Gm9825	-1,56	Best4-ps	1,92
Mypop	-1,56	2010015M23Rik	1,92
Ermn	-1,56	Cxcr5	1,92
Mettl18	-1,56	1700086P04Rik	1,91
Gm11603	-1,56	Gm23547	1,91
Rpl35a-ps3	-1,55	Camk4	1,90
Ccnd2	-1,55	Apoa1	1,89
Gyltl1b	-1,55	Itgb2l	1,89
KCNQ1OT1_5	-1,55	Clec10a	1,89
Gm16316	-1,55	Wap	1,89
Accs	-1,55	1700125H20Rik	1,89
Slco3a1	-1,55	Ccl6	1,89
Npr3	-1,55	Ccl9	1,89
Ltb	-1,55	Aoc3	1,89
Ush1c	-1,55	Nr2e1	1,89
Zfp112	-1,55	Tcp11l2	1,89
Slc6a2	-1,55	Rdh12	1,89
Ces3a	-1,55	Slc34a1	1,89
Gm12942	-1,55	Dydc2	1,89
Ceacam20	-1,55	Msmb	1,89

Mansc4	-1,55	Tnfsf11	1,89
Mroh8	-1,55	Mrz11	1,89
Gm2214	-1,55	Baalc	1,89
BC002163	-1,55	Morc1	1,89
1700061H18Rik	-1,55	Cldn26	1,89
Gm13594	-1,55	Lrrc69	1,89
Gm12207	-1,55	Gabrr2	1,89
Gm15489	-1,55	Crisp2	1,89
Gm5561	-1,55	Slc25a45	1,89
Gm26668	-1,54	Myadml2	1,89
Anpep	-1,54	Cdh9	1,89
Pmm1	-1,54	Pih1d3	1,89
Wdr38	-1,54	Atp6v1g3	1,89
4921525B02Rik	-1,54	Dpt	1,89
Rps19-ps4	-1,54	Myoc	1,89
Gm14634	-1,53	Kif12	1,89
Zfp467	-1,53	Calr4	1,89
Hspb8	-1,53	Draxin	1,89
Plagl1	-1,53	Tesc	1,89
Zfp473	-1,53	Wnt7a	1,89
Tmem219	-1,53	Art4	1,89
BC100451	-1,53	Slco1c1	1,89
6330403N20Rik	-1,53	Hapln3	1,89
Tmem108	-1,53	Ctrl	1,89
Irs2	-1,52	Ctrb1	1,89
Bmp8b	-1,52	Crtam	1,89
Mapk8ip2	-1,52	4931429I11Rik	1,89
Rpp38	-1,52	Drd2	1,89
Six5	-1,52	Cd300ld	1,89
Fzd4	-1,52	Olfr1509	1,89
Gm16794	-1,52	Dgkb	1,89
Eno2	-1,52	Mbl1	1,89
Nptxr	-1,51	Gm4955	1,89
Afap1l1	-1,51	Fgd3	1,89
Napb	-1,51	Cpa4	1,89
Ppp1r16b	-1,51	Chad	1,89
Ccdc40	-1,51	Nlrc4	1,89
Rnf207	-1,51	Il7	1,89
Cyp17a1	-1,51	Arhgap9	1,89
Tbx1	-1,51	Ltb4r2	1,89
Arhgef25	-1,51	Bbox1	1,89
Lrrc46	-1,51	Prrxl1	1,89
1700026L06Rik	-1,51	Vwa1	1,89
Tm4sf1	-1,51	Olfr1123	1,89
Sparcl1	-1,51	Fam25c	1,89
Tfr2	-1,51	Muc19	1,89
Fgf3	-1,51	Pcdhb14	1,89
Ephx4	-1,51	Hepacam	1,89
Kcnh5	-1,51	Adam29	1,89
Epgn	-1,51	Kcnv2	1,89
Pax1	-1,51	Als2cr12	1,89
Pomk	-1,51	Olfr1417	1,89
Olfml2b	-1,51	Prss54	1,89
Mocos	-1,51	Gm9826	1,89
Lrrc17	-1,51	Ceacam19	1,89
Serpinb6b	-1,51	Olfr430	1,89
Disc1	-1,51	A930002I21Rik	1,89
Gm4835	-1,51	Abca12	1,89
Hoxd9	-1,51	4930548G14Rik	1,89
Klre1	-1,51	Pcdhb9	1,89
Oprd1	-1,51	Prss51	1,89
Zfp786	-1,51	Rasal3	1,89
Doc2a	-1,51	Rnase9	1,89
Ffar4	-1,51	5830454E08Rik	1,89
A930005H10Rik	-1,51	Dpep2	1,89
Mir30e	-1,51	Tmprss11e	1,89
AF357428	-1,51	Foxi3	1,89
Gm11444	-1,51	2810407A14Rik	1,89
Gm10433	-1,51	Rdh9	1,89
Igkv13-84	-1,51	Mab21l1	1,89
Gm25506	-1,51	Musk	1,89
Fam186b	-1,51	Rpl27a-ps1	1,89
Gm13529	-1,51	1700112E06Rik	1,89
Gm15049	-1,51	Cntn4	1,89

Gm12470	-1,51	Gm23517	1,89
Gm7206	-1,51	Gm23099	1,89
Gm9673	-1,51	Mir218-1	1,89
Gm11609	-1,51	Gm22351	1,89
Gm12656	-1,51	Gm24445	1,89
Gm5883	-1,51	Gm25628	1,89
Gm16209	-1,51	Gm10172	1,89
Gm14020	-1,51	Wfdc13	1,89
Gm22960	-1,51	Mas1	1,89
Gm14019	-1,51	9930111J21Rik2	1,89
Gm11459	-1,51	Olfr894	1,89
Gm20667	-1,51	Ntn5	1,89
Gm22474	-1,51	Ccin	1,89
D830044I16Rik	-1,51	Mboat4	1,89
C630004M23Rik	-1,51	Tex24	1,89
mmu-mir-7578	-1,51	Timm8a2	1,89
SNORA21	-1,51	D6Ertd474e	1,89
Gm11983	-1,51	Arl14epl	1,89
Rab32	-1,50	Olfr472	1,89
Anxa1	-1,50	Olfr561	1,89
Arsi	-1,50	Mrgprx2	1,89

REFERENCE

Alakuijala A, TalviOja K, Pasternack A, Pasternack M. 2005. Functional characterization of rat rho2 subunits expressed in HEK 293 cells. *Eur J Neurosci*. 21:692-700.

Allshire RC, Nimmo ER, Ekwall K, Javerzat JP, Cranston G. 1995. Mutations derepressing silent centromeric domains in fission yeast disrupt chromosome segregation. *Genes Dev*. 9:218-33.

Anokye-Danso F, Trivedi CM, Juhr D, Gupta M, Cui Z, Tian Y, Zhang Y, Yang W, Gruber PJ, Epstein JA, Morrisey EE. 2011. Highly efficient miRNA-mediated reprogramming of mouse and human somatic cells to pluripotency. *Cell Stem Cell*. 8:376-88.

Arnold SJ, Robertson EJ. 2009. Making a commitment: cell lineage allocation and axis patterning in the early mouse embryo. *Nat Rev Mol Cell Biol*. 10:91-103.

Ayyanathan K, Lechner MS, Bell P, Maul GG, Schultz DC, Yamada Y, Tanaka K, Torigoe K, Rauscher FJ 3rd. 2003. Regulated recruitment of HP1 to a euchromatic gene induces mitotically heritable, epigenetic gene silencing: a mammalian cell culture model of gene variegation. *Genes Dev*. 17: 1855-1869.

Baldwin HS, Shen HM, Yan HC, DeLisser HM, Chung A, Mickanin C, Trask T, Kirschbaum NE, Newman PJ, Albelda SM, et al. 1994. Platelet endothelial cell adhesion molecule-1 (PECAM-1/CD31): alternatively spliced, functionally distinct isoforms expressed during mammalian cardiovascular development. *Development.* 120:2539-53.

Bannister AJ, Zegerman P, Partridge JF, Miska EA, Thomas JO, Allshire RC, Kouzarides T. 2001. Selective recognition of methylated lysine 9 on histone H3 by the HP1 chromo domain. *Nature*. 410:120-4.

Bartolomei MS, Ferguson-Smith AC. 2011. Mammalian genomic imprinting. *Cold Spring Harb Perspect Biol*. 3:1-17.

Ben-Haim N, Lu C, Guzman-Ayala M, Pescatore L, Mesnard D, Bischofberger M, Naef F, Robertson EJ, Constam DB. 2006. The Nodal Precursor Acting via Activin Receptors Induces Mesoderm by Maintaining a Source of Its Convertases and BMP4. *Dev Cell*. 11: 313-323.

Bilodeau S, Kagey MH, Frampton GM, Rahl PB, Young RA. 2009. SetDB1 contributes to repression of genes encoding developmental regulators and maintenance of ES cell state. *Genes Dev*. 23:2484-9.

Boyer LA, Plath K, Zeitlinger J, Brambrink T, Medeiros LA, Lee TI, Levine SS, Wernig M, Tajonar A, Ray MK, Bell GW, Otte AP, Vidal M, Gifford DK, Young RA, Jaenisch R. 2006. Polycomb complexes repress developmental regulators in murine embryonic stem cells. *Nature*. 441:349-53.

Bönisch C, Hake SB. 2012. Histone H2A variants in nucleosomes and chromatin: more or less stable? *Nucleic Acids Res*. 40:10719-10741.

Bradford MM. 1976. A rapid and sensitive method for the quantitation of microgram quantitiesof protein utilizing the principle of protein-dye binding. *Anal Biochem.* 72:248-254.

Brennan J, Lu CC, Norris DP, Rodriguez TA, Beddington RS, Robertson EJ. 2001. Nodal signalling in the epiblast patterns the early mouse embryo. *Nature*. 411:965-9.

Cadigan KM, Liu YI. 2006. Wnt signaling: complexity at the surface. *J Cell Sci.* 119:395-402.

Camus A, Perea-Gomez A, Moreau A, Collignon J. 2006. Absence of Nodal signaling promotes precocious neural differentiation in the mouse embryo. *Dev Biol.* 295:743-755.

Card DA, Hebbar PB, Li L, Trotter KW, Komatsu Y, Mishina Y, Archer TK. 2008. Oct4/Sox2-regulated miR-302 targets cyclin D1 in human embryonic stem cells. *Mol Cell Biol*. 28:6426-38.

Chazaud C, Yamanaka Y, Pawson T, Rossant J. 2006. Early lineage segregation between epiblast and primitive endoderm in mouse blastocysts through the Grb2-MAPK pathway. *Dev Cell.* 10:615-24.

Chen J, Liu H, Liu J, Qi J, Wei B, Yang J, Liang H, Chen Y, Chen J, Wu Y, Guo L, Zhu J, Zhao X, Peng T, Zhang Y, Chen S, Li X, Li D, Wang T, Pei D. 2013. H3K9 methylation is a barrier during somatic cell reprogramming into iPSCs. *Nat Genet*. 45:34-42.

Clapier CR, Cairns BR. 2009. The Biology of Chromatin Remodeling Complexes. *Annu. Rev. Biochem.* 78:273-304.

Clements D, Taylor HC, Herrmann BG, Stott D. 1996. Distinct regulatory control of the Brachyury gene in axial and non-axial mesoderm suggests separation of mesoderm lineages early in mouse gastrulation. *Mech Dev*. 56:139-49.

Coffinier C, Thépot D, Babinet C, Yaniv M, Barra J. 1999. Essential role for the homeoprotein vHNF1/HNF1beta in visceral endoderm differentiation. *Development.* 126:4785-94.

Compton SJ, Jones CG. 1985. Mechanism of dye response and interference in the Bradford protein assay. *Anal Biochem*. 151:369-374.

Dambacher S, Hahn M, Schotta G. 2010. Epigenetic regulation of development by histone lysine methylation. *Heredity*. 105:24-37.

Dodge JE, Kang YK, Beppu H, Lei H, Li E. 2004. Histone H3-K9 methyltransferase ESET is essential for early development. *Mol Cell Biol*. 2:2478-86.

Doetschman TC, Eistetter H, Katz M, Schmidt W, Kemler R. 1985. The in vitro development of blastocystderived embryonic stem cell lines: formation of visceral yolk sac, blood islands and myocardium. *J Embryol Exp Morphol*. 87:27-45.

Duan Q, Chen H, Costa M, Dai W. 2008. Phosphorylation of H3S10 blocks the access of H3K9 by specific antibodies and histone methyltransferase. Implication in regulating chromatin dynamics and epigenetic inheritance during mitosis. *J Biol Chem.* 283:33585-90.

Dunn TL, Mynett-Johnson L, Wright EM, Hosking BM, Koopman PA, Muscat GE. 1995. Sequence and expression of Sox-18 encoding a new HMG-box transcription factor. *Gene*. 161:223-5.

Engert S, Liao WP, Burtscher I, Lickert H. 2009. Sox17-2A-iCre: a knock-in mouse line expressing Cre recombinase in endoderm and vascular endothelial cells. *Genesis*. 47:603-10.

Eskeland R, Leeb M, Grimes GR, Kress C, Boyle S, Sproul D, Gilbert N, Fan Y, Skoultchi AI, Wutz A, Bickmore WA. 2010. Ring1B compacts chromatin structure and represses gene expression independent of histone ubiquitination. *Mol Cell*. 38:452-64.

Estève PO, Chin HG, Smallwood A, Feehery GR, Gangisetty O, Karpf AR, Carey MF, Pradhan S. 2006. Direct interaction between DNMT1 and G9a coordinates DNA and histone methylation during replication. *Genes Dev*. 20:3089-103.

Feldman N, Gerson A, Fang J, Li E, Zhang Y, Shinkai Y, Cedar H, Bergman Y. 2006. G9a-mediated irreversible epigenetic inactivation of Oct-3/4 during early embryogenesis. *Nat Cell Biol*. 8:188-94.

Fitzpatrick GV, Soloway PD, Higgins MJ. Regional loss of imprinting and growth deficiency in mice with a targeted deleion of KvDMR1. *Nat. Genet*. 2002. 32:426-431.

Flaus A, Martin DM, Barton GJ, Owen-Hughes T. *200*6. Identification of multiple distinct Snf2 sub-families with conserved structural motifs. *Nucleic Acids Res*. 34:2887-905.

Follit JA, San Agustin JT, Jonassen JA, Huang T, Rivera-Perez JA, Tremblay KD, Pazour GJ. 2014. Arf4 is required for Mammalian development but dispensable for ciliary assembly. *PLoS Genet.* 10:e1004170

Fritsch L, Robin P, Mathieu JR, Souidi M, Hinaux H, Rougeulle C, Harel-Bellan A, Ameyar-Zazoua M, Ait-Si-Ali S.2010. A subset of the histone H3 lysine 9 methyltransferases Suv39h1, G9a, GLP, and SETDB1 participate in a multimeric complex. *Mol Cell*. 37:46-56.

Fujita N, Watanabe S, Ichimura T, Ohkuma Y, Chiba T, Saya H, Nakao M. 2003. MCAF mediates MBD1-dependent transcriptional repression. *Mol Cell Biol*. 23:2834-43.

García-Martín E, Martínez C, Alonso-Navarro H, Benito-León J, Lorenzo-Betancor O, Pastor P, Puertas I, Rubio L, López-Alburquerque T, Agúndez JA, Jiménez-Jiménez FJ. 2011. Gamma-aminobutyric acid (GABA) receptor rho (GABRR) polymorphisms and risk for essential tremor. *J Neurol*. 258:203-11.

Giepmans BN. 2004. Gap junctions and connexin-interacting proteins. *Cardiovasc Res*. May.62:233-45.

Green MR. 2005. Eukaryotic Transcription Activation: Right on Target. *Mol Cell*. 18: 399-402.

Greer EL, Shi Y. 2012. Histone methylation: a dynamic mark in health, disease and inheritance. *Nat Rev Genet*. 13:343-57.

Hahn M, Dambacher S, Schotta G.2010. Heterochromatin dysregulation in human diseases. *J Appl Physiol*. 109:232-42.

Hansen KH, Bracken AP, Pasini D, Dietrich N, Gehani SS, Monrad A, Rappsilber J, Lerdrup M, Helin K. 2008. A model for transmission of the H3K27me3 epigenetic mark. *Nat Cell Biol.* 10:1291-300.

Hart AH, Hartley L, Sourris K, Stadler ES, Li R, Stanley EG, Tam PP, Elefanty AG, Robb L. 2002. Mixl1 is required for axial mesendoderm morphogenesis and patterning in the murine embryo. *Development*. 129:3597-608.

Hark AT, Schoenherr CJ, Katz DJ, Ingram RS, Levorse JM, Tilghman SM. 2000. CTCF mediates methylation-sensitive enhancer-blocking activity at the H19/Igf2 locus. *Nature*. 405:486 -489.

Hashimoto M, Hamada H. 2010. Translation of anterior-posterior polarity into left-right polarity in the mouse embryo. *Curr Opin Genet Dev*. 20:433-7.

Herrmann BG. 1991. Expression pattern of the Brachyury gene in whole-mount TWis/TWis mutant embryos. *Development.* 113:913-7.

Hiemisch H, Schütz G, Kaestner KH. 1997.Transcriptional regulation in endoderm development: characterization of an enhancer controlling Hnf3g expression by transgenesis and targeted mutagenesis. *EMBO J.* 16:3995-4006.

Hirrlinger J, Requardt RP, Winkler U, Wilhelm F, Schulze C, Hirrlinger PG. 2009. Split-CreERT2: temporal control of DNA recombination mediated by split-Cre protein fragment complementation. *PLoS One.* 4:e8354.

Ichimura T, Watanabe S, Sakamoto Y, Aoto T, Fujita N, Nakao M. 2005. Transcriptional repression and heterochromatin formation by MBD1 and MCAF/AM family proteins. *J Biol Chem*. 280:13928-35

Ideraabdullah FY, Vigneau S, Bartolomei MS. 2008. Genomic imprinting mechanisms in mammals. *Mutat Res*. 647:77-85.

Iwashita H, Shiraki N, Sakano D, Ikegami T, Shiga M, Kume K, Kume S. 2013. Secreted cerberus1 as a marker for quantification of definitive endoderm differentiation of the pluripotent stem cells. *PLoS One*. 8:e64291.

Izumi N, Era T, Akimaru H, Yasunaga M, Nishikawa S. 2007. Dissecting the molecular hierarchy for mesendoderm differentiation through a combination of embryonic stem cell culture and RNA interference. *Stem Cells.* 25:1664-74.

Jenuwein T, Laible G, Dorn R, Reuter G. 1998. SET domain proteins modulate chromatin domains in eu- and heterochromatin. *Cell Mol Life Sci*. 54:80-93.

Jiang W, Zhang D, Bursac N, Zhang Y. 2013. WNT3 Is a Biomarker Capable of Predicting the Definitive Endoderm Differentiation Potential of hESCs. *Stem Cell Reports.* 1:46-52.

Kaji K, Caballero IM, MacLeod R, Nichols J, Wilson VA, Hendrich B. 2006. The NuRD component Mbd3 is required for pluripotency of embryonic stem cells. *Nat Cell Biol*. 8: 285-92.

Kanai-Azuma M, Kanai Y, Gad JM, Tajima Y, Taya C, Kurohmaru M, Sanai Y, Yonekawa H, Yazaki K, Tam PP, Hayashi Y. 2002. Depletion of definitive gut endoderm in Sox17-null mutant mice. *Development*. 129:2367-79.

Kanai Y, Kanai-Azuma M, Noce T, Saido TC, Shiroishi T, Hayashi Y, Yazaki K. 1996. Identification of two Sox17 messenger RNA isoforms, with and without the high mobility group box region, and their differential expression in mouse spermatogenesis. *J Cell Biol*. 133:667-81.

Kawamoto S, Niwa H, Tashiro F, Sano S, Kondoh G, Takeda J, Tabayashi K, Miyazaki J. 2000. A novel reporter mouse strain that expresses enhanced green fluorescent protein upon Cre-mediated recombination. *FEBS Lett.* 470:263-8.

Kim I, Saunders TL, Morrison SJ. 2007. Sox17 dependence distinguishes the transcriptional regulation of fetal from adult hematopoietic stem cells. *Cell.* 130:470-83.

Kinder SJ,Tsang TE, Wakamiya M, Sasaki H, Behringer RR, Nagy A, Tam PP. 2001. The organizer of the mouse gastrula is composed of a dynamic population of progenitor cells for the axial mesoderm. *Development.* 128:3623-34.

Klaus A, Birchmeier W. 2008. Wnt signalling and its impact on development and cancer. *Nat Rev Cancer*. 8:387-98

Klose RJ, Bird AP. 2006. Genomic DNA methylation: the mark and its mediators. *Trends Biochem Sci.* 31:89-97.

Koerner MV, Pauler FM, Huang R, Barlow DP. 2009. The function of non-coding RNAs in genomic imprinting. *Development*. 136:1771-83.

Kooistra SM, Helin K. 2012. Molecular mechanisms and potential functions of histone demethylases. *Nat Rev Mol Cell Biol*. 13:297-312.

Kouzarides T. 2007. Chromatin modifications and their function. *Cell.* 128:693-705.

Kraushaar DC, Zhao K. 2013. The Epigenomics of Embryonic Stem Cell Differentiation. *Int J Biol Sci*. 9:1134-1144.

Kwon GS, Fraser ST, Eakin GS, Mangano M, Isern J, Sahr KE, Hadjantonakis AK, Baron MH. 2006. Tg (Afp-GFP) expression marks primitive and definitive endoderm lineages during mouse development. *Dev Dyn*. 235:2549-58.

Lee DH, Chung HM. 2011. Differentiation into Endoderm Lineage: Pancreatic differentiation from Embryonic Stem Cells. *Int J Stem Cells*. 4:35-42.

Lee JS, Smith E, Shilatifard A. 2010. The Language of Histone Crosstalk. *Cell*. 142:682-685.

Lehnertz B, Ueda Y, Derijck AA, Braunschweig U, Perez-Burgos L, Kubicek S, Chen T, Li E, Jenuwein T, Peters AH. 2003. Suv39h-mediated histone H3 lysine 9 methylation directs DNA methylation to major satellite repeats at pericentric heterochromatin. *Curr Biol*. 13:1192-200.

Lemaire P, Darras S, Caillol D et al. 1998. A role for the vegetally expressed Xenopus gene Mix1 in endoderm formation and in the restriction of mesoderm to the marginal zone. *Development.* 125:2371-2380.

Liang J, Wan M, Zhang Y, Gu P, Xin H, Jung SY, Qin J, Wong J, Cooney AJ, Liu D, Songyang Z. 2008. Nanog and Oct4 associate with unique transcriptional repression complexes in embryonic stem cells. *Nat Cell Biol*. 10:731-9

Lickert H, Kutsch S, Kanzler B, Tamai Y, Taketo MM, Kemler R. 2002. Formation of multiple hearts in mice following deletion of beta-catenin in the embryonic endoderm. *Dev Cell*. 3:171-81.

Lim SM, Pereira L, Wong MS, Hirst CE, Van Vranken BE, Pick M, Trounson A, Elefanty AG, Stanley EG. 2009. Enforced expression of Mixl1 during mouse ES cell differentiation suppresses hematopoietic mesoderm and promotes endoderm formation. *Stem Cells.* 27:363-74.

Lin SP, Youngson N, Takada S, Seitz H, Reik W, Paulsen M, Cavaille J, Ferguson-Smith AC. 2003. Asymmetric regulation of imprinting on the maternal and paternal chromosomes at the Dlk1-Gtl2 imprinted cluster on mouse chromosome 12. *Nat Genet*. 35:97-102.

Li B, Carey M, Workman JL. 2007. The Role of Chromatin during Transcription. *Cell*. 128:707-719.

Lohmann F, Loureiro J, Su H, Fang Q, Lei H, Lewis T, Yang Y, Labow M, Li E, Chen T, Kadam S. 2010. KMT1E mediated H3K9 methylation is required for the maintenance of embryonic stem cells by repressing trophectoderm differentiation. *Stem cells*. 28:201-12.

Loh YH, Zhang W, Chen X, George J, Ng HH. 2007. Jmjd1a and Jmjd2c histone H3 Lys 9 demethylases regulate self-renewal in embryonic stem cells. *Genes Dev*. 21:2545-57

Matsui T, Leung D, Miyashita H, Maksakova IA, Miyachi H, Kimura H, Tachibana M, Lorincz MC, Shinkai Y. 2010. Proviral silencing in embryonic stem cells requires the histone methyltransferase ESET. *Nature*. 464:927-31

McKnight KD, Hou J, Hoodless PA. 2007. Dynamic expression of thyrotropin-releasing hormone in the mouse definitive endoderm. *Dev Dyn*. 236:2909-17.

McKnight KD, Hou J, Hoodless PA. 2010. Foxh1 and Foxa2 are not required for formation of the midgut and hindgut definitive endoderm. *Dev Biol*. 337:471-81.

Minkovsky A, Sahakyan A, Rankin-Gee E, Bonora G, Patel S, Plath K. 2014. The Mbd1-Atf7ip-Setdb1 pathway contributes to the maintenance of X chromosome inactivation. *Epigenetics Chromatin*. 7:12

Monaghan AP1, Kaestner KH, Grau E, Schütz G. 1993. Postimplantation expression patterns indicate a role for the mouse forkhead/HNF-3 alpha, beta and gamma genes in determination of the definitive endoderm, chordamesoderm and neuroectoderm. *Development*. 119:567-78.

Monnier P, Martinet C, Pontis J, Stancheva I, Ait-Si-Ali S, Dandolo L. 2013. H19 lncRNA controls gene expression of the Imprinted Gene Network by recruiting MBD1. *Proc Natl Acad Sci U S A*. 110:20693-8.

Morris SA. 2011. Cell fate in the early mouse embryo: sorting out the influence of developmental history on lineage choice. *Reprod Biomed Online*. 22:521-4.

Nagano T, Mitchell JA, Sanz LA, Pauler FM, Ferguson-Smith AC, Feil R, Fraser P. 2008. The Air noncoding RNA epigenetically silences transcription by targeting G9a to chromatin. *Science.* 322:1717-20.

Nakamura T, Colbert MC, Robbins J. 2006. Neural crest cells retain multipotential characteristics in the developing valves and label the cardiac conduction system. *Circ Res.* 98:1547-54.

Nakanishi M, Kurisaki A, Hayashi Y, Warashina M, Ishiura S, Kusuda-Furue M, Asashima M. 2009. Directed induction of anterior and posterior primitive streak by Wnt from embryonic stem cells cultured in a chemically defined serum-free medium. *FASEB J*. 23:114-22.

Niakan KK, Ji H, Maehr R, Vokes SA, Rodolfa KT, Sherwood RI, Yamaki M, Dimos JT, Chen AE, Melton DA, McMahon AP, Eggan K. 2010. Sox17 promotes differentiation in mouse

embryonic stem cells by directly regulating extraembryonic gene expression and indirectly antagonizing self-renewal. *Genes Dev*. 24:312-26.

Nishikawa S, Jakt LM, Era T. 2007. Embryonic stem-cell culture as a tool for developmental cell biology. *Nat Rev Mol Cell Biol*. 8:502-7.

Niwa H, Toyooka Y, Shimosato D, Strumpf D, Takahashi K, Yagi R, Rossant J. t. 2005. Interaction between Oct3/4 and Cdx2 Determines Trophectoderm Differentiation. *Cell*. 123:917-929.

Nomura N, Nagase T, Miyajima N, Sazuka T, Tanaka A, Sato S, Seki N, Kawarabayasi Y, Ishikawa K, Tabata S. 1994. Prediction of the coding sequences of unidentified human genes. II. The coding sequences of 40 new genes (KIAA0041-KIAA0080) deduced by analysis of cDNA clones from human cell line KG-1. *DNA Res*. 1:223-9.

Norris DP, Robertson EJ. 1999. Asymmetric and node-specific nodal expression patterns are controlled by two distinct cis-acting regulatory elements. *Genes Dev*. 13:1575-88.

Oeda S, Hayashi Y, Chan T, Takasato M, Aihara Y, Okabayashi K, Ohnuma K, Asashima M. 2013. Induction of intermediate mesoderm by retinoic acid receptor signaling from differentiating mouse embryonic stem cells. *Int J Dev Biol.* 57:383-9.

Olins DE, Olins AL. 2003. Chromatin history: our view from the bridge. *Nat Rev Mol Cell Biol*. 4:809-814.

Onder TT, Kara N, Cherry A, Sinha AU, Zhu N, Bernt KM, Cahan P, Marcarci BO, Unternaehrer J, Gupta PB, Lander ES, Armstrong SA, Daley GQ. 2012. Chromatin-modifying enzymes as modulators of reprogramming. *Nature*. 483:598-602

Orkin SH, Hochedlinger K. 2011. Chromatin Connections to Pluripotency and Cellular Reprogramming. *Cell*. 145:835-850.

Peters AH, Kubicek S, Mechtler K, O'Sullivan RJ, Derijck AA, Perez-Burgos L, Kohlmaier A, Opravil S, Tachibana M, Shinkai Y, Martens JH, Jenuwein T. 2003. Partitioning and plasticity of repressive histone methylation states in mammalian chromatin. *Mol Cell*. 12:1577-89.

Perea-Gomez A, Vella FD, Shawlot W, Oulad-Abdelghani M, Chazaud C, Meno C, Pfister V, Chen L, Robertson E, Hamada H, Behringer RR, Ang SL. 2002. Nodal Antagonists in the Anterior Visceral Endoderm Prevent the Formation of Multiple Primitive Streaks. *Dev Cell*. 3:745-756.

Peters AH, O'Carroll D, Scherthan H, Mechtler K, Sauer S, Schöfer C, Weipoltshammer K, Pagani M, Lachner M, Kohlmaier A, Opravil S, Doyle M, Sibilia M, Jenuwein T. 2001. Loss of the Suv39h histone methyltransferases impairs mammalian heterochromatin and genome stability. *Cell*. 107:323-37.

Rea S, Eisenhaber F, O'Carroll D, Strahl BD, Sun ZW, Schmid M, Opravil S, Mechtler K, Ponting CP, Allis CD, Jenuwein T. 2000. Regulation of chromatin structure by site-specific histone H3 methyltransferases. *Nature*. 406:593-9.

Rice JC, Briggs SD, Ueberheide B, Barber CM, Shabanowitz J, Hunt DF, Shinkai Y, Allis CD. 2003. Histone methyltransferases direct different degrees of methylation to define distinct chromatin domains. *Mol Cell*. 12:1591-8.

Plusa B, Piliszek A, Frankenberg S, Artus J, Hadjantonakis AK. 2008. Distinct sequential cell behaviours direct primitive endoderm formation in the mouse blastocyst. *Development*. 135:3081-3091

Polavarapu N, Bowen NJ, McDonald JF. 2006. Identification, characterization and comparative genomics of chimpanzee endogenous retroviruses. *Genome Biol.* 7:R51.

Rougeulle C, Heard E. 2002. Antisense RNA in imprinting: spreading silence through Air. *Trends Genet.* 18:434-7.

Rowe HM, Jakobsson J, Mesnard D, Rougemont J, Reynard S, Aktas T, Maillard PV, Layard-Liesching H, Verp S, Marquis J, Spitz F, Constam DB, Trono D. 2010. KAP1 controls endogenous retroviruses in embryonic stem cells. *Nature*. 463:237-40.

Saiz N, Plusa B. 2013. Early cell fate decisions in the mouse embryo. *Reproduction*. 2013. 145:65-80.

Sajan SA, Hawkins RD. 2012. Methods for Identifying Higher-Order Chromatin Structure. *Annu. Rev. Genomics Hum. Genet.* 13:59–82.

Sarraf SA, Stancheva I. 2004. Methyl-CpG binding protein MBD1 couples histone H3 methylation at lysine 9 by SETDB1 to DNA replication and chromatin assembly. *Mol Cell*. 15:595-605.

Sass GL, Henikoff S. 1998. Comparative analysis of position-effect variegation mutations in Drosophila melanogaster delineates the targets of modifiers. *Genetics.* 148:733-41.

Saund RS, Kanai-Azuma M, Kanai Y, Kim I, Lucero MT, Saijoh Y. 2012. Gut endoderm is involved in the transfer of left-right asymmetry from the node to the lateral plate mesoderm in the mouse embryo. *Development*. 139:2426-35.

Schaniel C, Ang YS, Ratnakumar K, Cormier C, James T, Bernstein E, Lemischka IR, Paddison PJ. 2009. Smarcc1/Baf155 couples self-renewal gene repression with changes in chromatin structure in mouse embryonic stem cells. *Stem Cells*. 27:2979-91.

Scholzen T, Gerdes J. 2000. The Ki-67 protein: from the known and the unknown. *J Cell Physiol.* 182:311-22.

Schultz DC, Ayyanathan K, Negorev D, Maul GG, Rauscher FJ 3rd. 2002. SETDB1: a novel KAP-1-associated histone H3, lysine 9-specific methyltransferase that contributes to HP1-mediated silencing of euchromatic genes by KRAB zinc-finger proteins. *Genes Dev*. 6:919-32.

Shahbazian, M.D and Grunstein, M. 2007. Functions of site-specific histone acetylation and deacetylation. *Annu. Rev. Biochem*. 76:75–100.

Shinkai Y, Tachibana M. 2011. H3K9 methyltransferase G9a and the related molecule GLP. *Genes Dev*. 25:781-8

Simpson EH, Johnson DK, Hunsicker P, Suffolk R, Jordan SA, Jackson IJ. 1999. The mouse Cer1 (Cerberus related or homologue) gene is not required for anterior pattern formation. *Dev Biol.* 1213:202-6.

Skene PJ, Henikoff S. 2013. Histone variants in pluripotency and disease. *Development*.140:2513-24.

Sleutels F, Zwart R, Barlow DP. 2002. The non-coding Air RNA is required for silencing autosomal imprintedgenes. *Nature*. 415:810-813.

Srinivas S. 2006.The anterior visceral endoderm-turning heads. *Genesis*. 44:565-72.

Sripathy SP, Stevens J, Schultz DC. 2006. The KAP1 corepressor functions to coordinate the assembly of de novo HP1-demarcated microenvironments of heterochromatin required for KRAB zinc finger protein-mediated transcriptional repression. *Mol Cell Biol*. 26:8623-38.

Stoye JP. 2012. Studies of endogenous retroviruses reveal a continuing evolutionary saga. *Nat Rev Microbiol*. 10:395-406.

Surface LE, Thornton SR, Boyer LA. 2010. Polycomb group proteins set the stage for early lineage commitment. *Cell Stem Cell*. 7:288-98.

Tachibana M, Ueda J, Fukuda M, Takeda N, Ohta T, Iwanari H, Sakihama T, Kodama T, Hamakubo T, Shinkai Y. 2005. Histone methyltransferases G9a and GLP form heteromeric complexes and are both crucial for methylation of euchromatin at H3-K9. *Genes Dev*. 19:815-26.

Tachibana M, Matsumura Y, Fukuda M, Kimura H, Shinkai Y. 2008. G9a/GLP complexes independently mediate H3K9 and DNA methylation to silence transcription. EMBO J. 2008. 27:2681-90.

Takaoka K, Hamada H. 2012. Cell fate decisions and axis determination in the early mouse embryo Development. *Development*. 139:3-14.

Tam PP, Loebel DA. 2007. Gene function in mouse embryogenesis: get set for gastrulation. *Nature Reviews Genetics*. 8:368-381.

Tan SL, Nishi M, Ohtsuka T, Matsui T, Takemoto K, Kamio-Miura A, Aburatani H, Shinkai Y, Kageyama R. 2012. Essential roles of the histone methyltransferase ESET in the epigenetic control of neural progenitor cells during development. *Development.* 139:3806-16.

Talbert PB, Henikoff S. 2010. Histonevariants — ancient wrap artists of the epigenome. *Nat Rev Mol Cell Biol*. 11:264-275.

Thomson M, Liu SJ, Zou LN, Smith Z, Meissner A, Ramanathan S. 2011. Pluripotency factors in embryonic stem cells regulate differentiation into germ layers. *Cell.* 145:875-89.

Torres-Padilla ME, Richardson L, Kolasinska P, Meilhac SM, Luetke-Eversloh MV, Zernicka-Goetz M. 2007. The anterior visceral endoderm of the mouse embryo is established from both preimplantation precursor cells and by de novo gene expression after implantation. *Dev Biol.* 309:97-112.

Tremblay KD, Duran KL, Bartolomei MS. 1997. A 5' 2-kilobase-pair region of the imprinted mouse H19 gene exhibits exclusive paternal methylation throughout development. *Mol. Cell. Biol*. 17:4322–4329.

Uchimura Y, Ichimura T, Uwada J, Tachibana T, Sugahara S, Nakao M, Saitoh H. 2006. Involvement of SUMO modification in MBD1- and MCAF1-mediated heterochromatin formation. *J Biol Chem.* 281:23180-90

Ueda J, Tachibana M, Ikura T, Shinkai Y. 2006. Zinc finger protein Wiz links G9a/GLP histone methyltransferases to the co-repressor molecule CtBP. *J Biol Chem*. 281:20120-8.

Vandesompele J, De Preter K, Pattyn F, Poppe B, Van Roy N, De Paepe A, Speleman F. 2002. Accurate normalization of real-time quantitative RT-PCR data by geometric averaging of multiple internal control genes. *Genome Biol*. 3:RESEARCH0034

Viotti M, Niu L, Shi SH, Hadjantonakis AK. 2012. Role of the gut endoderm in relaying left-right patterning in mice. *PLoS Biol*. 10:e1001276.

Viotti M, Nowotschin S, Hadjantonakis AK. 2011. Afp::mCherry, a red fluorescent transgenic reporter of the mouse visceral endoderm. *Genesis*. 49:124-33.

Walsh CP, Chaillet JR, Bestor TH. 1998. Transcription of IAP endogenous retroviruses is constrained by cytosine methylation. *Nat Genet.* 20:116-7.

Wang H, An W, Cao R, Xia L, Erdjument-Bromage H, Chatton B, Tempst P, Roeder RG, Zhang Y. 2003. mAM facilitates conversion by ESET of dimethyl to trimethyl lysine 9 of histone H3 to cause transcriptional repression. *Mol Cell*. 12:475-87.

Wang Z, Oron E, Nelson B, Razis S, Ivanova N. 2012. Distinct lineage specification roles for NANOG, OCT4, and SOX2 in human embryonic stem cells. *Cell Stem Cell.* 10:440-54

Watabe T. 2012. Roles of Dppa2 in the regulation of the present status and future of pluripotent stem cells. *J Biochem*. 152:1-3.

Waterston RH, Lindblad-Toh K, Birney E, Rogers J, Abril JF, Agarwal P, Agarwala R, Ainscough R, Alexandersson M, An P. et al. 2002. Initial sequencing and comparative analysis of the mouse genome. *Nature*. 420:520-62.

Whitman M. 2001. Nodal signaling in early vertebrate embryos: themes and variations. *Dev Cell*. 1:605-17.

Wilson V1, Manson L, Skarnes WC, Beddington RS. 1995. The T gene is necessary for normal mesodermal morphogenetic cell movements during gastrulation. *Development.* 121:877-86.

Wolf D, Goff SP. 2007. TRIM28 mediates primer binding site-targeted silencing of murine leukemia virus in embryonic cells. *Cell.* 131:46-57.

Woodcock CL, Dimitrov S. 2001. Higher-order structure of chromatin and chromosomes. *Curr Opin Genet Dev*. 11:130-135.

Xi Q, Wang Z, Zaromytidou AI, Zhang XH, Chow-Tsang LF, Liu JX, Kim H, Barlas A, Manova-Todorova K, Kaartinen V, Studer L, Mark W, Patel DJ, Massagué J. 2011. A poised chromatin platform for TGF-β access to master regulators. *Cell*. 147:1511-24

Yamanaka Y. 2011. Response: Cell fate in the early mouse embryo-sorting out the influence of developmental history on lineage choice. *Reprod Biomed Online*. 22:525–527.

Yang L, Xia L, Wu DY, Wang H, Chansky HA, Schubach WH, Hickstein DD, Zhang Y. 2002. Molecular cloning of ESET, a novel histone H3-specific methyltransferase that interacts with ERG transcription factor. *Oncogene*. 21:148-52.

Yang D, Lutter D, Burtscher I, Uetzmann L, Theis FJ, Lickert H. miR-335 promotes mesendodermal lineage segregation and shapes a transcription factor gradient in the endoderm. 2014. *Development*. 141:514-25.

Yasunaga, M., Tada, S., Nishikawa, S. T., Nakano, Y., Okada, M., Jakt, L. M., Nishikawa, S., Chiba, T., Era, T., and Nishikawa, S. I. 2005 Induction and monitoring of definitive and visceral endoderm differentiation of mouse ES cells. *Nat Biotechnol*. 23:1542-1550

Ying, Q. L., Stavridis, M., Griffiths, D., Li, M. and Smith, A. 2003.Conversion of embryonic stem cells into neuroectodermal precursors in adherent monoculture. *Nat Biotechnol*. 21:183-186.

Yoshiba S, Shiratori H, Kuo IY, Kawasumi A, Shinohara K, Nonaka S, Asai Y, Sasaki G, Belo JA, Sasaki H, Nakai J, Dworniczak B, Ehrlich BE, Pennekamp P, Hamada H. 2012. Cilia at the node of mouse embryos sense fluid flow for left-right determination via Pkd2. *Science*. 338:226-31.

Yoshikawa Y, Fujimori T, McMahon AP, Takada S. 1997. Evidence that absence of Wnt-3a signaling promotes neuralization instead of paraxial mesoderm development in the mouse. *Dev Biol*. 183:234-42.

Yuan L, Liu JG, Hoja MR, Wilbertz J, Nordqvist K, Höög C. 2002. Female germ cell aneuploidy and embryo death in mice lacking the meiosis-specific protein SCP3. *Science*. 296:1115-8.

Yuan L, Liu JG, Zhao J, Brundell E, Daneholt B, Höög C. 2000. The murine SCP3 gene is required for synaptonemal complex assembly, chromosome synapsis, and male fertility. *Mol Cell*. 5:73-83.

Yuan P, Han J, Guo G, Orlov YL, Huss M, Loh YH, Yaw LP, Robson P, Lim B, Ng HH. 2009. Eset partners with Oct4 to restrict extraembryonic trophoblast lineage potential in embryonic stem cells. *Genes Dev*. 23:2507-20.

Zhang H, Roberts DN, Cairns BR. 2005. Genome-widedynamics of Htz1, a histone H2A variant that poises repressed/basalpromoters for activation through histone loss. *Cell*. 123:219–231.

Zhang Y, Reinberg D. 2001. Transcription regulation by histone methylation: interplay between different covalent modifications of the core histone tails. *Genes Dev*. 15:2343-60.

Zhang Z, Huynh T, Baldini A. 2006. Mesodermal expression of Tbx1 is necessary and sufficient for pharyngeal arch and cardiac outflow tract development. *Development*. 133:3587-95.

Zhu D, Fang J, Li Y, Zhang J. 2009. Mbd3, a Component of NuRD/Mi-2 Complex, Helps Maintain Pluripotency of Mouse Embryonic Stem Cells by Repressing Trophectoderm Differentiation. *Plos one*. 4:e7684.